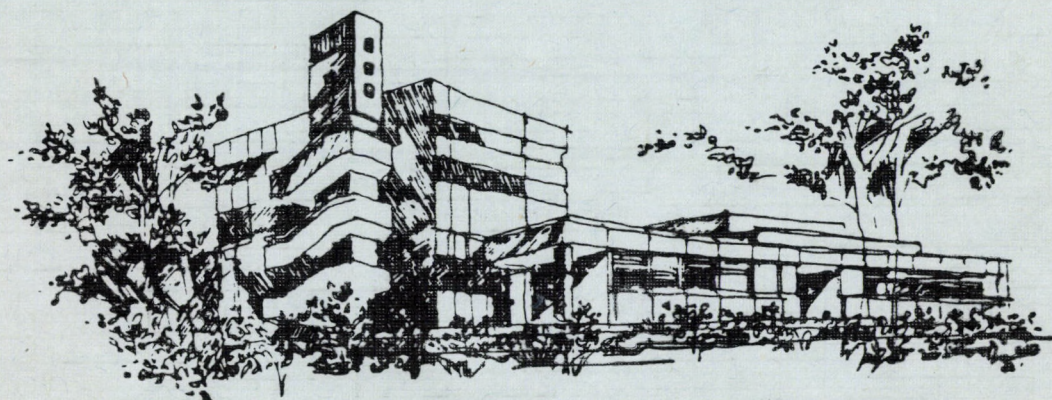


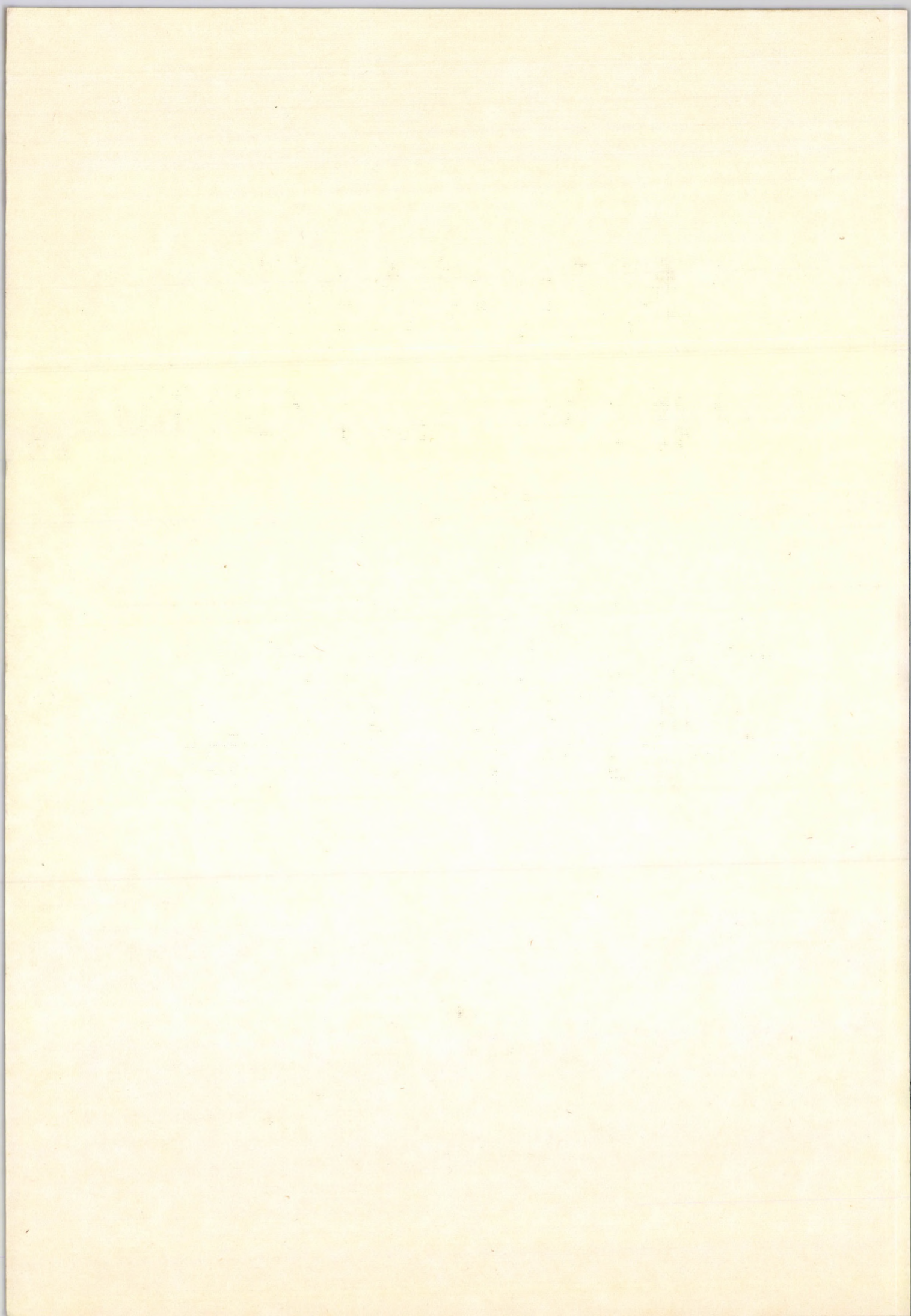
ATOMKI

ANNUAL REPORT

1991



INSTITUTE OF NUCLEAR RESEARCH
OF THE HUNGARIAN ACADEMY OF SCIENCES
DEBRECEN, HUNGARY



INSTITUTE OF NUCLEAR RESEARCH
OF THE HUNGARIAN ACADEMY OF SCIENCES
DEBRECEN, HUNGARY

ANNUAL REPORT 1991

ATOMKI

Postal address:

Debrecen

P. O. Box 51

H-4001

Hungary

Edited by Z. Gácsi

HU ISSN 0231-3596

ATOMKI

Preface

In a considerably changed outside environment the research activity of the Institute in 1991 remained on the same track as in the previous years, and the versatility of our activity remained too. The year 1991 has brought several administrative changes in the Institute. The most apparent ones may be the change of the director and deputy directors and some of the section leaders at the beginning of the year. Our research activities seem to survive the changes.

In this introduction I would like to touch upon the most important developments of the year and give some information about the Institute in general. Further general information can be found in the first section of the Annual Report; it gives some insight into the organisation, personnel and finance of the Institute.

The title of the section on **nuclear physics** has been changed to nuclear and particle physics this year. Well, the change might seem a little premature considering that there is only one contribution in particle physics, but the change of the title indicates our intention to encourage growth in this field. The main branch of our experimental nuclear physics research is "in beam" nuclear spectroscopy, and in 1991 a wealth of new results has been produced for the $^{66,68}\text{Ga}$, $^{72,74}\text{As}$, ^{116}Sn and $^{112,114,118}\text{Sb}$ isotopes. Studies of nuclear reactions at low energies have been going on with some shift towards reactions of astrophysical interest, which are anticipated to be important in the future. The application and refinement of the cluster model of light nuclei remains a healthy and vigorous project of our nuclear theorists. Their widespread interest, however, ranges from supersymmetric quantum mechanics to the problems of α decay of heavy nuclei.

In our **atomic collision physics** research the study of the electron capture and electron loss cusps was a dominating line. The observed and unexplained discrepancy between the velocity of the projectile and that of the cusp electrons lost to the continuum of the projectile caused some excitement, and initiated further studies. The classical trajectory Monte Carlo calculations of ion-atom collisions gained some momentum, and the theoretical description of single and double ionization of H_2 by protons kept some of our atomic physicists busy during the year.

Biological and medical research in an institute for nuclear physics might seem strange at first, but the application of nuclear and atomic physics in medical and biological research has a long tradition in the Institute. This line of research was given even more emphasis in the past years. The establishment of our cyclotron laboratory — the only one in Hungary — made the Institute the centre of nuclear medicine in Hungary. The neutron irradiation of living cells and isotope production for practical purposes continue to be important services in the Institute. The impact of environmental radioactivity and heavy element pollution on human health has been investigated with the use of analytical and detection methods available in the Institute.

Materials science and analysis is gaining strength in the Institute. Apart from the genuine solid state physics research in superconductivity and Si(Li) detector materials, our works on materials science and analysis originate from nuclear and atomic physics. Wear measurements with the use of radioactive isotopes and PIXE and PIGE applications are the most obvious examples. The application of X-ray and electron spectroscopy in material analysis continued to be the main line of our research activity in this field.

Environmental research is certainly the issue of the end of this century, and Hungary is no exception in this respect. Physics and, more specifically, analytical methods using results in atomic and nuclear physics will have a growing share in environmental monitoring and even in the solution of some acute problems. This line of research is not new in the Institute and we are well prepared to take up work in certain type of environmental monitoring. The measurement of radon concentration in natural caves and in some less traditional places of human residence, like apartment houses, seems to interest both our scientists and our cooperating partners. Mass spectroscopy contributes significantly to the solution problems in **earth sciences** and, more specifically, to the solution of problems in geochronology and hydrology. The investigation of air pollution and aerosol transfer is believed to be very important for environmental research, and our PIXE and XRFA are adequate tools for such analyses.

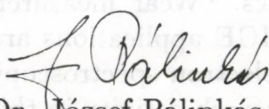
The **development of methods and instruments** is a prerequisite of efficient experimental physics research. Our development activity focusses primarily on detectors and data acquisition systems. The design and construction of special electron spectrometers are undoubtedly the most important of our development activity, and 1991 brought to life our new UV photoelectron spectrometer. The development of ion sources is a new field in the Institute, and, considering our plans on a heavy-ion facility (see below), it is hopefully a growing one. Next to detector development on the priority list of our technical physicists is data acquisition, and 1991 brought promising new results in digital data processing.

To say something about our **educational activity**, the first year of our Joint Physics Department with Lajos Kossuth University brought to life a course on the Physics of the Environment, the importance of which is self-evident. Several diploma works and doctoral theses were completed in 1991 and, generally, the educational work of the Institute is increasing.

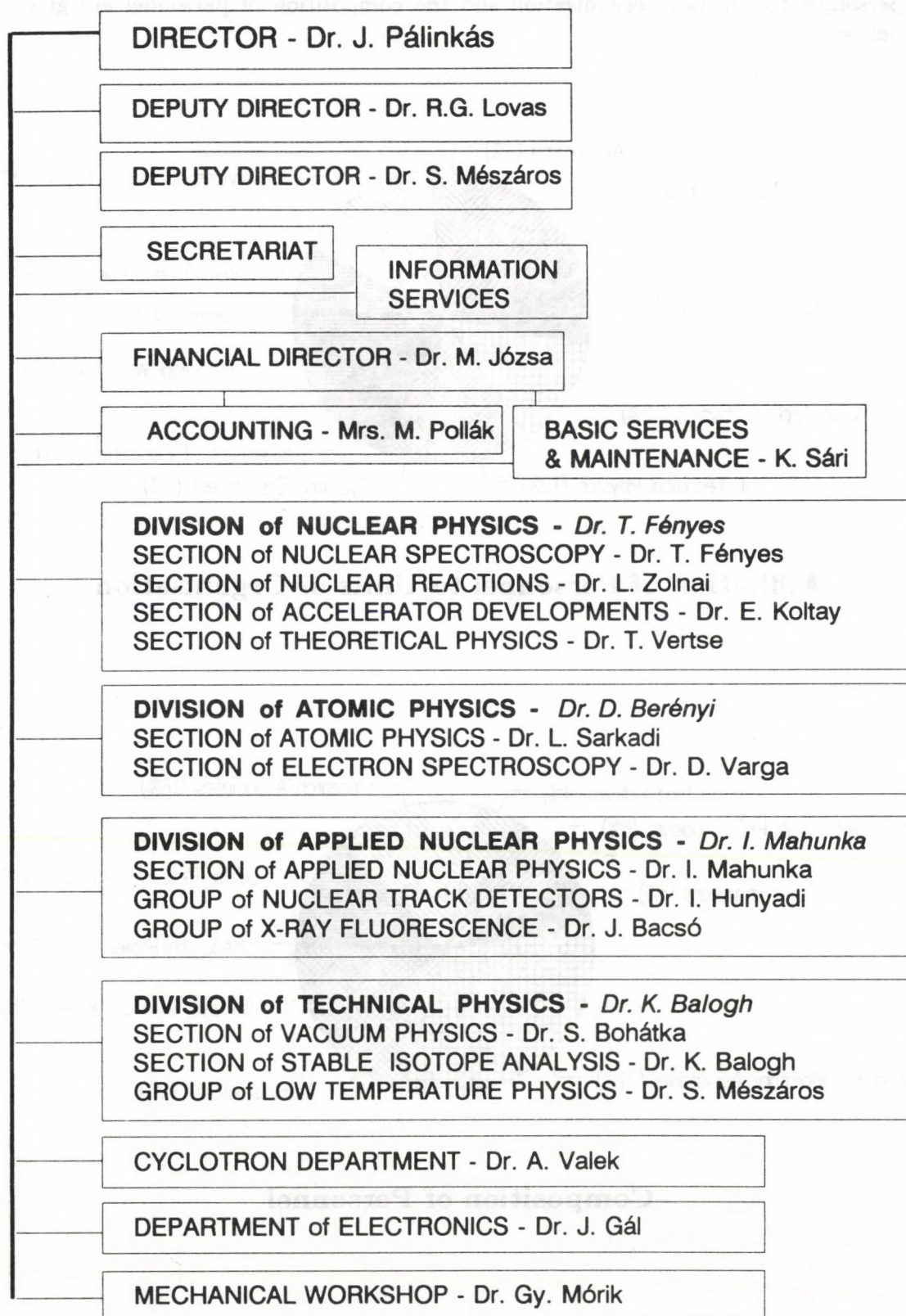
My report on the *progress* in 1991 is not complete without mentioning our **plans for the future**. We have two main development objects: a Positron Emission Tomograph (PET) laboratory and a heavy-ion facility based on an Electron Cyclotron Resonance (ECR) ion source. The general state of Hungarian economy might cause some delays in these developments, but the promising direction of changes keeps our hopes high and our plans ready.

In 1991 a decisive step was made towards the reunification of university education in Debrecen. Back in the early fifties, similarly to other universities in Hungary, the University of Debrecen was split into three independent educational institutions, and later the College of Agriculture was also granted the rank of university. Now these educational institutions and our Institute signed an association treaty and declared the foundation of the **University of Debrecen**. This is the first full-fledged university in Hungary, and our hopes are high again that, after our good start, this new structure will help in the economical use of resources in research and education.

Debrecen, February 28, 1992

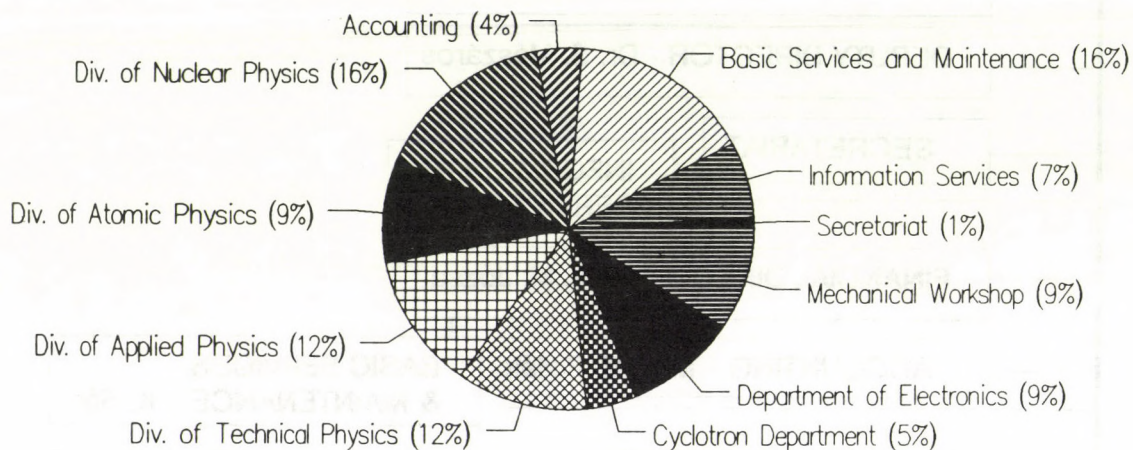

Dr. József Pálincás
Director

The organisation structure of the
Institute of Nuclear Research
of the Hungarian Academy of Sciences

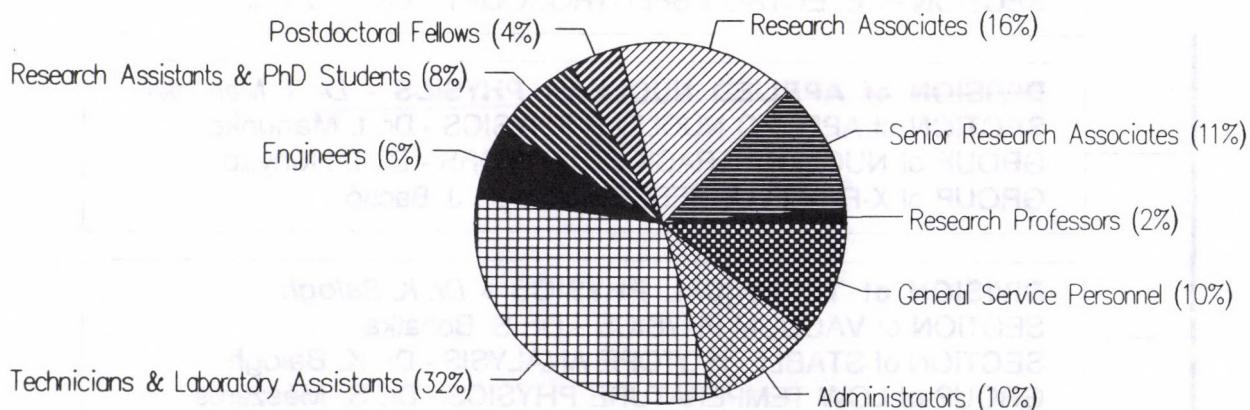


Personnel

The Institute at present employs a total of 244 persons. The affiliation of personnel to units of organisation and the composition of personnel are given below.



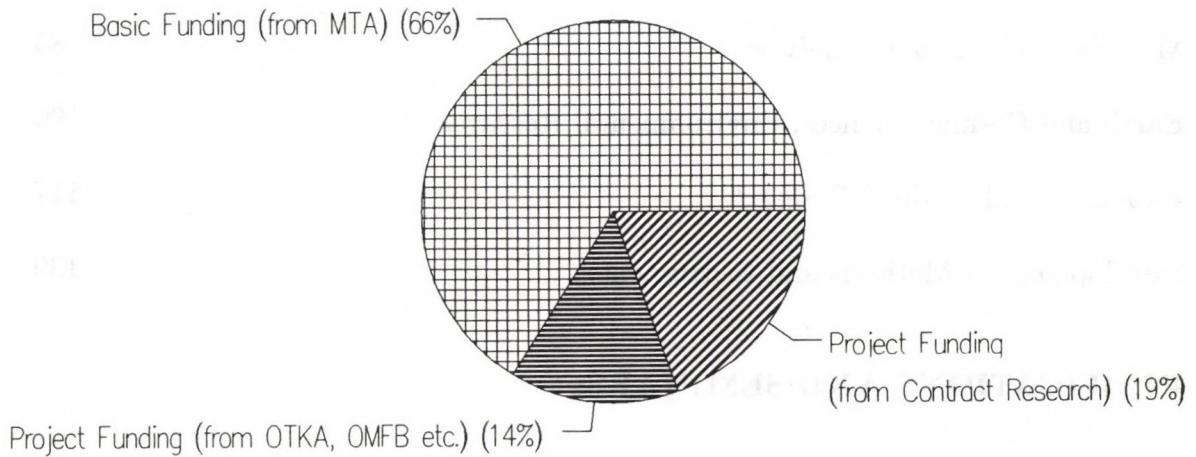
Affiliation of Personnel to Units of Organisation



Composition of Personnel

Finance

The total budget of the Institute in 1991 was 148 Million Hungarian Forints. The composition of the budget and the breakdown of expenditure according to different categories are given below.

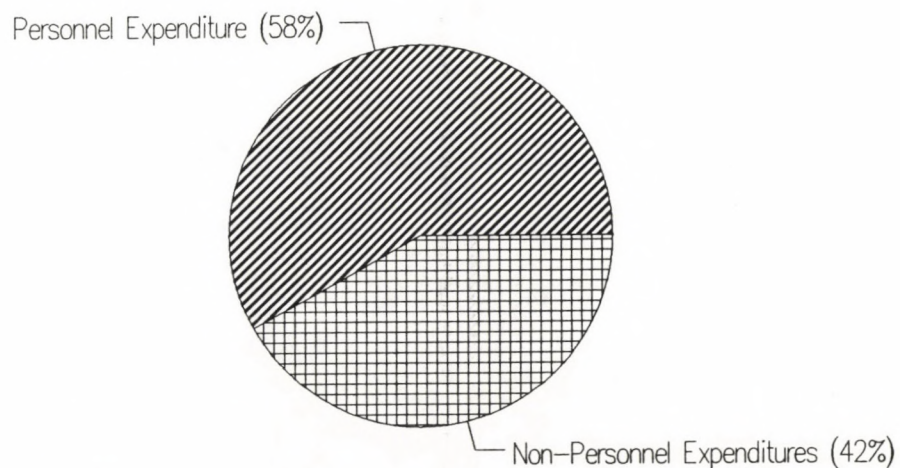


Composition of the Institute's Budget

MTA: Hungarian Academy of Sciences

OTKA: National Fund for Scientific Research

OMFB: National Committee for Technological Development



Breakdown of Expenditure into Personnel and Non-Personnel Expenditures

CONTENTS

REPORTS:

Nuclear and Particle Physics	1
Atomic Physics	63
Materials Science and Analysis	85
Earth and Cosmic Sciences, Environmental Research	106
Biological and Medical Research	117
Development of Methods and Instruments	139

PUBLICATIONS AND SEMINARS:

Papers Published in 1991	163
Conference Contributions and Talks	171
Theses Completed	187
Hebdomadal Seminars	189
Author Index	192



NUCLEAR
AND
PARTICLE PHYSICS

NUCLEAR
AND
PARTICLE PHYSICS

Isotopic Dependence of Electron Screening in Fusion Reactions

S.Engstler *, G.Raimann *, C.Angulo *, U.Greife *, C. Rolfs *,
U.Schröder *, E.Somorjai, B.Kirch ** and K.Langanke **

*Institut für Physik mit Ionenstrahlen, Ruhr-Universität Bochum,
Germany

**Institut für Theoretische Physik, Universität Münster, Germany

The fusion reactions ${}^6\text{Li}(p, \alpha){}^3\text{He}$, ${}^6\text{Li}(d, \alpha){}^4\text{He}$ and ${}^7\text{Li}(p, \alpha){}^4\text{He}$ have been studied over the c.m. energy range $E = 10$ to 1450 keV. Each reaction involved the use of hydrogen projectiles and LiF solid targets as well as Li projectiles and hydrogen molecular gas targets.

In all cases the effects of electron screening on the low-energy fusion cross sections (exponential enhancement) have been observed. The effect for ${}^6\text{Li} + p$ is shown in Fig. 1. together with the literature values [1, 2, 3].

The screening effects are somewhat stronger in the case of atomic p or d projectiles compared to the case of molecular H_2 or D_2 gas targets. If isotopic effects on electron screening are negligible, all three reactions should exhibit the same enhancements for each set of experimental techniques. The measurements confirmed this expectation to a large extent.¹

References

1. W. Gemeinhardt, D. Kamke and Chr.von Rhöneck, Z. Phys. **197** (1966) 58
2. O. Fiedler and R. Kunze, Nucl. Phys. **A96** (1967) 513
3. J. F. Harmon, Nucl. Instr. Meth. **40/41** (1989) 507

¹ Accepted for publication in Z. Phys.

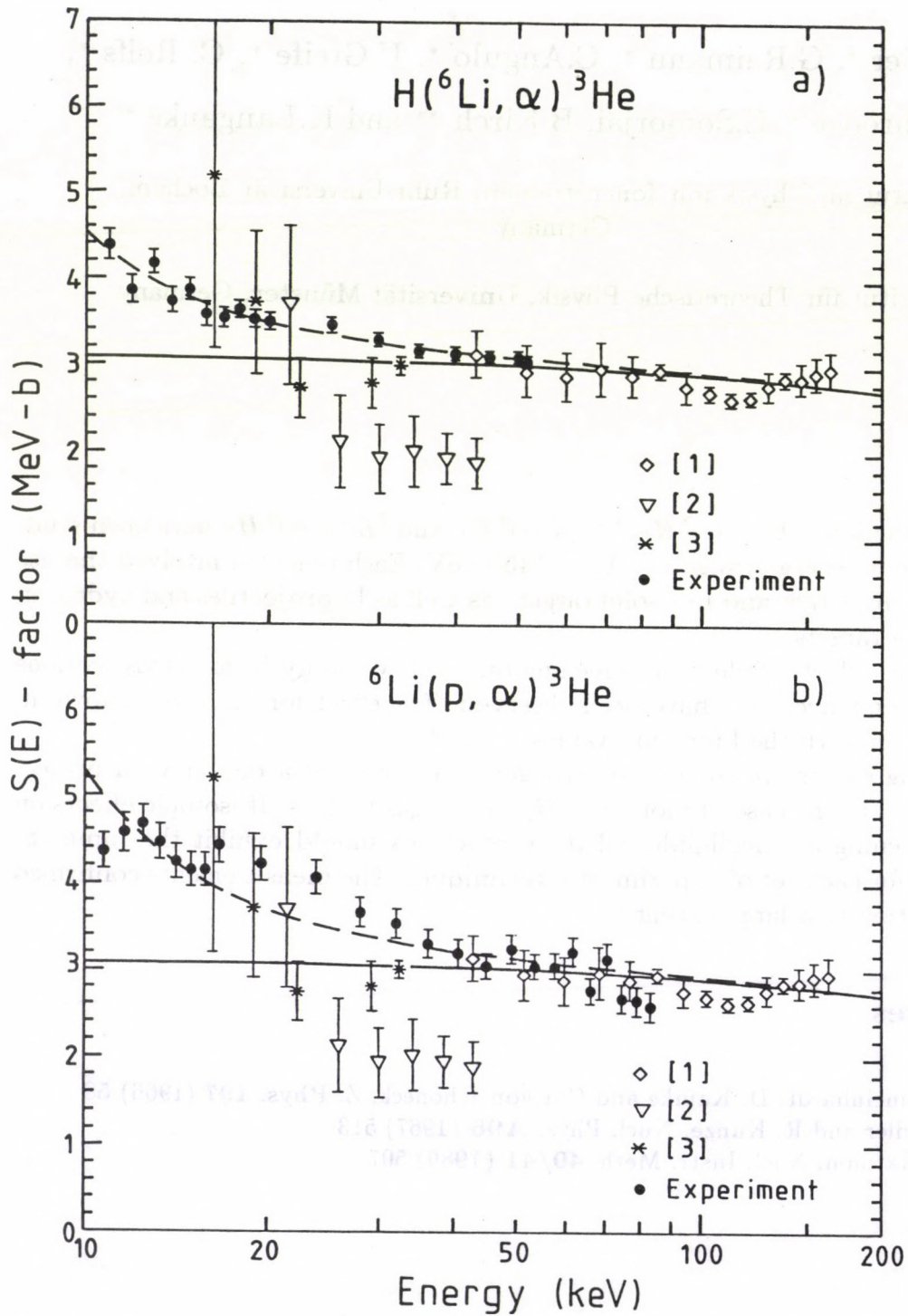


Fig. 1. Enhancement caused by electron screening for $^6\text{Li} + p$ with gas (a) and solid target (b).

Lifetime Measurements in ^{28}Si

Zs. Fülöp, Á.Z. Kiss, E. Somorjai

P. Tikkanen *, J. Keinonen * and A. Kangasmäki *

* Accelerator Laboratory, Department of Physics, University of Helsinki,
SF-00170 Helsinki, Finland

Although ^{28}Si is one of the most intensively studied nucleus in the sd-shell region yet many ambiguities are found among its level parameters, especially among the lifetimes of excited states. The aim of the present work is to determine reliable and consistent lifetimes for this nucleus applying an improved Doppler shift attenuation (DSA) method we have already used for many nuclei of the sd-shell (see e.g. ref. [1]).

The ^{28}Si states were excited in the reactions $^{27}\text{Al}(p, \gamma)^{28}\text{Si}$ and $^{14}\text{N}(^{16}\text{O}, pn)^{28}\text{Si}$. The latter reaction carried out using 17 to 28 MeV ^{16}O beams supplied by the 5MV tandem accelerator at the Helsinki University is the first study on short lifetimes for the higher excited states using heavy ions and high recoil velocities. The capture reaction served for lifetime determinations of lower lying bound states excited by the $E_p = 655, 767, 992$ and 1317 keV resonances having recently determined accurate gamma-ray branchings [2].

During the measurements implanted ^{14}N and ^{27}Al targets in Ta were used. In the case of the capture reaction targets implanted in Si were also used in order to get more accurate values of the longer ($\tau > 200$ fs) lifetimes. For the lifetime determination the stopping powers for both stopping materials were measured experimentally and the gamma-lineshapes were simulated using the Monte Carlo method. The final determination of the lifetimes and the comparison of the experimentally deduced transition strengths with shell model calculations based on large-basis multi-shell wave functions is in progress.

References

1. P. Tikkanen, J. Keinonen, A. Kangasmäki, Zs. Fülöp, Á. Z. Kiss, E. Somorjai, Phys. Rev. C43 (1991) 2162
2. P. M. Endt, C. Alderliesten, F. Zijderhand, A. A. Wolters and A. G. M. Van Hees, Nucl. Phys. A510 (1990) 209-243

Spectroscopy of ^{38}Ar via the $^{34}\text{S}(\alpha, \gamma)$ Reaction

Zs. Fülöp, Á. Z. Kiss, E. Koltay, E. Somorjai,

J.Keinonen *, P. Tikkanen *

*Accelerator Laboratory, Department of Physics, University of Helsinki,
SF-00170 Helsinki, Finland

As a part of our study of α -capture reactions on Sulphur targets excitation curves of the $^{34}\text{S}(\alpha, \gamma)^{38}\text{Ar}$ reaction have been measured over the energy range $E_\alpha = 3.4 - 4.4\text{MeV}$. A part of the excitation function is shown on Fig. 1. Five new resonances (at energies $E_\alpha = 3.799, 3.853, 3.920, 3.968, 4.008\text{MeV}$ corresponding to excited states of ^{38}Ar at $E_x = 10.61, 10.66, 10.72, 10.76, 10.79\text{MeV}$, respectively) have been found. Thanks to the lower background provided by the 100% enriched (implanted) target some resonances attributed earlier to the ^{32}S contamination of the target [1] proved to be resonances of the investigated reaction.

The study of the decay schemes, resonance strengths, spin-parity values of the new resonances and the reinvestigation of decays for the known ones [2] is under course.

References

1. A. Chevallier, E. Bozek, J. Chevallier, A. Pape and R. Armbruster, Nucl. Phys **A191** (1972) 201-208
2. P. M. Endt and C. van der Leun **A521** (1990) 1

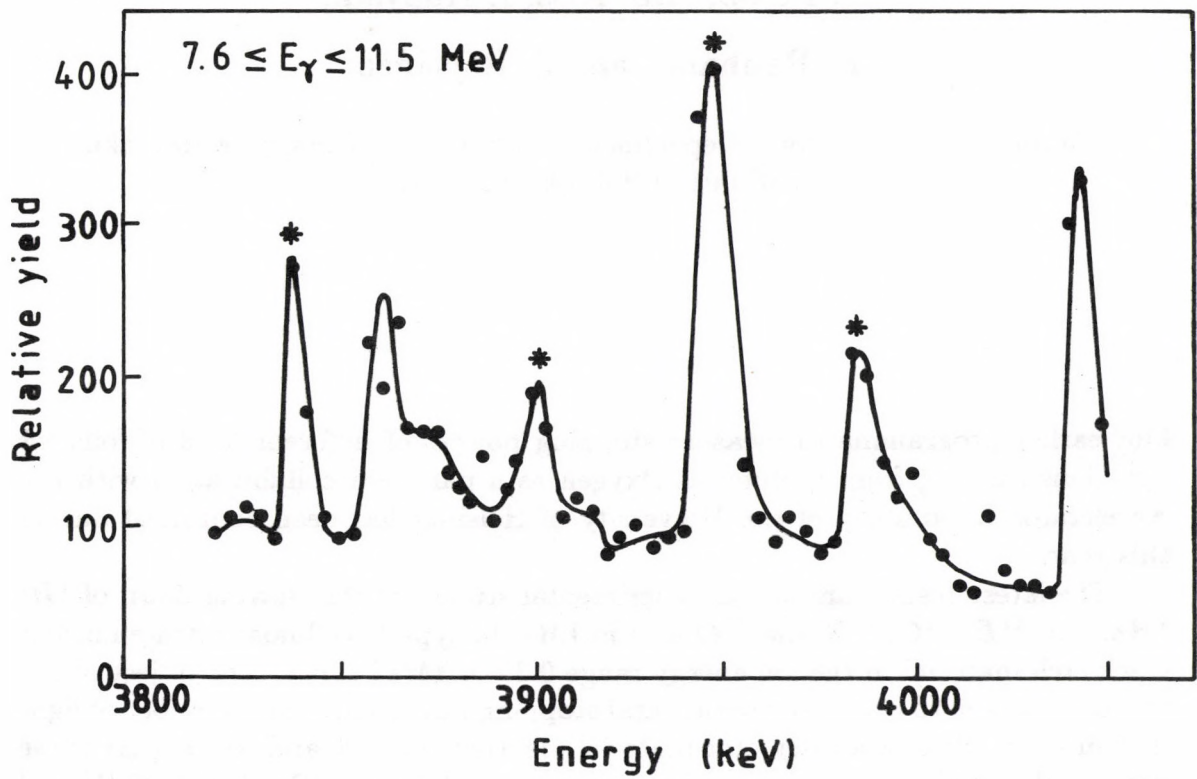


Fig. 1. Yield curve for the reaction $^{34}\text{S}(\alpha, \gamma)^{38}\text{Ar}$ obtained for energy window 7.6 – 11.5 MeV. The new resonances are marked by asterisk.

Slowing Down of Light Ions in LR-115 Nuclear Track Material

Zs. Fülöp, Á.Z. Kiss, I. Hunyadi,

E. Rauhala * and J. Räsänen *

*Accelerator Laboratory, Department of Physics, University of Helsinki,
SF-00170 Helsinki, Finland

Our earlier programme to measure stopping powers of different kind of foils for light ions ranging from protons to Oxygen as a part of a collaboration with the Accelerator Laboratory of the University of Helsinki has been continued during this year.

The latest results are in the experimental studies of the slowing down of 1H , 4He , 7Li , ^{11}B , ^{12}C , ^{14}N and ^{16}O ions in LR-115 type II cellulose nitrate nuclear track etch material in the ion energy range $0.3 - 4.3 MeV/amu$. The object of the present study is to provide experimental stopping power data for a number of light ions in the nuclear track detector material mentioned above and to compare these data to the predictions of two recent semiempirical models (Ziegler, 1980 [1] and TRIM-91 [2]) for calculating the stopping powers.

The 1H and 4He beams were obtained from the 2.5 MV Van de Graaff accelerator of the Helsinki University and from the 5MV Van de Graaff accelerator (energies $< 5 MeV$) and from the MGC-20 cyclotron (energies $> 5 MeV$) at our institute. The 7Li , ^{11}B , ^{12}C , ^{14}N and ^{16}O ion beams were supplied by the 5 MV tandem accelerator EGP-10-II of the Accelerator Laboratory of the University of Helsinki. The experimental arrangement used in the energy loss measurements performed at our institute was similar to the one described in detail in our earlier study [3], while the experimental setup used in the measurements at the Helsinki University is described in ref. [4].

As an example Fig. 1. shows stopping powers of the LR-115 material for 1H and 4He ions in comparison with stopping powers calculated by the code TRIM-91. For the stopping power data (including also experimental results for heavier ions than He) an absolute uncertainty of $\pm 3\%$ is assigned. From the comparisons of the data with semiempirical stopping power predictions based on the TRIM-91 computer code and semiempirical curves calculated by the Ziegler parameters [1] we have concluded that the predictions underestimate the observed stopping powers for 7Li , ^{11}B and ^{12}C ions. The deviations are below 10 % [5].

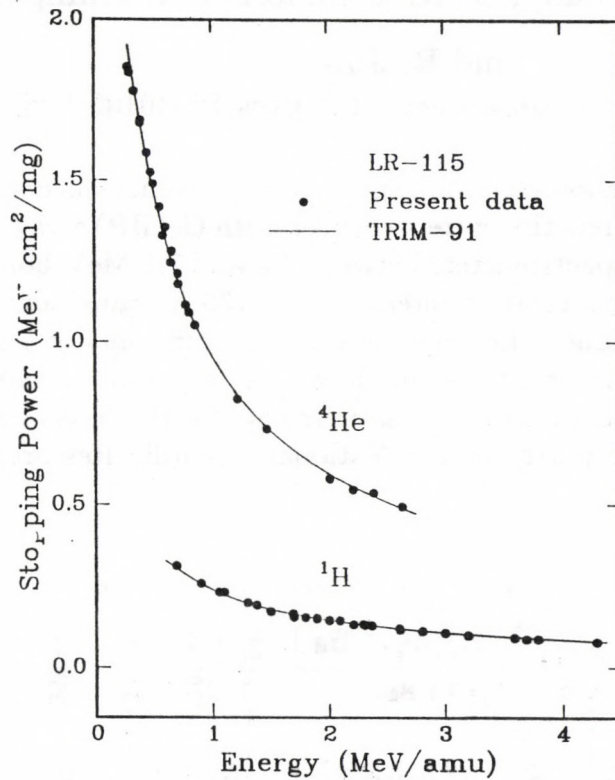


Fig. 1. Stopping powers of LR-115 for ^1H and ^4He ions. The curves represent the stopping power as predicted by TRIM-91.

References

1. J. F. Ziegler, *The Stopping and Ranges of Ions in Matter*. Vol. 5. Plenum Press, New York, 1980.
2. J. F. Ziegler (1991) TRIM computer code, private communication.
See also J.P. Biersack and L.G. Haggmark, *Nucl. Instr. Meth.* **174** (1980) 257
3. Á. Z. Kiss, E. Somorjai, J. Räsänen and E. Rauhala, *Nucl. Instr. Meth.* **B39** (1989) 15
4. J. Räsänen, E. Rauhala, *Phys. Rev.* **B41** (1990) 3951
5. E. Rauhala, J. Räsänen, Zs. Fülöp, Á.Z. Kiss and I. Hunyadi, Submitted to *Nucl. Tracks and Rad. Meas.*

Spectroscopic study of the $^{66}\text{Zn}(p,n\gamma)^{66}\text{Ga}$ reaction

J. Tímár, T. X. Quang, A. Krasznahorkay, J. Kumpulainen †

and R. Julin †

†University of Jyväskylä, Department of Physics, SF-40100 Jyväskylä, Finland

γ -ray, internal conversion electron (fig. 1) and $\gamma\gamma$ -coincidence spectra (fig. 2) from the $^{66}\text{Zn}(p,n\gamma)^{66}\text{Ga}$ reaction were measured with Ge(HP) γ -ray and magnetic lens plus Si(Li) electron spectrometers between 6.5 and 7.1 MeV bombarding proton energies. Energies and relative intensities of 130 γ transitions of the ^{66}Ga nucleus have been determined. Internal conversion coefficients of >30 transitions have been deduced for the first time enabling determination of many new γ -ray multiplicities and unambiguous parity assignments for the levels below 800 keV. This work was supported partly by the National Scientific Research Foundation /OTKA/.

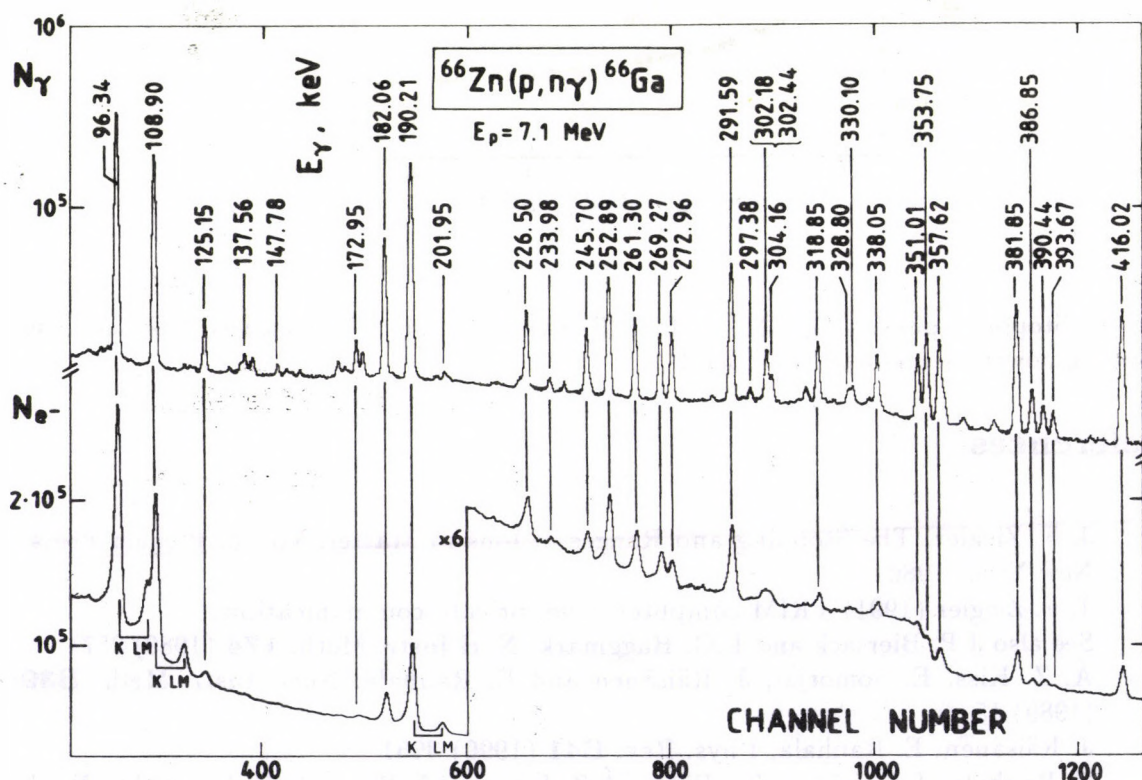


Fig. 1. Typical γ -ray and internal conversion electron spectra from the $^{66}\text{Zn}(p,n\gamma)^{66}\text{Ga}$ reaction.

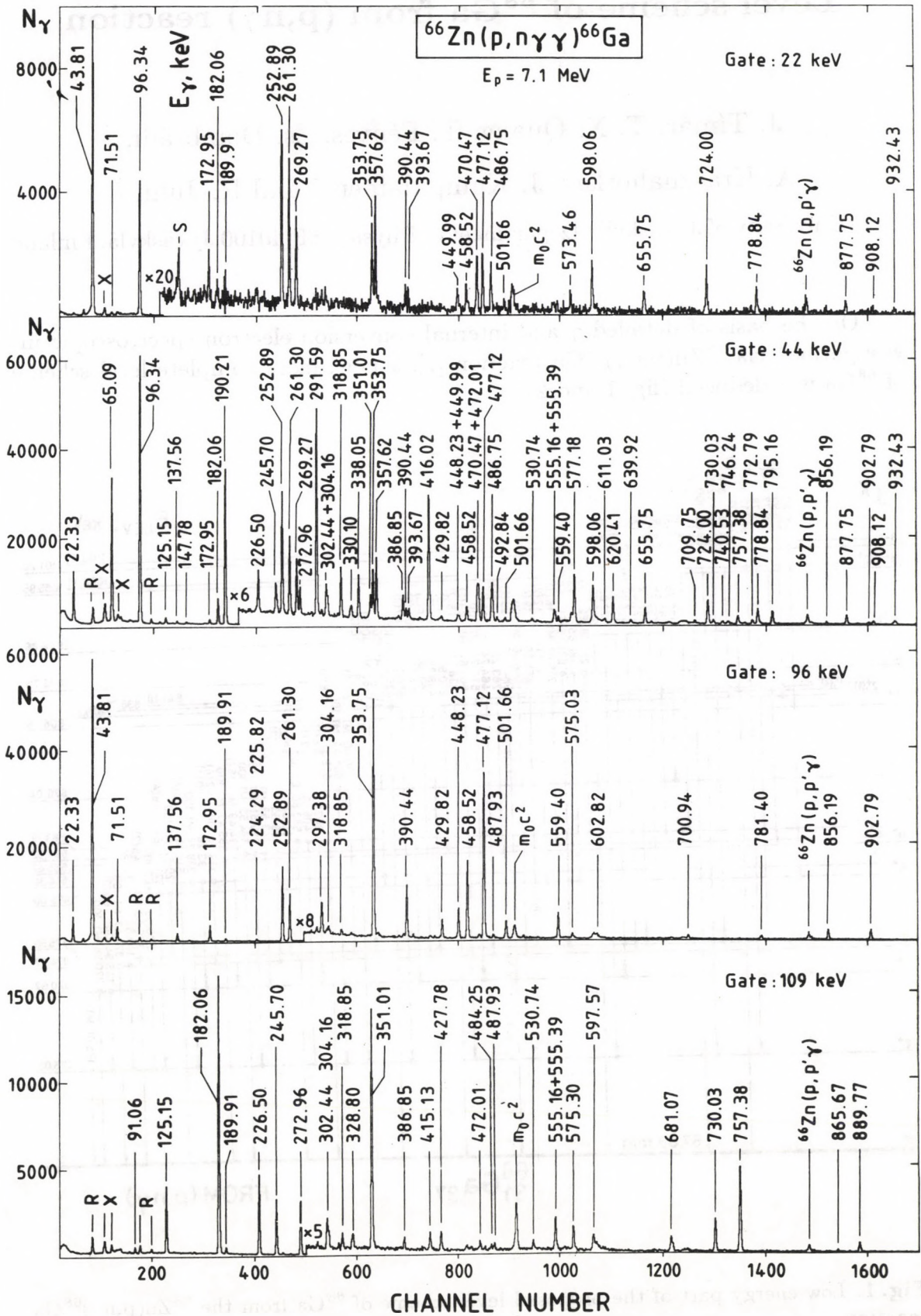


Fig. 2. Typical $\gamma\gamma$ coincidence spectra of ^{66}Ga . S, R and X denote summa and random coincidences and X-rays, respectively.

Level scheme of ^{68}Ga from $(p,n\gamma)$ reaction

J. Tímár, T. X. Quang, T. Fényes, Zs. Dombrádi,

A. Krasznahorkay, J. Kumpulainen [†] and R. Julin [†]

[†]University of Jyväskylä, Department of Physics, SF-40100 Jyväskylä, Finland

On the basis of detailed γ and internal conversion electron spectroscopic investigations via $^{68}\text{Zn}(p,n\gamma)^{68}\text{Ga}$ reaction [1], a new, more complete level scheme of ^{68}Ga was deduced (fig. 1 and 2).

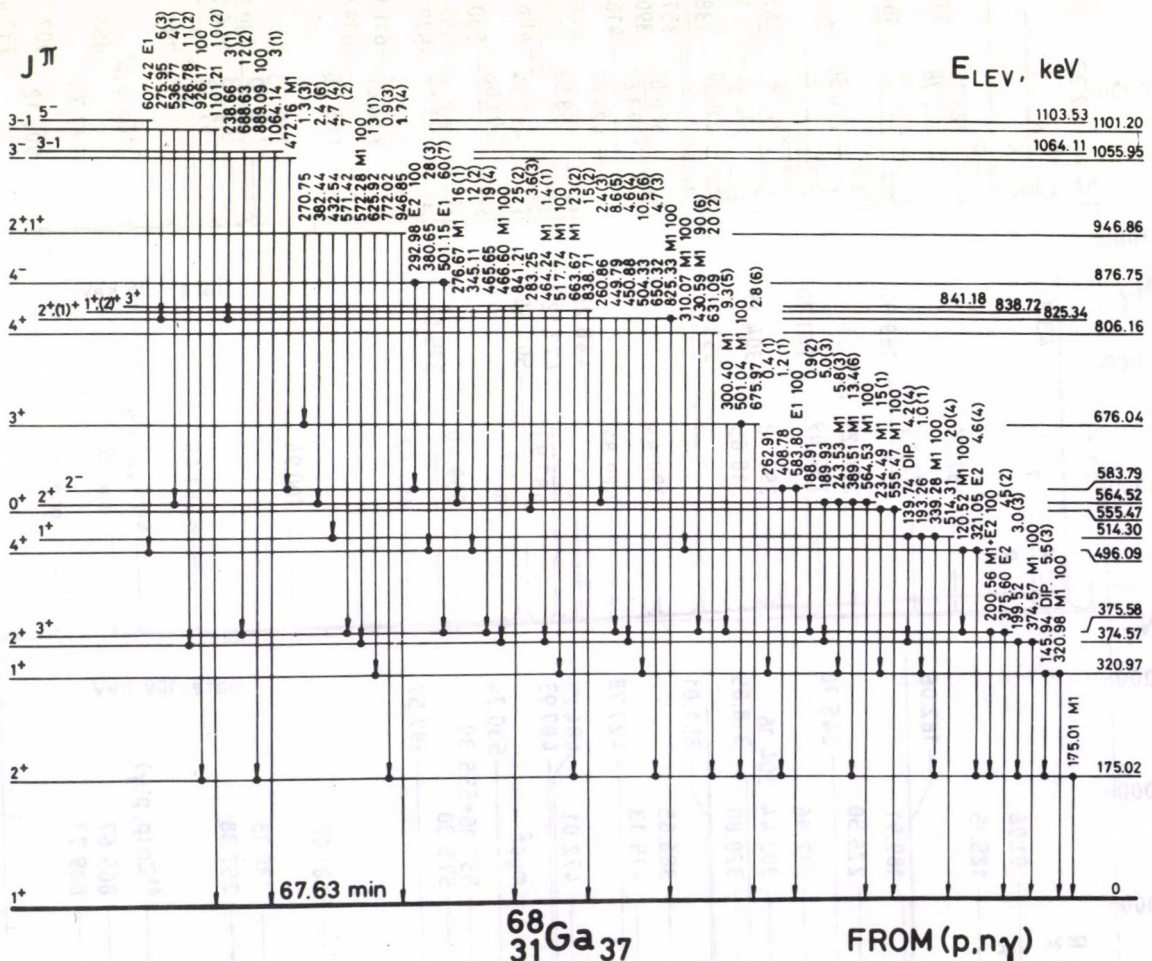


Fig. 1. Low-energy part of the proposed level scheme of ^{68}Ga from the $^{68}\text{Zn}(p,n\gamma)^{68}\text{Ga}$ reaction.

Spin and parity values have been deduced from internal conversion coefficients of transitions, Hauser-Feshbach analysis of (p,n γ) reaction cross sections and other arguments. The energy splitting of the different p-n multiplets has been calculated on the basis of the parabolic rule. Several p-n multiplet states have been identified. This work was supported partly by the National Scientific Foundation /OTKA/.

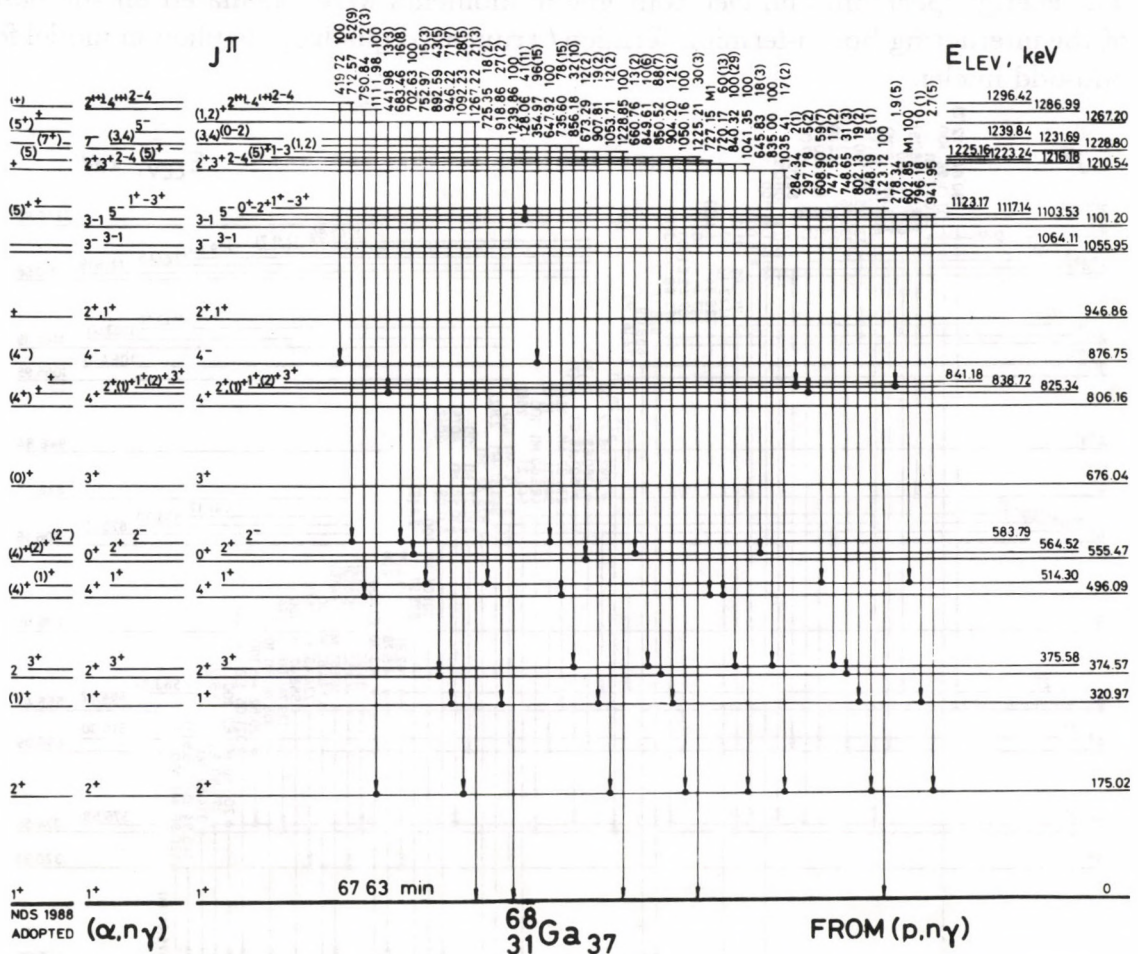


Fig. 2. High-energy part of the ^{68}Ga level scheme from (p,n γ) reaction.

Reference

1. J. Tímár, T. X. Quang, A. Krasznahorkay, T. Fényes, J. Kumpulainen and R. Julin, ATOMKI Ann. Rep. 1990, p.12.

Structure of ^{68}Ga from $(\alpha, n\gamma)$ reaction

J. Tímár, T. X. Quang, T. Fényes, Zs. Dombrádi,

A. Krasznahorkay and V. Paar \dagger

\dagger Prirodoslovno-matematički fakultet, University of Zagreb, 41000 Zagreb, Croatia

On the basis of detailed in-beam spectroscopic study of ^{68}Ga [1] a new, more complete level scheme (fig. 1 and 2) was deduced from $^{65}\text{Cu}(\alpha, n\gamma)^{68}\text{Ga}$ reaction. The energy spectrum and electromagnetic moments were calculated on the basis of the interacting boson-fermion-fermion/ truncated quadrupole phonon model for odd-odd nuclei.

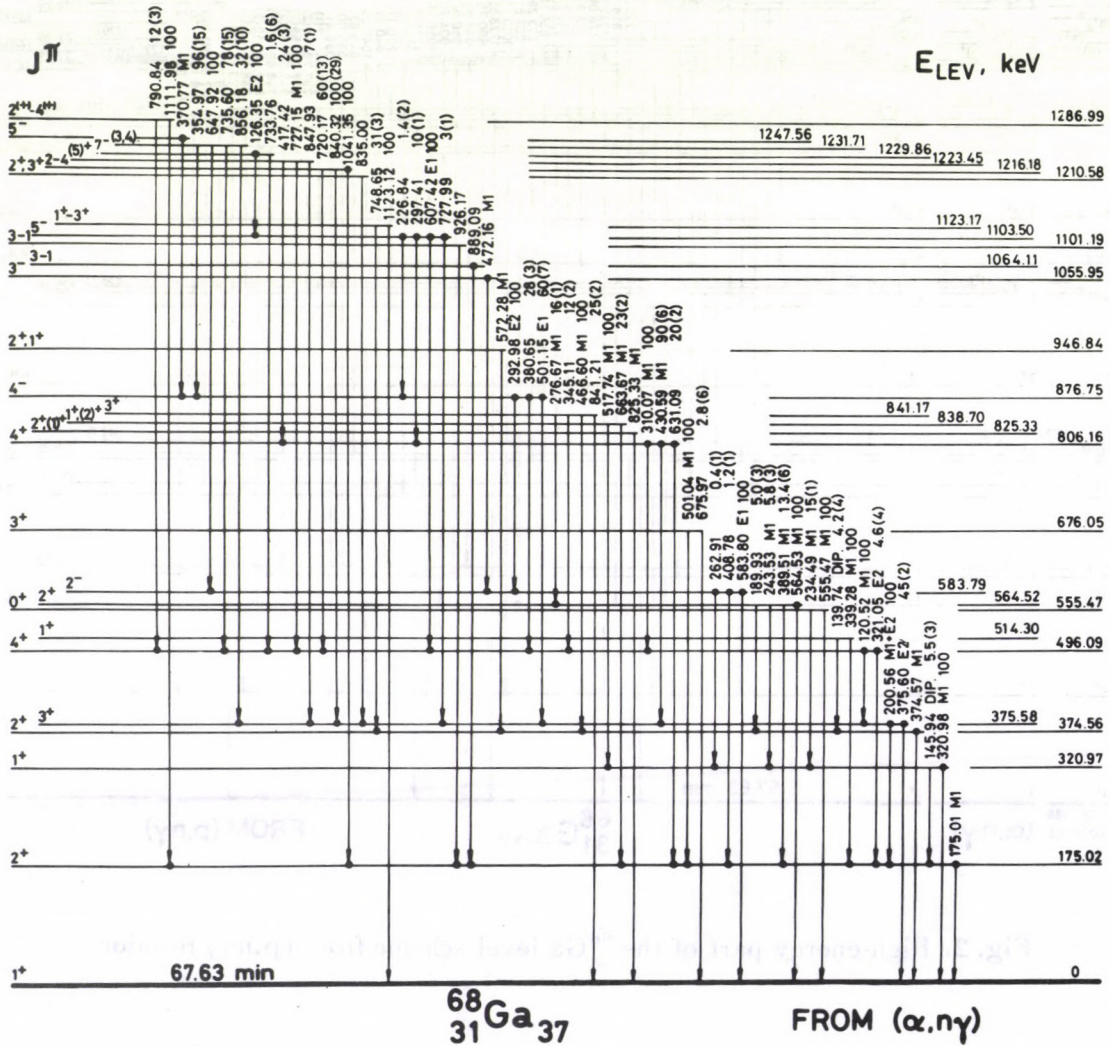


Fig. 1. Low-energy part of the proposed level scheme of ^{68}Ga from $(\alpha, n\gamma)$ reaction.

Reference

1. J. Tímár, T. X. Quang and A. Krasznahorkay, ATOMKI Ann. Rep. 1990 p.10.

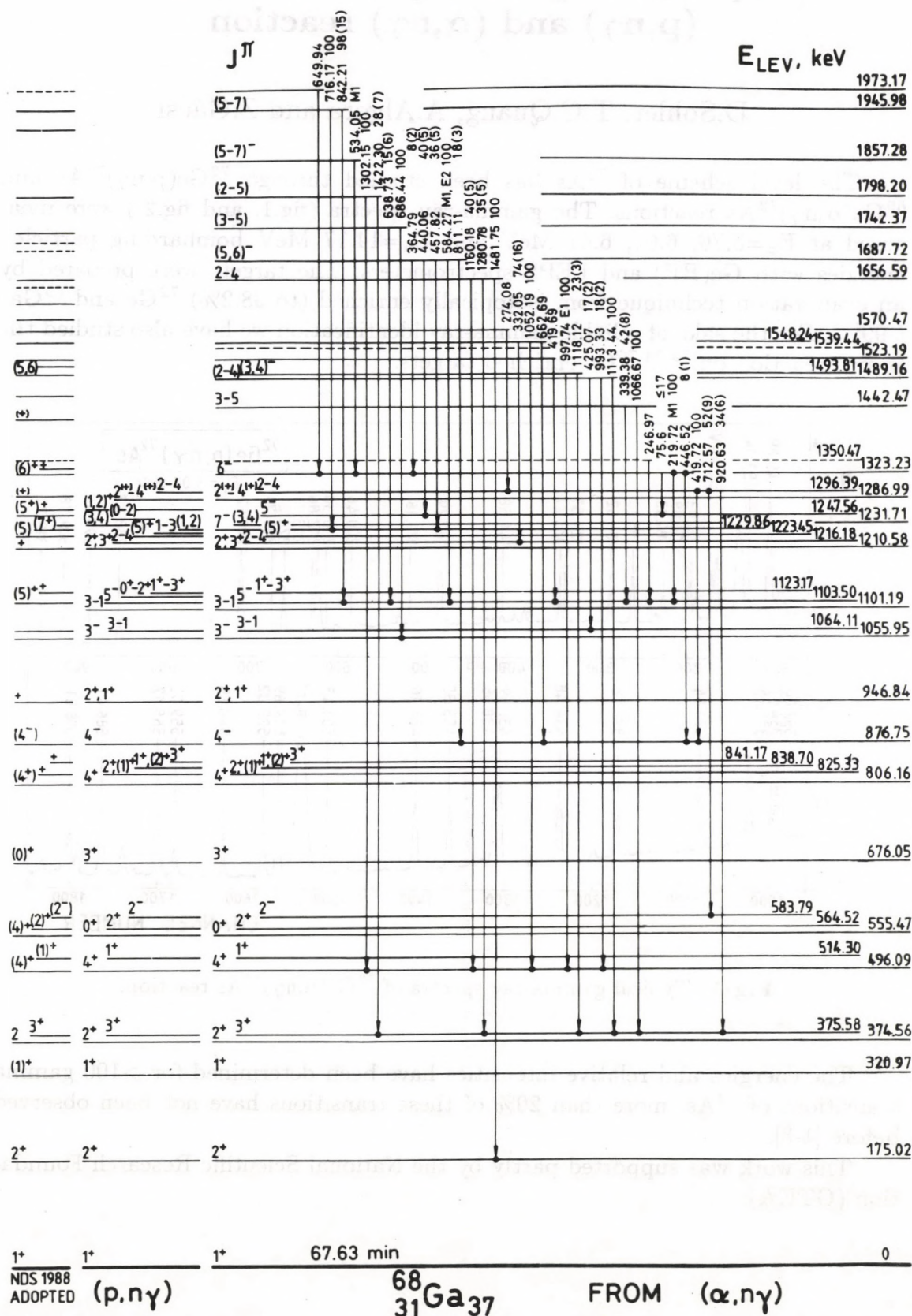


Fig. 2. High-energy part of the ⁶⁸Ga level scheme from (α, γ) reaction.

Spectroscopic study of ^{72}As from $(p,n\gamma)$ and $(\alpha,n\gamma)$ reaction

D.Sohler, T.C.Quang, A.Algora and Z.Gácsi

The level scheme of ^{72}As has been studied through $^{72}\text{Ge}(p,n\gamma)^{72}\text{As}$ and $^{69}\text{Ga}(\alpha,n\gamma)^{72}\text{As}$ reactions. The gamma-ray spectra (fig.1. and fig.2.) were measured at $E_p=5.76, 6.01, 6.41$ MeV and $E_\alpha=14.17$ MeV bombarding particle energies with Ge(HP) and LEPS spectrometers. The targets were prepared by an evaporation technique from isotopically enriched (to 98.2%) ^{72}Ge and ^{69}Ga (99%). For the sake of reliable gamma-ray identification we have also studied the $(p,n\gamma)$ reaction on $^{73,74,76}\text{Ge}$ enriched targets.

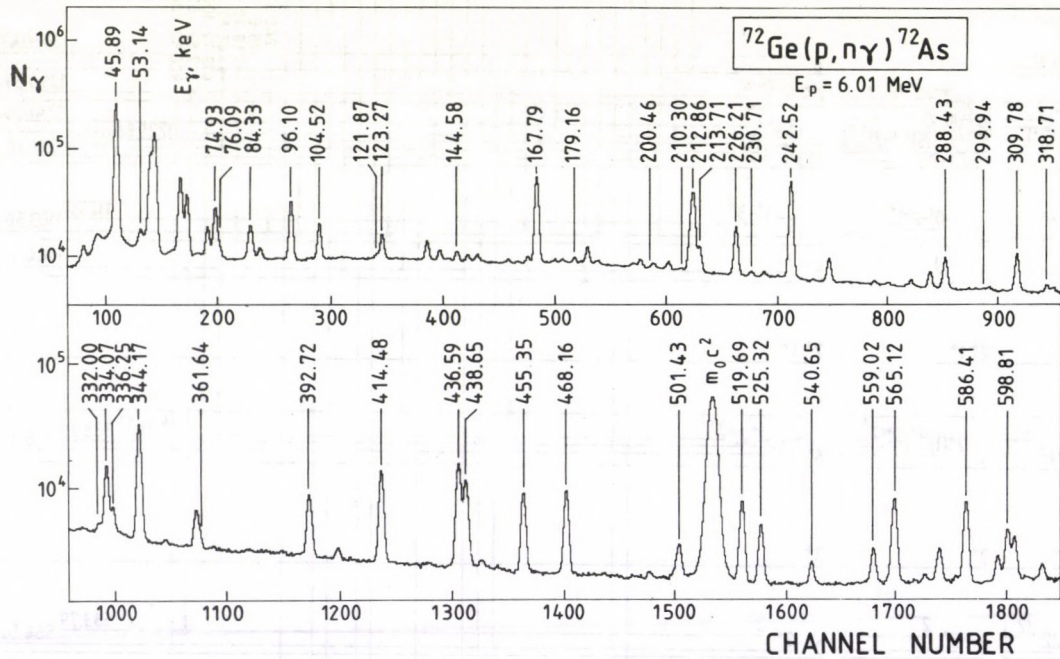


Fig. 1. Typical gamma-ray spectra of $^{72}\text{Ge}(p,n\gamma)^{72}\text{As}$ reaction.

The energies and relative intensities have been determined for >100 gamma transitions of ^{72}As , more than 20% of these transitions have not been observed before [1-3].

This work was supported partly by the National Scientific Research Foundation (OTKA).

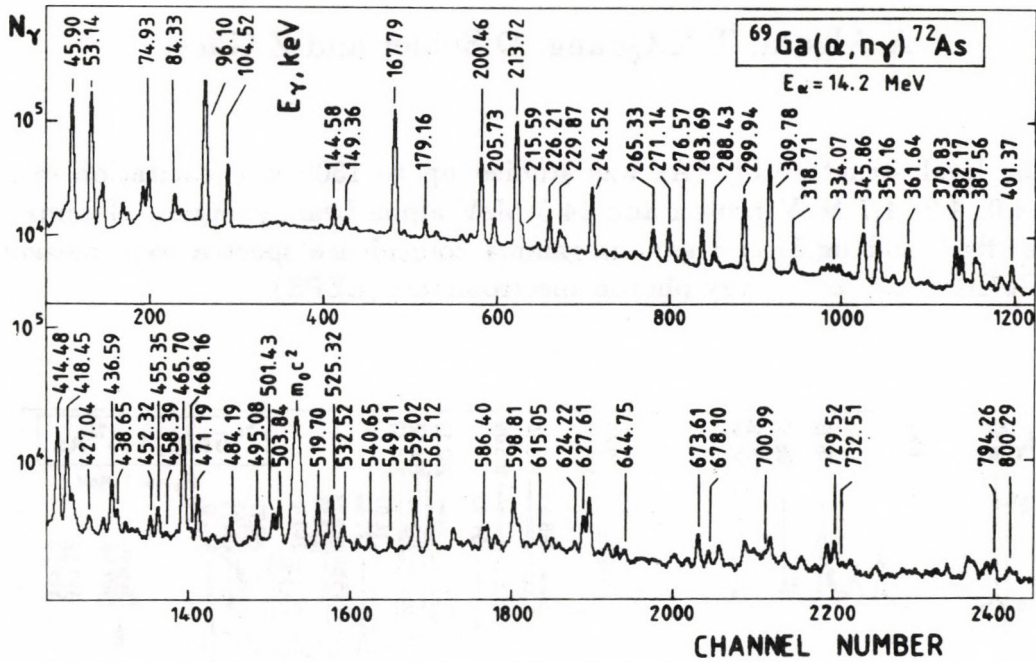


Fig. 2. Typical gamma-ray spectra of $^{69}\text{Ga}(\alpha, n\gamma)^{72}\text{As}$ reaction.

References

1. M.M.King, Nuclear Data Sheets, **56** 1 (1989).
2. K.Kimura, N. Takagi, M. Tanaka, Nucl. Phys. **A272** 381 (1976).
3. M.A.J.Mariscotti, M.Behar, A. Filevich, G. García Bermúdez, A. M. Hernandez, C. Kohan, Nucl. Phys. **A260** 109 (1976).

Spectroscopic Study of ^{74}As from $^{74}\text{Ge}(p,n\gamma)^{74}\text{As}$ and $^{71}\text{Ga}(\alpha,n\gamma)^{74}\text{As}$ Reaction

A. Algora, T.X. Quang, D. Sohler and Z. Gácsi

The level structure of ^{74}As was studied up to 1300 keV excitation energy using 4.0, 4.2, 4.7 MeV proton and 14.5 MeV alpha beam energies. Gamma-ray singles (fig.1 and fig.2) and gamma-gamma coincidence spectra were measured with Ge(HP) and low-energy photon spectrometers (LEPS).

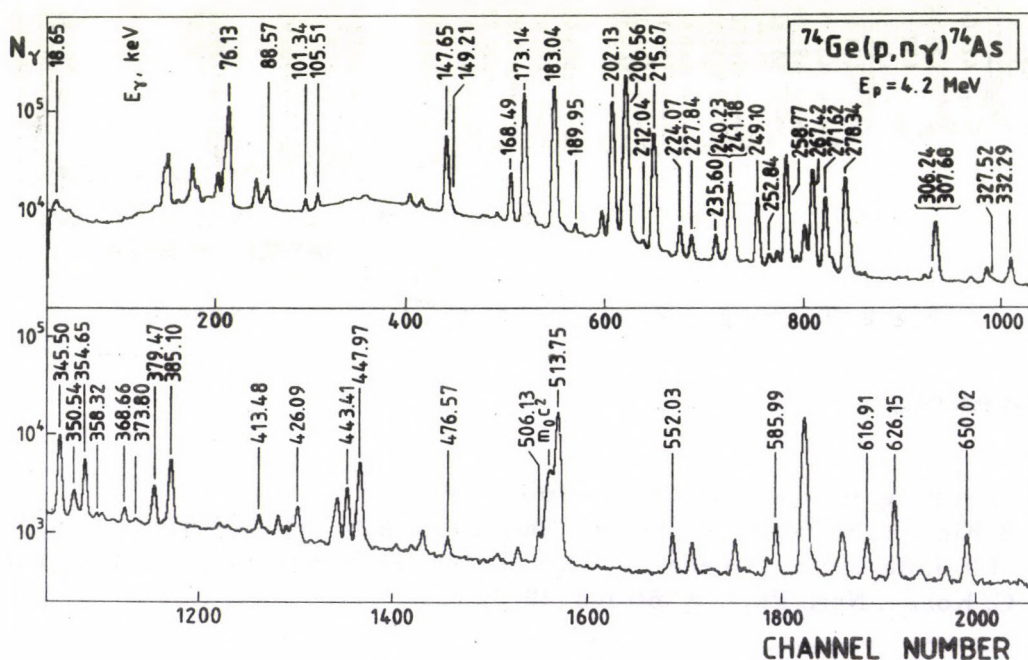


Fig. 1. Typical gamma-ray spectrum of $^{74}\text{Ge}(p,n\gamma)^{74}\text{As}$ reaction.

The targets were prepared by evaporating isotopically enriched GeO_2 (99.1%) and Ga (99.6%) onto a thin carbon backing. For the sake of reliable γ -ray identification we have also studied the same reactions on $^{72,73,76}\text{Ge}$ isotopes.

Energies and relative intensities have been determined for > 100 gamma transitions. More than 30 % of these transitions have not been observed before [1-4].

This work was supported partly by The National Scientific Research Foundation (OTKA).

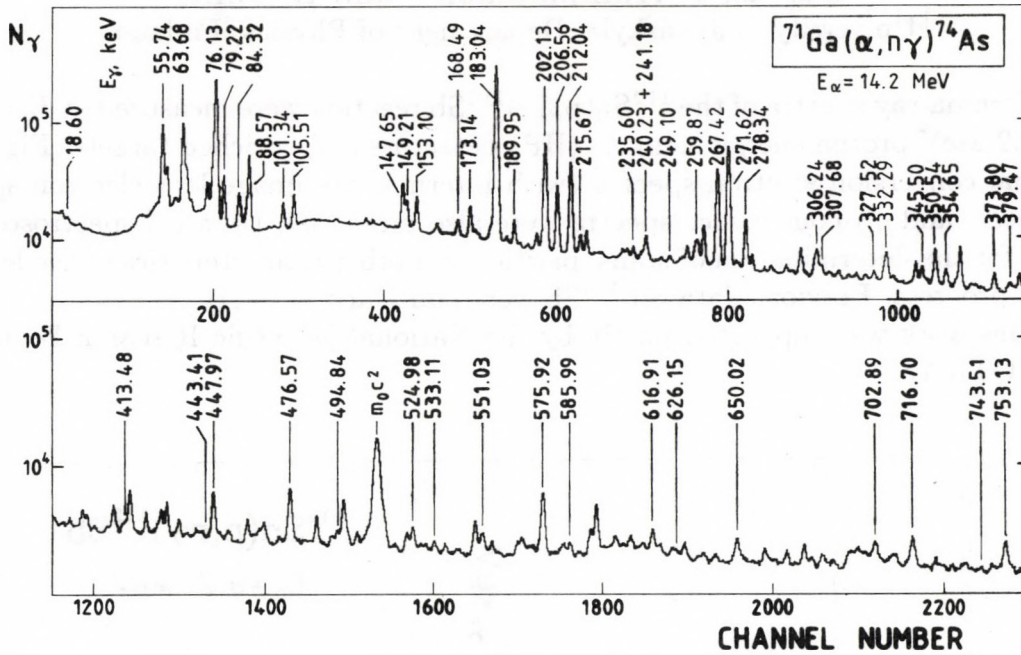


Fig. 2. Typical gamma-ray spectrum of $^{71}\text{Ga}(\alpha, n\gamma)^{74}\text{As}$ reaction.

References

- 1 Kikuo Kimura, Nucl. Phys. **A213** (1973) 61
- 2 B. Lal, Y. K. Agarwal, C. V. K. Baba, S. M. Bharathi and S. K. Bhattacharjee, Pramana **6** (1976) 209
- 3 G. García Bermúdez, M. Behar, A. Filevich, M. A. J. Mariscotti, Phys. Rev. C **14** (1976) 1776
- 4 B. Singh and D. A. Viggars, Nucl. Data Sheets **51** (1987) 225

Study of ^{112}Sb from $(p,n\gamma)$ reaction

J. Gulyás, J. Kumpulainen [†] and R. Julin [†]

[†]University of Jyväskylä, Department of Physics, Finland

Gamma-ray spectra of the $^{112}\text{Sn}(p,n\gamma)^{112}\text{Sb}$ reaction were measured at $E_p=8.7$ and 9.2 MeV proton energy using Ge(HP) detectors and enriched targets (Fig. 1). Internal conversion electron spectra (with intermediate image lens electron spectrometer) and $\gamma\gamma$ -coincidence spectra were also measured. Detailed spectroscopic study for the determination of spins, parities and other characteristics of the levels are in progress. Previous data on ^{112}Sb were summarized in [1]:

This work was supported partly by the National Scientific Research Foundation /OTKA/.

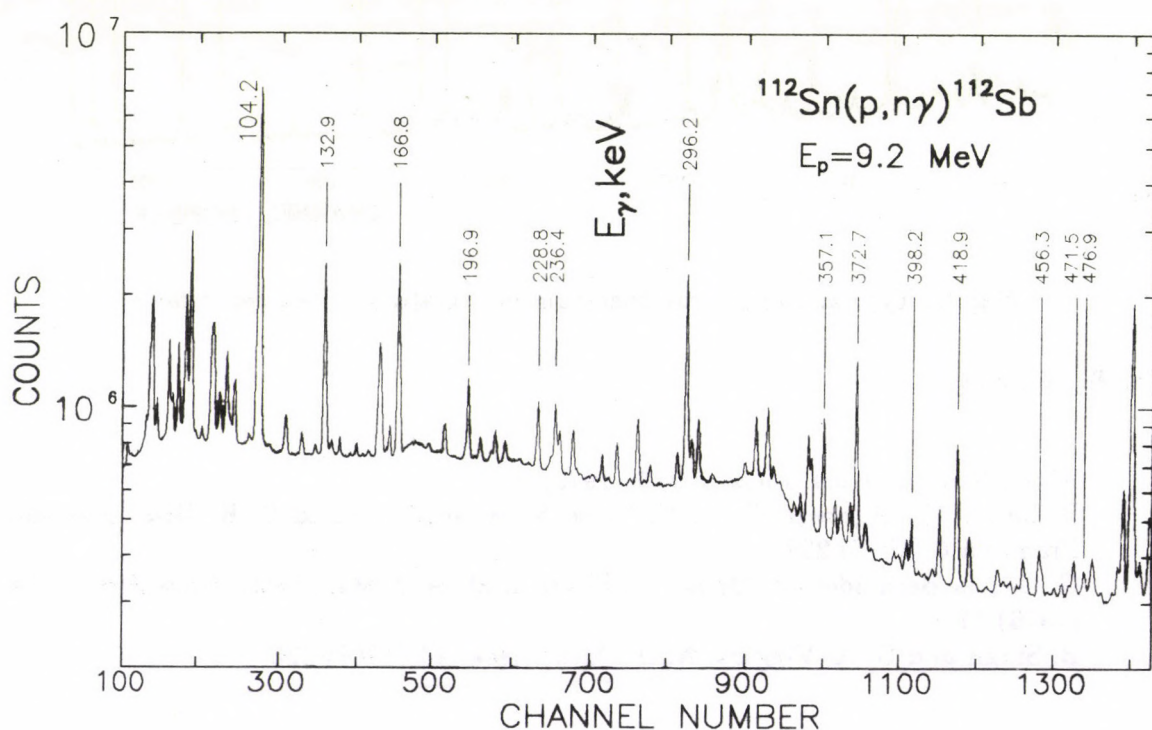


Fig. 1. Part of a typical γ -spectrum. Energies of the strongest ^{112}Sb γ -rays are indicated.

1. D. De Frenne, E. Jacobs and M. Verboven, Nucl. Data Sheets **57** (1989) 443.

Spectroscopy of ^{114}Sb from (p,n γ) reaction

Z. Gácsi

As a continuation of the study of $Z=51$ odd-odd nuclei [1,2], the γ -ray and internal conversion electron spectra of the $^{114}\text{Sn}(p,n\gamma)^{114}\text{Sb}$ reaction were measured at $E_p=8.2$ MeV bombarding proton energies with Ge(HP) (2 keV resolution at 1333 keV), Ge(HP,LEPS) (1.9 keV resolution at 1333 keV), and superconducting magnetic transporter plus Si(Li) electron spectrometers. The spectrometers were calibrated with ^{133}Ba and ^{152}Eu sources. In order to improve the accuracy of energy determination, gamma rays from these sources together with those of ^{114}Sb were also measured simultaneously. Self-supporting targets of 0.5–3.0-mg/cm² thickness were prepared by an evaporation technique from isotopically enriched (to 70.0 %) ^{114}Sn . For the sake of reliable γ -ray identification, we also studied (p,n) reaction at the same energy on different tin isotopes. The $\gamma\gamma$ -coincidence data were acquired in a two-dimensional mode at $E_p=8.2$ MeV, with fixed $\tau=50$ ns resolving time. The 20% and 25% detectors were placed at 125° and 235° angles to the beam direction. Approximately 40 million $\gamma\gamma$ -coincidence events were recorded on magnetic tapes in event-by-event mode for subsequent analysis. Typical $\gamma\gamma$ -coincidence gate spectra are shown in Fig. 1. Angular distribution of γ rays were also measured at 8.2 MeV bombarding proton energy at different angles with respect to the beam direction from $\theta_{lab}=35^\circ$ to 90° varied in 5° steps.

The results of the present experimental studies can be summarized as follows.

For approximately 60 γ transitions assigned to ^{114}Sb , accurate E_γ and I_γ values have been given, compared with 27 previously known gamma rays [3]. Experimental internal conversion coefficients have been determined for about 20 transitions, 18 of them are obtained for the first time. A more complete level scheme has been constructed incorporating more than 50 transitions among more than 25 levels, 20 of which have not been found before.

This work was supported partly by the National Scientific Research Foundation (OTKA).

References

1. J. Gulyás, T. Fényes, Zs. Dombrádi, and T. Kibédi, ATOMKI Annual Report 1990, p19; J. Gulyás, J. Kumpulainen, and R. Julin, ATOMKI Annual Report 1990, p21; and to be published.
2. Z. Gácsi, T. Fényes, and Zs. Dombrádi, Phys. Rev. C44, 626 (1991); Z. Gácsi, Zs. Dombrádi, T. Fényes, S. Brant, and V. Paar, Phys. Rev. C44, 642 (1991).
3. J. Blachot, G. Marguier, Nuclear Data Sheets 60, 139 (1990).

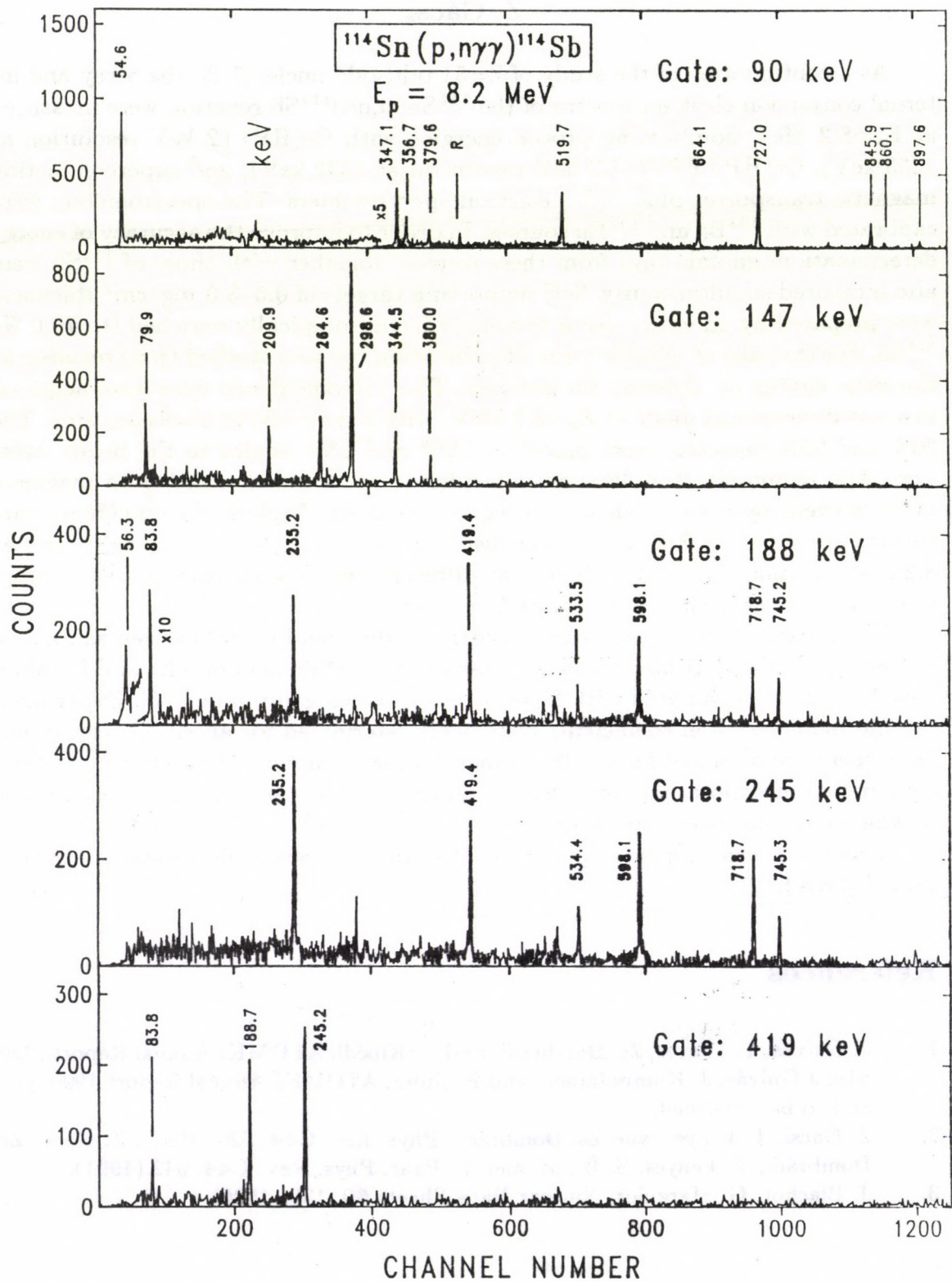


Fig. 1. Typical $\gamma\gamma$ -coincidence gate spectra. The background was subtracted. R denotes random coincidences.

New levels in ^{116}Sn

Z. Gácsi

The nuclear excited states in ^{116}Sn have been extensively studied [1]. The most recent and complete work [2] finds ~ 100 levels below 4.3 MeV in $^{115}\text{Sn}(n,\gamma)$ and $^{116}\text{Sn}(n,n'\gamma)$ reactions. Nevertheless, it is striking to find that among the wealth of methods employed, the exploration of the radioactive decays of the ($Z=51$) ^{116}Sb nucleus is still far from complete and accurate. These decays were last studied about two decades ago using semiconductor detectors with rather good resolution, but the results are available only as internal reports.

This contribution presents briefly the results obtained in Debrecen utilizing the 60-min ^{116}Sb ($\beta+\epsilon$) decay. The 8^- , 60-min excited mother state was populated via bombarding ^{113}In (enriched) target with 16 MeV α beams of the Debrecen cyclotron. Singles and $\gamma\gamma$ -coincidence spectra were recorded using Ge(HP) detectors of 1.8-2.0-keV/1333 keV resolution. Accurate energy values (~ 10 ppm), intensities, and coincidence relations were determined and a more complete level scheme has been constructed. The overall agreement with previous studies is good, but the current work establishes levels at 2909, 3228, and 3986 keV excitation energies not found in decay studies before. The level at 3986 keV has not been observed in any other work yet. The reason for others to miss this level may be quite simple. This new level can have a spin and parity of 7^- , 8^- , and 9^- , thus will not be excited in (n,γ) or $(n,n'\gamma)$ reactions, furthermore, heavy ions and more energetic light ions capable of exciting higher-spin states tend to populate states with more collective structure, while in decay, probably states with dominating single particle components are preferably excited.

This work was supported partly by the National Scientific Research Foundation (OTKA).

References

1. J. Blachot, G. Marguier, Nuclear Data Sheets **59**, 333 (1990).
2. S. Raman, T. A. Walkiewicz, S. Kahane, E. T. Journey, J. Sa, Z. Gácsi, J. L. Weil, K. Allaart, G. Bonsignori, J. F. Shriver, Jr., Phys. Rev. **C43**, 521 (1991).

Proton-neutron multiplets in ^{118}Sb

J. Gulyás, M. Favez F. M. Hassan, T. Fényes, and

Zs. Dombrádi

On the basis of complex γ and internal conversion electron spectroscopic study of the $^{118}\text{Sn}(p,n\gamma)^{118}\text{Sb}$ reaction new level scheme of ^{118}Sb has been deduced (Fig. 1). Former results were summarized in [1].

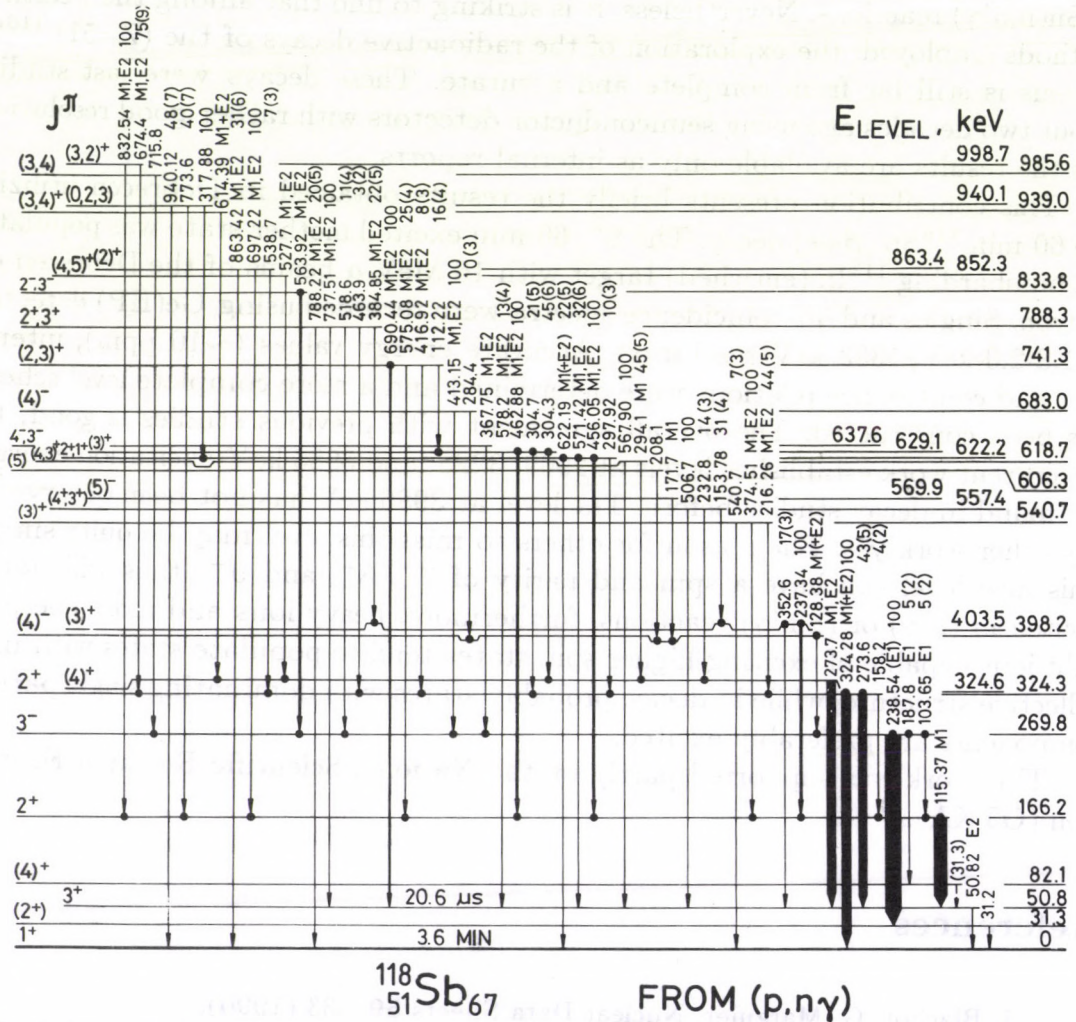


Fig. 1. The low-energy part of the proposed level scheme of ^{118}Sb nucleus from the $^{118}\text{Sn}(p,n\gamma)^{118}\text{Sb}$ reaction. Solid circles at the ends of arrows indicate $\gamma\gamma$ -coincidence relations. After the energies of the transitions multipolarities and relative γ -ray intensities (branching ratios) are given.

Level spins and parities have been determined on the basis of Hauser-Feshbach analysis, internal conversion coefficients, and γ -ray angular distribution data. Fig. 2 shows the comparison of calculated and experimental excitation cross sections for different levels.

The energies of several ^{118}Sb proton-neutron multiplet states were calculated on the basis of the parabolic rule [2]. Many members of the $\pi d_{5/2}\nu s_{1/2}$, $\pi d_{5/2}\nu d_{3/2}$, $\pi d_{5/2}\nu g_{7/2}$, $\pi d_{5/2}\nu h_{11/2}$, $\pi g_{7/2}\nu s_{1/2}$ and $\pi g_{7/2}\nu d_{3/2}$ proton-neutron multiplets have been identified.

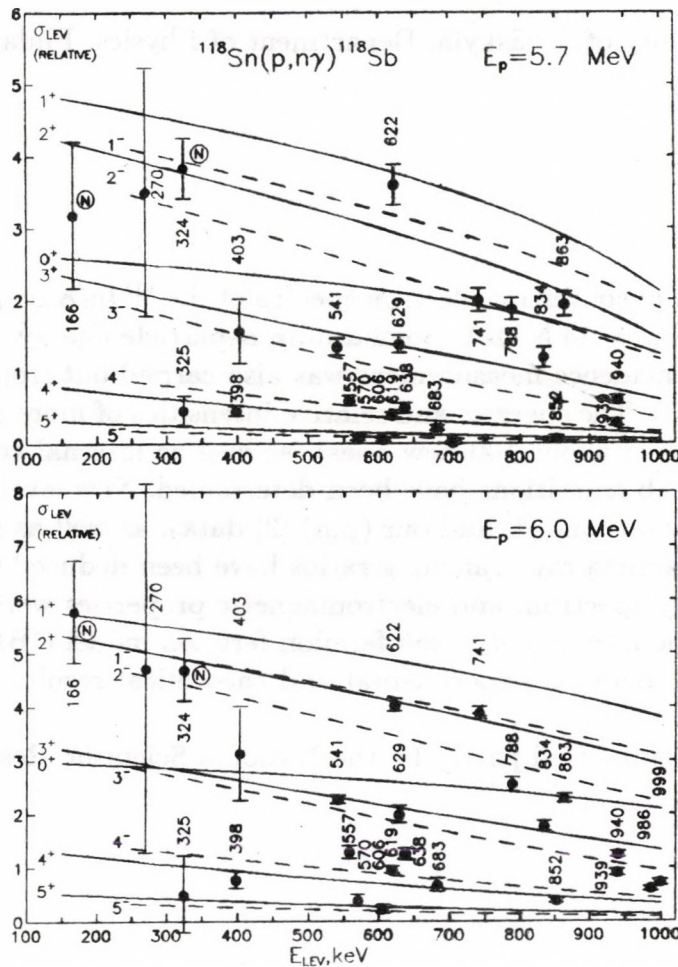


Fig. 2. Experimental relative cross sections (σ_{LEV}) of the $^{118}\text{Sn}(p, n\gamma)^{118}\text{Sb}$ reaction (dots with error bars) as a function of the excitation energy (E_{LEV}). The solid lines show results of Hauser-Feshbach calculations. The normalization of experimental and theoretical data was done on the average of two 2^+ points indicated by N.

This work was supported partly by the National Scientific Research Foundation /OTKA/.

1. T. Tamura, K. Miyano and S. Ohya, Nucl. Data Sheets **51** (1987) 329.
2. V. Paar, Nucl. Phys., **A331** (1979) 16.

Structure of low-lying levels of ^{118}Sb nucleus

J. Gulyás, M. Fayez F. M. Hassan, T. Fényes, Zs. Dombrádi,

J. Kumpulainen [†] and R. Julin [†]

[†]University of Jyväskylä, Department of Physics, Finland

γ -ray and internal conversion electron spectra of the $^{115}\text{In}(\alpha, n\gamma)^{118}\text{Sb}$ reaction were measured at $E_\alpha = 14.5$ MeV bombarding α -particle energy (in Debrecen). Gamma-gamma coincidence measurement was also carried out from the same reaction (in Jyväskylä). The energies and relative intensities of more than 150 ^{118}Sb gamma-rays (including about 100 new ones), as well as internal conversion coefficients of many ^{118}Sb transitions have been determined. New level scheme (complementing the previous one [1] and our (p,n) [2] data), as well as multipolarities of transitions and gamma-ray branching ratios have been deduced (Fig. 1).

The level energy spectrum and electromagnetic properties were calculated in the framework of the interacting boson-fermion-fermion model (IBFFM) and satisfactory agreement between experimental and theoretical results have been obtained.

This work was supported partly by the National Scientific Research Foundation /OTKA/.

References

1. T. Tamura, K. Miyano and S. Ohya, Nucl. Data Sheets **51** (1987) 329.
2. J. Gulyás, M. Fayez F. M. Hassan, T. Fényes, and Zs. Dombrádi, in this volume

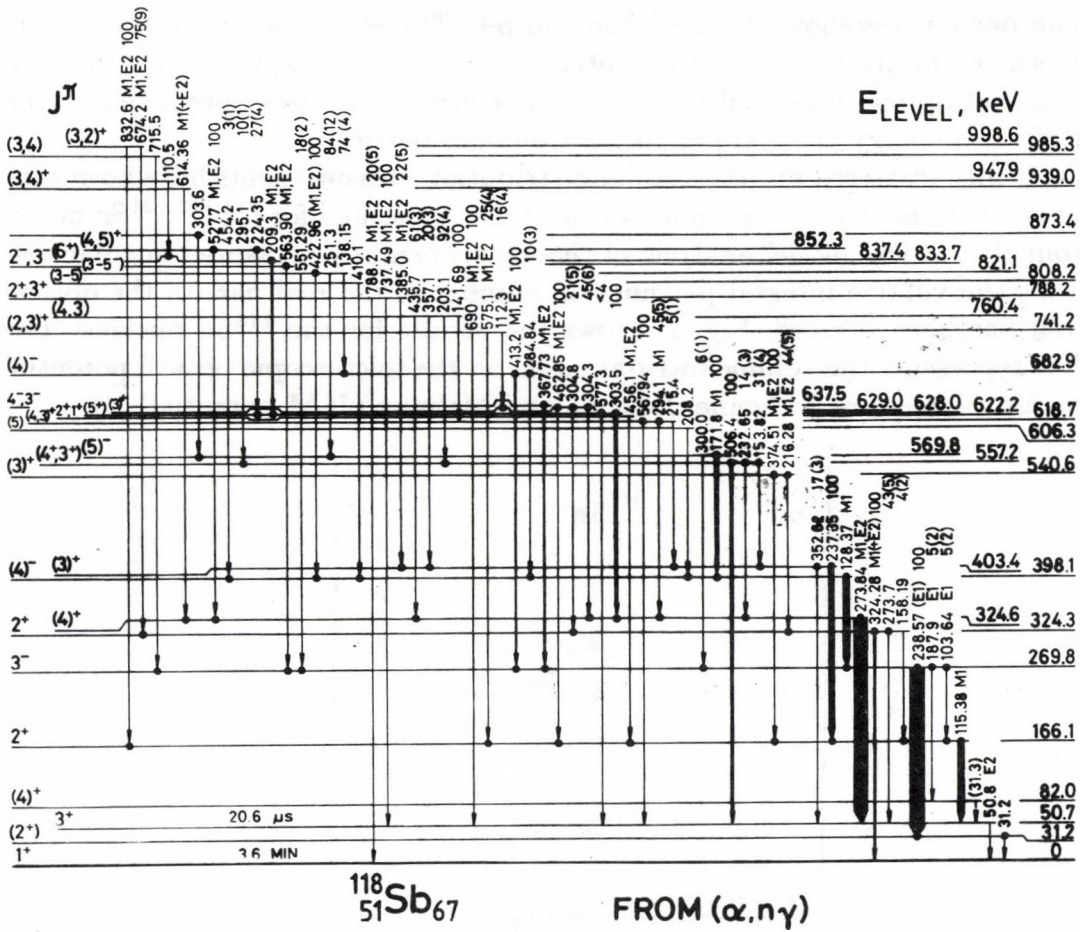


Fig. 1. The low-energy low-spin part of the level scheme of ^{118}Sb nucleus deduced from $^{115}\text{In}(\alpha, \gamma)^{118}\text{Sb}$ reaction. Solid circles indicate $\gamma\gamma$ -coincidence relations. Multipolarities and γ -ray branching ratios are also given (after γ -ray energies).

Low energy optical potential for ^{118}Sn

L. Zolnai, M. Józsa, Z. Máté

The anomalous behaviour of the optical potential in the neighbourhood of the Coulomb barrier was shown for $p+^{116}\text{Sn}$ and $p+^{120}\text{Sn}$ elastic scattering [1,2]. The real depth of the proton optical potential increased more rapidly than the well known global optical potential fits (Perey, Becchetti-Greenlees) predicted as the center-of-mass energy came closer to the Coulomb barrier.

Elastically scattered proton angular distribution measurements have been continuing on ^{118}Sn nucleus in the same way as it was presented for $^{114,122,124}\text{Sn}$ nuclei [3]. From the optical model analysis of the experimentally measured angular distributions the volume integral per nucleon number of the real part of the optical potential has been derived. Fig. 1. shows the results for the ^{118}Sn nucleus. The solid line represents the volume integral based on the microscopic optical potential calculus introduced by Jeukenne, Lejeune and Mahaux (JLM potential) [4].

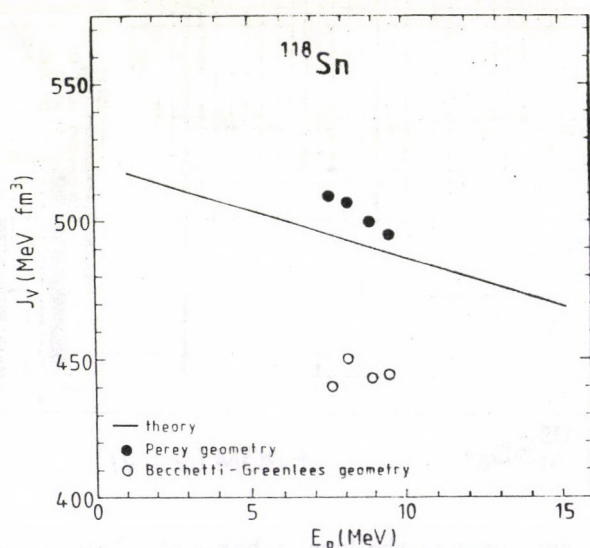


Fig. 1. The energy dependence of the real part of the volume integral of the proton optical potential for ^{118}Sn . The experimental values were obtained from optical model analysis with the Perey and Becchetti-Greenlees geometry

References

1. B. Gyarmati et al., *J. Phys. G.* **5** 1225 (1979)
2. A. F. Gurbich, V. P. Lunev and N. N. Titarenko, *Yad. Fiz.* **40** 310 (1984)
3. M. Józsa et al., *ATOMKI Annual Report* 18 (1988)
4. J. P. Jeukenne, A. Lejeune and C. Mahaux, *Phys. Rev.* **C16** 80 (1977)

Evidence for Core Polarization Interaction in Odd-Odd In Nuclei

Zs. Dombrádi, S. Brant ^a and V. Paar ^a

^aPrirodoslovno-Matematički Fakultet, University of Zagreb,
41000 Zagreb, Croatia

The presence of a core-polarization interaction was searched for in the strongly deformed and in the doubly magic regions by analysing the empirical matrix elements of the effective interaction [1-4]. In the deformed region the presence of an additional quadrupole-quadrupole interaction was excluded [1], while in the doubly magic region its existence is doubtful [3,4].

Recently the structure of the odd-odd $^{106-114}\text{In}$ nuclei was investigated through $(p,n\gamma)$ and $(\alpha,n\gamma)$ reactions in a Debrecen-Jyväskele-Zagreb collaboration. On the basis of the spin values, electromagnetic properties and spectroscopic factors we assigned more than 100 states to proton-neutron multiplets in $^{106-116}\text{In}$ nuclei.

The large amount of recent experimental data provided a new possibility to extend the search for the core-polarization interaction in the single closed shell region, too. We have accepted those multiplets of the above nuclei, which contain more than three known members, as the experimental basis of the analysis.

We used two methods to study the multipole structure of the effective interaction: for the complete multiplets we deduced the multipole coefficients of the interaction directly from the experimental multiplet energies, while for all the multiplets we fitted a dipole-plus-quadrupole interaction to the experimental data.

From the multipole analysis of the $\pi g_{9/2}^{-1} \nu \tilde{d}_{5/2}$ multiplet of $^{106-110}\text{In}$, the $\pi g_{9/2}^{-1} \nu \tilde{g}_{7/2}$ multiplet of ^{112}In and the $\pi g_{9/2}^{-1} \nu \tilde{d}_{3/2}$ multiplet of ^{116}In the $\beta_2 = 3.17 \pm 0.76$ value was obtained for the Quadrupole component. The same multipole analysis on the proton-neutron multiplets of the doubly magic region resulted in $\beta_2 = 1.93 \pm 0.2$ value.

The strength of the dipole and quadrupole interactions was fitted to the splitting of the proton-neutron multiplets of odd-odd In nuclei. The obtained average quadrupole-quadrupole interaction strength was independent of whether the strength of the dipole component was treated as a free parameter or was fixed to some reasonable value.

The $\beta_2 = 3.31 \pm 0.88$ value obtained this way is highly consistent with the one obtained from the full multipole analysis (3.17 ± 0.76) and is much stronger than the value characteristic for the doubly magic nuclei (1.93 ± 0.2). Although the

multipole coefficients of the empirical matrix elements determined from the doubly magic region also deviate somewhat from the delta interaction, there remains a significant difference ($\approx 75\%$) between the quadrupole components of the empirical effective interactions determined in the doubly and single closed shell regions.

If we assume that the effective delta interaction approximation is a reasonable universal interaction, then the large strength of the quadrupole component of the empirical interaction found in the odd-odd In nuclei can be interpreted as an indication of the presence of an additional quadrupole-quadrupole interaction with $V_{QQ} = -0.35 \pm 0.16$ MeV strength.

The strength of this additional quadrupole-quadrupole interaction can be compared with the value of the core-polarization interaction strength estimated on the basis of the particle-vibration theory. Using the parameters of the tin cores this value is $V_{cpi} = -0.32 \pm 0.06$ MeV, which is in a good agreement with the strength of the experimentally found quadrupole-quadrupole interaction.

If the change of the effective interaction is really caused by the core polarization process, then also an increase of the effective charges is expected. To search for the presence of this effect, the effective charge (e_{eff}) of the neutron was fitted to the electric quadrupole moments of some $^{106-116}\text{In}$ states within the frame of the quasiparticle model, keeping the proton effective charge as $e_{eff} + 1$. The 3.8e effective charge obtained contains $\approx 0.5e$ contribution from the high energy core polarization, the average neutron charge in the odd-odd In nuclei is $3.3 \pm 1.0e$.

The value of the polarization charge estimated on the basis of particle-vibration theory is $e_{pol} = 4.4 \pm 0.9e$ approximating $\langle R^2 \rangle$ with its constant density value. This effective charge is in a reasonable agreement with the one determined from the quadrupole moments.

From the analysis of the experimental data on proton neutron multiplet states the nearly doubling of the quadrupole-quadrupole interaction strength, as well as a strong increase of the effective charges was deduced. The good agreement with the theoretical estimate of both quantities indicates that the additional quadrupole-quadrupole interaction found, corresponds to the core polarization interaction.

References

1. J.P. Boisson, R. Piepenbring and W. Ogle, Physics Reports **26C**, 101 (1976)
2. J.P. Schiffer and W.W True, Rev. Mod. Phys. **48**, 191 (1976)
3. A. Molinari, M.B. Johnson, H.A. Bethe and W.M. Alberico, Nucl. Phys. **A239**, 45 (1975)
4. W.F. Daehnick, Physics Reports **96**, 317 (1983)

Single Nucleon Transfer Spectroscopy of Odd-Odd Sb Nuclei

Zs. Dombrádi, S. Brant ^a and V. Paar ^a

^aPrirodoslovno-Matematički Fakultet, University of Zagreb,
41000 Zagreb, Croatia

The low-lying levels of $^{120,122,124}\text{Sb}$ were investigated through (d,p), (d,t) and (p,d) reactions [1-3]. Although the determined single nucleon transfer spectroscopic factors are sensitive to the details of the nuclear wave functions, their theoretical interpretation was missing. In the present work we have calculated the level energies and spectroscopic factors for the low-lying states of $^{120,122,124}\text{Sb}$ within the framework of the interacting boson-fermion-fermion model (IBFFM).

The calculated and measured spectroscopic factors agree in most cases within a factor of two. The ^{120}Sb spectroscopic factors fit well for all states, suggesting that the calculated wave functions are good approximations to the real ones.

The IBFFM and experimental spectroscopic factors are compared in Table 1. for single nucleon transfer reactions leading to ^{122}Sb . In the case of the pick up reactions not the theoretical spectroscopic factors are given in the table, instead they are divided by $2j_{\text{target}} + 1$ according to the convention of the experimental papers.

In the case of 3_1^+ and 3_3^+ states of ^{122}Sb , the deviation of the calculated and measured spectroscopic factors suggest that the calculated wave function differs somewhat from the real one. The large difference between the calculated and measured spectroscopic factors for the 283 and 311 keV ^{122}Sb levels may have experimental origin, because the experimental spectroscopic factors are well above the sum rule limit. Even if we assume that the 283 keV peak is doublet, containing the 8^- member of the $\pi d_{5/2} \nu h_{11/2}$ multiplet predicted at about this energy, the experimental spectroscopic factor remains too large.

In the case of ^{124}Sb , there is a general agreement between the calculated and experimental data. A detailed comparison cannot be given due to the poor resolution in the (d,p) experiment.

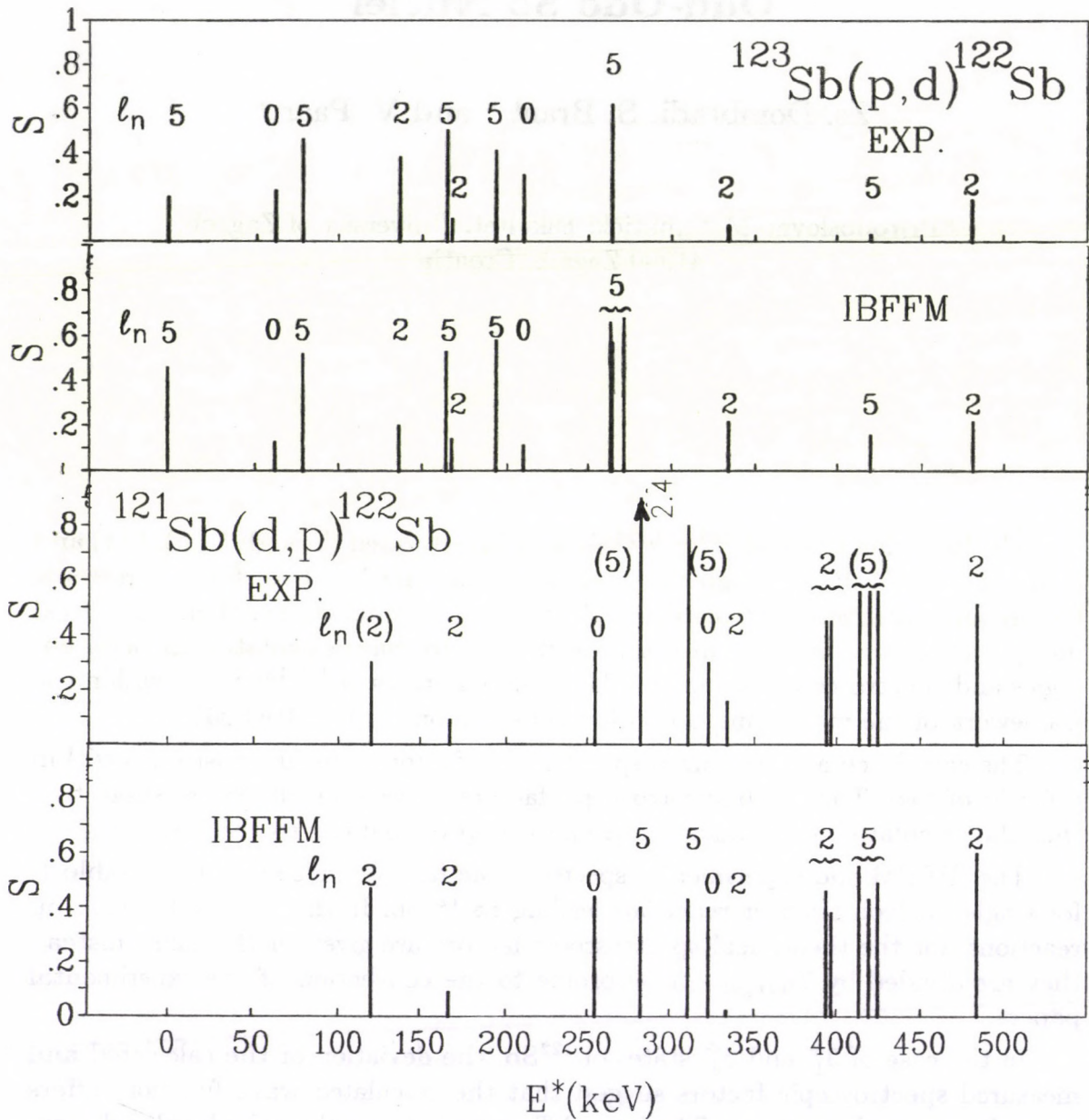


Fig. 1. Comparison of measured and calculated in IBBFM spectroscopic factors for the one-neutron transfer reactions leading to ^{122}Sb . The experimental are taken from refs. [2,3]. In the IBBFM parts also the experimental energies are used.

1. S. A. Hjorth, Ark. Fys. **33**, 183 (1967)
2. R. A. Emigh, C. A. Fields, M. L. Gartner, L. E. Samuelson and P. A. Smith, Z. Phys. A **308**, 165 (1982)
3. V. L. Alexeev, B. A. Emelianov, A. I. Egorov, L. P. Kabina, D. M. Kaminker, Yu. L. Khazov, I. A. Kondurov, E. K. Leushkin, Yu. E. Loginov, V. V. Martynov, V. L. Rumiantsev, S. L. Sakharov, P. A. Sushkov, H. G. Börner, W. F. Davidson, J. A. Pinston and K. Schreckenbach, Nucl. Phys. **A297**, 373 (1978)

Effect of Collectivity on the Splitting of Proton-Neutron Multiplets

Zs. Dombrádi, S. Brant ^a and V. Paar ^a

^aPrirodoslovno-Matematički Fakultet, University of Zagreb,
41000 Zagreb, Croatia

Systematic studies of the doubly magic region show that the empirical proton-neutron interaction matrix elements lie on two universal curves, causing a significant odd-J even-J staggering in the energy splitting of the p-n multiplets as a function of J, the spin of the multiplet states. On the other hand, in the single closed shell (SCS) region the splitting of many p-n multiplets can be approximated with smooth parabolas.

The main difference between the two regions is the appearance of the surface vibration modes in the SCS nuclei. The particle vibration coupling leads to a quadrupole-quadrupole core polarization interaction. The simple summation of the polarization and the delta interactions really leads to some smoothing of the splitting, but cannot cancel the staggering feature of the short range interaction.

To search for the reason of the smoothing we performed calculations both in the frame of interacting boson-fermion-fermion model (IBFFM) and quasiparticle model. The difference between the IBFFM and its quasiparticle approximation, leading to different splitting, lies in the structure of the wave functions. While the IBFFM wave functions contain admixture from one, two, etc. d-boson components, in the quasiparticle model the multiplets are pure in this sense.

The difference in wave functions implies some difference in the matrix element of the effective interaction, namely, instead of the simple matrix element of the quasiparticle approximation we obtain a weighted average of the matrix elements of the effective interaction using the neighbouring multiplet states in IBFFM. The weights are determined by the dynamical interaction strength. In other words, the explicit treatment of the d-boson components leads to an averaging procedure, which is quite similar to a five point smoothing method.

The effect of the smoothing is shown in Fig. 1. In the calculations $\Gamma_\nu = 0$ was applied in order to avoid the disturbance of the polarization interaction. It is seen that the multiplet gets smoother and smoother, and the large $1^+ - 2^+$ distance, characteristic for the delta interaction, is gradually decreasing. It is to be mentioned that the splitting gets also weaker and weaker, while the average interaction strength remains practically the same (not shown in the figure).

As the smoothing is caused by mixing of wave functions, it can be approximated by renormalizing the effective interaction. Our analysis shows that in order

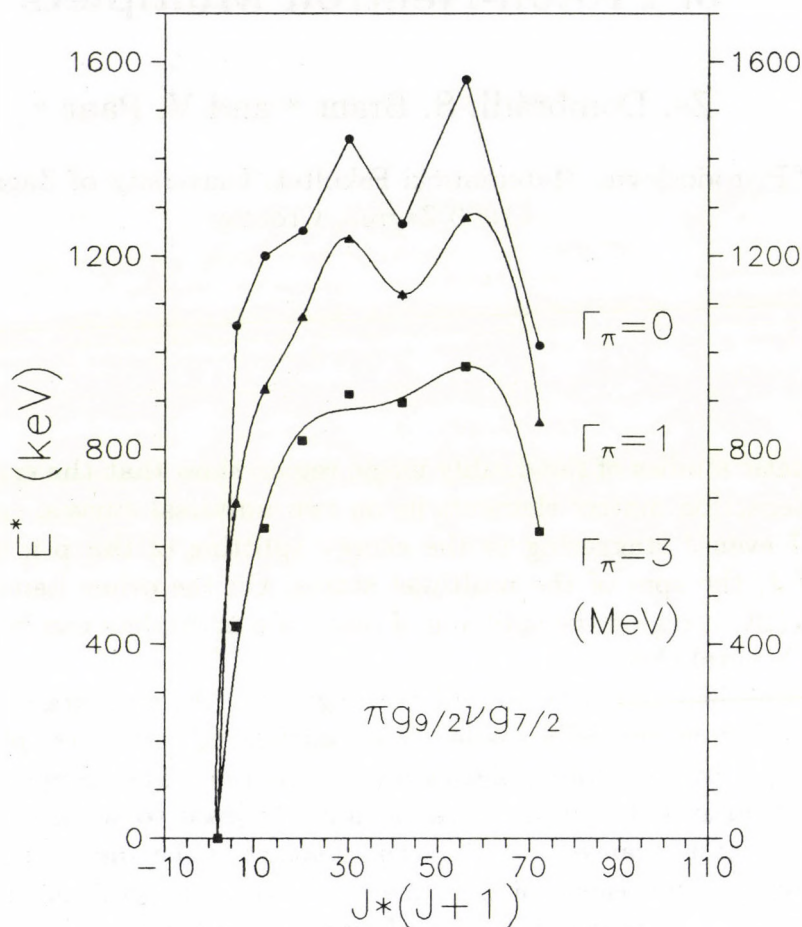


Fig. 1. Calculated splitting of the $\pi g_{9/2}\nu h_{11/2}$ multiplet as a function $J*(J+1)$ assuming different proton dynamical interaction strength.

to precisely renormalize the effective interaction not only the quadrupole coefficient should be increased, but all of the multipole coefficients of the proton-neutron interaction must be renormalized, which can be well approximated by the lengthening its range. For the case of the boson-fermion dynamical interaction strengths characteristic for In and Sb nuclei, a 2 fm gaussian interaction is a good estimation.

The deviation of the IBFFM and quasiparticle description is even more noteworthy when the neutron occupation probability is around 0.5. In this case in quasiparticle approximation the multiplet splitting is governed by the spin dependent interactions, which taking into account the smoothing effect lead to a linear splitting. In the IBFFM the neutron exchange interaction also acts. Although it works only for the d-boson states, the proton dynamical interaction admixes also d-boson components to the wave function of the proton-neutron multiplets, and makes effective the exchange interaction for multiplet-like states, too. In this way the proton-boson dynamical and the neutron quasiparticle-boson exchange interactions together produce an additional splitting of the multiplets. The energy splitting produced is a fourth order polynomial as a function of $J*(J+1)$ in agreement with the experiment.

Pole structure of the $\frac{3}{2}^+$ resonance of ${}^5\text{He}$

A. Csótó, R. G. Lovas and A. T. Kruppa†

Present address: Daresbury Laboratory, Warrington, UK

The $\frac{3}{2}^+$ resonance of ${}^5\text{He}$ at the excitation energy of 16.8 MeV is one of the most important resonances of nuclear physics owing to its overwhelming role in the thermonuclear reaction $t + d \rightarrow \alpha + n$, which is a key step in astrophysical nucleosynthesis as well as in thermonuclear energy production.

The fact that this resonance produces an extremely strong transition is very surprising because the partial waves that contribute can only couple via the relatively weak tensor term of the nucleon–nucleon interaction. Recently, a phenomenological fit to the scattering amplitudes has invoked an “exotic object”, a so-called shadow pole [1], to reproduce the strong transition.

A resonance can generally be associated with a pole of the scattering matrix, as a multivalued function of the complex energy, on the lower half of the non-physical Riemann sheet adjacent to the physical sheet in the energy region of the resonance. In n -channel problems to each resonance there correspond $2^{n-1} - 1$ other poles on different non-physical Riemann sheets, and the shadow poles are those located on Riemann sheets other than the one adjacent to the physical sheet at the resonance energy. Because of the remoteness of the shadow poles, it had been believed that they cannot have a significant effect. In nuclear physics this is the first indication that the contribution of a shadow pole may be appreciable, and there is just one more example in other branches of physics, namely, in particle physics [3].

This two-pole structure of the resonance deprives the partial widths of their probability meaning, and leaves one in doubt as to the relative weights of the $\alpha + n$ and $t + d$ components in the resonance. In fact, although in ref. [1] it was suggested that the resonance is dominated by the $\alpha + n$ configuration, we have found that it can be represented in a reaction satisfactorily by omitting the $\alpha + n$ component [4], with which the shadow pole disappears.

The existence of the shadow pole is borne out by a phenomenological two-channel model, in which the potentials were fitted to reproduce the experimental scattering amplitudes [2]. We wished to see whether the interaction of the five nucleons gives rise to the same pole structure.

We have performed dynamical microscopic calculations in our $\{\alpha + n, t + d\}$ model. We go beyond our earlier model [4] in that we include the tensor (as well as the spin–orbit) interaction so as to give rise to the coupling of $\alpha + n$ and $t + d$

Pole positions (in keV)

	Ordinary pole	Shadow pole
Ref. [1]	47-37i	82-3.7i ^a)
Ref. [2]	47-37i	82-3.4i
Present work	47-38i	82-1.1i

^a) The Riemann sheet differs from that obtained in the other works.

channels in the $\frac{3}{2}^+$ partial wave, and extend our model to complex energy. The interaction has been chosen so as to reproduce the $\alpha + n$ and $t + d$ scattering data as well as the experimental $t + d \rightarrow \alpha + n$ reaction cross section [5]. Preliminary results for the pole positions are given in the table above.

Our results give evidence for the existence of the shadow pole in the realistic dynamical problem with parameters close to the phenomenologically extracted values. However, in contrast with the statements made in refs. [1] and [2], we have clearly demonstrated that the resonance is associated with the $t + d$ channel. A detailed study of the behaviour of the poles as functions of the parameters is in progress.

References

1. G. M. Hale, R. E. Brown and N. Jarmie, Phys. Rev. Lett. **59** (1987) 763
2. L. N. Bogdanova, G. M. Hale and V. E. Markushin, Phys. Rev. **44** (1991) 1289
3. Particle Data Group, Phys. Lett. B **204** (1988) 1
4. J. B. J. M. Lanen, R. G. Lovas, A. T. Kruppa, H. P. Blok, J. F. J. van den Brand, R. Ent, E. Jans, G. J. Kramer, L. Lapikás, E. N. M. Quint, G. van der Steenhoven, P. C. Tiemeyer and P. K. A. de Witt Huberts, Phys. Rev. Lett. **63** (1989) 2793; R. G. Lovas, A. T. Kruppa and J. B. J. M. Lanen, Nucl. Phys. **A516** (1990) 325
5. G. Blüge and K. Langanke, Few-Body Systems **11** (1991) 137

Triton+³He admixture in the ground state of ⁶Li

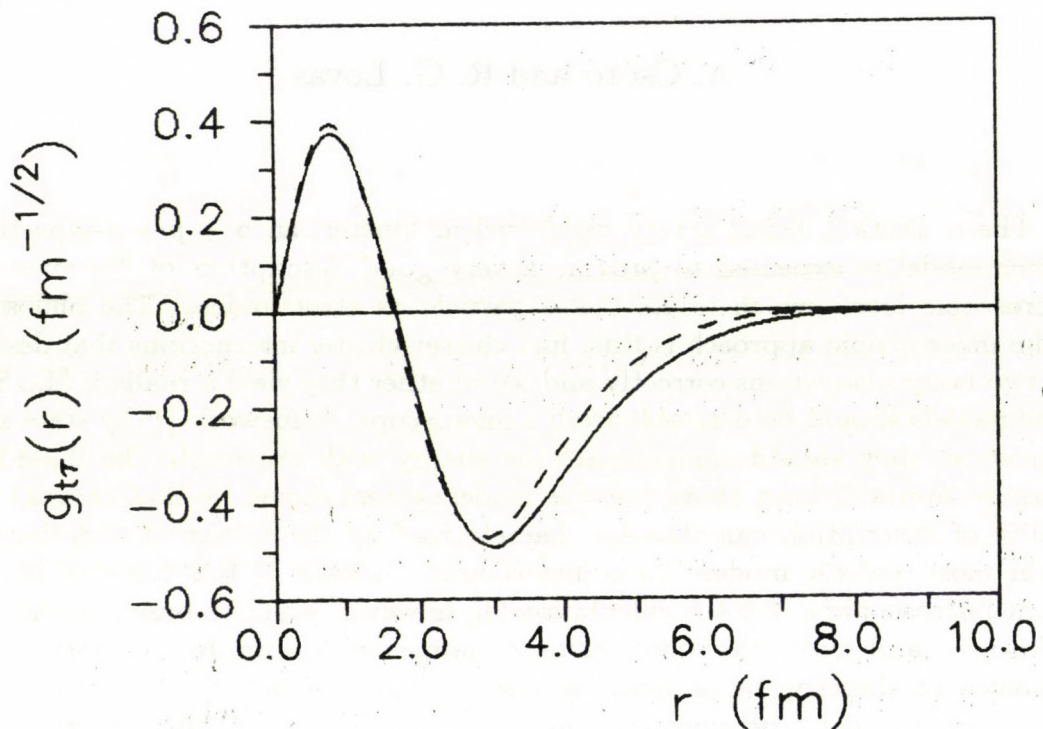
A. Csótó and R. G. Lovas

The α particle being a very rigid nuclear cluster, an $\alpha + p + n$ -type three-cluster model is expected to provide a very good description of ⁶Li even at a macroscopic level, which treats the α particle as structureless. The philosophy of the macroscopic approach is this: find cluster-cluster interactions that describe the two-body subsystems correctly and see whether they yield a realistic ⁶Li. Since these models should be derivable from a microscopic framework [1] by state space truncation, they should approximate the energy with respect to the three-body breakup threshold from above (i.e. the model system should be *underbound*). The quality of description can thus be characterized by the extent of underbinding. In the most realistic models ⁶Li is underbound typically by 0.2–0.5 MeV [2]. Our recent microscopic $\alpha + p + n$ calculation [3], however, which is based on the same philosophy, and treats the three-cluster dynamics with a similar accuracy, underestimates the binding by as much as 1 MeV. This contradicts the results of the macroscopic models and suggests that there must be three-cluster effects ignored by our model.

The most prominent three-cluster effect must be a rearrangement of the $\alpha + p + n$ system into a $t + \tau$ ($\tau = {}^3\text{He}$) configuration. We therefore extended our model [4] by inclusion of such configurations and found a gain of 0.6 MeV in binding energy. This correction is surprisingly high because the overlap of the $t + \tau$ configurations with the $\alpha + d$ components included in the model might have been expected almost complete. We emphasize that this effect appears in excess of a virtually complete $\alpha + p + n$ subspace, so there is room for further improvement only in the $t + \tau$ component, which cannot but enlarge the effect.

If the contribution to the binding energy is so significant, it must also appear as an enhancement of the $t + \tau$ spectroscopic factor. Indeed, we found an increase of 0.06. The figure shows preliminary results for the spectroscopic amplitude functions calculated in the $\alpha + p + n$ model (dashed line) and in the $\{\alpha + p + n, t + \tau\}$ model (solid line).

To conclude, one can say that the $t + \tau$ subspace provides at least 0.6 MeV of the 1 MeV binding energy missing from the $\alpha + p + n$ model. The contradiction with the three-body model shows that the off-shell behaviour of the effective forces they use cannot be perfect.



References

1. R. G. Lovas, K. Varga and A. T. Kruppa: *Microscopic versus macroscopic treatment of clusters in nuclei*, to appear in Proc. Int. Conf. on Nuclear and Atomic Clusters, Turku, 1991 (Springer Lecture Notes on Physics, 1992); K. Varga and R. G. Lovas, Phys. Rev. C **43** (1991) 1201
2. D. R. Lehman, M. Rai and A. Ghovanlou, Phys. Rev. C **17** (1978) 744; J. Bang and C. Gignoux, Nucl. Phys. **A313** (1979) 119; V. I. Kukulín, V. M. Krasnopol'sky, V. T. Voronchev and P. B. Sazonov, Nucl. Phys. **A417** (1984) 128; B. V. Danilin, M. V. Zhukov, A. A. Korshennikov and L. V. Chulkov, Yad. Fiz. **53** (1991) 71
3. A. Csótó and R. G. Lovas: *Dynamical microscopic three-cluster description of ${}^6\text{Li}$* , contribution to this Annual Report
4. K. Varga, A. Csótó, K. F. Pál, A. T. Kruppa and R. G. Lovas: *Microscopic formalism for light multicluster systems*, contribution to this Annual Report

Dynamical microscopic three-cluster description of ${}^6\text{Li}$

A. Csóto and R. G. Lovas

In recent years we have done extensive work on the description of the ground state (g.s.) of the nucleus ${}^6\text{Li}$ [1-4]. We solve a six-nucleon problem ('microscopic model') with an effective nucleon-nucleon interaction ('dynamical model') in a truncated state space treating the Pauli principle as well as the centre-of-mass motions exactly. Our previous approach [2] depicted ${}^6\text{Li}$ as an $\alpha + p + n$ three-cluster system arranged as $(pn)\alpha$, with an excitable α cluster in which the six nucleons interact via a central effective nucleon-nucleon force. This interaction allows no mixing in the summed nucleon spin S , and relative orbital momenta l_{pn} , $l_{d\alpha}$, and their sum, L , such that they are to be set to $S = 1$ and $l_{pn} = l_{d\alpha} = L = 0$ in the ${}^6\text{Li}$ g.s.

We have now [4] attempted to achieve the perfection of macroscopic $\alpha + p + n$ three-body models. We use a generator-coordinate approach, which includes $(pn)\alpha$, $(\alpha n)p$, and $(\alpha p)n$ partitions with all angular-momentum components of any significance. The trial function is constructed out of $0s$ and a set of $0s$, $0p$, $0d$ harmonic-oscillator (h.o.) eigenfunctions of the α intrinsic and of intercluster Jacobi coordinates, respectively, with the generator coordinates being the h.o. size parameters.

The effective nucleon-nucleon force used contains tensor and spin-orbit terms. We have determined its parameters by fitting to the properties of the subsystems. We found that the description of the subsystems is less perfect than with central forces, and explained this by the inconsistency of the use of a tensor force with describing the α g.s. by $0s$ oscillator states.

The binding of ${}^6\text{Li}$ with this force was found to be about 1 MeV too weak. After readjusting the force to yield the correct ${}^6\text{Li}$ energy, we found the weights of the components with summed nucleon spin and orbital momentum $(S, L) = (1, 0)$, $(1, 1)$, $(1, 2)$, and $(0, 1)$ to be 94.6%, 0.2%, 3.9%, and 1.3%, respectively. The $(1, 2)$ component comes predominantly from clusterization $(pn)\alpha$; the others can be attributed to any of the highly overlapping partitions.

The $\alpha + d$ and ${}^5\text{He} + p$ spectroscopic factors were calculated with a new formula, which expresses them in the generator-coordinate basis directly, without resort to integral transformations. The estimates for the $\alpha + d$ spectroscopic factor, ~ 0.9 , are realistic, but those for ${}^5\text{He} + p$ are a factor of 2 too high. This is understood to be a consequence of the model's tendency to compress the low-energy continuum, which appears to be a general defect of forces that are constrained to reproduce the bulk properties of the α particle in terms of $0s$ states. Thus a radical remedy would require an improvement of the description of the cluster internal motion.

References

1. R. Beck, F. Dickmann and R. G. Lovas, Nucl. Phys. **A446** (1985) 703
2. R. Beck, F. Dickmann and A. T. Kruppa, Phys. Rev. C **30** (1984) 1044;
A. T. Kruppa, R. G. Lovas, R. Beck and F. Dickmann, Phys. Lett. **179B** (1986) 317;
R. Beck, F. Dickmann and R. G. Lovas, Ann. Phys. (N.Y.) **173** (1987) 1;
R. G. Lovas, A. T. Kruppa, R. Beck and F. Dickmann, Nucl. Phys. **A474** (1987) 451;
A. T. Kruppa, R. Beck and F. Dickmann, Phys. Rev. C **36** (1987) 327;
J. B. J. M. Lanen, R. G. Lovas, A. T. Kruppa, H. P. Blok, J. F. J. van den Brand, R. Ent, E. Jans, G. J. Kramer, L. Lapikás, E. N. M. Quint, G. van der Steenhoven, P. C. Tiemeyer and P. K. A. de Witt Huberts, Phys. Rev. Lett. **63** (1989) 2793;
R. G. Lovas, A. T. Kruppa and J. B. J. M. Lanen, Nucl. Phys. **A516** (1990) 325;
R. G. Lovas, K. Varga and A. T. Kruppa: *Microscopic versus macroscopic treatment of clusters in nuclei*, to appear in Proc. Int. Conf. on Nuclear and Atomic Clusters, Turku, 1991 (Springer Lecture Notes on Physics, 1992)
3. K. Varga and R. G. Lovas, Phys. Rev. C **43** (1991) 1201
4. A. Csótó and R. G. Lovas: *Dynamical microscopic three-cluster description of ${}^6\text{Li}$* , submitted to Phys. Rev. C

Microscopic formalism for light multicluster systems

K. Varga, A. Csótó, K. F. Pál, A. T. Kruppa[†] and

R. G. Lovas

[†]Present address: Daresbury Laboratory, Warrington, UK

The description of light weakly bound nuclei, like ${}^{6,7,9,11}\text{Li}$, may require the explicit treatment of more than two clusters. For ${}^6\text{Li} = \alpha + p + n$, we used to use a two-cluster $\alpha + d$ formalism, with the $p + n$ motion represented by a combination of excited deuteron states [1]. With composite clusters or mixed angular-momentum relative motions, however, this is not a viable method.

Our new multiconfiguration multicluster formalism is based on a linear variational approximation to the A -nucleon problem with a trial function of the generator-coordinate type. The nucleon-nucleon interaction is assumed to be a sum of central, *tensor*, *spin-orbit* and Coulomb terms. The clusters are restricted to be 0s clusters.

The trial function is a sum over various cluster arrangements, each associated with a particular set of intercluster Jacobi coordinates. In an 1+2+3 three-cluster model a general term describing the arrangement (12)3 has the form

$$\Psi_{S,(l_1 l_2)L}^{(12)3} = \mathcal{A} \left\{ \left[\Phi_S [\chi_{l_1}^{12}(\mathbf{r}_1) \chi_{l_2}^{(12)3}(\mathbf{r}_2)]_L \right]_{JM} \right\},$$

where \mathcal{A} is the intercluster antisymmetrizer, $\Phi_{SM_S} = [(\Phi^1 \Phi^2) \Phi^3]_{SM_S}$ is composed of the cluster intrinsic wave functions Φ^i , the $\chi(\mathbf{r})$ are functions of the intercluster Jacobi coordinates, and $[]_{jm}$ denotes angular-momentum coupling. The cluster intrinsic states are harmonic-oscillator (h.o.) Slater determinants, of different size parameters, each projected onto the 0s h.o. wave function describing the respective zero-point vibration of the cluster centres of mass. Such a set of cluster intrinsic states comprises, in addition to the ground state, a set of breathing vibrational states as well, whose inclusion is to allow for the distortion of the clusters in each other's vicinity. The intercluster functions $\chi_{lm}(\mathbf{r}_i)$ are expanded as

$$\chi_{lm}(\mathbf{r}_i) = \sum_k^{N_i} C_k r_i^l \exp(-\frac{1}{2} \gamma_{ik} r_i^2) Y_{lm}(\hat{\mathbf{r}}_i). \quad (1)$$

The matrix elements involving the basis functions are expressed as integral transforms of matrix elements of multicentre shell-model Slater determinants projected to total momentum zero. One can derive such a relationship by using the

fact that a shifted Gaussian is the generating function of the functions involved in the expansion (1).

Because of the non-central potential terms, the matrix elements between the multicentre shell-model states are functions of the displacement *vectors* between the h.o. centres involved. The integral transformations involve integrations over all these vectorial variables. In the integration over the angular variables an angular-momentum projection is also implicit. The technical novelties in the formalism are in the treatment of these integral transformations. The formalism facilitates the implementation of computer algebra.

The formalism has first been applied to the ground state of ${}^6\text{Li}$. The results obtained in a pure $\alpha + p + n$ model and in a mixed $\{\alpha + p + n, t + \tau\}$ model are reported on in Refs. [2] and [3], respectively.

References

1. R. Beck, F. Dickmann and A. T. Kruppa, Phys. Rev. C **30** (1984) 1044;
R. G. Lovas, A. T. Kruppa, R. Beck and F. Dickmann, Nucl. Phys. **A474** (1987) 451
2. A. Csótó and R. G. Lovas: *Dynamical microscopic three-cluster description of ${}^6\text{Li}$* , contribution to this Annual Report
3. A. Csótó and R. G. Lovas: *Triton+ ${}^3\text{He}$ admixture in the ground-state of ${}^6\text{Li}$* , contribution to this Annual Report

A Semi-Microscopic Algebraic Cluster Model

J. Cseh†

Recently we have proposed an algebraic treatment of cluster structure of light nuclei, including non-closed-shell clusters [1]. The internal cluster degrees of freedom are described in this approach by the $SU(3)$ shell model [2], while the relative motion is treated in terms of the vibron model [3].

This description is semi-microscopic in the sense, that the Pauli forbidden states are excluded from the model space not only when the truncation can be done according to the quantum number of the relative motion [4], but also within a major shell. The spurious center of mass excitations are excluded, too. This model space is similar to that of the microscopic $SU(3)$ cluster model [5]. In fact, the solution of the norm-kernel problem of the microscopic description can be used to build up the model space of the semi-microscopic approach, but a simpler approximation based on the matching of the shell model and cluster model basis [6,1] also proved to be useful in several cases. Some other consequences of the antisymmetrization, which are normally beyond the capability of the phenomenological cluster models including the vibron model, are also incorporated in this description. An example is the equivalence of different cluster configurations.

Table I. $SU(3)$ representations for the $^{12}C + \alpha$ system from the matching of the cluster basis and shell model basis

n_π	(λ, μ)
4	(0, 0)
5	(2, 1)
6	(2, 0) (3, 1) (4, 2)
7	(3, 0) (4, 1) (5, 2) (6, 3)
8	(4, 0) (5, 1) (6, 2) (7, 3) (8, 4)
9	(5, 0) (6, 1) (7, 2) (8, 3) (9, 4)
⋮	⋮
⋮	⋮
⋮	⋮
⋮	⋮

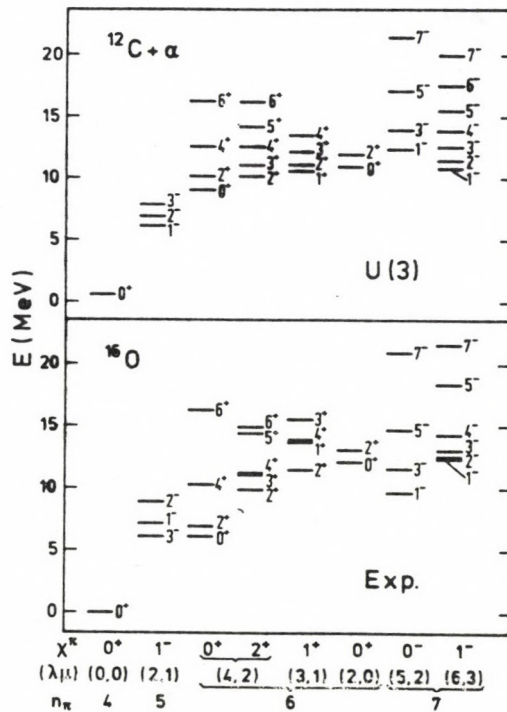


Figure 1. Experimental and model spectra of ^{16}O according to the $U(3)$ dynamical symmetry

The model is algebraic in the sense, that the quantum numbers of the states are provided as representation labels of some Lie groups and the interactions are expressed in terms of their generators.

As an illustrative example Table I. presents the model space of the $^{12}\text{C} + \alpha$ system, and Fig. 1. shows the low-lying part of the spectrum.

- † Alexander von Humboldt fellow; present address:
Institut für Theoretische Physik, Justus-Liebig Universität, Giessen, Germany
1. J. Cseh: ATOMKI Annual Report 1990, 42.
J. Cseh: Proc Int. Conf. on Nuclear and Atomic Clusters, Turku 1991, Inv. Papers, Springer-Verlag, in press
 2. J. P. Elliott: Proc. Roy. Soc. **A245** (1958) 128 and 562.
 3. F. Iachello: Phys. Rev. **C23** (1981) 2778.
F. Iachello and R. D. Levine: J. Chem. Phys. **77** (1982) 3046.
 4. J. Cseh and G. Lévai: Phys. Rev. **C38** (1988) 972.
J. Cseh: J. Phys. Soc. Jpn. Suppl. **58** (1989) 604.
 5. H. Horiuchi and K. Ikeda: Cluster Models and Other Topics (World Scientific 1986)

A semi-microscopic algebraic study of the α -cluster states of the ^{18}O nucleus

G. Lévai^{a),b)}, J. Cseh^{c),b)} and W. Scheid^{b)}

A well-known common feature of many light nuclei is the presence of α -cluster states in their spectra. These states have been interpreted in terms of both microscopic [1] and phenomenologic [2,3] cluster models. The Vibron Model [3] (which is a phenomenologic algebraic model of dipole collectivity,) was able to reproduce several important characteristics of nuclear cluster states, using the simplified picture of the rotational-vibrational motion of two structureless clusters [4]. In order to take into account the internal degrees of freedom, this model was developed further on a phenomenologic level by allowing collective quadrupole [5] and single-nucleon [6] excitations of the clusters.

Recently, a semi-microscopic version of the Vibron Model was formulated [7] as a general approach to nuclei consisting of non-closed shell clusters. This version describes the internal degrees of freedom of the clusters in terms of the $SU(3)$ shell model of Elliott [8], while the relative motion of the clusters is accounted for by the $U(3)$ limit of the Vibron Model. The construction of the model allows the exclusion of the Pauli-forbidden states and the spurious states related to the CM motion of the whole nucleus [7]. The first results from the model were the reproduction of the spectra of the $^{12}\text{C} + \alpha$ and the $^{12}\text{C} + ^{16}\text{O}$ systems [7], however, the thorough application of the *full* machinery of the model (including the description of $E2$ and $E1$ transitions) to some nucleus remained to be done.

The ^{18}O nucleus appeared ideal as the subject of such a study for at least two reasons. On the one hand, its relatively simple structure makes the application of the model straightforward and easy to test before turning to more complex systems, while, on the other hand, the enhanced $E1$ (and $E2$) transitions, confirmed by a recent work [9], clearly show the importance of the molecular ($^{14}\text{C} + \alpha$) structure of some of its states. The experimental data have been compared to the model spectra corresponding to the dynamical symmetries of the simple Vibron Model [9]. This description can account for the enhanced $E1$ transitions, (actually the experiment was inspired by this prediction,) however the model spectra contain considerably less states than what was found experimentally.

We have used the $(0,2)$ $SU(3)$ shell model representation to describe the internal structure of the ^{14}C nucleus, while the relative motion of the α and the ^{14}C clusters was characterised by the Vibron Model quantum number n_π , where (according to the Wildermuth condition) only states with $n_\pi \geq 6$ were considered. We identified 34 $T = 1$ states of the experimental spectrum with model states and assigned them to 11 bands with both positive and negative parity after fitting the model Hamiltonian with 7 parameters.

$E2$ and $E1$ transitions between the $SU(3)$ coupled model states were also calculated and specific non-trivial selection rules were found to hold for the phenomenologic transition operators. The three parameters of the $T^{(E2)}$ operator

and the two parameters of the $T^{(E1)}$ operator were fixed by requiring the reproduction of the strength of certain, precisely measured transitions [9,10]. The $E2$ transitions obtained this way were in good agreement with the experimental data set (of 16 items), moreover the quadrupole moment of the first excited (2^+) state was also excellently reproduced. The results were somewhat poorer for the $E1$ transitions (30 items), nevertheless the performance of our model was still better than that of a Generator-Coordinate Method (GCM) calculation [11] which overestimated the $B(E1)$ values significantly. A remarkable finding was that our results (especially the $B(E2)$ values) showed non-negligible correlation with the GCM results in the sense that the same transitions were found to be strong (or weak) in the two models, sometimes even in contradiction with the experimental data.

These first results obtained from the $SU(3)$ dynamical symmetry of the new semi-microscopic algebraic cluster model are encouraging with respect to its possible applications to more complex systems, which we plan to carry out in the near future.

^{a)} DAAD fellow ; present address, ^{b)}

^{b)} Institut für Theoretische Physik, Justus-Liebig Universität, Giessen, Germany

^{c)} Alexander von Humboldt fellow; present address, ^{b)}

References

1. see for example: Prog. Theor. Phys. Suppl. **68** (1980) 1
2. B. Buck, C. B. Dover and J. P. Vary: Phys. Rev. C **11** (1975) 1803
3. F. Iachello: Phys. Rev. C **23** (1981) 2778
4. J. Cseh and G. Lévai: Phys. Rev. C **38** (1988) 972
J. Cseh: J. Phys. Soc. Jpn. Suppl. **58** (1989) 604
J. Cseh, G. Lévai and K. Katō: Phys. Rev. C **43** (1991) 165
5. H. J. Daley and F. Iachello: Ann. Phys. (N.Y.) **167** (1986) 73
6. G. Lévai and J. Cseh: Phys. Rev. C **44** (1991) 152 and 166
7. J. Cseh: in Proc. Int. Conf. on Nuclear and Atomic Clusters, Turku 1991, Inv. Papers, Springer-Verlag, in press
J. Cseh: Universität Giessen, Preprint, 1991
8. J. P. Elliott: Proc. Roy. Soc. **A245** (1958) 128 and 562
9. M. Gai, M. Ruscev, D. A. Bromley and J. W. Olness: Phys. Rev. C **43** (1991) 2127
10. F. Ajzenberg-Selove: Nucl. Phys. **A475** (1987) 1
11. P. Descouvemont and D. Baye: Phys. Rev. C **31** (1985) 2274

Algebraic $^{12}\text{C} + ^{12}\text{C}$ cluster model description of ^{24}Mg

J. Cseh^{a),b)}, G. Lévai^{c),b)} and W. Scheid^{b)}

A Possible $^{12}\text{C} + ^{12}\text{C}$ cluster structure of ^{24}Mg was suggested for the first time in connection with the highly excited states of ^{24}Mg , which are populated as molecular resonances in the $^{12}\text{C} + ^{12}\text{C}$ reactions [1]. The explanation of their appearance was given in terms of phenomenological models, like the Nogami-Imanishi model [2], double resonance model [3], and band-crossing model [4]. Later on the phenomenological algebraic description of the vibron model [5] was also applied to this system [6,7]. Furthermore, microscopic [8] and semi-microscopic [9] calculations were carried out, concentrating on the high-lying quasi-bound states.

More recently the low-energy part of the ^{24}Mg spectrum has been described [10] in terms of the coupled channel extension of the local potential approach [11].

Here we report the preliminary results of our application of the semi-microscopic algebraic cluster model [12] to the $^{12}\text{C} + ^{12}\text{C}$ system. In this approach the internal cluster degrees of freedom are described by the $SU(3)$ shell model [13], while the relative motion is treated in terms of the vibron model [5]. Furthermore several effects of the antisymmetrization are taken into account [12].

In particular, we have addressed the question of the description of the ^{24}Mg nucleus when both the low-lying spectrum and the quasi-molecular resonances are considered. Both ^{12}C nuclei are characterised by the (0,4) shell model representation, i.e. their relative orientations can change, but no other internal excitations are involved. (In the previous algebraic descriptions [5-7] both clusters were considered to be structureless.) The $SU(3)$ basis of this semi-microscopic model combined with simple interactions corresponding to the $SU(3)$ dynamical symmetry result in reasonable agreement between the experimental and model spectra. The Hamiltonian contains terms up to the third order. The number of experimental $T = 0$ states taken into account is circa 180. The molecular resonances have $2\hbar\omega$ excitations in our model, similarly to Ref. [8]. The strongest $B(E2)$ values, which are associated in this description to intraband transitions between states with same (λ, μ) quantum numbers of the combined $SU(3)$ group, are reproduced also fairly well. However, some weaker $E2$ transitions are missing from this description; they show evidence for a weak breaking of the $SU(3)$ dynamical symmetry.

The effects of these cluster states on the $^{12}\text{C} + ^{12}\text{C}$ reaction cross section can be studied by combining the present nuclear structure calculation with the R -matrix description of the reaction, like in Ref. [14].

- a) Alexander von Humboldt fellow; present address: b)
b) Institut für Theoretische Physik, Justus-Liebig Universität, Giessen, Germany
c) DAAD fellow; present address: b)
1. See e.g. K. A. Erb and D. A. Bromley: *Treatise on Heavy-Ion Science* (Ed.: D. A. Bromley, Plenum Press) **3** (1984) 201, and references therein
 2. B. Imanishi: *Phys. Lett.* **27B** (1968) 267,
B. Imanishi: *Nucl. Phys.* **A125** (1969) 33.
 3. W. Scheid, W. Greiner and R. Lemmer: *Phys. Rev. Lett.* **25** (1970) 176,
H. J. Fink, W. Scheid and W. Greiner: *Nucl. Phys.* **A188** (1972) 259,
J. Y. Park, W. Greiner and W. Scheid: *Phys. Rev.* **C16** (1977) 2276.
 4. T. Matsuse, Y. Kondo and Y. Abe: *Prog. Theor. Phys.* **59** (1978) 1009,
Y. Abe, Y. Kondo and T. Matsuse: *Prog. Theor. Phys.* **59** (1978) 1393.
 5. F. Iachello: *Phys. Rev.* **C23** (1981) 2778,
F. Iachello and R. D. Levine: *J. Chem. Phys.* **77** (1982) 3046.
 6. K. A. Erb and D. A. Bromley: *Phys. Rev.* **C23** (1981) 2781.
 7. J. Cseh: *Phys. Rev.* **C31** (1985) 692.
 8. K. T. Hecht, H. M. Hofmann and W. Zahn: *Phys. Lett.* **103B** (1981) 92,
K. T. Hecht, E. J. Reske, T. H. Seligman, and W. Zahn: *Nucl. Phys.* **A356** (1981) 146.
 9. M. Ohkubo, K. Kato and H. Tanaka: *Prog. Theor. Phys.* **67** (1982) 207,
K. Kato and H. Tanaka: *Prog. Theor. Phys.* **81** (1989) 390.
 10. R. A. Balbock and B. Buck: *J. Phys.* **G12** (1986) L29,
B. Buck, P. D. B. Hopkins and A. C. Merchant: *Nucl. Phys.* **A513** (1990) 75.
 11. B. Buck, C. B. Dover and J. P. Vary: *Phys. Rev.* **C11** (1975) 1803.
 12. J. Cseh: *Proc. Int. Conf. on Nuclear and Atomic Clusters, Turku 1991, Inv. Papers, Springer-Verlag, in press*
 13. J. P. Elliott: *Proc. Roy. Soc.* **A245** (1958) 128 and 562.
 14. R. Maass, W. Scheid and A. Thiel: *Nucl. Phys.* **A460** (1986) 324,
R. Maass, and W. Scheid: *J. Phys.* **G16** (1990) 1359 and in press

On the Relation Between Cluster and Superdeformed States of Light Nuclei

J. Cseh^{a),b)} and W. Scheid^{b)}

We have investigated the relation between cluster and superdeformed states of light nuclei [1,2] both in terms of Harvey's prescription [3] and in terms of the connection between the shell and cluster model basis [4]. It turns out that these two prescriptions associate the same α -like clusterisations with local minima of the potential energy surfaces of $N = Z$ even-even nuclei [5].

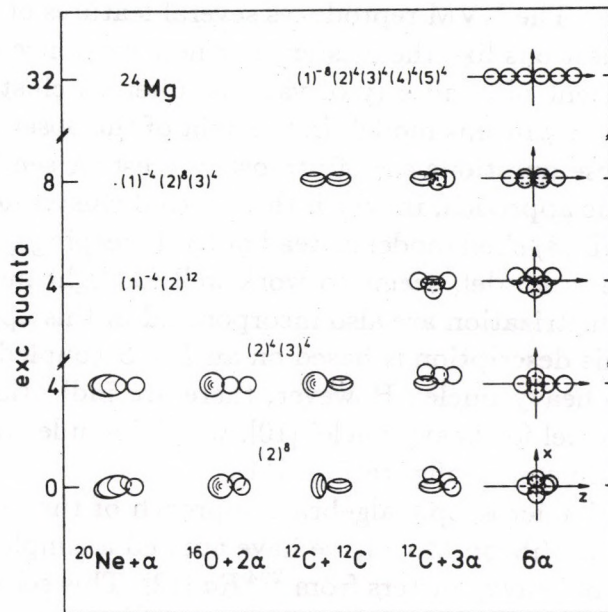


Fig. 1. Possible cluster configurations of some highly deformed states of ^{24}Mg . Only the directions of symmetry axes and the directions of amalgamations of the clusters carry physical content, while the relative distances do not.

- a) Alexander von Humboldt fellow; present address: b)
 b) Institut für Theoretische Physik, Justus-Liebig Universität, Giessen, Germany
1. J. Cseh and W. Scheid: Contribution to the European Research Conference "Nuclear Physics: Nuclear Shapes" Balatonfüred 1991
 2. J. Cseh and W. Scheid: Universität-Giessen, Preprint 1991
 3. M. Harvey: Proc. 2nd Int. Conf. on Clustering Phenomena in Nuclei (College Park 1975, USDERA report ORO-4856-26) p. 549.
 4. K. Wildermuth and Th. Kanellopoulos: Nucl. Phys. **7** (1958) 150.
 5. G. Leander and S. E. Larsson: Nucl. Phys. **7** (1975) 93.

Pseudo $SU(3)$ Approach to Clusterization in Heavy Nuclei

J. Cseh^{a),b)}, R. K. Gupta^{b),c)} and W. Scheid^{b)}

Cluster configurations in heavy nuclei have been discussed in the past in terms of a phenomenological algebraic cluster model, called Nuclear Vibron Model (NVM) [1-4], in which the collective states of the core are accounted for by the Interacting Boson Model (IBM) [5]. The NVM reproduces several features of the experimental data. Nevertheless, questions like the existence or non-existence of a specific clusterization, and the extent of similarity of various different cluster configurations can not be answered easily in this model. In the light of the observed heavy-cluster radioactivity [6,7], these questions are of utmost interest. A semi-microscopic extension of the algebraic approach, in which the internal cluster degrees of freedom are described by the $SU(3)$ shell model instead of IBM, keeping the relative motion described by the Vibron Model, seems to work well for light nuclei [8,9]. Several effects of the antisymmetrization are also incorporated in this approach. Since the shell model part of this description is based on an $L - S$ coupled scheme, it is not applicable directly to heavy nuclei. However, there are indications in favour of a pseudo $SU(3)$ shell model for heavy nuclei [10], which includes the validity of this scheme also for some cluster configurations [11].

Based on the semi-microscopic algebraic approach of the pseudo $SU(3)$ shell model coupled with the Vibron Model, we have applied a simple selection rule for the possible emission of heavy clusters from ^{224}Ra [12]. This selection rule is given by a matching requirement between the $U(3)$ and $U^{ST}(4)$ representations of the cluster basis and the shell model basis of the united nucleus. We find that this selection rule is sensitive to the microscopic structure of the nuclei. For example, supposing a zero occupation of the intruder neutron subshells, the ^{14}C emission is forbidden, while α and ^{12}C emissions are allowed. However, if we take the intruder states into account, then for the configuration $(j_{15/2})_n^2 \otimes (26, 4)_n \otimes (18, 0)_p$, which corresponds to a realistic deformation of ^{224}Ra , the $^{14}\text{C} + ^{210}\text{Pb}$ clusterization is allowed. Then not only the ground-state band $(44, 4)$, but also the lowest-lying negative parity band $(49, 2)$ can be obtained in this model. Furthermore, due to the antisymmetrization effect, we find that some cluster configurations, like ^4He , ^{12}C , and ^{14}C clusters plus the corresponding cores, are equivalent in this approximation.

2 J. Cseh^{a),b)}, R. K. Gupta^{b),c)} and W. Scheid^{b)}

- a) Alexander von Humboldt fellow; present address: b)
 - b) Institut für Theoretische Physik, Justus-Liebig Universität, Giessen, Germany
 - c) Permanent address: Physics Department, Panjab University, Chandigar-160014, India
1. H. J. Daley and F. Iachello: Phys. Lett. **131B** (1981) 281.
 2. H. J. Daley and F. Iachello: Ann. Phys. (N.Y.) **167** (1986) 73.
 3. H. J. Daley and M. A. Nagarajan: Phys. Lett. **166B** (1986) 379.
 4. H. J. Daley and B. Barrett: Nucl. Phys. **A449** (1986) 256.
 5. F. Iachello and A. Arima: The Interacting Boson Model (Cambridge University Press, Cambridge, England, 1987)
 6. P. B. Price: Proc. Int. Conf. on Nuclear and Atomic Clusters, Turku 1991, Inv. Papers, Springer-Verlag, in press
 7. W. Greiner: Proc. Int. Conf. on Nuclear and Atomic Clusters, Turku 1991, Inv. Papers, Springer-Verlag, in press
 8. J. Cseh: Proc. Int. Conf. on Nuclear and Atomic Clusters, Turku 1991, Inv. Papers, Springer-Verlag, in press
 9. J. Cseh: Universität-Giessen, Preprint 1991.
 10. J. P. Draayer: Nucl. Phys. **A520** (1990) 259c.
 11. D. Braunschweig, K. T. Hecht and J. P. Draayer: Phys. Lett. **76B** (1978) 538.
 12. J. Cseh, R. K. Gupta and W. Scheid: Proc. Int. Conf. on Nuclear and Atomic Clusters, Turku 1991, Cont. Papers, (Ed: T. Lönnroth, Turku 1991) p. 9.

Dynamical Symmetry Breaking in $SU(2)$ Model and the Quantum Group $SU(2)_q$

R. K. Gupta^{a),b)}, J. Cseh^{c),d)}, A. Ludu^{a),e)}, W. Greiner^{a)} and
W. Scheid^{d)}

We have studied the quantum analogues of the limiting symmetries $U(1)$ and $O(2)$ of the $U(2)$ algebra [1]. In particular, we have investigated the question whether the q -deformation parameter in the algebra of $SU(2)_q$ group can be looked upon as a dynamical symmetry breaking parameter of taking us from one limiting case to another. We find that in the limiting case of $U(2) \supset U(1)$, partially the real and imaginary q -deformations and more completely the complex q -deformations give a transition from $U(1)$ towards $O(2)$ and also show intermediate results.

- a) Institut für Theoretische Physik, Johann Wolfgang Goethe-Universität, Frankfurt am Main, Germany
 - b) Permanent address: Physics Department, Panjab University, Chandigarh-160014, India
 - c) Alexander von Humboldt fellow; present address: d)
 - d) Institut für Theoretische Physik, Justus-Liebig Universität, Giessen, Germany
 - e) Permanent address: University of Bucharest, Faculty of Physics, Department of Theoretical Physics and Mathematics, Bucharest, Romania
1. R. K. Gupta, J. Cseh, A. Ludu, W. Greiner and W. Scheid: J. Phys. G, in press

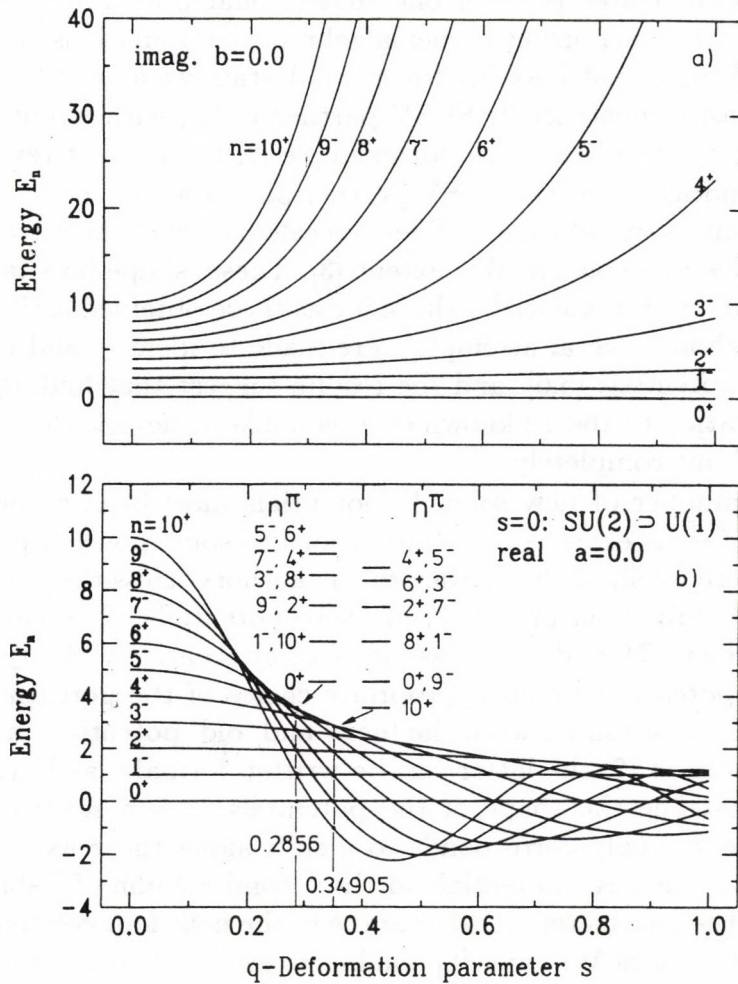


Fig. 1. Energy spectrum as a function of q-deformation parameter s for $SU(1)$. Here in (a) $s (= a)$ is real and in (b) $s (= ib)$ is imaginary-valued. The energy spectra observed at $b = 0.2856$ and 0.34905 are shown as an inset.

On some recent developments concerning solvable potentials obtained from SUSYQM

G. Lévai

The introduction of supersymmetric quantum mechanics (SUSYQM) [1] generated renewed interest in solvable problems of nonrelativistic quantum mechanics. This new approach relates pairs of one-dimensional potentials ('SUSY partner potentials') to each other using (super)algebraic manipulations, and has led to the remarkable finding that knowing the ground-state wavefunction of a potential $V_-(x)$ one can easily construct its SUSY partner $V_+(x)$ with essentially the same bound-state energy spectrum. (See, for example [2] for a recent review.)

It was soon noticed that the SUSY partner potentials often depend on the coordinate in the same way, which simplifies the calculation of the wavefunctions and energy eigenvalues to a considerable extent [3]. These 'shape invariant' potentials were, in fact, found to be essentially the same as those obtained earlier [4] from the factorisation method. Several attempts were made to identify and classify *all* the shape invariant potentials [5,6], and the results suggest that finding further such potentials in addition to the 12 known ones is unlikely, nevertheless its possibility can not be ruled out completely.

Recently a number of new solvable potentials have been reported either as basic new results or as examples or illustrations to some novel approach inspired by SUSYQM. Here we show that although the authors stress the novelty [7,8,9,10] and the shape invariant nature [9,10] of these potentials, they can be obtained from already known *PI* and *PII* class [6] (or, alternatively [4], type *A* and *E*) shape invariant potentials by an appropriate choice of the potential parameters. We summarise the relation between the 'new' and 'old' potentials in Table 1. [11]. Using the notations of [6] the latter can be written formally as $V_-(A, B; ax + \delta)$, where *A* and *B* define the shape of the potentials, *a* is a scaling factor of the coordinate, while δ simply corresponds to a shift along the *x* axis. We displayed the parameters of the 'new' potentials in the second column of Table 1. and gave their relation to the parameters *A*, *B*, *a* and δ in the next four columns. In order to get the 'new' potential of Williams [8] one has to rewrite hyperbolic functions into exponential ones and also has to add a constant term to the resulting expression. The expression of the energy eigenvalues E_n also has to be rearranged somewhat.

The 'new' potentials were obtained using various approaches. Williams [8] followed earlier works [6,12] to construct a new class of solvable potentials related to the Jacobi polynomials, but, as it can be seen from Table 1., what he found is a *PII* class potential shifted along the *x* axis. Arai [9] also obtained shifted *PI* and *PII* class potentials as 'new' ones by using 'deformed hyperbolic functions' like e.g. $\sinh_q x = \frac{1}{2}(e^x - q e^{-x})$. Both authors notice that the energy spectrum of their 'new' potentials is independent of the *a* ([8]) and *q* ([9]) parameters. The interpretation of this result is clear, since as we see, these parameters represent practically only a shift along the *x* axis, so they should not be relevant to the basic

results. Cerveró [7] obtained a 'new' potential as a special case of a new approach based on the Jacobi elliptic functions. Here we also mention that his expectations about the reflectionlessness of this potential seem to be false, as can be seen from an earlier work [13].

Table 1. The 'new' potentials of refs. [7,8,9,10] expressed in terms of known shape invariant potentials [6]

Ref.	'New' potentials parameters	'Old' shape invariant potentials $V_-(A, B; ax + \delta)$				
		A	B	a	δ	Class ($g(x)$) [6]
[7]	ρ, ϕ	$\rho \cos \phi - \frac{1}{2}$	$\rho \sin \phi$	1	0	$PI(i \sinh x)$
[8]	α, A, a	$-\frac{\alpha+1}{4}$	$\frac{1-\alpha^2}{16} - \frac{A}{4}$	$-\frac{1}{2}$	$\frac{1}{2} \ln \frac{a}{2}$	$PII(\coth x)$
[9] Ex. 1.	$\alpha, \beta, \lambda, q$	$-\lambda$	β	α	$-\frac{1}{2} \ln q$	$PII(\tanh x)$
Ex. 2.	α, λ, μ, q	$-\lambda$	$-\mu q^{-1/2}$	α	$-\frac{1}{2} \ln q$	$PI(i \sinh x)$
[10] (33)	a, b	a	$-b$	1	0	$PI(\cosh 2x)$
(39)	a, b	$-a$	b	1	$\frac{\pi}{2}$	$PII(-i \cot x)$
(40)	a, b	a	$-b$	1	$\frac{\pi}{2}$	$PI(\cos x)$

In conclusion we can say that the twelve-member 'club' of shape invariant potentials appears to be exclusive, and admission of further members seems unlikely despite all the efforts initiated by the recent developments of SUSYQM. Nevertheless, these studies may open the way towards other exactly solvable problems of nonrelativistic quantum mechanics and may help our understanding of this field.

References

1. E. Witten: Nucl. Phys. **B188** (1981) 513
2. A. Lahiri, P. K. Roy and B. Bagchi: Int. J. Mod. Phys. **A5** (1990) 1383
3. L. Gendenshtein: Zh. Eksp. Teor. Fiz. Pis. Red. **38** (1983) 299; (JETP Lett. **38** (1983) 356)
4. L. Infeld and T. E. Hull: Rev. Mod. Phys. **23** (1951) 21
5. F. Cooper, J. N. Ginocchio and A. Khare: Phys. Rev. D **36** (1987) 2458
6. G. Lévai: J. Phys. A:Math. Gen. **22** (1989) 689
7. J. M. Cerveró: Phys. Lett. A **153** (1991) 1
8. B. W. Williams: J. Phys. A:Math. Gen. **24** (1991) L667
9. A. Arai: J. Math. Anal. Appl. **158** (1991) 63
10. C. X. Chuan: J. Phys. A:Math. Gen. **24** (1991) L1165
11. G. Lévai: to be published
12. G. Lévai: J. Phys. A:Math. Gen. **24** (1991) 131
13. A. Khare and U. P. Sukhatme: J. Phys. A:Math. Gen. **21** (1988) L501

Absolute alpha decay width of ^{212}Po in a mixed shell-and-cluster model

K. Varga, R. G. Lovas and R. J. Liotta [†]

[†]Manne Siegbahn Institute of Physics, Stockholm

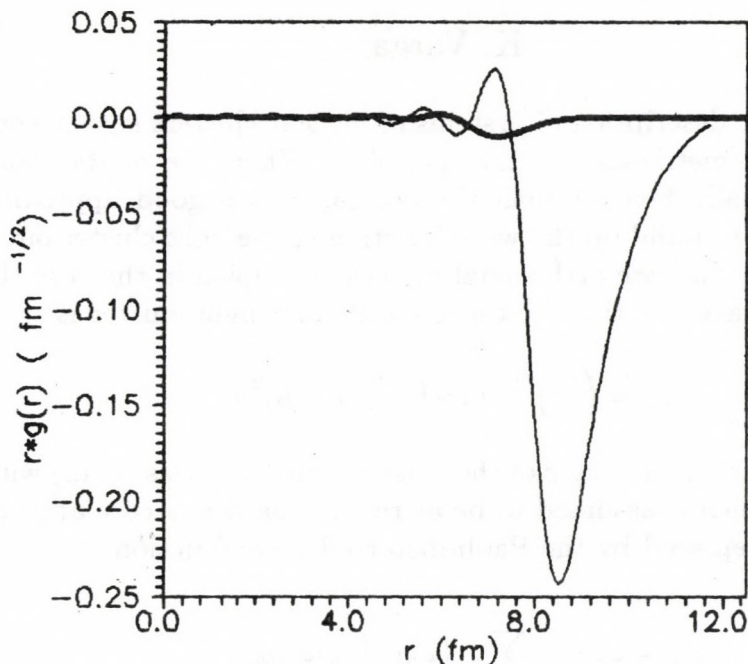
We cannot say that we understand the dynamics of α decay until we are able to predict absolute α decay rates, widths or, equivalently, the probability of α -particle pre-formation. Obviously, such a model should treat the valence nucleons of the parent nucleus microscopically, and a really fundamental approach calls for the shell model of the parent nucleus. A shell-model wave function, however, can only be used for this purpose if it is correct in a far-enough region where the nuclear interaction as well as Pauli exchanges are negligible, and that requires prohibitively large basis dimensions.

To overcome this hitch, we complement the shell-model basis by cluster-model basis states of the type of α particle plus residual nucleus. With the core assumed to be infinitely heavier than the α particle, the cluster-model states are tractable as some generalized shell-model states. They only require extra treatment because they involve single-particle (s.p.) orbits not orthogonal to each other, to the other valence orbits and to orbits occupied by the core nucleons. Thus, to reduce the cluster-model part as well to a four-valence-nucleon problem, the Pauli principle has to be allowed for by an orthogonality condition on the s.p. orbits.

In the model we developed along these lines in the past years [1] everything can be calculated analytically, though we had severe technical difficulties in its implementation and testing [1]. This is the first preliminary report on the results.

Our approach differs from the similar approach of Steinmayer, Sünkel and Wildermuth [2] in that our shell model is a realistic shell model by itself, from the approach of Okabe [3] in that we do not assume the existence of a single-particle model state nearby, and from both in that we use a realistic s.p. potential.

In the actual application of the model to the decay of the ground state of ^{212}Po we start with a reasonably realistic shell model with a Woods-Saxon-shaped s.p. potential. The parameters are fixed at this level by fitting to independent experimental data for the energy levels of the core + one-nucleon and core + two-nucleon systems and for core + s.p. scattering. We then include the cluster-model states. The decay width is calculated as $\Gamma = 2P(r_c)\gamma^2(r_c)$, where γ is the formation amplitude calculated analytically from the parent-state wave function and from a consistent α intrinsic wave function, and P is the Coulomb penetration factor. Γ has proved weakly dependent on the channel radius r_c as it should be. The resulting



value is not very sensitive to the shell-model and cluster-model configurations either. The only ingredients whose effect is crucial are the s.p. potential and the α separation energy because these affect the size and shape of the Coulomb barrier to be overcome by the α -particle.

In the above figure the two curves are the two contributions to the formation amplitude: the shell-model term (thick line) and the cluster-model term (thin line). The α spectroscopic factor is 0.07. The resulting decay width is 1.3×10^{-15} MeV, while the experimental value is 1.5×10^{-15} MeV. Since the uncertainty of the input parameters can well account for the difference between these two values, agreement with experiment may be said to be perfect.

To our knowledge, this is the best-ever estimate obtained in a fundamental microscopic approach for the absolute decay width of an α -radioactive nucleus.

References

1. R. J. Liotta, R. G. Lovas, K. Varga and T. Vertse, ATOMKI Annual Report (1990) p. 35;
K. Varga: *Matrix elements between Pauli-distorted single-particle orbits*, contribution to this Annual Report
2. T. Steinmayer, W. Sünkel and K. Wildermuth, Phys. Lett. **125B** (1983) 437
3. S. Okabe, Proc. 5th Int. Conf. on Clustering Aspects in Nucl. and Subnucl. Systems, J. Phys. Soc. Japan **58** (1989) Suppl. p. 516

Matrix elements between Pauli-distorted single-particle orbits

K. Varga

The microscopic description of systems of nuclear clusters is very complicated because the antisymmetrization is indispensable. When one of the clusters (the "core") is substantially heavier than the others, it is a good approximation to antisymmetrization to build up the wave function of the light cluster out of single-particle (s.p.) states that are orthogonal to those occupied in the core [1-3].

A typical s.p. wave function for the nucleons of a light cluster is

$$\varphi_{\mathbf{s}} = \left(\frac{\alpha}{\pi}\right)^{3/4} \exp\left(-\frac{\alpha}{2}(\mathbf{r} - \mathbf{s})^2\right),$$

where \mathbf{s} is the displacement vector of the cluster centre of mass (c.m.) with respect to the core c.m., which is assumed to be at rest in the heavy-core approximation. This is then to be replaced by the Pauli-distorted wave function

$$\hat{\varphi}_{\mathbf{s}} = \varphi_{\mathbf{s}} - \sum_{\text{occupied}} \langle \varphi_{nlm} | \varphi_{\mathbf{s}} \rangle \varphi_{nlm} \quad (1a)$$

$$= \sum_{\text{unoccupied}} \langle \varphi_{nlm} | \varphi_{\mathbf{s}} \rangle \varphi_{nlm} \quad (1b)$$

To calculate the one-body and two-body matrix elements of the Pauli-distorted states, one usually uses [2-3] the harmonic oscillator expansion (1b). To get convergence in this way is not only computer time consuming [2] but may lead to numerical inaccuracies [4] as well. Therefore, we propose to use the expression (1a) directly.

For this purpose, we constructed a generating function

$$g(q) = \left(\frac{4\alpha\beta^2}{\pi(\alpha + \beta)^2}\right)^{3/4} \exp\left(-\frac{1}{2} \frac{\alpha\beta}{\alpha + \beta} s^2\right) \exp\left(-\frac{1}{2} \beta r^2\right) \frac{1}{(1 - z^2)^{3/2}} \exp\left(-\frac{z^2}{(1 - z^2)}(\beta r^2 + \gamma s^2) + \frac{2z\beta\gamma\mathbf{r}\mathbf{s}}{(1 - z^2)}\right),$$

where

$$\gamma = \frac{\alpha^2\beta}{(\alpha + \beta)(\alpha - \beta)} \quad \text{and} \quad z = \left(\frac{\alpha - \beta}{\alpha + \beta}\right)^{1/2} q.$$

The matrix elements of the generating function are well known (see e.g. [1]) as it has simple gaussian \mathbf{r} dependence. From this the matrix elements of the Pauli-distorted wave function can be derived by using the relationship

$$\hat{\varphi}_{\mathbf{s}} = g(0) - \frac{d^{2n+l}}{dq^{2n+l}} g(q)|_{q=0}. \quad (2)$$

One can easily perform the operations prescribed by equation (2) using computer algebra or a recurrence relation.

We have successfully applied this method in the cluster+shell model description of the alpha-decay of ^{212}Po [4].

References

1. H. Horiuchi, Suppl. of Prog. Theor. Phys. **62** (1977) 90
2. T. Steinmayer, W. Sünkel and K. Wildermuth, Phys. Lett. **125B** (1983) 437
3. R. Blendowske, T. Fließbach and H. Walliser, Z. Phys. A **339** (1991) 121
4. K. Varga, R. G. Lovas and R. J. Liotta, Contribution to this Annual Report

Continuum RPA calculation of escape widths.

T. Vertse, P. Curutchet ¹, R. J. Liotta ¹, J. Bang ², N. Van Giai ³

The effect of an external field on a nucleus can be characterized by the response function which is a complex function of the energy and is constructed from the operator of the field and the Green's function of the system concerned. The imaginary part of the response function is proportional to the strength function and a complex pole of the response function lying close to the real E -axis represents a resonance of the nuclear system. In a work reported earlier [1] the dependence of the particle-hole response function on the real energy E was studied in a very simple model. It represented a continuum RPA (CRPA) calculation if the exact form of the single-particle Green's function was used. In order to speed up the calculations we also applied approximations to the CRPA, in which two sorts of pole expansions of the single particle Green's function were used. The result of the approximate methods were checked against that of the exact CRPA. The agreements encouraged us to use these pole expansions even if we extended the study of the p-h response function to complex energies.

The ultimate goal of all this efforts motivated by recent experimental studies is to develop a new and efficient method for the calculation of the particle decay width of giant resonances in heavy nuclei. Here one of the main complications is to include the contribution of the continua of many p-h configurations which all sum up coherently in the building up of a giant resonance. In a realistic case CRPA calculations become hopelessly time consuming besides they give no insight into the structure of the resonance whose decay width is calculated. In order to overcome these difficulties some of us [2] suggested an approximate method called resonant RPA (RRPA) where the continuum is approximated by a discrete set of bound and resonant single particle states. A stringent test of the RRPA (against the CRPA) and another pole expansion method based on the Mittag-Leffler expansion of the Green's function were carried out [3] in a simple model case of ref.[1]. There the unperturbed Hamiltonian contained a square well potential (with/without Coulomb term) and the residual interaction had a separable multipole form. In this case the p-h response function has a simple form and the partial decay widths is proportional to its residue. The complex pole of the response function and the corresponding residue were determined numerically. Though the model is oversimplified the parameters of the calculation were chosen so as to simulate giant multipole resonances in ^{208}Pb . The exact CRPA produced narrow giant resonances for the isoscalar 0^+ , 2^+ and the isovector 1^- cases. The sum of the partial widths calculated for these resonances coincided with the total width of the resonance (coming from the imaginary part of the energy) up to 3-4 decimal digits. This fact proved the reliability of the CRPA calculations. The

fact that both the RRPA and the other approximate calculation reproduced the partial width of the CRPA within 10% accuracy shows that the pole expansion methods can be used to get a reliable estimate of the partial width. The RRPA calculations not only took several orders of magnitudes shorter time to be completed than the CRPA but gave some hint about the importance of the different p-h configuration in the giant resonance. The other expansion method which in principle must be more reliable[4] was also much faster than the CRPA (but slower than the RRPA) and sometimes gave closer value to the exact result but due to the overcompleteness of the basis has difficulties in extracting structure information . Another experience we gained from this work is that the partial widths are better reproduced by the approximate calculations than the complex energy of the resonance therefore the sum of the partial width values give much better estimate to the total width than the one related to the imaginary part of the energy.

The extention of the calculations to realistic potentials is under way.

References

1. T. Vertse, P. Curutchet and R. J. Liotta, Phys. Rev. **42** (1990) 2605.
2. P. Curutchet, T. Vertse and R. J. Liotta, Phys. Rev. **C39** (1989) 1020.
3. T. Vertse, P. Curutchet, R. J. Liotta, J. Bang and N. Van Giai, Phys. Lett. **264B** (1991) 1.
4. T. Berggren and P. Lind private communication.

¹Manne Siegbahn Institute of Physics, Stockholm,

²The Niels Bohr Institute, Copenhagen,

³Institut de Physique Nucléaire, Orsay

Test of CP and CPT Symmetries at LEAR

S.Szilágyi

The CPLEAR (PS195) Collaboration

Univ.Athens, Univ.Basel, Univ.Boston, CERN, Univ.Coimbra,
Delft Techn.Univ., Democritos INP, Univ.Fribourg, Ioannina Univ.,
Univ.Liverpool, J.Stefan Inst.Ljubljana, Marseille CPPM,
Orsay CSNSM, Stockholm MSI, Univ.Thessaloniki, Zurich ETH

As a research fellow from ATOMKI, S.Szilágyi has been participating in the particle physics experiment called CPLEAR for four years. The experiment is being performed at the European Organization for Nuclear Research (CERN, Geneva) in a large international collaboration. As a member of the particle physics group at the Manne Siegbahn Institute of Physics (MSI Stockholm), he has worked on several aspects of the CPLEAR experiment, taking actively part in the construction and test of the detector, working especially on both hardware and software developments of the Particle Identification Detector for CPLEAR. Now he is involved in the physics analysis program of the experiment.

The idea and the main features of the CPLEAR experiment are briefly summarized as follows.

The physics motivation of the CPLEAR (PS195) experiment is to study CP violation phenomena using the improved source of antiprotons at LEAR (Low Energy Antiproton Ring, CERN).

The study of the invariance under the combined operation CP is connected to several fundamental questions in physics, like the observed asymmetry of particles and antiparticles in the Universe. Since its first observation in 1964 in the decay of the long-lived neutral kaon into two pions, CP violation remains one of the enigmas in particle physics.

While previous and other current experiments (e.g. NA31 at CERN and E731 at Fermilab) measure decays of K_L^0 and interferences with generated K_S^0 , CPLEAR starts with pure $|K^0\rangle$ and $|\bar{K}^0\rangle$ states, which are related by the CP operator: $CP|K^0\rangle = |\bar{K}^0\rangle$. The time evolution of these states is studied, and any difference (asymmetry) between K^0 and \bar{K}^0 decay rates is a direct evidence of CP violation.

An intense ($2 \times 10^6 s^{-1}$) beam of low momentum (200 MeV/c) antiprotons is stopped in a hydrogen gas target to obtain a high flux of tagged K^0 and \bar{K}^0 mesons through the annihilation channels (called *golden events*)

$$\bar{p}p \text{ (at rest)} \rightarrow \pi^\pm K^\mp K^0(\bar{K}^0)$$

The average kaon momentum in these channels is around 550 MeV/c. Both annihilation channels have the same branching ratio (0.2 %) due to C invariance in strong interactions. In the CPLEAR experiment the decays of the neutral kaon

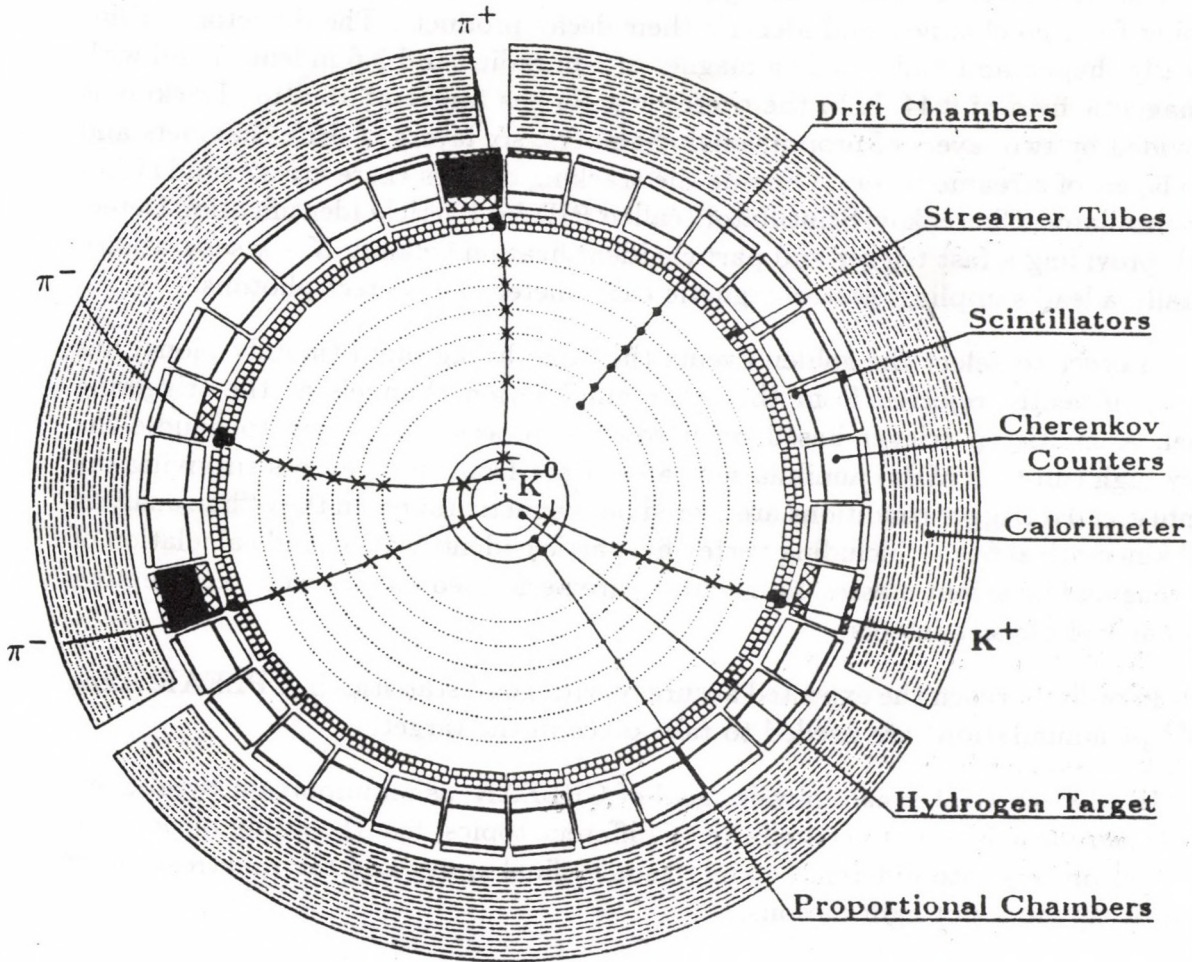


Fig. 1. Cross-section of the CPLEAR detector indicating a golden event

into 2π , 3π and semileptonic final states are studied. A new approach is used by measuring directly the $K_S^0 K_L^0$ interference effects and the asymmetries of different decay amplitudes in the neutral kaon system.

The quantity to be measured for different states f is

$$A_f \equiv \frac{R(\bar{K}^0 \rightarrow f) - R(K^0 \rightarrow f)}{R(\bar{K}^0 \rightarrow f) + R(K^0 \rightarrow f)}$$

where R denotes the decay rate. By this method of symmetrical production of particles and antiparticles in the $p\bar{p}$ annihilation at rest and the identical detection of their decay products, not only will the systematic errors be minimized, but CP violation in other than the 2π channel can be detected for the first time as well.

The CPLEAR detector (*see figure*) has been designed to tag neutral kaons arising from $p\bar{p}$ channels and identify their decay products. The detector is cylindrically shaped and built inside a magnet of 1 m radius and 3.6 m length and with a magnetic field of 0.44 T. In the centre is a H_2 gas target at 15 atm. Tracking is provided by two layers of proportional chambers, six layers of drift chambers and two layers of streamer tubes. Outside the tracking devices there are 32 sandwiches of Scintillator-Cherenkov-Scintillator (called PID for Particle Identification Detector), providing a fast trigger and particle identification (mainly $K - \pi$ separation). Finally a lead sampling electromagnetic calorimeter is to detect photons.

In order to select the golden events the large background (mainly pions) has to be efficiently rejected from the other annihilation channels at the triggering level. A multistep trigger based on hardwired processors is used to handle the very high (up to 2 MHz) annihilation rates. Data from those events surviving the sophisticated trigger conditions are stored on magnetic tapes. In the offline analysis full kinematical fits — including vertex fit, particle identification and calculation of missing and invariant masses, momenta — are performed on all events representing channels of physics interest.

In order to reach the expected accuracy with good statistics in CPLEAR, some 10^{13} $p\bar{p}$ annihilations are needed to take place in the target.

In addition to the main physics goal of CPLEAR, as an important byproduct, the experiment is able to contribute to different topics, like the study of $p\bar{p}$ annihilation process into different (mainly kaonic) final states and the spectroscopy of rare decay modes of light mesons.

References

1. The CPLEAR Collaboration: *Initial Performance of CPLEAR*
Proc.Conf. Low Energy Antiproton Physics, LEAP'90 MSI Stockholm, 2-6 July 1990. World Scientific Publishing, Singapore, 1991, Editors P.Carlson, A.Kerek and S.Szilágyi, pages 414-420.
2. The CPLEAR Collaboration: *The CPLEAR Particle Identification Detector*.
Nucl. Inst. and Meth. in Physics Research **A311** (1992) 78-90
3. The CPLEAR Collaboration: *Determination of the Relative Branching Ratios for $p\bar{p} \rightarrow \pi^+\pi^-$ and $p\bar{p} \rightarrow K^+K^-$*
Physics Letters **B 267** (1991) 154-158
4. The CPLEAR Collaboration: *First Determination of CP Violation Parameters from $K^0 - \bar{K}^0$ Decay Asymmetry*
Submitted to Physics Letters **B** (1992)

ATOMIC PHYSICS

An Exact Comparison of the Experimental and Theoretical ECC Cusp Energies

S. Ricz, I. Kádár, J. Végh, Zs. Fülöp, E. Takács, K. Wakiya[#],

Gy. Szabó, L. Tóth

It is generally accepted that the ECC (Electron Capture to the Continuum) cusp electrons have the same velocity as the projectiles capturing them^{1,2,3}. To test this hypothesis the energy of the ECC cusp has been accurately measured in proton-noble gas atom collisions at accurately known proton energies at 0° with high electron energy resolution. High resolution and accurate calibration of both ion and electron energy scales is of utmost importance. Also, for an exact ECC cusp energy determination the electrons should be measured exactly in the direction of the beam.

Earlier experiments^{4,5} revealed a definite change in the energy of the ECC cusp electrons in function of the observation angle, but no exact comparison of the measured and calculated energies was made.

The proton energy scale was calibrated with high accuracy using well defined resonances of the $^{27}\text{Al}(p,\gamma)^{28}\text{Si}$ reaction (1519.7 ± 0.2 keV ($\Gamma=3.7$ keV), 760.39 ± 0.04 keV ($\Gamma<0.04$ keV)). The energy resolution of the electron spectrometer was 5×10^{-4} , the acceptance angle at zero degree $\pm 3.2^\circ$. The maximum possible angular deviation from 0° is $\leq 0.1^\circ$, as limited by the beam-shaping collimators. The alignment of the spectrometer with the scattering chamber is much better than ± 0.04 degree. The total angular uncertainty of the center of the 0° spectrometer channel is $\leq 0.14^\circ$, the possible energy shift caused by it is negligible^{4,5}. The electron energy scale was calibrated by the Ne $\text{KL}_{2,3}\text{L}_{2,3}^1\text{D}_2$ (804.5 ± 0.1 eV^{6,7}) and the argon $\text{L}_{3}\text{M}_{2,3}\text{M}_{2,3}^1\text{D}_2$ (203.49 ± 0.02 eV⁷) Auger lines.

Table 1. Experimental and theoretical energy values for the cusp shaped peak due to ECC electrons at two proton energies in different p - noble gas atom collisions.

Target	Proton energy [keV]	Theoretical ECC electron energy [eV]	Experimental ECC cusp energy [eV]
Ar	1519.7 ± 1.5	827.68 ± 0.8	813.5 ± 2.9
Ne	1519.7 ± 1.5	827.68 ± 0.8	812.9 ± 4.6
He	1519.7 ± 1.5	827.68 ± 0.8	812.4 ± 1.5
Ar	760.39 ± 1.0	414.13 ± 0.5	408.7 ± 2.5

The results of the measurements are summarized in Table 1. The electron spectra and their theoretical estimates are presented in Fig. 1. The calculations were made according to Ref. 2 by using Roothan-Hartree-Fock target wavefunctions.

The theoretical value of the ECC cusp energy deviates from the measured one. The energy difference depends on the projectile energy.

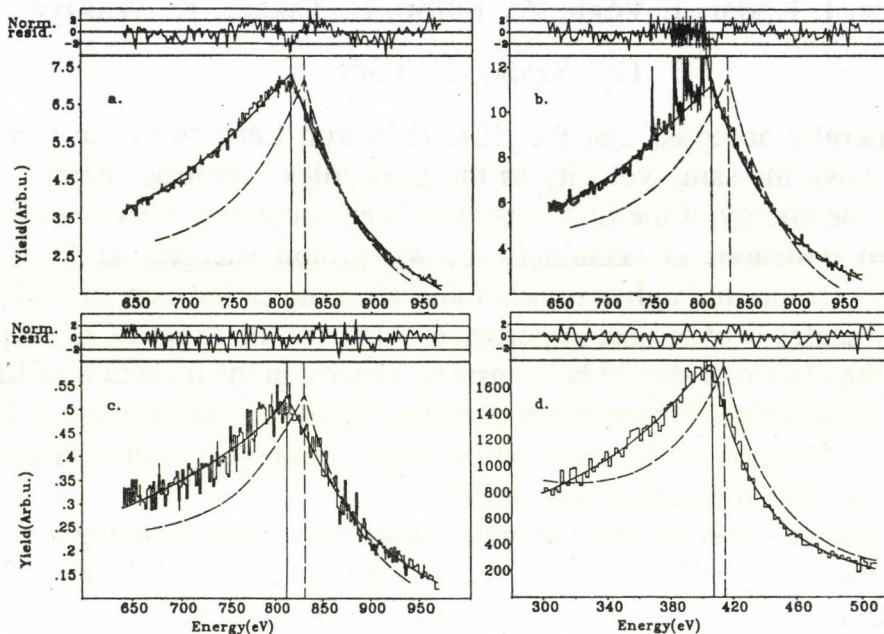


Fig. 1 Electron spectra in the ECC cusp region: a. in the 1519.7 keV p-Ar, b. p-Ne, c. p-He, and d. in the 760.39 keV p-Ar collisions. The fitted curve (continuous line), the residual and the theoretical estimate of the spectrum (dashed line) are also shown. The vertical continuous line indicates the position of the cusp peak, the dashed one its theoretical estimate.

This work was sponsored by the Hungarian National Scientific Research Foundation.

References

1. M. Breinig, S.B. Elston, S. Huldt, L. Liljeby, C.R. Vane, S.D. Berry, G.A. Glass, M. Schauer, I.A. Sellin, G.D. Alton, S. Datz, S. Overbury, R. Laubert, and M. Suter, *Phys. Rev. A* **25** 3015 (1982)
2. J.E. Miraglia, V.H. Ponce, *J. Phys. B.* **13** 1195 (1980)
3. M. Rålbjro and F.D. Andersen *J. Phys. B* **12**, 2883 (1979)
4. J. Macek, J.E. Potter, M.M. Duncan, M.G. Menendez, M.W. Lucas and W. Steckelmacher, *Phys. Rev. Lett.* **46** 1571 (1981)
5. G. Bissinger and R. Mehta, *Nucl. Instr. Meth.* **B56/57** 92 (1991)
6. L. Petterson, J. Nordgren, L. Selander, C. Nordling and K. Siegbahn, *J. El. Spectrosc. Relat. Phenom.* **27** 29 (1982)
7. G. Johanson, J. Hedman, A. Berndtsson, M. Klasson, and R. Nilsson, *J. Electr. Spectrosc. Rel. Phenom.* **2** 295 (1973)

*Permanent address: Department of Physics, Sophia University, Kioicho 7-1, Chiyoda-ku, Tokyo 102, Japan

Projectile energy dependence of the ECC cusp shape

P. Závodszky, L. Sarkadi, T. Vajnai, J. Pálinkás,
L. Gulyás and D. Berényi*

This work is a continuation of our study [1] of the asymmetry of the ECC cusp peak in $H^+ \rightarrow He$ collisions. The projectile energy range has been extended considerably in this study and now it is between 75 and 1400 keV. The proton beam has been obtained from the 1.5 MeV Van de Graaff accelerator of ATOMKI. The electron spectra were taken by a distorted-field double-pass cylindrical mirror electron spectrometer (ESA-13) at 0° ejection angle and fixed angular acceptance (about 2°).

The electron spectrometer has been calibrated using the known energies of the LMM and KLL Auger lines of Ar and Ne, respectively. The calibration spectra were taken at $\theta = 30^\circ$ and 50° relative to the beam direction where the PCI shift is expected to be very small.

To compare the velocity of the ECC cusp electrons and that of projectile, which is one of the aims of this work, it is necessary to determine precisely the beam velocity (energy). This has been achieved by a careful calibration of the analysing magnet of the accelerator. For this purpose we used the ${}^7\text{Li}(p,\alpha){}^8\text{Be}^* \rightarrow {}^8\text{Be} + \gamma$ nuclear reaction at the 340, 671 and 935 keV resonances. The target was a very thin LiF film vacuum-evaporated on Al backing. The beam current was small enough (max. 10 nA) to avoid the target contamination which is especially critical at low energy. The gamma rays were measured with a NaI(Tl) scintillator. The field of the analysing magnet was measured with an NMR based magnetometer.

We obtained the following formula between the proton energy E_p (in eV) and magnetic field B (in gauss):

$$E_p = (C \pm \Delta C) \cdot B^2$$

The values obtained for C and ΔC are shown in Tab.1.

At the fixed resonance energies of the above nuclear reaction we have taken the cusp electron spectra from the $H^+ \rightarrow He$ collision. The energy values of the maxima of these cusp spectra (ϵ^{exp}) are also shown in Tab.1, together with the corresponding theoretical energy values (ϵ^{th}) calculated assuming $v_e = v_p$. An excellent agreement can be observed between the two electron energy values. This verifies the theoretical assumption that the projectile and the ECC cusp electron have the same velocity at the maximum of spectrum.

To analyse the asymmetry of the ECC cusp we have taken 14 spectra of good statistics, every spectra in the velocity range from $0.9 v_e$ to $1.1 v_e$. These spectra corrected for the spectrometer efficiency and constant relative energy resolution (about 0.0025), are shown in Fig.1.

The shape analysis is in progress. We use the method proposed by Meckbach et al.[2] based on the series expansion of the cross-section. We wish to compare our experimental results with the recent theoretical results obtained by Moiseiwitsch [3].

Tab.1. The proton energies (E_p), the calibration constants (C) obtained and used to calculate the theoretical energy (ϵ^{th}) of the ECC cusp. The ϵ^{exp} values are the measured energies of the maximum of the ECC cusp.

E_p (keV)	$C \pm \Delta C$	ϵ^{th} (eV)	ϵ^{exp} (eV)
340 ± 1.0	0.1838 ± 0.0005	185.2 ± 0.5	185.5 ± 0.4
671 ± 2.6	0.1837 ± 0.0007	365.5 ± 1.4	365.6 ± 0.6
935 ± 2.0	0.1847 ± 0.0004	509.3 ± 1.0	508.5 ± 0.8

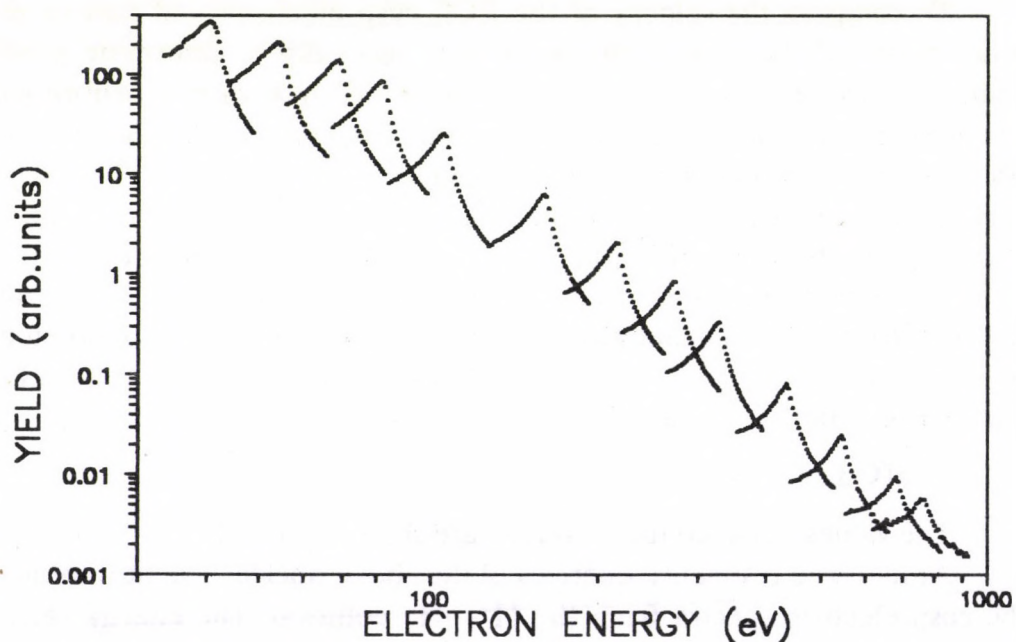


Fig.1. Electron energy spectra of the ECC cusp at different impact energies in $H^+ \rightarrow He$ collisions.

This research work was supported by OTKA Grant no.3011.

References

- On leave from the University of Miskolc, H-3515 Miskolc
- 1. Gulyás, A. Kövér, Gy. Szabó, T. Vajnai, D. Berényi: 4th Workshop on High-Energy Ion-Atom Collision Processes, Debrecen 1990, Lecture Notes in Physics, eds. D. Berényi and G. Hock (Springer, Berlin 1991) p.56
- 2. W. Meckbach, I.B. Nemirovsky, C.R. Garibotti: Phys. Rev. **A24**(4), 1793 (1981)
- 3. B.L. Moiseiwitsch: J. Phys.: At. Mol. Opt. Phys. **24**, 983, (1991)

Versatility of the CTMC exit channels in 3-body collisions

K. Tőkési and G. Hock

In atomic collisions investigated in terms of the Classical Trajectory Monte Carlo (CTMC) methods Newton's (e.g., [1]) or Hamilton's (e.g., [2]) classical (non-relativistic) equations of motions are used for the three-body system of colliding (bare or 'dressed') particles. These systems of coupled differential equations are solved numerically for a statistically large number of trajectories with initial conditions determined pseudorandomly.

We developed a CTMC computer code [3,4] for calculating total cross sections of processes in atomic collisions, in which we assumed three bare particles to have arbitrary masses and charges and the forces acting among the three bodies were taken to be pure Coulombic ones. The projectile (particle 1) collided with a target (particles (2,3) with the nucleus (particle 3) and electron (particle 2)) chosen always to be bound and characterized by means of Kepler orbits oriented randomly in space [5].

In most of the CTMC calculations of atomic collisions in literature, only the three main channels, the direct inelastic (involving the quasielastic), break-up and simple rearrangement (such as charge transfer) channels are taken as final channels. The splitting up of the phase space among the final channels is however, motivated by the aim of the given tasks. Thus, one distinguishes sometimes between different break-up processes e.g., direct, transfer [1] or saddle-point [6] ionization as well.

Following from the general assumptions on the three particles involved in the collisions, we had to extend the categories of the final channels step-by-step, since we observed various 'non-regular' cases. Among them, there appeared need to include the (positive / negative) particle exchange and quasibound 3-body (negative ion / quasi-molecule) channels, too. These latter are alternatives of each other, corresponding to the kinds of charges of the 3 particles. Finally, to our knowledge, there is no direct proof to exclude the 3-particle bonding channel of a molecule.

Particle exchange processes were observed in a non-negligible amount for identical particles, while 3-body (quasi-)bound states are strongly 'integration time-dependent' so their real existence need further careful investigations.

Table 1. Test conditions for the final states considered. A plus sign means that the test must be passed, a minus sign that it must not be passed, and a zero that it is not made. The entries and quantities are defined as follows: D:= direct (excitation), DI:= direct ionization, TI:= transfer ionization (ECC), CT:= charge transfer (EC), EX:= 'negative' particle exchange, TX:= 'positive' particle exchange, NI:= negative ion state, QM:= quasi-molecular state, MO:= molecular state, E_{Pe} := centre-of-mass energy of (Pe) at time $t(+\infty)$, E_{Te} := centre-of-mass energy of (Te) at time $t(+\infty)$, E_{TP} := centre-of-mass energy of (TP) at time $t(+\infty)$, V_{Pe}^L := velocity of the (Pe) system in lab, V_T^L := velocity of the Target in Lab, $E_{3B(rel)}$:= 3-body relative energy, \vec{A} , \vec{B} , \vec{C} relative positions of three particles, \vec{V}_A , \vec{V}_B , \vec{V}_C relative velocities of three particles, U := total potential energy of the electron in the total field of particles P and T , U_0 := maximum value of U

Test	D	DI	TI	CT	EX	TX	NI	QM	MO
$A < C$	0	+	-	0	0	0	0	0	0
$E_{Pe} > 0$	+	+	+	0	0	0	+	-	-
$E_{Te} > 0$	0	+	+	+	+	+	-	-	-
$E_{Pe} < U_0$	0	0	0	+	0	+	0	0	0
$E_{Te} < U_0$	+	0	0	0	0	0	0	0	0
$\vec{A} \vec{V}_A$	0	+	+	0	0	0	0	0	0
$\vec{B} \vec{V}_B$	+	0	0	+	0	+	0	0	0
$\vec{C} \vec{V}_C$	0	+	+	0	+	0	0	0	0
$B < A$	0	0	0	0	+	0	0	0	0
$E_{TP} < U_0$	0	-	-	0	+	0	0	0	0
$V_{Pe}^L < V_T^L$	0	0	0	-	0	+	0	0	0
$E_{3B(rel)} < 0$	0	0	0	0	0	0	0	-	+
$E_{TP} < 0$	-	0	0	0	0	0	+	0	0

References

- [1] R. Abrines and I.C. Percival, Proc. Phys. Soc. **88** (1966) 861, 873
- [2] R.E. Olson, and A. Salop, Phys. Rev. **A16** (1977) 531
- [3] K. Tökési and G. Hock, ATOMKI Ann. Rep. **1989** (1990) 49
- [4] K. Tökési and G. Hock, *submitted to Am. J. Phys.*
- [5] J.S. Cohen, Phys.Rev. **A26** (1982) 3008
- [6] G. Bandarage and R. Parson, Phys. Rev. **A41** (1990) 5878

Total Cross Sections in $\mu^\pm, \pi^\pm \rightarrow \text{H}(1s)$ Collisions

*G. Hock*¹, *K. Tőkési*¹, *H. Nakamatsu*² and *T. Mukoyama*²

¹ Institute of Nuclear Research of the Hungarian Academy of Sciences (ATOMKI),
H-4001 Debrecen, P.O.Box 51, Hungary

² Institute for Chemical Research, Kyoto University, Uji, Kyoto-Fu, 611 Japan

The collision systems $\mu^\pm, \pi^\pm \rightarrow \text{H}(1s)$ are treated in the 3-body Classical Trajectory Monte Carlo (CTMC) approximation. The total cross sections of direct (excitation), break-up (ionization), transfer and exchange processes (if any), simultaneously obtained in the CTMC calculations are determined with (full 3-body) and without the inclusion of the projectile—target potential (restricted 3-body). This latter case simulates the straight-line semiclassical or plain wave Born approximations.

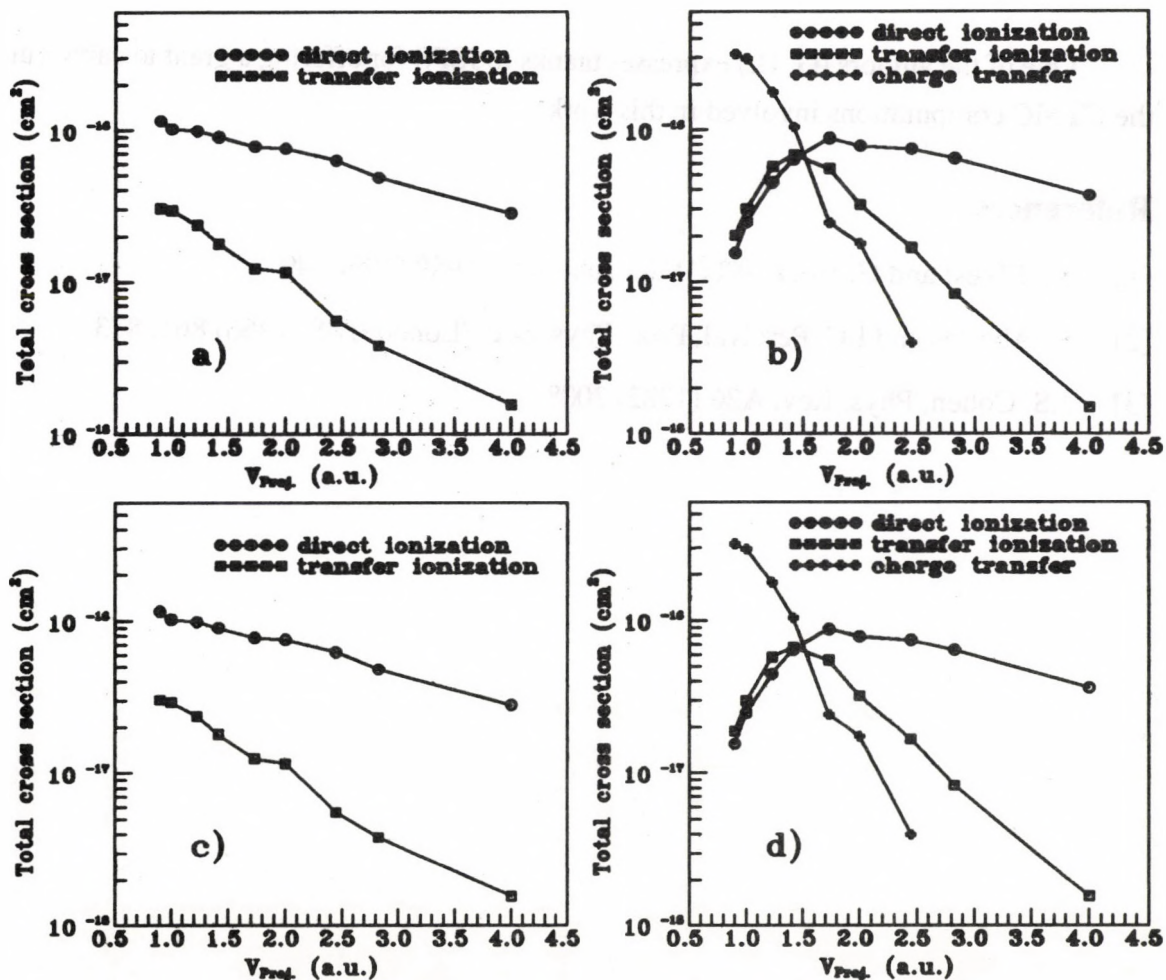


Fig.1. Total cross sections of the $\mu^\pm, \pi^\pm \rightarrow \text{H}(1s)$ collisions as functions of the projectile velocity for full 3-body CTMC calculations. The projectile is: a) μ^- , b) μ^+ , c) π^- , d) π^+ .

The calculations were carried out in the Computer Centre of Kyoto University, Uji, using the CTMC code written earlier [1]. These calculations are based on the 3-body CTMC method by the authors [2,3] for bare Coulomb particles. Results are seen in Fig. 1, for the different projectiles and full 3-body case. No significant exchange processes have been registered, therefore such data are missing from the figures. The excitation cross-sections (including the elastic channel), at the same time, amount to about 1–2 orders of magnitude larger than the ionization and capture cross-sections.

These kinds of data may be instructive for e.g. muon catalysed fusion calculations or experiments, where the presence of these inelastic channels may influence the productive mechanisms in the fusion. The calculations may be extended to include real life times of the decaying particles involved in the collisions and to determine channel probabilities along with cross sections and towards various states and kinds of target atoms.

One of the authors (G. H.) expresses thanks to JSPS for offering a grant to carry out the CTMC computations involved in this work.

References

- [1] K. Tókési and G. Hock, *ATOMKI Ann. Rep.* **1989** (1990) 49
- [2] R. Abrines and I.C. Percival, *Proc. Phys. Soc. (London)* **88** (1966) 861, 873
- [3] J.S. Cohen, *Phys. Rev.* **A26** (1982) 3008

Al K_{α} satellite polarization measurements in metal and in sapphir (Al_2O_3)

V. P. Petukhov ¹, I. Török, P. Závodszy, J. Pálinkás, L. Sarkadi

¹Moscow State University, Institute of Nuclear Physics, Moscow, USSR.

In the last two decades several attempts were made to measure and calculate the degree of polarization of X-ray satellite transitions [1-6]. Most of these studies dealt with the K satellites of Al metal. It is expected that the degree of polarization of X-rays from an atomic species in different chemical environment (different electron density in the neighbourhood of the radiating atom) will also be different. We measured the polarization of Ti K_{α} satellites from metal and different titanates (perovskite type crystal form) [7], but the resolution and statistics permitted only to get an average value for the polarization of the whole KL^1 satellite group of metallic Ti. For aluminium we could get much better resolution and statistics, therefore we started to determine the polarization for this metal and for one of its oxides, sapphir.

Our Soller-type X-ray polarimeter [8] installed on the beam line of the 5 MV Van de Graaff generator of ATOMKI was used to measure the K_{α} satellites of aluminium. A 99.99% purity aluminium metal disc of 1 mm thickness and a disc of a sapphir substrate (used in semiconductor industry) of 0.3 mm thickness were bombarded by 3.2 MeV He^+ ions. The $K_{\alpha}L^0$ - $K_{\alpha}L^3$ region was scanned several times, and the spectra were summed up to obtain good statistics (about 16 000 pulse/channel for the metal, and about 2700 pulse/channel for the oxide in the most intense peak).

The evaluation of the summed spectra by the EWA code [9] is in progress. The nominal energies of the distinct satellite features like $K_{\alpha'}$, $K_{\alpha 3}$, $K_{\alpha 4}$ [10] are used in the fitting. For both target materials, and for both measuring positions (i. e. parallel and perpendicular relative to the incoming ion beam) the intensities of the satellite features will be determined, relative to the $K_{\alpha 1}$ peak. The degree of polarization will be calculated from these relative intensities. At the present stage of evaluation it seems that for the sapphir the degree of polarization is smaller, than for the metal.

The results of these measurements will be compared to the values obtained from former similar measurements and theoretical estimations for Al metal [1-6]. Similar measurements have been performed recently in Berlin at the Humboldt University, with the participation of one of the authors (V. P. P.), where the target was also Al metal, but the bombarding particles were 350 keV protons. The experiments were performed also by a polarimeter of Moscow- design, and we intend to use the same evaluation process for the spectrum fitting, etc..

This work was supported by OTKA, grant: No. 3011.

References

1. K. A. Jamison, Patrick Richard, Phys. Rev. Lett. **38** (1977) 484.
2. K. A. Jamison, Patrick Richard, F. Hopkins, D. L. Matthews, Phys. Rev. **A17** (1978) 1642.
3. G. J. Pedrazzini, J. Palinkas, R. L. Watson, D. A. Church, R. A. Kenefick, Nucl. Instrum. Meth. **B10/11** (1985) 904.
4. B. Cleff, Acta Phys. Pol. **A61** (1982) 285.
5. L. Kocbach, K. Taulbjerg, in Tenth International Conference on the Physics of Electronic and Atomic Collisions, Paris, 1977 (CEA, Paris, 1977), p.44.
6. E. Merzbacher, J. Wu, in Tenth International Conference on the Physics of Electronic and Atomic Collisions, Paris, 1977 (CEA, Paris, 1977), p.46.
7. V. P. Petukhov, S. M. Blokhin, I. Török, P. Závodszy, J. Pálinkás, L. Sarkadi, T. Papp, B. Sulik, E. Takács: Polarization measurements of light element $K_{\alpha}L^n$ x-ray satellites; poster at International Symposium on Ion-Atom Collisions - ISAC XII, Ana Hotel, Gold Coast, Australia, 18-19 July 1991.
8. V. P. Petukhov: Prib. Tech. Expt., No.1, p. 195 (1990) (*in Russian*)
9. J. Végh: Thesis, 1990, ATOMKI, Debrecen
10. Y. Cauchois, C. Senemaud: *Wavelengths of X-ray emission lines and absorption edges*, Pergamon Press, Oxford, etc., 1978.

The Rough Determination of Ti $K_{\alpha 5}$ and $K_{\alpha 6}$ X-Ray Satellite Energies at Ion Bombardment

I. Török, P. Závodszy

When the energy resolving power of our Soller-type X-ray crystal spectrometer was measured, a lot of K spectra of different elements from Mg to Cu have been taken. Some of the satellites could be seen, e. g. for Ti. In the first evaluations these satellites were not used, being rather weak, especially in the KL^2 group, and taken with not too good resolution. Later we needed the energy values mentioned in the title of this paper, but we could not find them in X-ray line catalogs, like [1], and in the current literature, either these or any other $K_{\alpha 5}$ and $K_{\alpha 6}$ lines for the 4th row elements. For Ti Hill et al.[2] gave an average energy of the KL^2 satellite group in the case of He ion bombardment: 4.5598 keV.

Therefore we decided to determine these values from our old calibration spectra. The 3.2 MeV He-ion induced Ti K_{α} spectrum—scans were summed up, and at first we graphically determined the values. As a test we also determined these values from a paper [3], where only a rough figure contained the information we needed. Fig. 2. of [3] gave a K_{α} spectrum of Ti bombarded by 125 MeV Xe^{8+} ions. (From this source we could estimate also the rough energy values for $K_{\alpha 8}$ and $K_{\alpha 9}$ satellite lines as 4.5954 and 4.6127 keV respectively.) Table 1. gives the numerical results from different determinations. Later using the EWA code [4], a third pair of data has been got. Fig. 1. shows the spectrum from the He ion bombarded Ti, fitted by the EWA. Equal width pseudo-Voigt peak shapes were used. The data obtained from it are presented as the third row of the table. (It is interesting to compare the manual and machine-made results.)

All these results are only rough estimations of the real value, because also the M shell is ionized in the energetic collision, especially in the case of the Xe ions. Several eV displacements are due to this effect. Even if the energy resolution is much better, this problem remains. However, these approximate energy values helped us in fitting the Ti spectra, when we were measuring the polarization degree of Ti K_{α} satellites [5].

Table 1.. Ti $K_{\alpha 5}$ and $K_{\alpha 6}$ X-ray satellite energies obtained by different methods.

	$K_{\alpha 5}$ [energy in keV]	$K_{\alpha 6}$ [energy in keV]
From Fig.1. graphically	4.5621	4.5721
From Fig.2. of [3] graphic.	4.5662	4.5725
From Fig.1. by EWA	4.5627±2.6eV	4.5701±1eV

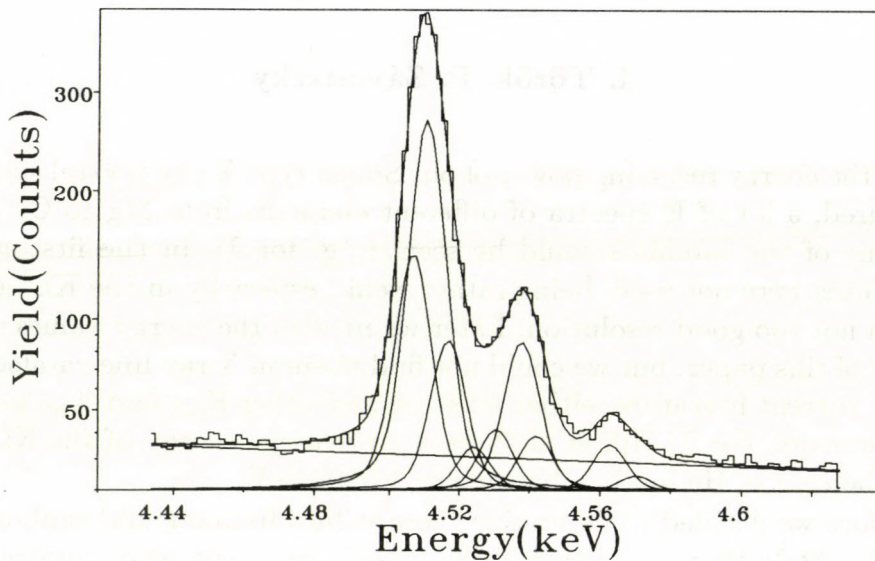


Fig. 1. K_{α} spectrum obtained by an ADP analyzer crystal in the third order of reflection, from He ion excited Ti metal. The nominal Soller-collimator divergence is about 0.3 degree.

In the meantime we got a finer Soller-collimator, so it is planned to repeat this measurement by higher resolution and with better statistics.

This work was supported by OTKA, grant No 3011.

References

1. Y. Cauchois, C. Senemaud, *Wavelengths of X-ray emission lines and absorption edges*, Pergamon Press, Oxford, etc., 1978.
2. K. W. Hill, B. L. Doyle, S. M. Shafroth, D. H. Madison, R. D. Deslattes, *Phys. Rev. A* **13** (1976) 1334.
3. V. A. Altynov, M. A. Blokhin, S. M. Blokhin, A. A. Polyakov, A. G. Artyukh, A. V. Eremin, *Izv. A. N. SSSR, ser. phys.* **46** (1982) 745.
4. J. Végh, *Thesis*, 1990, ATOMKI, Debrecen.
5. V. P. Petukhov, S. M. Blokhin, I. Török, P. Závodszy, J. Pálinkás, L. Sarkadi, T. Papp, B. Sulik, E. Takács: Polarization measurements of light element $K_{\alpha}L^n$ x-ray satellites; poster at International Symposium on Ion-Atom Collisions - ISIAC XII, Ana Hotel, Gold Coast, Australia, 18-19 July 1991.

PIXE with Crystal Spectrometer, Using Different Orders of Reflection

I. Török

Closely spaced higher order and lower order reflections can be used to determine element ratios. The method is based on empirical calibration curves giving the K_α peak area ratios as a function of element (or its compounds) concentration ratio. If the low intensity higher order peak comes from the major element and the lower order strong reflection peak is originated from a minor element one can determine efficiently a minor lower Z element in a sample of a major higher Z element. As an example we have measured small amounts of Mg in the presence of much Ca, using first order Mg K_α and third order Ca K_α lines. Such measurements can be optimized by using proper analyzer crystal, efficient position sensitive detector for the X-rays, selective excitation (performing measurements at bombarding energies, where the cross section of X-ray production is at about the maximum for the minor element), and by using low absorption materials in the X-ray path (windows of detector and vacuum chamber, etc.).

The Mg/Ca ratios are important data for geologists for limestones. The so-called dolomitization grade gives some information on the genetics of the stone, one can conclude what type of water the stone was sedimented from. The durability of concretes also strongly depends on Mg content.

First we recognised this possibility from a spectrum of a natural limestone from the Bükk mountains (northern Hungary) [1,2]. We made a series of calibration measurements on artificial $\text{CaCO}_3 + \text{MgCO}_3$ mixtures at 2 MeV proton bombarding energy [3-5]. Later a more precise series of measurements was performed using 1 MeV protons.

Fig. 1 gives a spectrum obtained from an artificial $\text{CaCO}_3 + \text{MgCO}_3$ sample, showing that without changing analyzer crystal (in our case ADP), one can get well separated peaks. Fig. 2. shows a calibration curve deduced from spectra of different composition mixtures of the two materials. Such measurements at the moment are too expensive and difficult for geologists, who would like to get the information in the terrain. At the same time for other element pairs, perhaps in semiconductor industry or in materials science one can use the method efficiently, because in these industries many small accelerators are already in use.

Further information on this method can be found in two recently published work from our laboratory [6,7].

The high resolution PIXE method is available at many accelerators, but its proper applications are not really found. ¹ Perhaps from discussing as much material as possible, a promising direction for the high resolution PIXE research can be drawn.

¹ The author would like to prepare a review of the available systems and the applications attempted to use them, therefore any contributions made in this field are welcome, including reprints, preprints, research reports, personal views, etc..

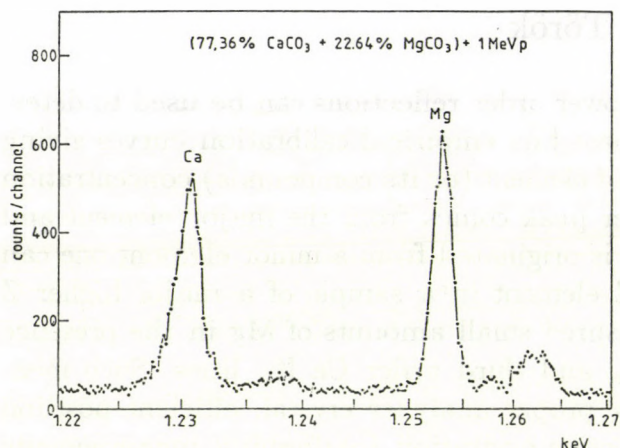


Fig. 1. Third order Ca and first order Mg K_{α} peaks, taken by an ADP crystal from a $\text{CaCO}_3 + \text{MgCO}_3$ mixture.

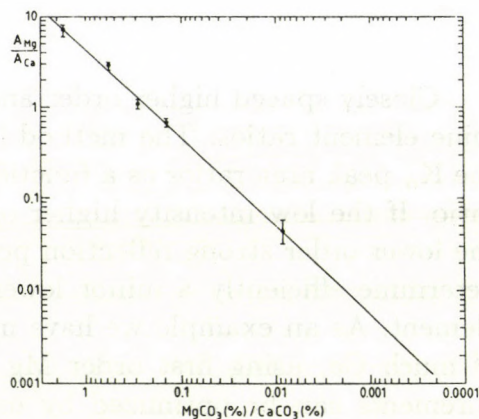


Fig. 2. A calibration curve deduced from measurements of different composition mixtures of the two materials.

Acknowledgement. Thanks are due to Zs. Türk and A. Ágoston for their help. The stable ion beams produced by the crew of the Van de Graaff generator is highly appreciated. This work was partly supported by the OTKA grants No. 1184-85, and No. 576.

References

1. I. Török, B. Tóth, *J. Physique* **48**(1987)C-9, 79.
2. I. Török, B. Tóth, *ATOMKI Ann. Rep.* 1987(1988)p. 66.
3. I. Török, *ATOMKI Ann. Rep.* 1988(1989)p. 49.
4. I. Török, *Radioisotopy* **31**(1990)98.
5. I. Török, *Izotóptechnika, Diagnosztika* **33**(1990)161.
6. I. Török, *Nucl. Instrum. Meth.* **B61**(1991)94.
7. I. Török, *Nucl. Instrum. Meth.* **B** in print. Proceedings of the 2nd ECAART conf.

Ionization of H_2 by proton impact

I. Single ionization

L. Nagy and L. Végh

The knowledge of the total and differential ionization cross sections is a basic requirement for many fields connected with the interaction of radiation with the matter. While in many cases, the irradiated material has some molecular structure, the available cross section values have been measured mainly for atomic or simpler molecular targets. Generally, using the recommended cross section values, the molecular character of the irradiated matter is neglected. Really, making some binding energy modification to take into account the different binding energies in atomic and molecular orbitals, the total cross sections can be well described approximating the molecule as an entity of its atoms.

In paper[1] we investigate the approximation of molecular cross sections by the sum of cross sections of the constituent free atoms. For the investigation we have chosen the simplest diatomic system, the hydrogen molecule. We discuss the problem why the assumption, that the molecular hydrogen is identical with two independent hydrogen atom, is so successful in the description of proton induced ionization cross sections.

To analyse the significance of two-center effects, we use simple Heitler-London type molecular wave functions as a target wave function to calculate the ionization amplitudes. Single ionization cross sections of the proton - hydrogen molecule collision are calculated in semiclassical approximation by using atomic and Heitler-London like two-center molecular wave functions for ground state of H_2 . In transition matrix elements calculated with two-center wave functions the factors depending on $|\mathbf{r} - \boldsymbol{\rho}/2|$ ($\boldsymbol{\rho}$ is the vector of the molecular axis) are expanded into Legendre series. The calculated cross sections are compared to the data and the dependence of the cross sections on target wave functions are discussed.

The success of approximation using the twice the calculated cross sections for hydrogenic atoms is explained by the dominance of monopole contributions in the expansion in terms of $\boldsymbol{\rho}$. While for homonuclear diatomic molecules the differential cross sections could be well described as twice of the atomic cross sections, for other molecules such approximations may be inaccurate for the calculation of total and mainly for differential cross sections.

References

1. L. Nagy and L. Végh submitted to Phys. Rev. A

Ionization of H_2 by proton impact

II. Two-electron processes

L. Nagy and L. Végh

The cross sections for two-electron processes that occur during collisions of fast charged projectiles have been reported recently by Edwards et al[1-3]. These processes have included double ionization and ionization plus excitation channels. The projectiles interact with the H_2 molecule forming dissociative states of H_2^{++} and H_2^+ . The fragments that are ejected from these dissociative states were analyzed[1-3] at specified angles relative to the beam direction.

Cross sections for the double ionization and ionization plus excitation of H_2 by high-energy protons have been calculated in independent electron approximation as a function of orientation of the internuclear axis of the molecular target. The model is formulated using the semiclassical (SCA) approximation where the projectile path is described classically. The ground state of the target is described by Heitler-London type wave functions and the molecular orbitals for the excited states of H_2^+ are constructed from Slater-type atomic functions. We have restricted ourselves to study of the double-collision mechanism when the projectile interacts separately with each electron to produce the final state.

The calculated cross sections have been compared to the data of Edwards et al. The calculated and measured cross sections have the same magnitude for double ionization but the contribution of other mechanisms involving electron-electron interactions are relevant to reproduce the differences between the cross sections induced by protons and electrons. The remarkable dependence of the calculated cross sections on the target wave functions suggests that the model could be improved by using more realistic H_2 wave functions, too. For the excitation of the $2p\sigma_u$, $2p\pi_u$, and $2s\sigma_g$ states the calculated cross sections are much lower than the measured ones. The small values of the calculated cross section suggests that the double-collision mechanism does not give the dominant contribution to the amplitude of the ionization plus excitation processes. The details are discussed in paper[4].

References

1. A. K. Edwards, R. M. Wood, J. L. Davis, and R. L. Ezell: Phys. Rev. A **42** 1367 (1990) and Phys. Rev. A **44** 797 (1991)
2. A. K. Edwards, R. M. Wood, M. W. Dittmann, J. F. Browning, M. A. Magnan, and R. L. Ezell: Nucl. Instrum. Meth. Phys. Res. B **53** 472 (1991)
3. R. L. Ezell, A. K. Edwards, R. M. Wood, M. W. Dittmann, J. F. Browning, and M. A. Magnan: Nucl. Instrum. Meth. Phys. Res. B **56/57** 292 (1991)
4. L. Nagy and L. Végh submitted to Phys. Rev. A

Determination of a $\beta_2 > 0$ value at the cusp shape study in He^+ -He collision

L. Gulyás, L. Sarkadi, J. Pálinkás, Á. Kövér, T. Vajnai ¹,
Gy. Szabó, J. Végh, D. Berényi and S.B. Elston ²

¹University of Miskolc, Physics Department, H-3515 Miskolc, Hungary

²University of Tennessee and Oak Ridge National Laboratory, Oak Ridge, Tennessee, P.O.Box 2008, USA

There are theoretical predictions [1,2] according to which at low impact energy values (less than several hundred keV), the β_2 values in the series expansion analysis [3] of the ELC cusp in the emitted electron spectrum should be positive. The positive value of β_2 means a so-called cusp inversion (cf. ref. 1,2).

The study of this phenomenon, however, is rather difficult. First of all, in the case of He^+ impact there is a possibility for an ECC contribution as well and so to study the ELC cusp a coincidence arrangement should be applied (e-spectrum in coincidence with He^{2+}). In the impact energy region concerned, however, the relative ELC contribution is only 5-10 per cent [4] and thus a rather long measuring time is needed to obtain experimental values of good statistics enough.

In this study we used the same experimental arrangement at the 1.5 MV Van de Graaff accelerator of ATOMKI which was used before [4].

The singles and coincidence spectra were taken in the collision $\text{He}^+(200 \text{ keV}) - \text{He}$ and they were analysed by the series expansion method in the cusp region of the spectra.

In Table 1 the values of the experimentally determined parameters are given for the coincidence spectrum in comparison with the theoretical values. It can be seen that the parameter β_2 is definitely positive and its value is not in contradiction with the theoretical values calculated in PWBA approximation with analytic Roothaan-Hartree-Fock wave functions for the target electrons [5]. On the basis of the present experimental data, however, the relative 1s-2s contribution cannot be determined.

In this study a non-zero value of β_1 was also found which is not allowed for ELC cusp according to the first Born approximation.

Further details is given on the whole investigation in ref. [6].

Table 1. Cusp-shape parameters β_1 and β_2 at He^+ (200 keV) impact determined on the basis of electron - outgoing He^+ projectile coincidence measurements

	Target		
	He		
	exp	theor.+	
1s		2s	
β_1	0.28 ± 0.10		
β_2	0.35 ± 0.18	0.18	0.28

⁺There is a possibility for the mixture of the proportion of the different initial 1s and 2s states [6].

References

- 1 J. Burgdörfer, M. Breinig, S.B. Elston and I.A. Sellin, *Phys. Rev. A* **28** 3277 (1983)
- 2 J. Burgdörfer, *Phys. Rev. Lett.* **51** 374 (1983)
- 3 W. Meckbach, I.B. Nemirovsky and C.R. Garibotti, *Phys. Rev. A* **24** 1973 (1981)
- 4 Á. Kövér, L. Sarkadi, J. Pálinkás, D. Berényi, Gy. Szabó, T. Vajnai, O. Heil, K.O. Groeneveld, J. Gibbons and I.A. Sellin, *J. Phys. B* **22** 1595 (1989)
- 5 Gy. Szabó, J. Burgdörfer and Á. Kövér, *ATOMKI Ann. Rep.* 1989, Debrecen, 1990, p.43
- 6 L. Gulyás, L. Sarkadi, J. Pálinkás, Á. Kövér, T. Vajnai, Gy. Szabó, J. Végh, D. Berényi and S.B. Elston, in course of publication in *Phys. Rev. A*

Determination of 3p and 3d core-level widths in ammonium pertechnetate by internal conversion electron spectroscopy

I. Cserny and L Kövér, V. Brabec*, M. Fišer*, O. Dragoun* and J. Novák*
 *Nuclear Physics Institute, Czechoslovak Academy of Sciences, 250 68 Rez near to Prague

The applicability and use of internal conversion electron spectroscopy (ICES) in the determination of 3p and 3d core-level widths in metallic technetium have been demonstrated in a previous study [1]. Here we present an extension of that work: 3p and 3d core-level widths in a non-metallic sample (NH_4TcO_4) have been determined experimentally.

Source preparation and measurements [1] were carried out at Nuclear Physics Institute, Rez near Prague. Peak positions, background parameters and FWHM values have been determined by the EWA v2.23 program[2].

The 3d level widths have been determined from the comparison of M4, M5 ICES spectra measured earlier [1] on non-metallic (NH_4TcO_4) and metallic Tc samples assuming that these spectra are identical except for the difference in the lifetime broadening, and the metallic state produces asymmetric line-shape in contrary to the fairly symmetric lines observed from the non-metallic state. The pertechnetate M4, M5 lines were fitted by using Voigt line profiles and linear background. In the case of metallic Tc M4, M5 spectra a more complicated model (Doniach-Sunjić profile convoluted by a Gaussian and Tougaard background) was used. The overall widths evaluated from the pertechnetate M4,5 lines are higher by about 0.1 eV than that of the Tc M5 line (Table 1). This small change may be partially or completely caused by the difference in the phonon broadening between the two samples.

The determination of 3p core-level widths in NH_4TcO_4 based on the assumption that the shape of the M2 and M3 conversion lines (Fig. 1) is similar to that of the M5 line except for the difference in the lifetime broadening. Folding the measured M5 conversion line with Lorentzians of different widths and comparing the line obtained this way to the measured M2,3 lines, the difference between the M5 and M2 or M3 level widths can be obtained (Fig. 2). The resulted value (2.05 ± 0.1 eV) is very close to the value determined earlier [1] for Tc metal.

Table 1. Core level widths and kinetic energy of conversion electrons determined in this work compared with values obtained for metal[1].

Level	Level width [eV]		Kinetic energy [eV]	
	metal	NH_4TcO_4	metal	NH_4TcO_4
3p _{1/2}	2.08(15) ^a	2.27(20)	1726.5(2) ^a	1721.3(2)
3p _{3/2}	2.08(10) ^a	2.27(20)	1746.3(2) ^a	1741.2(2)
3d _{3/2}	0.48(15) ^a	0.22(10)	1916.1(2) ^a	1910.8(2) ^a
3d _{5/2}	0.13(10) ^a	0.22(10)	1919.9(2) ^a	1914.4(2) ^a

^a data taken from Ref. 1

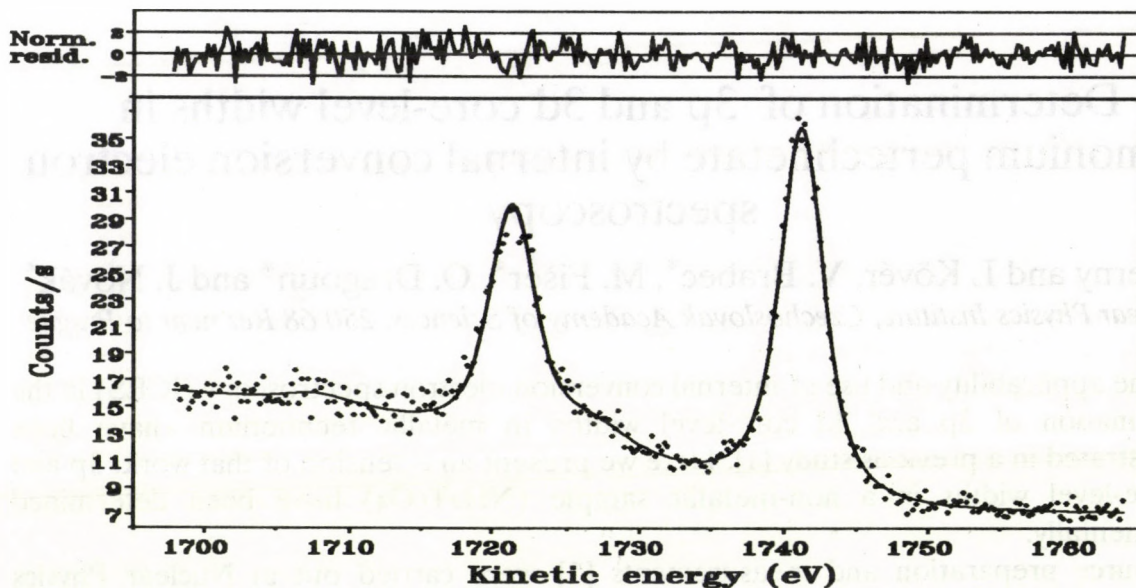


Fig. 1 The M2,3 conversion spectrum from a NH_4TcO_4 sample fitted by Voigt profiles and Tougaard background.

The pertechnetate level width values determined by us (Table 1) may also contain an unknown contribution from phonon broadening. The corresponding value for Tc metal was estimated at 95 meV [3].

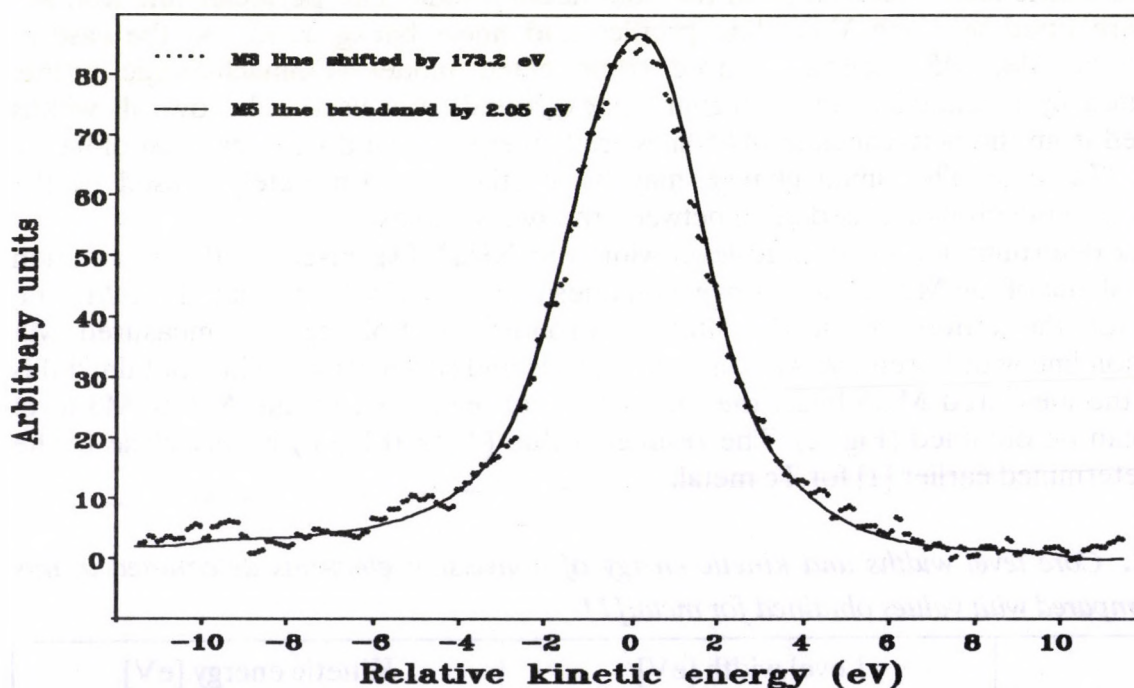


Fig. 2 The M3 conversion spectrum from a NH_4TcO_4 sample compared to the M5 line broadened by a Lorentzian having an FWHM of 2.05 eV

References

1. L. Kövér, I. Cserny, V Brabec, M. Fiser, O. Dragoun and J. Novák, Phys. Rev. B, Vol 42, No 1, (1990) 643
2. J. Végh, unpublished
3. L. Kövér, I. Cserny, V Brabec, M. Fiser, O. Dragoun and J. Novák, Proceedings of ECASIA 89, Surface and Interface Analysis, Vol 16, No 1-12, (1990) 215

Coupled-States Model Calculations of the L_3 -Subshell Alignment Induced by Ion Bombardment in Ag and U

L. Sarkadi and T. Mukoyama [†]

The subshell coupling effects are known to influence the ionization of the L subshells significantly, especially for heavy-ion impact. For the inclusion of these effects into the standard first-order descriptions of the ionization process (PWBA, SCA) the so-called coupled-states model has been developed [1]. The model is based on the solution of eight coupled equations governing the time-evolution of the L-substate amplitudes. The coupling effects are expressed in the form of a correction factor (for each subshells), which can be applied to cross sections obtained from an accurate first-order theory. Due to the great complexity of the problem, the correction factors are determined using series of approximations. In spite of the simplifications, the coupled-states model has been successfully applied for the interpretation of measured subshell cross sections, subshell ratios, ionization probabilities, and L_3 -subshell alignment.

Recent alignment measurements provided further possibilities to test the performance of the model. Jesus and Ribeiro [2] studied the L_3 -subshell alignment of uranium induced by protons and alpha particles in the energy range 0.35–1.00 MeV/nucleon by measuring the angular distribution of the L_1 x-ray line. They compared the results of the experiments to our previous second-order SCA and coupled-states model calculations. They concluded that the agreement between the experiment and theory was good. Unfortunately, a firm conclusion could not be drawn from their comparison, because the calculations had been made for gold, and the use of the same alignment parameters for uranium was questionable.

Meierkord *et al.* [3] have measured L_3 -subshell alignment parameters for Mo and Ag target following impact ionization by ions with atomic number $Z_1=2-18$. The measurements were performed with a high-resolution crystal spectrometer in order to get information about the amount of the multiple ionization. Significant deviations have been observed between the experimental data and the alignment parameters calculated in a first-order theory. The deviations were attributed to multiple ionization effects, as well as to possible subshell coupling effects.

To analyse the results of the above experiments theoretically, we have performed coupled-states calculations for p, He, N on Ag and p, He on U collisions. Making the calculations we have applied several further approximations to improve the model. For example, according to the suggestion of Legrand *et al.* [4], we used such renormalized interaction matrix elements, which were in accordance with the experimental binding energies of the united atom in the limit of the very slow, adiabatic collisions. A significant improvement in the description of the experimental data was achieved correcting one of the basic assumptions of the model connected with the energy transfer to the ionized electron. Until now only excita-

tions with minimum energy transfer were considered, in the modified version these were replaced by excitations with an average energy transfer.

The calculations reproduced the main tendencies of the experimental data, but the agreement is only qualitative (for uranium see fig.1.). Further improvement is expected replacing the non-relativistic hydrogenlike wave functions in the model by more realistic ones.

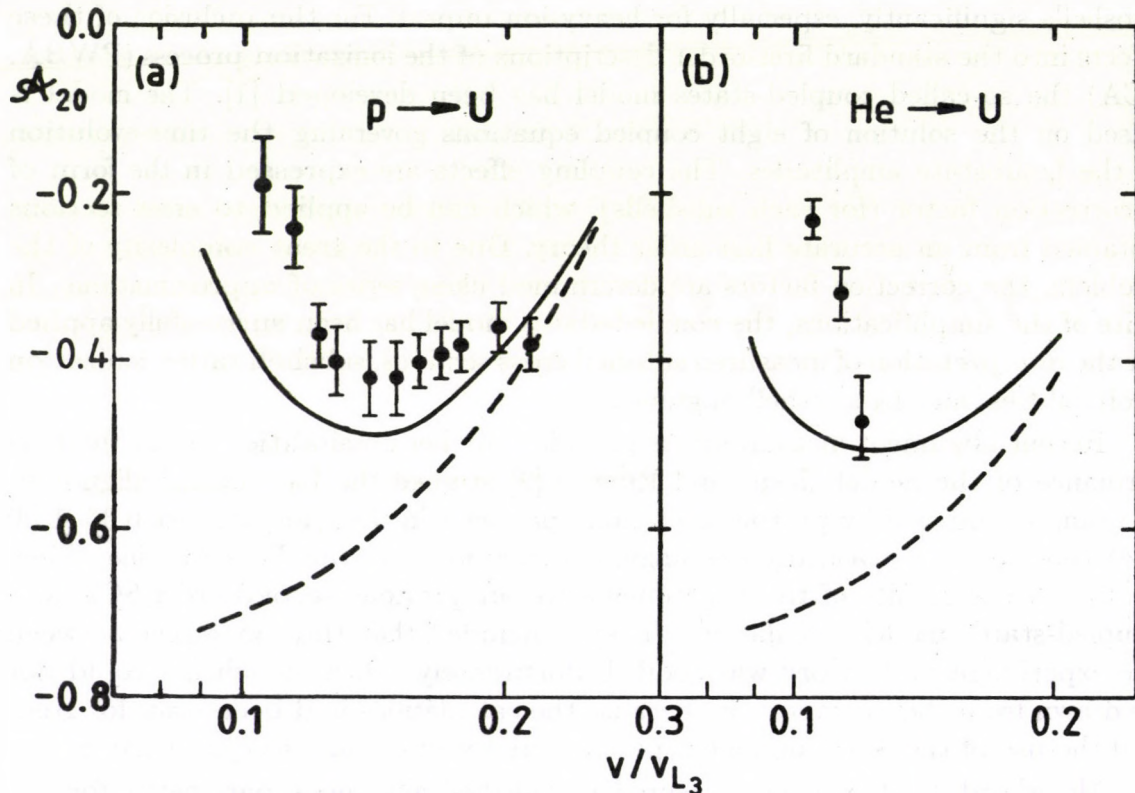


Fig. 1. The L_3 -subshell alignment parameter of uranium for proton (a) and helium (b) bombardment as a function of the relative collision velocity. The experimental data are from Jesus and Ribeiro [2]. The dashed and the solid line denote the PWBA and the coupled-states theory, respectively.

References

† Institute for Chemical Research, Kyoto University, Uji, Kyoto, 611 Japan

1. L. Sarkadi: *J. Phys. B* **19** L755 (1986)
2. A. P. Jesus, J. P. Ribeiro: *Nucl. Instr. and Meth. B* **48** 93 (1990)
3. W. Meierkord, T. Blümke, M. Brüssermann, J. Hofste, H.-U. Menzebach, J. F. Pennings, Z. Stachura, W. Vollmer, J. Wigger, B. Cleff: *Z. Phys. D* **18** 75 (1991)
4. I. C. Legrand, A. Berinde, C. Ciortea, A. Enulescu, D. Flueraşu, I. Piticu, V. Zoran: *Nucl. Instr. and Meth. B* **56/57** 21 (1991)

MATERIALS SCIENCE
AND
ANALYSIS

Wear Measurement of Cutting Edges of Superhard Turning Tools

I. Mahunka, S. Takács, F. Ditrói and L. Vasváry

During last years the conditions for introducing superhard cutting tools in machinery industry increased rapidly. The most important demands for using superhard cutting tools are as follow:

- high cutting speed;
- high accuracy of machining;
- high quality of machined surface.

To fulfil these demands one first of all should have the possibility to measure and monitor ("on-line") of the wear of the cutting edge with high accuracy.

Our group started a project to develop a method and instrument for measuring and monitoring of the wear of superhard cutting edges of turning tools by using nuclear method.

The cyclotron based Thin Layer Activation (TLA) method was used to measure the wear of the cutting edges. The investigated tools were made from Boron Nitride (BN) and industrial Diamond (DIA). At the first step the cutting edges were irradiated with proton beams. The irradiation geometry was chosen to produce a cylindrical ($\varnothing 200 \mu\text{m}$) activated volume, parallel to the main axis of the tool. The position of the cutting edges relative to the collimator was checked under microscope. Due to several considerations (irradiation damage of material, depth distribution of generated activity, target material, nuclear reaction, possibly short irradiation time, ...) $E_p = 8.0 \text{ MeV}$ for DIA and $E_p = 5.4 \text{ MeV}$ beam energy for BN was used. The beam current was kept at 10 nA. In the BN material ${}^7\text{Be}$ isotope ($T_{1/2} = 53.3 \text{ d}$) was produced via ${}^{10}\text{B}(p,\alpha){}^7\text{Be}$ reaction. In the case of DIA ${}^{56}\text{Co}$ isotope ($T_{1/2} = 77.7 \text{ d}$) was produced via ${}^{56}\text{Fe}(p,n){}^{56}\text{Co}$ reaction from the iron content of the material that fills in the gaps and keeps together the diamond particles in the DIA.

The realistic wear of cutting edges was simulated by grinding away of the activated volume step by step on diamond wheel. Wear of back surface of the turning tools were measured by microscope and the residual activity by gamma-spectrometer after each step of grinding.

Using this method an activity-wear calibration curve was produced for both the BN and DIA materials. Calibration curves for BN materials measured with scintillation and HpGe detectors are shown in Fig. 1. It is easy to see that the low cost scintillation technique gives a result as good as the HpGe system.

Analyzing these curves one can see that the irradiation geometry used results

low sensitivity for the early stage of wear, but the rapid increase of the incline of the calibration curve at the end of measured interval indicates high sensitivity. This fact makes possible to detect the moment, when the tool has worn out and must be changed. Using these calibration curves it is possible to monitor "on-line" the wear of tuning tools.

Changing the irradiation geometry is the way to modify the activity distribution and the shape of the activated volume as well as to increase the sensitivity of the method to measure the actual wear of the working tool.

This work was made in cooperation with the Department of Technology in Machinery of the Technical University of Miskolc.

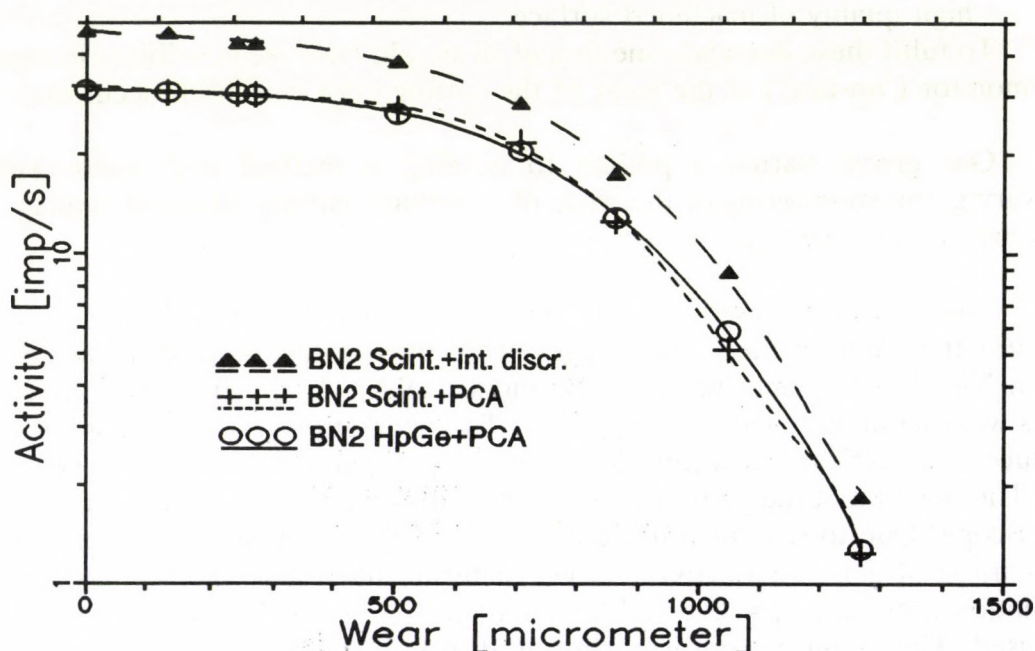


Figure 1. Calibration curves for BN material measured by HpGe and Scintillation spectrometers

References

1. I. Mahunka, I. Dombi, S. Takács, F. Ditrói, IAEA 1989 INDC(Hun)-027/G p.21
2. S. Takács, F. Ditrói, I. Mahunka, IAEA 1989 INDC(Hun)-027/G p.18
3. I. Mahunka, F. Ditrói, IAEA Consultants' meeting ; IAEA, Vienna, 15-18 May 1990.
4. Mahunka Imre, Ditrói Ferenc, Takács Sándor; Kutatási jelentés, 1990, ATOMKI, Debrecen

Thick dead layer in a Si(Li) detector

G. Kalinka

There has been a puzzle for a long time about the ultimate limit of undepleted uncompensated p-type Si layer thickness in Si(Li) detectors and on the nature and structure of so called dead layers assumed to be responsible for low energy tail and shelf (see for example Campbell's review article [1]).

As a contribution to solving this problem we have investigated the response of a Si(Li) detector to ArK X-rays as a function of detector bias. The particular detector chosen had earlier been left uncooled for a couple of years thus, like most other Si(Li) detectors, had extremely thick decompensated p-Si layer providing us a unique possibility to "tune" the dead layer thickness in very wide range by the applied detector bias U_d .

The Ar spectra acquired were fitted by sum of Gaussian photo (P), escape (ESC) and silicon (Si) peaks as well as smooth polynomial (at lower bias) or a more or less flat continuum (S , at higher bias). The residue left to P was considered as tail (T) of the ArK line. By extrapolation of photopeak intensities $P(U_d)$ to $U_d \rightarrow \infty$ a P^o value was determined and photo dead layer thickness x_d^P was defined according to $P/P^o = \exp(-\mu x_d^P)$. Note that x_d^P defines the boundary between the complete charge collection (CCC, $\eta = 1$) and incomplete charge collection (ICC, $0 \leq \eta < 1$) regions. On the other hand, by a simple model it was proved that at lower biases (below full depletion) the ICC region coincides the undepleted part of the decompensated p-Si which had been formed during the long term storage at room temperature. The total decompensated thickness was $\sim 45 \mu\text{m}$, while the depletion voltage was $\sim 420 \text{ V}$. Varying the bias from 200 to 1000 V, x_d^P changed from 15 to $0.25 \mu\text{m}$.

From the dependence of all the spectrum components (P, T, S, ESC, Si) and their sum (TOT) on x_d^P the following conclusions have been reached:

(I) There is a transition region between approximately $x_d^P = 1 \div 2 \mu\text{m}$, below this no undepleted p-Si exists.

(II) In the upper x_d^P range the undepleted p-Si layer ($0 \leq \eta < 1$) can be divided into two regions: (i) adjacent to the metal-semiconductor interface ($x = 0$) there is a completely inactive region with no charge collection at all (NCC, $\eta = 0$) with thickness x_d^A , (ii) next to it from x_d^A to x_d^P is located the "true" ICC^t region ($0 < \eta < 1$).

As a consequence only in this case can be detected fluorescent Si line originating from the window. The 3 dimensional model derived for the SiK intensity assuming NCC as the source and ICC^t as an absorber fits the experimental observations quite well. A similar model for the relative escape intensity ESC/P , with CCC as the emitter and ICC^t as absorber, however, does not seem to be as good: experimental points suggest $NCC + ICC^t = ICC$ to be the absorber. The "shelf" component S shows an approximate linearity with x_d^P up to $1/\mu \sim 4 \mu\text{m}$, but it seems unlikely to vanish as $x_d^P \rightarrow 0$.

(III) In the lower dead layer region where there is no NCC region except for an infinitesimal MOS interface with assumed high surface recombination rate [2] it is the T tail component which seems to be assigned to photons absorbed in the ICC layer for we observed $T = TOT[1 - \exp(-\mu x_d^P)]$.

In order to get more information about the nature of dead layers additional measurements of S/TOT and T/TOT ratios versus energy were made at x_d^P values of 0.3 and 8 μm (low and high region, respectively) as shown in Fig. 1. (The tail could not be determined with certainty due to the high shelf at 8 μm .) Detailed analysis of this figure will be given elsewhere.

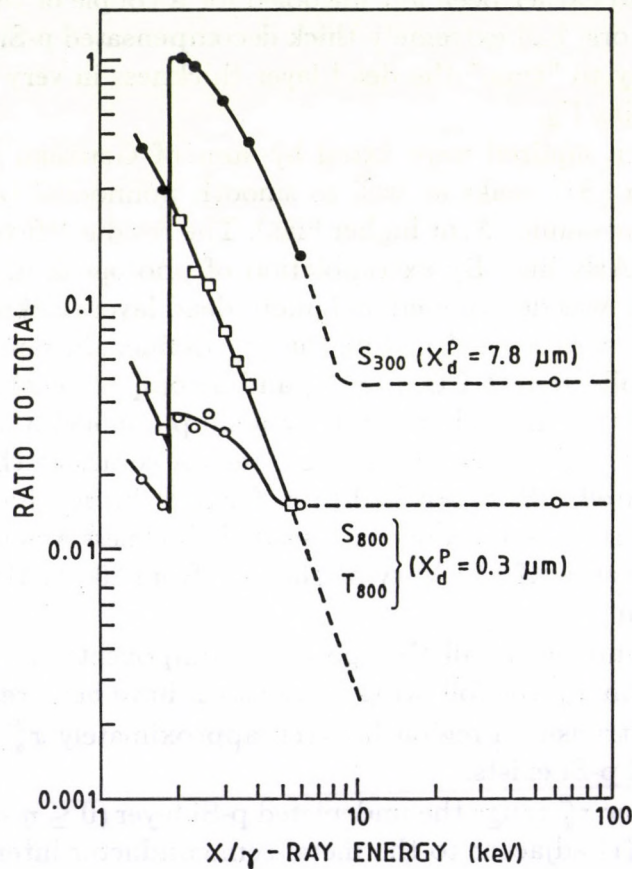


Fig. 1. Tail/total and shelf/total intensity ratios vs photon energy for a Si(Li) detector at 300 V ($x_d^P = 8\mu\text{m}$) and 1000 V ($x_d^P = 0.3\mu\text{m}$) biases

References

1. J.L. Campbell, Nucl. Instr. and Meth. **B49** (1990) 115
2. C.S. Rossington J.T. Walton, J.M. Jaklevic, IEEE Trans. Nucl. Sci. **NS-38**, No.2 (1991) 239

A Si(Li) detector with improved low energy response

G. Kalinka

Though in principle a semiconductor detector with bulk trapping only must have true Gaussian line shape at low enough photon energies, real X-ray detectors always exhibit more or less severe low energy tailing and shelf due to near surface interactions [1, 2]. This is pronounced at low penetration depths typically just above the K or L absorption edge of the detector material.

There have been simultaneously investigations [3-5] on the nature and origin of the so called dead layer responsible for the surface effect and a continuous effort for diminishing it by appropriate entrance window technology [6-9].

On the basis of previously published works in the field of Si detectors and of metal-semiconductor interfaces [8-15] we have been developing modified Schottky barrier with conventional polarity (entrance electrode is negative) for Si(Li) detectors with improved low energy response. The best result to date is shown in Fig.1.: a K X-ray spectrum of elemental phosphorus excited by ^{55}Fe together with the fitting components of the PK_α line. The best fit was achieved by the following function:

$$F(i) = G_o(i) + G_1(i) + T_1(i) + S(i) + B(i)$$

where $G_o(i)$ denotes the main Gaussian, $G_1(i)$ a second Gaussian, $T_1(i)$ an exponential tail of $G_1(i)$, the latter two both responsible for the skewing (tailing) of $G_o(i)$ while $S(i)$ is the standard shelf component and $B(i)$ is a general background caused by the excitation source (note the gap between the main Gaussian and its tail components).

The line and component parameters are given in Tables 1. and 2. It is worth noting that the total degraded event fraction ($G_1 + T_1 + S$) is 5.3 % which corresponds to an equivalent affected silicon layer thickness of about 0.08 μm .

References

1. J.L.Campbell, Nucl.Instr. and Meth. **B22** (1987) 13
2. J.L.Campbell, Nucl.Instr. and Meth. **B49** (1990) 115
3. J.Llacer, E.E.Haller, R.C.Cordi, IEEE Trans.Nucl.Sci. **NS-24**, No.1 (1977) 53
4. J.X.Wang, J.L.Campbell, Nucl.Instr. and Meth. **B54** (1991) 499
5. J.L.Campbell, J.X.Wang, X-ray Spectrom. **20** (1991) 191
6. M.Slapa et.al., Adv. X-Ray Anal. **25** (1982) 23
7. C.E.Cox, B.G.Love, R.A.Sareen, IEEE Trans.Nucl.Sci. **NS-35**, No.1 (1988) 28
8. J.M.Jaklevic et.al., Nucl.Instrum. and Meth. **A266** (1988) 598
9. C.S.Rossington, J.T.Walton, J.M.Jaklevic,IEEE Trans.Nucl.Sci. **NS-38**, No.2 (1991) 239
10. G.Forcinal, P.Siffert, A.Coche IEEE Trans.Nucl.Sci. **NS-15**, No.3 (1968) 275
11. K.E.Haq, K.H.Behrndt, I.Kobin, J.Vac. Sci.Technol. **6** (1969) 148
12. C.Inskeep, E.Elad, R.A.Sareen, IEEE Trans.Nucl.Sci. **NS-21**, No.1 (1974) 379
13. J.P.Ponpon, P.Siffert, J.Appl.Phys. **49** (1978) 6004
14. J.P.Ponpon, P.Siffert, J.Appl.Phys. **50** (1979) 505
15. L.J.Brillson, Surf. Sci Rep. **2** (1982) 13

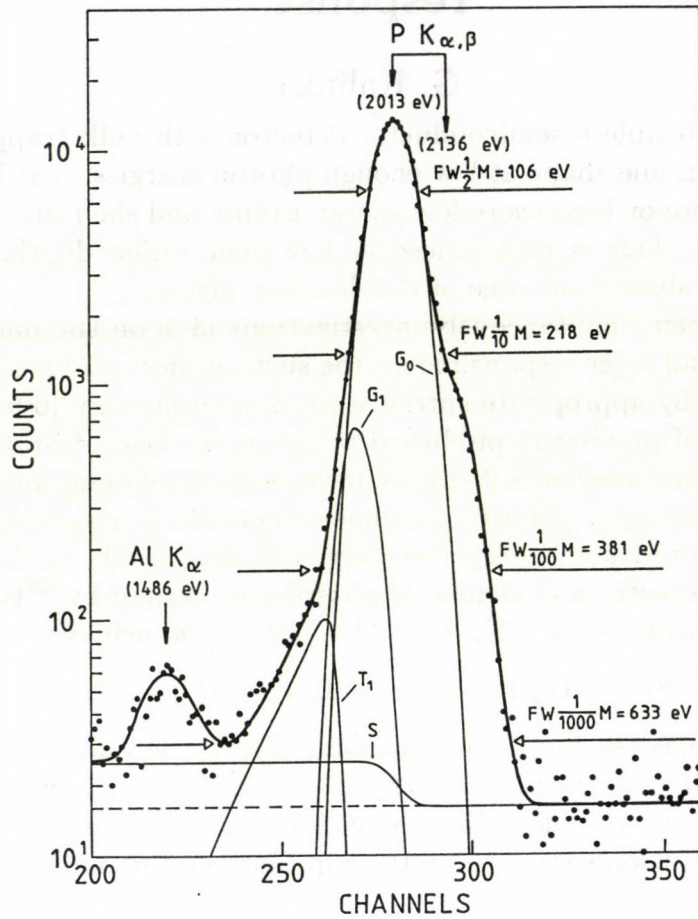


Fig. 1. A phosphorus K X-ray line taken with improved entrance window Si(Li) detector

	$PK_{\alpha+\beta}$	PK_{α}	measured/true Gaussian
FW 0.5 M	106	106	1.00
FW 0.1 M	218	194	1.83 : 1.82 = 1.005
FW 0.01 M	381	323	3.05 : 2.58 = 1.18
FW 0.001M	633	500	4.72 : 3.16 = 1.49

Table 1. Width parameters in eV of phosphorus K lines shown on Fig. 1.

	G_0	G_1	T_1	S
FWHM (eV)	106	86	-	-
AREA	0.947	0.037	0.005	0.011
E_0-E (eV)	-	90	165	-

Table 2. Parameters of PK_{α} line components

A line shape model of planar Si(Li) X-ray detectors

G. Kalinka

It is well known that bulk trapping of charge carriers in semiconductor detectors degrades the line shape. The effect is more pronounced at higher photon energies where the penetration depth is comparable to or more than the thickness w of the detector due to the position dependent charge collection efficiency and its statistical fluctuation.

The basis of presently used line shape models is the equation established by Trammel and Walter [1]. McMath and Martini were the first to involve into the equation position dependent variance as extracted from their experimental investigations on Si(Li) and Ge(Li) detectors [3]. Later these models were successfully applied to large coaxial HPGe detectors without [4] and with taking into account ballistic deficit [5] but still using empirically determined expression for the signal variance due to trapping.

Now for the first time we present a model for planar Si(Li) X-ray detectors using theoretically derived variance assuming:

constant and homogeneous electric field, charge carrier mobilities ($\mu_i = const.$, $i = e, h$), trapping with no detrapping ($\tau_i^+ = const.$, $\tau_{Di} = \infty$) and mean free path ($\lambda_i = const.$) respectively, as a consequence.

The line shape is given by the modified Trammel-Walter equation:

$$\frac{dN(E_0, E)}{dE} = \int_0^w P(E_0, x) \frac{1}{\sigma(x)\sqrt{2\pi}} \exp\left[-\frac{(E - \eta(x)E_0)^2}{2\sigma^2(x)}\right] dx \quad (1)$$

where $P(E_0, x)$ is the absorption probability density function:

$$P(E_0, x) = \frac{\mu(E_0) \exp[-\mu(E_0)(w-x)]}{1 - \exp[-\mu(E_0)w]} \quad (2)$$

$\eta(x)$ is charge collection efficiency:

$$\eta(x) = \frac{\lambda_e}{w} \left[1 - \exp\left(-\frac{w-x}{\lambda_e}\right)\right] + \frac{\lambda_h}{w} \left[1 - \exp\left(-\frac{x}{\lambda_h}\right)\right] \quad (3)$$

and the total variance is $\delta^2(x) = \delta_{st}^2 + \delta_{el}^2 + \delta_{coll}^2(x)$, where δ_{st}^2 and δ_{el}^2 are the contributions due to charge creation statistics and electronic noises respectively, while that from the charge collection is :

$$\sigma_{coll}^2(x) = E_0 \varepsilon \left\{ \frac{\lambda_e^2}{w^2} \left[1 - 2\frac{w-x}{\lambda_e} \exp\left(-\frac{w-x}{\lambda_e}\right) - \exp\left(-2\frac{w-x}{\lambda_e}\right)\right] + \frac{\lambda_h^2}{w^2} \left[1 - 2\frac{x}{\lambda_h} \exp\left(-\frac{x}{\lambda_h}\right) - \exp\left(-2\frac{x}{\lambda_h}\right)\right] \right\} \quad (4)$$

The flow diagram of line formation is illustrated in Fig.1., while in Fig.2. the effect of trapping asymmetry on line shape is shown under the following conditions: $E_0 = 59.56$ keV, $1 - \bar{\eta} = 0.0067$, asymmetry is characterised by y_e/y_h , with $y_i = \lambda_i/w$.

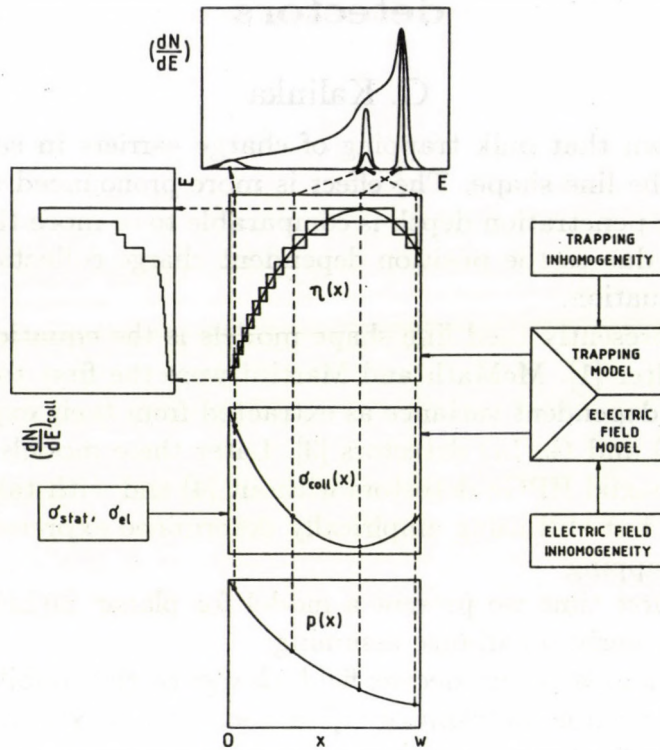


Fig. 1. Illustrative flow diagram of line shape formation

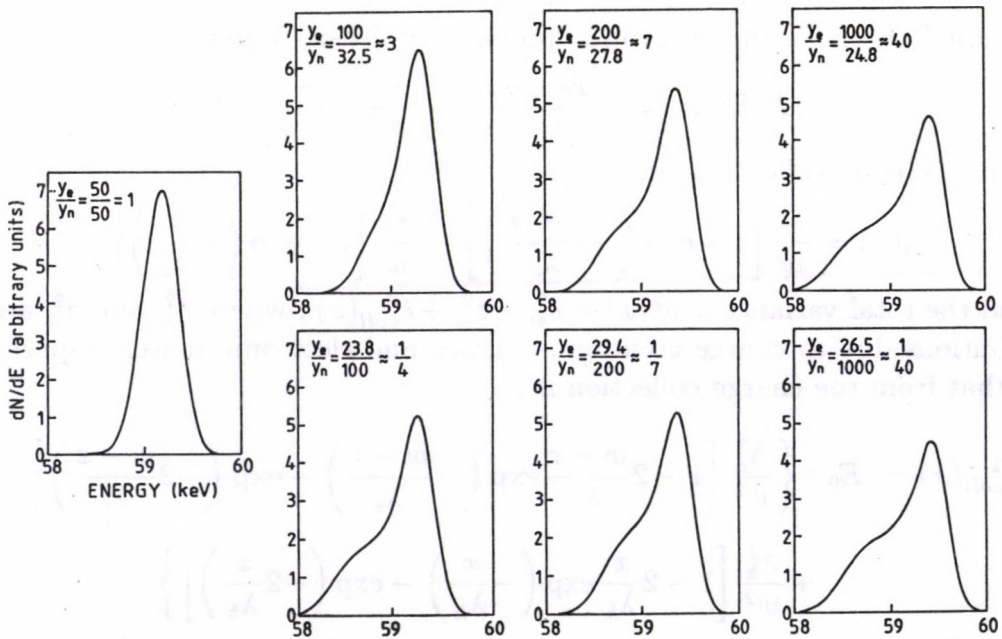


Fig. 2. Effect of trapping asymmetry on line shape (for details see the text)

References

1. R.Trammel, F.J.Walter, Nucl.Instr. and Meth. **76** (1969) 317
2. T.A.McMath, M.Martini, Nucl.Instr. and Meth. **86** (1970) 245
3. M.Martini, T.A.McMath, Nucl.Instr. and Meth. **79** (1970) 259
4. T.W.Raudorf,R.H.Pehl,Nucl.Instr. and Meth. **A255** (1987) 538
5. M.L.Simpson, T.W.Raudorf, T.J.Paulus, R.C.Trammel, IEEE Trans.Nucl.Sci. **NS-37**, No.2 (1990) 444

Calibration of electron spectrometers using ^{99m}Tc internal conversion sources

L. Kövér

For obtaining analyzer functions of electron energy analyzers used for surface analysis, the following requirements should be considered regarding the electron sources applied for calibration:

- Electrons should be emitted isotropically and homogeneously from a solid sample in the same sample-analyzer input geometry as in the case of the surface analytical measurements.
- The width of the energy distribution of electrons from the calibration electron source should be much smaller than the energy broadening caused by the analyzer.
- If possible, the number of the electrons emitted from the calibration source should be determined with high precision.

On the basis of these requirements new methods are proposed for resolution and efficiency calibration of electron spectrometers.

Internal Conversion Electron Spectroscopy (ICES) of ^{99m}Tc sources (combined with XPS measurements for a precise energy calibration) provides a unique tool for both resolution and absolute efficiency calibration of electron spectrometers. The 2.2 keV energy, highly (99 %) converted nuclear transition from a long lifetime isomeric state to a prompt decaying intermediate nuclear state induces narrow energy width electron peaks [1] and other appropriate conditions (for e- γ coincidence experiments) are available as well for using these lines in various calibration methods.

Resolution calibration

The lineshape of the ^{99m}Tc M₄M₅ internal conversion lines has no contribution from X-ray excitation in contrast with XPS lines available for calibration. The respective core hole lifetime broadenings can be determined from independent measurements [1,2] and in the case of NH_4TcO_4 samples symmetric lineshapes can be obtained. For determination of analyzer functions, the measured M₅ spectrum can be deconvoluted of contributions [1] due to the M₄ line and to the inherent (Lorentzian) lifetime broadening and the remaining part can be fitted e.g. with a Gaussian.

Absolute efficiency calibration

The aim of the procedures to determine the ratio η of the number N_D of the detected electrons to the total number N_T of the monochromatic electrons leaving the sample surface in 2π solid angle, $\eta = N_D/N_T$. Measuring the respective internal conversion electrons in coincidence with the γ -ray photons which are following the decay of the nuclear isomeric level (Fig. 1), the absolute number N_0 of the decays per unit time can be determined.

Methods: a) 4π β - γ coincidence measurements of monolayer ^{99m}Tc samples following the respective calibration ICES measurements.

For a simple two-stage β - γ decay:

$$\begin{aligned} N_\beta &= N_0 \varepsilon_\beta \\ N_\gamma &= N_0 \varepsilon_\gamma \\ N_c &= N_0 \varepsilon_\beta \varepsilon_\gamma \end{aligned} \quad \rightarrow \quad N_0 = N_\beta N_\gamma / N_c \quad (1)$$

where $N_{\beta,\gamma,c}$ denotes the numbers of the measured counts in the electron, the gamma and the coincidence channels, respectively, and $\varepsilon_{\beta,\gamma}$ refers to the efficiencies of the respective detectors.

For the case of ^{99m}Tc , (1) is shown [3] to be valid, with: $N_o(\text{observed}) \rightarrow N_o(\text{"true"})$, if $\varepsilon_{\beta} \rightarrow 1$.

Varying ε_{β} (the discriminator level of the $4\pi \beta$ proportional counter) and extrapolating to $\varepsilon_{\beta} = 1$, $N_o(\text{"true"})$ can be obtained [3] from (1), with a precision better than 1%.

The number N_T of the M5 conversion electrons emitted (per unit time) during the calibrating ICES measurements is:

$$N_T^o = N_o^t * \frac{\alpha}{\alpha+1} * \beta * e^{t/\tau_{1/2}} \quad (2)$$

where $\alpha/(1+\alpha)=0.88$ [3] is the probability of the IC process (as opposed to the γ -ray emission) in the 2.2 keV transition; β is the relative probability (branching ratio) of the M5 conversion in the same transition; $\tau_{1/2} = 6.0$ h (half lifetime of the isomeric state); and t is the time interval elapsed between the calibrating ICES and the succeeding $4\pi \beta-\gamma$ coincidence measurements.

b) Measurements of a selected subshell conversion electron (e.g. M5) peak with the electron spectrometer in coincidence with the respective γ photons using a "built in" scintillation γ -ray detector.

$$\frac{\eta}{2} = N_c / N_{\gamma} \quad (3)$$

In both cases, by choosing different subshell IC peaks and using calculated values [4] for β , the energy dependence of the spectrometer efficiency can be determined.

References

1. L. Kövér, I. Cserny, V. Brabec, M. Fišer, O. Dragoun, J. Novák, *Phys. Rev. B* **42** (1990) 643
2. I. Cserny, L. Kövér, V. Brabec, M. Fišer, O. Dragoun, J. Novák, this volume
3. R. L. Ayres, A. T. Hirshfeld, *Int. J. Appl. Radiat. Isot.* **33** (1982) 835
4. M. Band, M. B. Trzhaskovskaya, "Tables of Gamma Ray Internal Conversion Coefficients for K, L and M subshells, $10 \leq Z \leq 104$ " (Leningrad Nuclear Physics Institute, Leningrad, 1978)

Preliminary Results on Multiple Angular Detection Auger Spectroscopy

J. Cazaux *, T. Bardoux *, D. Mouze *, J.M. Patat *,

G. Salace *, X. Thomas *, J. Tóth

From elementary calculations of the Auger signal intensities issued from a specimen at 2 different take-off angles Θ_1 and Θ_2 , it is shown that the simultaneous acquisition of these spectra allows to distinguish between homogeneous alloys and stratified samples. It also signs the presence of topographic effects.

The preliminary results confirm the potential of the Multiple Angular Detection Auger Electron Spectroscopy (MADAES) that can be developed by using only one analyzer of CMA type. Further developments are also indicated in our paper (title and authors: see above) presented at ECASIA '91 (European Conference on Applications of Surface and Interface Analysis, 14-18, Oct, 1991; Budapest, Hungary) and to be published in SIA, (Surface and Interface Analysis), ECASIA 91 Proceedings.

The references in that paper are the followings:

1. M.M. El Gomati, M. Prutton, B. Lamb and C.G. Tuppen: Surf. Interf. Anal., **11** 251 1988
2. I.R. Barkshire, M.M. El Gomati, J.C. Greenwood, P.G. Kenny, M. Prutton and R.H. Roberts: Surf. Interf. Anal., **17** 203 1991
3. J. Cazaux, O. Jbara, K.H. Kim: Surf. Sci., **247** 360 1990
4. L. Reimer in Scanning Electron Microscopy, Springer Series in Optical Sciences, Springer Verlag, 1985 -P-
5. C.J. Harland, G. Cox, D.J. Fathers, P.S. Flora, M. Hardiman, G. Raynend, M. Whitehouse - Yeo and J.A. Venables: Inst. Phys. Conf. Series, **90** 9 1987
6. D. Briggs and J.C. Rivière in Practical Surface Analysis by Auger and X-Ray Photoelectron Spectroscopy edited by D. Briggs, M.P. Seah, John Wiley and Sons 1983 Ch3
7. M. Prutton, M.M. El Gomati and P.G. Kenny: Electron Spectros. Relat. Phenom. **52** 197 1990

We have some new results on ultrathin layers (20 Å) of epitaxial erbium silicide (prepared by LEPES-CNRS, Grenoble) as an application of MADAES.

An other part of our angular dependent experiments are inner shell EELS (Electron Energy Loss Spectroscopy) on graphite specimen concerning the momentum transfer relating to transitions of C $1s \rightarrow \pi^*$ and $1s \rightarrow \sigma^*$.

These results will be presented in a paper entitled "Double detection angulaire en spectroscopie Auger et pertes d'énergie" (in French) by Bardoux T., Tóth J., Salace G., Mouze D., Patat J. M., Thomas X., Cazaux J., at the Journées Surfaces et Interfaces, Nice-30 et 31 janvier 1992.

*LASSI (Laboratoire d'Analyse des Solides Surfaces et Interfaces) BP 347 Faculté des Sciences 51062 Reims Cédex France

Energy Dispersive X-Ray Spectrometer for Archaeological Use

M. Kis-Varga, P. Kovács, G. Kalinka, S. Fekete ¹, J. Szádai,
and L. Költő ²

¹DIGITMODUL Ltd., Debrecen

²Kaposvár Museum, Kaposvár

In the ATOMKI, in collaboration with the Kaposvár Museum, we have since many years been investigating the composition of archaeological objects (mostly bronzes, silver- and golden alloys) by XRF analysis [1]. Utilizing the experiences gained during that work an energy dispersive XRF spectrometer has been introduced in the Kaposvár Museum. This is the first analytical equipment of that type in a Hungarian museum.

The spectrometer is based on the ATOMKI NZ-860 Si(Li) detector and NZ-853 pulse processor which is connected to an IBM AT through an analogue-digital converter board developed for that purpose. The data acquisition software [2] provides usual multichannel analyzer functions: timing, setting up measurement parameters, spectrum accumulation, energy calibration, identification of elements by KLM markers, simple peak evaluation by ROIs, storing of spectrum- and result files, etc.

The XRF program calculates the composition by using the fundamental parameter approach. The built-in automatic element identification routine provides easy operation for the analyst. Although the x-ray yields are simply calculated in ROI windows, and only experimentally determined overlap corrections are used if necessary, the concentrations achieved are in good agreement with that of using the intensities provided by least squares fit of AXIL code [3] (see Table 1.). The spectrometer has been tested with known composition stainless steel, brass, bronze, silver and golden alloys. The accuracy of analyses satisfies the requirements for classification of archaeological findings.

Table 1. Concentrations calculated by using x-ray intensities of ROIs (a) and that of achieved from least squares fit with AXIL [3] code (b).

Specimen	Element	Concentration (w/w)	
		a	b
Brass No.1.	Cu	58.5	58.7
	Zn	39.6	39.6
	Pb	1.8	1.7
Brass No.2.	Cu	57.8	58.0
	Zn	39.9	39.3
	Pb	2.3	2.1
Stainless steel	Cr	18.8	18.7
	Fe	65.8	65.0
	Ni	12.7	13.2
	Mo	2.8	2.6

References

1. M.Kis-Varga, L.Költő, ATOMKI Annual Report (1989) 62
2. P.Kovács, to be published
3. P. Van Espen et al., Nucl. Instr. Meth. **142** (1977) 243

Energy Dispersive X-Ray Spectrometer with Reduced Background

M.Kis-Varga, G.Kalinka and P.Kovács

Preliminary results in improving the detection limit of our x-ray spectrometer achieved with a recently installed Siemens Kristalloflex 710H x-ray generator and Mo-tube are presented here. Most of the background in tube excited XRF spectra arises from elastic and Compton scattering of the primary photons by the specimen. To improve the detection limits the background has to be significantly reduced. The application of polarized x-rays for background reduction has been published by many authors [1-8].

We used the classical Barkla principle for polarization: if the unpolarized beam is scattered at a 90° angle from a low Z amorphous target (Be, B, C, etc.) the scattered beam will show linear polarization. Using this radiation for exciting characteristic x-rays in the three-axis geometry proposed by T.G. Dzubay et al [1], where the paths between the source, polarizer (or secondary target), sample and the detector represent three mutually orthogonal vectors, the scattered background will be highly reduced.

To somewhat compensate the intensity loss caused by polarization process we have constructed a compact irradiation block with the path lengths as follows: tube window-polarizer (secondary target) 20 mm, polarizer-sample 35 mm, sample-detector 15 mm. In order to accomplish this geometry we had to modify the detector cryostat (product of the Institute of Instrumental Technique of the Czechoslovakian Academy of Sciences, Brno [9]). The new cryostat is more flexible: it can be used from horizontal up to 45° upwards.

We have tested our three-axis geometry XRF system with boron-nitride and graphite polarizers as well as with different secondary targets (Mo, In, Sb, etc.). Fig. 1 shows the x-ray spectra of Soil-7 IAEA standard reference material as measured by using graphite polarizer in 2-axis geometry (the primary, the polarized and the fluorescence beam propagate in the same plane) and in 3-axis geometry as well. The drastic improvement in the scattered background is obvious. In Fig. 2 the detection limits as a function of atomic number are compared for I-125 radioisotope and tube excitation with In and graphite targets. The polarized tube excitation gives cca 2-5 times lower detection limits and decreases below one ppm level at medium atomic number elements.

Further improvements are expected after optimizing the target materials and their thicknesses, proper filtering the primary beam and replacing the detector crystal with a better one (the present detector has an intense low energy tailing as seen in Fig. 1 below 10 keV).

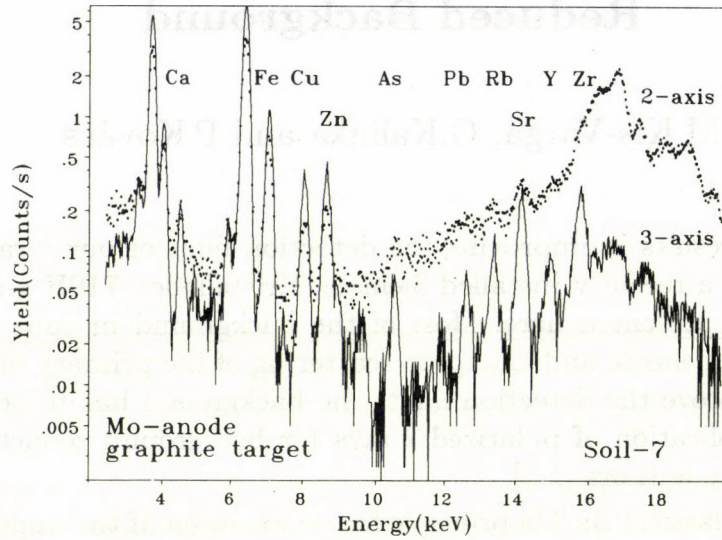


Fig. 1. The Soil-7 x-ray spectra excited by graphite polarizer. Upper: 2-axis geometry, lower: 3-axis geometry.

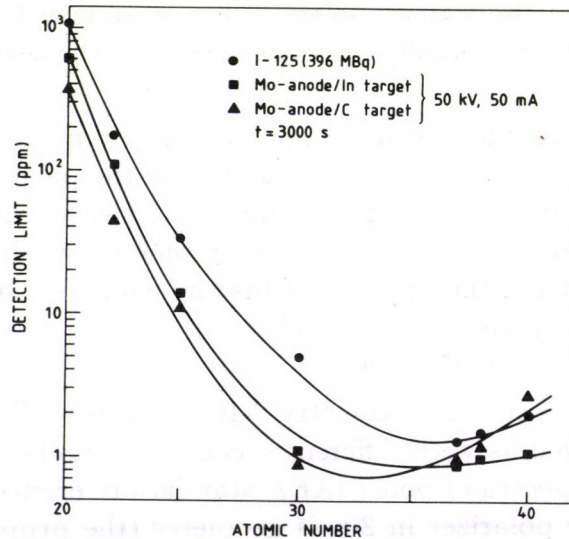


Fig. 2. Comparison of detection limits for I-125 radioisotope and tube excitation (Mo anode/In and graphite target, respectively).

References

1. T.G. Dzubay et al, Nucl. Instr. Meth. **115** (1974) 297
2. H. Aiginger et al, Nucl. Instr. Meth. **120** (1974) 541
3. R.W. Ryon, Adv. X-Ray Anal. **20** (1977) 575
4. R.W. Ryon, J.D. Zahrt, Adv. X-Ray Anal. **22** (1979) 453
5. P. Standzenieks, E. Selin, Nucl.Instr.Meth. **165** (1979) 63
6. P.Wobrauschek, H.Aiginger, X-Ray Spectrometry **9/2** (1980) 57
7. K. Maack Bisgard et al, X-Ray Spectrometry **10/1** (1981) 17
8. P.Wobrauschek, H.Aiginger, X-Ray Spectrometry **12/2** (1983) 72
9. J. Dupak, Jemnamechanika a optika **33** (1988) 249

Si(Li) Detector Line Shapes at Medium X-Ray Energies

M. Kis-Varga and J. Végh

The response functions of Si(Li) x-ray detectors has been widely investigated [1-8]. Although many different model functions has been succesfully tested and proposed for routine use, the physical mechanism of detection is still not well understood. The line shapes are described mostly by semiempirical equations including Gaussian shaped full energy and Si-escape peaks, a flat continuum (shelf) from zero to the full energy and a tailing function on the low energy side of the photopeak.

The line distortion is particularly significant at low x-ray energies due to near surface interactions in the detector crystal [5-8]. At medium or higher energies (above 15 keV) the line shapes of x-ray fluorescence spectra are strongly influenced by Compton scattering of fluorescence radiation in the sample [4,5].

We have been studying the XRF spectrometer response in the energy range of 2 to 30 keV for different Si(Li) detectors constructed in our laboratory. Pure metals and light matrices containing one element at 5000 ppm level were excited by I-125 isotope and by low power x-ray tube as well. The characteristic K-lines were fitted by using the computer code EWA [9]. The peak shapes were described by a modified version of Hypermet function [1]:

$$Y_i = Y_0 * (G_i^{Gauss} + E_i^{Escape} + C_i^{Tail} + P_i^{Shelf})$$

where G_i denotes the Gaussian photopeak, E_i is the Gaussian escape peak, C_i includes the short term and long term exponentials of Hypermet, as well as the truncated shelf proposed by J.L. Campbell et al, [4] for the Compton scattered part, P_i is a Shirley-type function [10,11] which describes the flat continuum from zero to the full energy.

Using the above form excellent fits have been achieved in the whole energy range except for thick and light matrices above 15 keV, where in many cases better fits have been realized by using a broad Gaussian instead of truncated shelf for fitting the Compton scattered region (see Fig 1.). Our studies have also shown that the area ratio of this component to the main Gaussian varies strongly with sample matrix and thickness.

The details of our line shape studies (e.g. the influence of instrumental and matrix parameters on the response function as well as the comparison of line shapes for different detectors) will be published elsewhere.

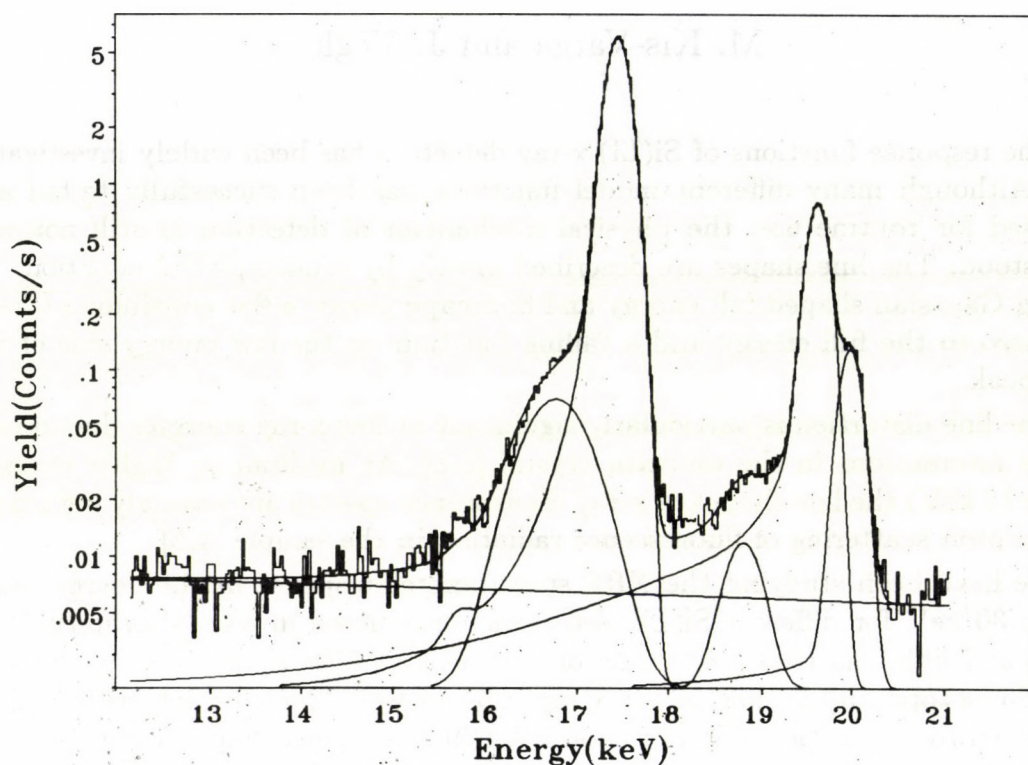


Fig. 1. The fit of Compton-tails of Mo K-lines with Gaussians.

References

1. G.W. Phillips, K.W. Marlow, Nucl.Instr.Meth. **37** (1976) 525
2. L.Wielopolski, R.P.Gardner, Nucl.Instr.Meth. **165** (1979) 297
3. J.L. Campbell et al, X-Ray Spectrometry **16** (1987) 195
4. J.L. Campbell et al, Nucl.Instr.Meth. **B43** (1989) 490
5. T. He et al, Nucl.Instr.Meth. **A299** (1990) 354
6. J.L. Campbell, J.X. Wang, X-Ray Spectrometry **20** (1991) 191
7. M. Geretschlager, Nucl.Instr.Meth. **B28** (1987) 289
8. Y. Inagaki et al, Nucl.Instr.Meth. **B27** (1987) 353
9. J. Végh, Thesis 1991
10. D.A. Shirley, Phys. Rev. **55** (1972) 4709
11. J.Végh, J.Electron Spectroscopy and Related Phenomena **46** (1988) 411

Combined Applications of the PIXE and PIGE Analytical Methods

I. Borbély-Kiss, Zs. Fülöp, A.Z. Kiss, E. Koltay,

E. Somorjai and Gy. Szabó

Aerosol research

During this year a regular aerosol sampling has been continued in collaboration with Central Institute of Atmospheric Physics. Samples of atmospheric aerosol particles collected in Budapest (two sampling stations), in a rural site (K-puszta) and in Debrecen (ATOMKI) were analysed up to 22 elements (Al, Si, P, S, Cl, K, Ca, Sc, Ti, V, Cr, Mn, Fe, Co, Ni, Cu, Zn, As, Se, Br, Ba, Pb) by PIXE method. They were searched for light element contents, especially boron and sodium by PIGE.

Balneology

PIGE trace element analysis has been performed from hot wells of the hydrotherapeutical thermal baths Zsóri (Mezőkövesd) and Hajduszoboszló. Special emphasis was given for the determination of their Li content.

Archeology

The determination of elemental concentrations of ancient glass pastes has been continued this year. On the collection of 26 specimens reported in our last year annual report [1] a complex mathematical study, a cluster analysis has been performed. The resulted dendrogram displaying the levels of similarity among the specimens supports the classification made according to the pattern seen on the glass sealings.

1. I. Borbély-Kiss, Zs. Fülöp, T. Gesztelyi, A. Z. Kiss, E. Koltay and Gy. Szabó, Atomki Annual Report, 1990, p.81.

Thermally activated flux motion in Bi(Pb)SrCaCuO thick films

K. Vad, S. Mészáros and N. Hegman

A mechanism of energy dissipation generated by DC transport currents in superconducting Bi(Pb)SrCaCuO screen-printed films was studied. Current-voltage characteristics were measured by the standard four contact method using both continuous and pulsed transport currents. We studied the magnetic field and temperature dependence of current-voltage characteristics for different film widths systematically. The magnetic field and temperature ranged from 0 to 10 mT and from 5 to 120 K respectively. Some peculiarities of the current-voltage characteristics were observed. The film carrying a current that was slightly higher than its critical current was found to be in an instable state. The weakly pinned vortices in intergrain Josephson junctions started to slip, which caused some energy dissipation in the film. This phenomenon appeared in current-voltage characteristics as a linear part just above the critical current. At higher currents the voltage increased much faster and the characteristics became strongly nonlinear. A clear distinction could be made between the critical current limitation caused by flux creep and the current value, at which the curve started to be strongly nonlinear. The difference between these two dissipation mechanisms was demonstrated by measurements of quantum interference patterns of an appropriate film.

References

1. K. Vad et al. Proc. 6th Int. Symp. on Weak Superconductivity, S. Benacka, M. Darula and M. Kedro (editors), World Scientific, 1991. p. 64.

Complex AC susceptibility of high- T_c superconductors in the RF range

S. Mészáros, N. Hegman and K. Vad

The AC susceptibility measurement is a good method of obtaining information about the magnetic behaviour of high- T_c superconducting materials. The measurements are usually performed in the frequency range from a few kHz to a few hundred KHz and in the microwave region. Much less experimental information has been gained in the RF range. In order to get a more complete picture we performed complex AC susceptibility measurements in the frequency range of 5 to 500 MHz. The experimental arrangement consisted of a low loss 50 Ohm RF cable shorted by a low inductance Helmholtz coil. This coil generated the excitation field using the cable in $n\lambda/4$ resonator mode. The generated magnetic moment of the sample was detected by a pick-up coil placed around the sample located in the centre of the Helmholtz coil. The pick up coil signal was connected to the 50 Ohm input of a high frequency lock-in by a coaxial cable. In-phase and quadrature components of the signal were detected by the lock-in and analysed by a computer to deduce the two components of the complex susceptibility. The probe was immersed into an experimental chamber, where the temperature and the static magnetic field could be regulated. AC susceptibility was studied as a function of excitation amplitude, frequency, temperature and static magnetic field for high temperature superconducting powders, ceramics and single crystals of YBaCuO and Bi(Pb)SrCaCuO.

Complex AC susceptibility of right-angle superconductors in the HF range

S. Mészáros, A. Hegman and M. Tóth

The AC susceptibility measurement is a well known method for studying superconductors. In this paper the complex behavior of right-angle superconductors is investigated in the frequency range from a few kHz to a few MHz. The experimental arrangement, consisting of a low temperature helium bath, a right-angle superconductor, and a measuring coil, is described. The results show that the AC susceptibility is a function of frequency and temperature. The real part of the susceptibility is a step function, while the imaginary part is a peak. The peak height and position depend on the frequency and temperature. The results are compared with the theoretical predictions of the Ginzburg-Landau theory. It is shown that the experimental results are in good agreement with the theory. The results also show that the AC susceptibility is a sensitive probe for studying the properties of right-angle superconductors. The results are discussed in the context of the Ginzburg-Landau theory and the implications for the study of right-angle superconductors are discussed.

EARTH AND COSMIC SCIENCES,
ENVIRONMENTAL RESEARCH

Radon measurements in Hungarian karstic regions*

J.Hakl, I.Hunyadi, I.Csige, G.Géczy ^a, L.Lénárt ^b, I.Törőcsik ^c

^aEötvös Loránd University, Dept. of Physical Geography, Budapest

^bUniversity Miskolc, Dept. of Hydrogeology and Engineering Geology

^cUniversity Medical School, Institute of Forensic Medicine, Debrecen

Starting from 1978 continuous radon observation was performed at about 150 sub- and near-to-surface monitoring stations in different substances (cave air, soil, water) of Hungarian karstic regions. The radon activity concentration was registered by monthly changed nuclear track detectors using diffusion cups. The mean value of the obtained time series fall in the range of 0.2-14 kBq/m³. In cave air, typically, summer maxima and winter minima were observed, their ratios fall in the range of 2-50. The soil gas measurements performed above a cave showed maxima in winter and minima in summer. In a few cases the radon content of waters was strongly related to the yield of the feeding stream.

All these phenomena are strongly connected with the geology of the investigated areas. Karstic caves are generally situated in highly fractured rocks with a few 'entrances', where some of them are only a complex of small openings and fissures. Such a configuration is favorable for emerging an air circulation through this fracture system. In first approximation, the strength of these air motions is proportional to dT/f , where dT is the temperature difference between the cave and outside air and f is a friction factor. These 'winds' in a seasonally changing direction wash out the air from the radon rich fracture system of karstic terrains. If this washing out process is taking place in the direction of rock or soil surface → fracture system → galleries → entrance then an increased radon level can be measured inside the caves. This is typical for summer in our country. In winter, when the flow direction reverses, the fresh atmospheric air dilutes the radon concentration in the caves. It is interesting to note that, according to this model, in the winter season an increased radon exhalation can also be expected on the surface. These winter maxima were detected at the 'top' of the biggest Hungarian vertical karstic cave system (Istvánlápa), in a few m deep vertical fracture and covering soil above the Hajnóczy cave and in some potholes in the Mecsek region. It is worth mentioning that due to gravitational reason in all these cases only minima could be expected in winter. The dilution effect of colder atmospheric air is reflected only in the smaller amplitudes of these winter maxima. The most convincing experimental results are presented in Fig. 1. The last three year section of mean radon concentration observed in the air of the Hajnóczy cave (a) is shown together with the radon concentration measured simultaneously in the surface soil (b) and in the air of an open fracture (c) on the upper side of the hill, where the cave is embedded. Approaching deeper parts of the karst, the strength of these winds decreases due to their $1/f$ dependence. In passages of a deep karst it also may cause lower radon activity concentration values. Due to saturation effects the

amplitude of changes will also decrease. Indeed much lower activity concentrations were found in the deep parts of the narrowest vertical caves in Hungary (Szepessy, Istvánláp), where the seasonal change was found also to be negligible. From the point of view of ventilation these caves can be considered as the most closed formations. In the longest and biggest cave of Hungary (Baradla), more effects take place simultaneously, which influence the radon concentration and finally in time and space a well balanced level is formed. These measurements showed that in karstic regions the structurally controlled convective radon transport is dominant over diffusive transport. Radon dissolved in circulating subsurface fluids migrates over a longer distances along caverns and fractures, depending on the velocity of transporting medium. Two important radiological consequences follow from the periodical behaviour of this karst breathing: In the radon concentration of the air of caves and mines used also for speleo- and balneotherapy big differences can occur between the summer and winter values consequently in the radon exposure received by the patients. On karstic terrains a notably increased surface exhalation can be expected seasonally, which may enhance the indoor radon concentration of houses built on this region.

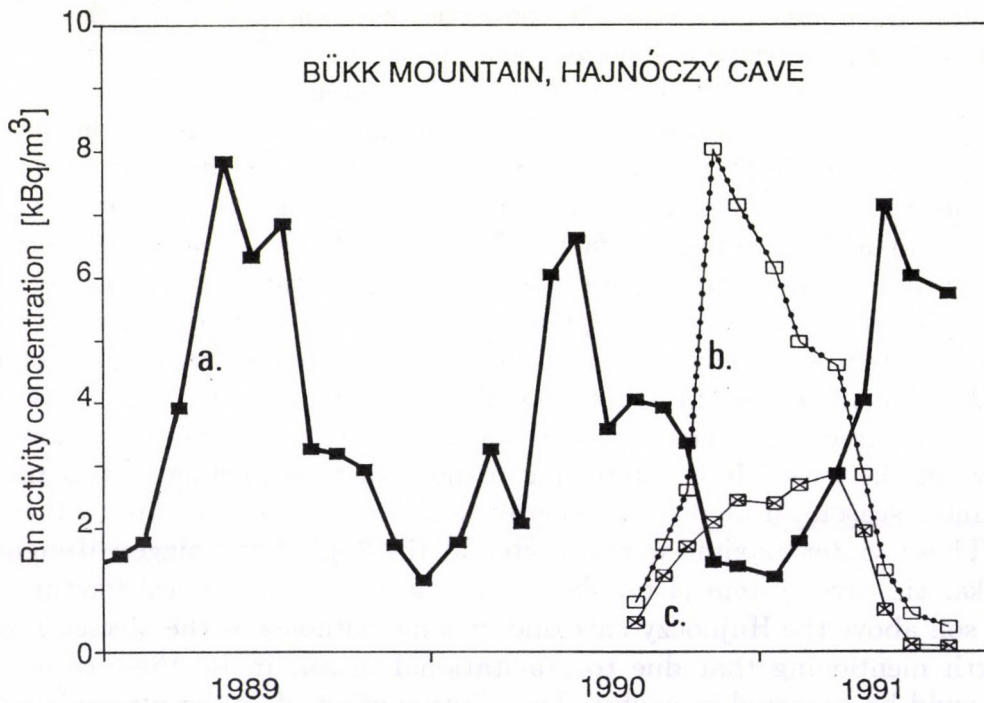


Fig. 1. Variation of the radon activity concentration in the air of a Hajnóczy cave (a), in the surface soil (b) and in the air of an open fracture (c) on the upper side of the hill, where the cave is embedded.

This work was supported in part by the Hungarian Academy of Sciences, National Scientific Research Funds (OTKA), contract No. 3005.

*Shortened from the paper presented at the 5th Int. Symp. on Natural Radiation Environment, Salzburg, Austria, Sept. 22-28, 1991.

Geochronological studies with the K/Ar method in 1991

K. Balogh, E. Árva-Sós, Z. Pécskay

A number of publications submitted in earlier years appeared in 1991.

An age of 156.8 ± 3.9 Ma has been established for the hydrothermal alteration and ore mineralization of the Kelasuri Massif, NW Caucasus, Georgia [1]. Two distinct phases, 8-12 Ma and 1-2 Ma, of the basaltic volcanism in the Bao Loc and Dilinh areas (Vietnam) were distinguished, and it has been demonstrated that bauxitization is connected only to the older phase [2]. Tertiary volcanic rocks in East Styria and Burgenland have been dated. The oldest ones are the trachyandesites (13-14 Ma) of Weitendorf and Gossendorf, 10.5-12 Ma has been measured for the alkali basalt and diabase of Oberpullendorf and Pauliberg. The nephelin basaltic activity lasted from 3.7 to 1.7 Ma B.P. [3]. In the Dráva-basin K/Ar age of $<2\mu$ illite gave the age of the last tectonic-thermal event (cca 30 Ma) corresponding to the end of horizontal displacement of blocks [4]. K/Ar ages of magmatic (ophiolites and island arc volcanites) and metamorphic rocks in NE Cuba reflect the time of tectonic events in the Upper Cretaceous [5].

In 1991 continued dating of $<2\mu$ illites in the Bükkium, NE Hungary, and closure ages from Upper Jurassic to Upper Cretaceous were obtained and interpreted as the time of low-grade metamorphism (Cooperation: Geochem. Res. Lab. Hung. Acad. Sci., Budapest; P. Árkai).

Upper Cretaceous uplift ages have been measured for the metamorphic rocks of Macskamező, Romania (Coop.: Hung. Geol. Inst., Budapest; Gy. Lelkes-Felvári).

In the southern part of Transdanubia Miocene and Paleogene volcanic rocks have been distinguished (coop.: Geophys. Res. Comp., Budapest).

The study of Neogene volcanic belt from the Gutin Mts. to the southern end of Harghita has been continued in cooperation with the Inst. Geol. Geophys., Bucharest and IPEG, Maramures. The results help the improvement of Pannonian and Pontian chronostratigraphy.

Tertiary tuffs from the Mecsek Mts. were dated and resulted Lower and Middle Miocene ages (coop.: Ore Mining Comp of Mecsek, Pécs; Z. Máthé).

On the basis of geochemical, geochronological and tectonic study of the basalt-tephrite-phonolite series, it has been concluded that the Lower Cretaceous volcanism of SE Transdanubia was the result of the final stage of an aborted rifting process at a passive continental margin (coop.: Dept. Petrogr. Geochem., Eötvös Univ., Budapest).

Several geochronological problems were studied in cooperation with the Faculty of Mining and Geology, Univ. Belgrade, Yugoslavia (S. Karamata). Partly Middle Triassic and partly Jurassic-Cretaceous ages were obtained on Mesozoic rocks from the Budva area. The younger ages correspond to tectonic events. In accordance with the geological position, Miocene ages were determined on the granites from Bukulja and Cer.

Biotite, feldspar and glauconite were dated from volcanoclastic rocks in the Marche Region in Italy, and cca 11 Ma age has been determined for the age of tectonism. (coop.: Univ. Urbino; Hung. Geol. Inst., Budapest).

References

1. Balogh, K., Ravasz-Baranyai, L., Dudaui, O., Togonidze, M.: *Chem. Erde* **51** (1991) 107.
2. Árváné Sós E., Balogh Kad., Nguyen Van Quy, Ravasz Cs., Ravaszné Baranyai L.: *Ann. Rep. Hung. Geol. Inst.*, 1988, Vol. 1. (1990) 485.
3. Balogh Kad., Lobitzer H., Pécskay Z., Ravasz Cs., Solti G.: *Ann. Rep. Hung. Geol. Inst.*, 1988, Vol. 1. (1990) 451.
4. Balogh, Kad., Kovách, Á., Pécskay, Z., Svingor, É., Árkai, P.: *Acta Geol. Hung.* **33** No. 1-4. (1990) 69.
5. Kozák M., Pécskay Z., Széky-Fux V., Andó J.: *Acta Geogr. Geol. Meteorol. Debrecina*, **26-27** (1987/88), (1990) 143.

Geochronologic and paloclimatic characterization of quaternary sediments in the Great Hungarian plain

E. Hertelendi, P. Sümegi † and GY. Szöör †

†Department of Mineralogy and Geology, Kossuth Lajos University,
H-4010 Debrecen, Hungary

The application of the "maloco-thermometer" method elaborated by P. Sümegi [1] was tested on a detailed eco-statistical analysis of the Upper Pleistocene-Holocene malacofauna of the Great Hungarian Plain. 10 malacofaunalistic levels and some species of chronological indicator role have been ascertained within the period 7000-32,000 BP years. The paleoclimatologic investigations, according to the rules of sedimentology, have been based on the oxygen isotope analysis of properly collected *Pupilla muscorum* shells. Oxygen isotope ratios of remote deposits from the same time period showed good agreement. Temperature values obtained from the results of the isotopic studies and of a malaco-thermometer constructed on the basis of the dispersion and climatic claims of the Mollusc species are also closely correlated.

For the interpretation of the results it was considered important to calibrate the temporal scale of our climatic curve with radiocarbon data. Radiocarbon measurements were performed, parallel to the determination of stable isotope ratios, on *Gastropoda*-shells.

Comprehensive studies of the paleoclimatic changes, chronological, isotope geochemical data as well bioindicative results showed the same climatic periods as found in Northern and Western Europe, although the climate of the studied area was of a rather continental character at the end of the Pleistocene (Fig.1.).

References

1. P. Sümegi (ms) 1989 Upper Pleistocene evolution history of the Hajdúság (Hungary) region on the basis of stratigraphical investigations. PhD dissertation, Debrecen: 93p.

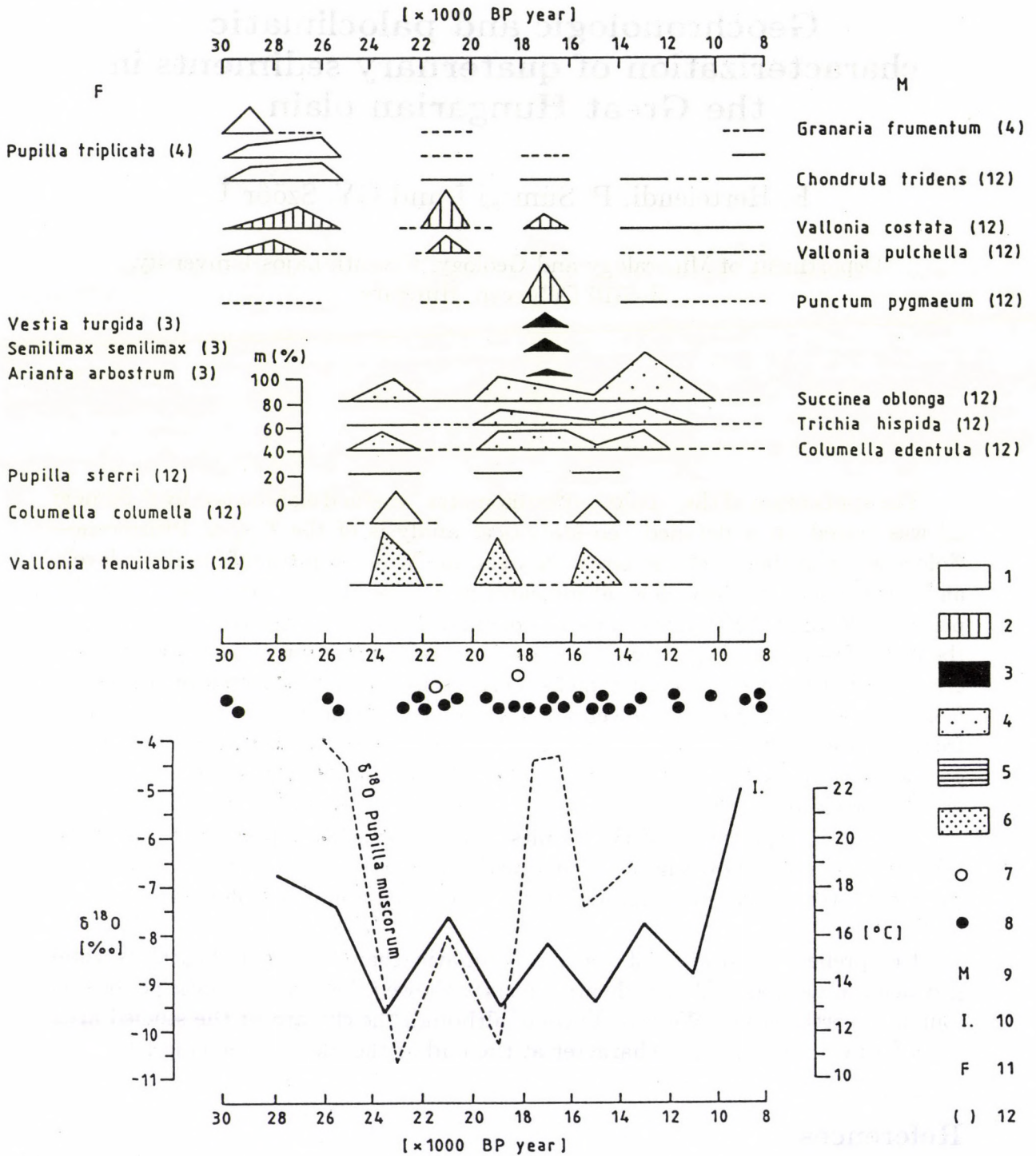


Fig. 1. Paleoclimatic and paleoecological reconstruction of the Great Hungarian Plain based on mollusk fauna and isotope geochemical data. Mean temperature values were obtained from 12 sequences: 1. Thermophilic, steppean species; 2. Mesophilic, steppean species; 3. Forest species; 4. Hygrophilic, cold-resistant, steppean fauna; 5. Hygrophilic, cold climate, steppean fauna; 6. Cold climate fauna, resistant to dry climate; 7. Radiocarbon data (from Hannover); 8. Radiocarbon data (from Debrecen); 9. Fossil species of the Great Hungarian Plain; 10. Malacothermometer (Sümegi 1989); 11. Current species of the Great Hungarian Plain; 12. Number of sequences used for the calculation of the mean percent ratio for a given species

Short-Range Transport of Aerosols Emitted by a Point Source of Mixed Character in Complex Terrain

S. Amemiya ¹, S.K. Biswas ², I. Borbély-Kiss, T. Katoh ¹,
E. Koltay, Gy. Szabó

¹Department of Nuclear Engineering, Faculty of Engineering, Nagoya
University, Furo-Cho, Chikusa-Ku, Nagoya, Japan

²Atomic Energy Centre, P.O.Box 164, Dhaka 1000, Bangladesh

As reported in the last volume of ATOMKI Annual Report longitudinal distribution of ground level aerosol concentrations have been measured in the neighbourhood of an emission source of mixed character by PIXE method. The source was located in a valley in hilly terrain. Repeated measurements and evaluation revealed the following features of short-range transport of the aerosols;

- the concentration of the plume as the function of distance calculated from a simple Gaussian model falls off much faster than the observed concentration of the various elements, even if only the diffusion is taken into account without dry and wet deposition. A plausible explanation for the slow decrease can be found in flow channeling due to the walls of the valley; the terrain strongly limits horizontal dispersion with respect to the width of a flat-area Gaussian plume.
- as a first orientation concerning the environmental effect of the emission source, a comparison is given in Table 1 between the total aerosol concentrations measured for the elements in different sampling stations in the valley, (source-to-sampler distances are indicated in km in the upper indices) and the total aerosol concentration observed in rural site, K-Pusztá [2] which is a reference station of atmospheric observations in Hungary. The elements in Table 1 are divided into two groups according to the magnitude of the fine-to-coarse concentration ratios. The small ratio approximately corresponds to dispersion mode, the large one to the accumulation mode aerosols. It is the crust-related (dispersion mode) elements and the sum of the concentrations of the observed constituents that are predominant in coarse fraction. They show strong decrease with transport distance. The oil-related (accumulation mode) elements emerge in the fine fraction. Their concentrations are

relatively stable during short-range transport. A build-up of the coarse sulphure fraction during transport due to condensation and adsorption can be observed with increasing distance. Under meteorological conditions given during the measurement the environmental effect was limited to a distance of 5 km. Beyond that the curves approached the values observed at the background station in a distance of 210 km from this site. Significant differences were experienced for zinc, lead and calcium. In the cases of zinc and lead the weak sedimentation is caused by high fine-to-coarse ratios. Another reason of the higher lead concentration may be a local enrichment of lead in pearlite stone. This was indicated by a PIXE analysis of a stone sample.

Table 1. Total aerosol concentrations in $\mu\text{g}/\text{m}^3$ measured at two sampling stations in the valley. For comparison corresponding data for a rural background station are also indicated. Upper indices show the source-to-sampler distances in km.

Mode	Elements	$\left\langle \frac{C_{\text{fine}}}{C_{\text{coarse}}} \right\rangle^{0.2-5.3}$	$C_{\text{total}}^{0.2}$	$C_{\text{total}}^{5.3}$	$C_{\text{total}}^{\text{rural}} [\text{ref.}^2]$
Dispersion	Si	0.63	61.6	0.874	0.81
	Cl	0.13	2.4	2.05	1.54
	Ca	0.31	2.59	0.88	0.005
	Fe	0.61	2.06	0.95	0.29
Accumulation	S	11.45	5.35	7.05	1.54
	Zn	2.71	0.27	0.25	0.025
	Pb	6.6	0.27	0.27	0.02

References

1. S.Amemiya, S.K.Biswas, I.Borbély-Kiss, T.Katoh, E.Koltay, Gy.Szabó ATOMKI Annual Report 1990. p. 79
2. I.Borbély-Kiss, E.Koltay, Gy.Szabó, L.Bozó, E.Mészáros and Á. Molnár, Nucl. Instr. Meth. B49 (1990) 388-394

Dry Deposition Velocities of Atmospheric Aerosol Particles from Vertical Concentration Profiles Measured by PIXE Method

S. Amemiya ¹, I. Borbély-Kiss, T. Katoh ¹, E. Koltay,
E. Mészáros ², Á. Molnár ², Gy. Szabó, M. Varga ²

¹Department of Nuclear Engineering, Faculty of Engineering, Nagoya University, Furo-Cho, Chikusa-Ku, Nagoya, Japan

²Institute for Atmospheric Physics, H-1675 Budapest, P.O.Box 39 Hungary

Vertical concentration profile measurements performed on aerosol samples by PIXE elemental analysis have been reported in the last volume of the Annual Report of ATOMKI [1]. From samples taken in two subsequent sampling experiments elemental concentrations have been obtained in coarse and fine size fractions for 13 elements as the function of height. Experiment 1 and 2 covered the air layers 0-100 m and 0-30 m, respectively, the first sampling was performed at noon in summer time while second sampling early next morning. Different meteorological conditions resulted in different character of the distribution curves. As an example, data for the cases of Si and S as well as the sum of concentrations of elements Al, Si, S, Cl, K, Ca, Ti, Mn, Fe, Cu, Zn, As and Pb are shown in Fig.1. The different behaviour of the distributions in experiment 1 and 2 can be clearly seen. The general decrease of the concentrations with increasing height, which was observed in experiment 1, revealed an upward air transport under the given meteorological conditions. This means that the lower-lying air surface represented the primary source of aerosols. This behaviour shows much similarity with that described in Ref.[2]. A direct determination of deposition velocities from this experiment seems to be impossible. The opposite behaviour found for the majority of the elements in experiment 2 suggested the application of the analysis described in Ref.[3] to deduce dry deposition velocities $v_{d,i}$ for the i -th element. For moderately unstable meteorological conditions the formula

$$v_{d,i} \approx \frac{C_i(z_2)}{C_i(z_1) - 1} \cdot \frac{(ku_*)}{\ln(z_2/z_1)}$$

is valid, where $C_i(z_j)$ is the concentration of the i -th element at height z_j , k is the Karman constant ($k \approx 0.41$), $u_* = 0.0071u_{wind}$ is the friction velocity. With a

fitting procedure, dry deposition velocities presented in Table 1 have been deduced for seven elements. Also shown are in the table the experimental data from Refs. 4,5,6,7,8,9. The large scattering of the measured data from Refs.4 and 6 as well as the large difference between the calculated values predicted by different models (Ref.10,11) reflect the complexity of the deposition process. Our data - with a single exception - are within the intervals covered by other author's results.

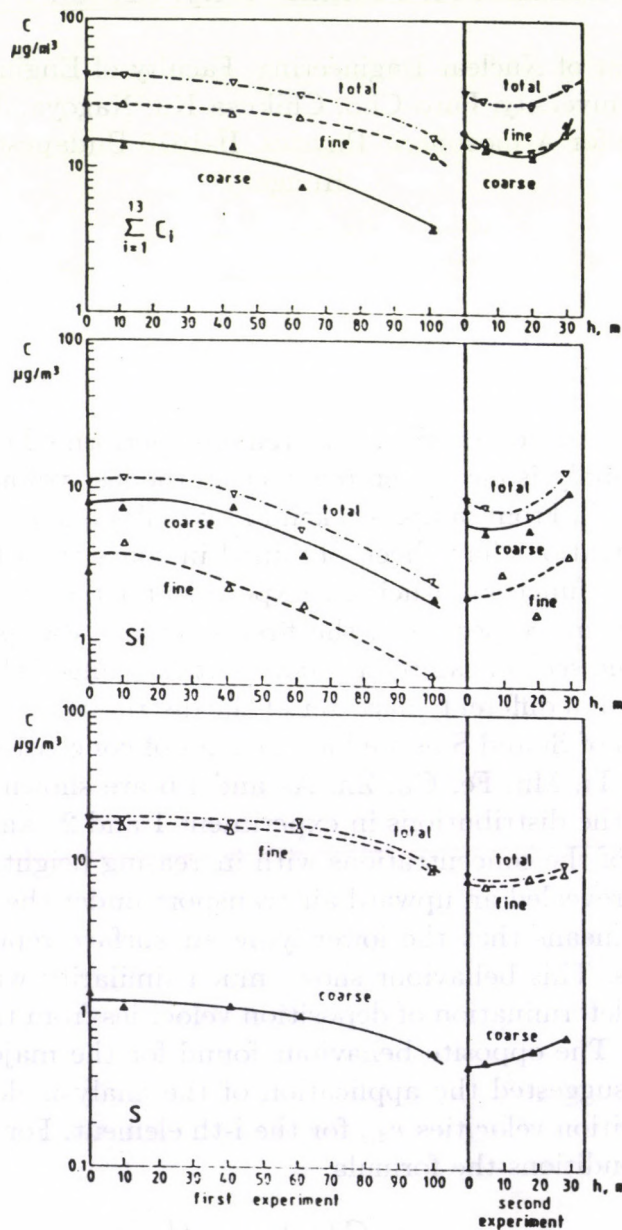


Fig. 1. Height distribution curves for elements Si and S as well as for the sum of concentrations of Al, Si, S, Cl, K, Ti, Mn, Fe, Cu, Zn, As, and Pb. Coarse and fine fractions and their sums are presented for both experiments

Element	This work	Ref. 4	Ref. 3	Ref. 5	Ref. 6	Ref. 7	Ref. 8	Ref. 9	Ref. 10
Al	0.20*	0.20-7.90 2.63		0.9-2.7	1.30			2.41	0.98
Si	0.39* 1.63+ 0.55#							1.91	0.71
S	1.10* 0.13+		1.0-1.4 1.0-1.4	0.2-2.9 0.2-2.9					
Cl	0.19+			0.2-6.3				1.61	0.67
Ti	0.03*	0.50-5.60 3.0		0.7-2.2	1.0			3.22	1.26
Mn	0.46+	0.27-6.40 1.70		0.4-0.9	0.56	0.4;2.2		1.31	0.60
Zn	0.10+	0.05-0.66 0.34		0.4-4.5	0.62		0.25	1.05	0.45

Table 1. Dry deposition velocities for atmospheric aerosol in cm/s from the present experiments compared to the data from the literature (measured on coarse [*], fine [+], and coarse+fine [#] fraction)

References

1. S. Amemiya, I. Borbély-Kiss, T. Katoh, E. Koltay, E. Mészáros, Á. Molnár, Gy. Szabó, M. Varga: ATOMKI Annual Report 1990, p.77
2. P. S. Guest, W. H. Mach and J. Winchester, *J. Geophys. Res.* 89 (1984) 1459-1467.
3. R. G. Everett, B. B. Hicks, W. W. Berg and J. W. Winchester, *Atmos. Environ.* 13 (1979) 931-934.
4. C. I. Davidson and Yee-Lin Wu, in *Control and Fate of Atmospheric Trace Metals*, eds. J. M. Pacyna and B. Ottar (Kluwer Academic Publishers, Dordrecht, 1989) pp. 147-202.
5. G. A. Sehmel, *Atmos. Environ.* 14 (1980) 983-1011.
6. T. A. McMahon and P. J. Denison *Atmos. Environ.* 13 (1979) 571-585.
7. J. B. Milford and C. I. Davidson, *J. Air Pollut. Contr. Ass.* 35 (1985) 1249-1260.
8. W. H. Chan, R. J. Vet, C. U. Ro, A. J. S. Tang and M. A. Lulis, *Atmos. Environ.* 18 (1984) 1001-1008.
9. C. J. Davidson, J. M. Miller and M. A. Peskov, *Water Air and Soil Pollut.* 18 (1982) 25-43.
10. S. A. Slinn and W. G. N. Slinn, in *Atmospheric Pollutants in Natural Waters* ed. S. J. Eisenreich (Ann Arbor Science, Ann Arbor, MI) pp.23-53

Year	1970	1971	1972	1973	1974	1975	1976	1977	1978	1979	1980
1	0.00	0.00	0.00	0.00	0.00	0.00	0.00	0.00	0.00	0.00	0.00
2	0.00	0.00	0.00	0.00	0.00	0.00	0.00	0.00	0.00	0.00	0.00
3	0.00	0.00	0.00	0.00	0.00	0.00	0.00	0.00	0.00	0.00	0.00
4	0.00	0.00	0.00	0.00	0.00	0.00	0.00	0.00	0.00	0.00	0.00
5	0.00	0.00	0.00	0.00	0.00	0.00	0.00	0.00	0.00	0.00	0.00
6	0.00	0.00	0.00	0.00	0.00	0.00	0.00	0.00	0.00	0.00	0.00
7	0.00	0.00	0.00	0.00	0.00	0.00	0.00	0.00	0.00	0.00	0.00
8	0.00	0.00	0.00	0.00	0.00	0.00	0.00	0.00	0.00	0.00	0.00
9	0.00	0.00	0.00	0.00	0.00	0.00	0.00	0.00	0.00	0.00	0.00
10	0.00	0.00	0.00	0.00	0.00	0.00	0.00	0.00	0.00	0.00	0.00

The dipositive solution of atmospheric pollution is a complex problem that requires a multi-faceted approach. This study aims to explore the various factors contributing to air quality degradation and to propose effective strategies for their mitigation.

References

1. Smith and Jones, *Journal of Environmental Science*, 1980, 10(1), 1-10.
2. Brown and White, *Atmospheric Pollution*, 1981, 25(1), 15-20.
3. Green and Black, *Environmental Science and Technology*, 1982, 16(1), 30-35.
4. Lee and Kim, *Journal of Air Quality Management*, 1983, 28(1), 45-50.
5. Park and Kim, *Journal of Environmental Science*, 1984, 14(1), 60-65.
6. Kim and Park, *Journal of Environmental Science*, 1985, 15(1), 70-75.
7. Kim and Park, *Journal of Environmental Science*, 1986, 16(1), 80-85.
8. Kim and Park, *Journal of Environmental Science*, 1987, 17(1), 90-95.
9. Kim and Park, *Journal of Environmental Science*, 1988, 18(1), 100-105.
10. Kim and Park, *Journal of Environmental Science*, 1989, 19(1), 110-115.

BIOLOGICAL
AND
MEDICAL RESEARCH

Dosimetical Parameters of a d + D Type High Pressure Gas Target with Double Entrance Foil

T. Molnár⁺, A. Fenyvesi, I. Mahunka

Intense fast neutron sources based on cyclotrons provide important opportunities for human purpose applications (e.g. radiotherapy treatments of some kinds of malignant tumors, fast neutron radiography, *in vivo* fast neutron activation analyses, *in vivo* experiments to study the radiobiological effects of fast neutrons, etc.).

At low energy cyclotrons ($E_{\text{proton}} \leq 20$ MeV), a pressurized D_2 -gas target bombarded by deuterons of the highest energy available at the accelerator is the best solution to fulfil the mean neutron energy and intensity requirements of these type of irradiations. A single entrance foil type gas target was developed by Schraube [1] for these purposes for the German Cancer Research Institute (Heidelberg). A double foil version of Schraube's target developed at the ATOMKI [2] has been installed at the MGC-20E cyclotron in order to make most of the mentioned applications possible also in Debrecen. This report presents some dosimetical parameters of the uncollimated mixed neutron-gamma field in air produced by our double entrance foil version.

The multi foil activation technique and the LSQUNF code [3] was applied to determine the spectral distribution of neutrons at SSD = 1 m from the center of the neutron emitting volume (Fig. 1.) produced at pressure $p_{\text{gas}} = 11$ bar. The average energy of neutrons above 1 MeV was 10.1 MeV.

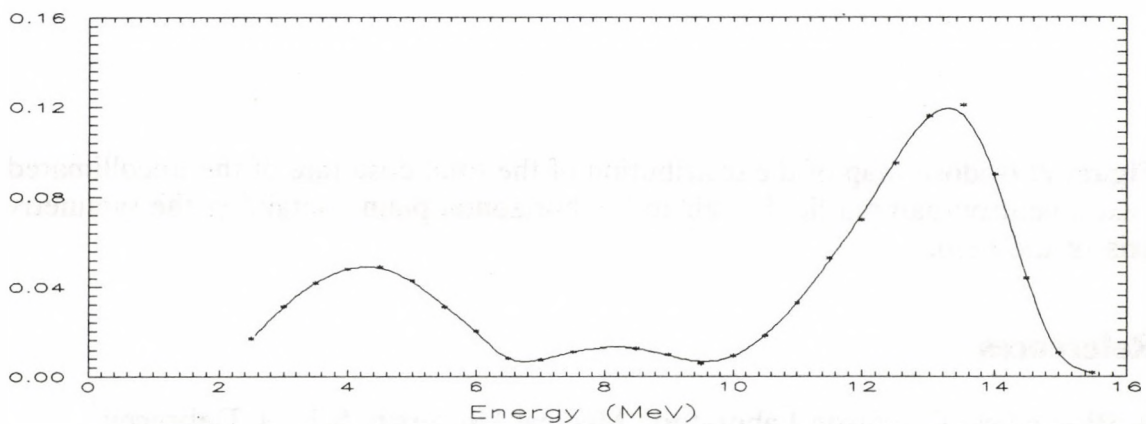


Figure 1: Spectral distribution of neutrons at forward direction and at SSD = 16 cm from the geometrical center of the pressurized D_2 -gas target.

2. T. Molnár⁺, ...

Neutron and gamma dose rate distributions were measured by the twin chamber technique using thimble type ionization chambers of different neutron and gamma sensitivities. The first one, the TE-TE chamber (Type: EXRADIN T2 with a build up cap of 3 mm thick) was made of A-150 tissue equivalent plastic and it was flushed with tissue equivalent gas. The second chamber was a Mg-Ar chamber (Type: EXRADIN M2 with 3 mm build up cap).

A map containing isodose curves of the total dose rate distribution of the uncollimated mixed neutron-gamma field produced in air at $p_{\text{gas}} = 11$ bar is shown in Fig. 2. It was measured in a horizontal plain containing the symmetry axis of the field.

At SSD = 1 m from the center of the neutron emitting volume, the total dose rate was $D_{\text{tot}} = (160 \pm 8)$ mGy/ μC and $D_{\gamma}/D_{\text{tot}} = 0.06 \pm 0.003$ was resulted for the gamma component.

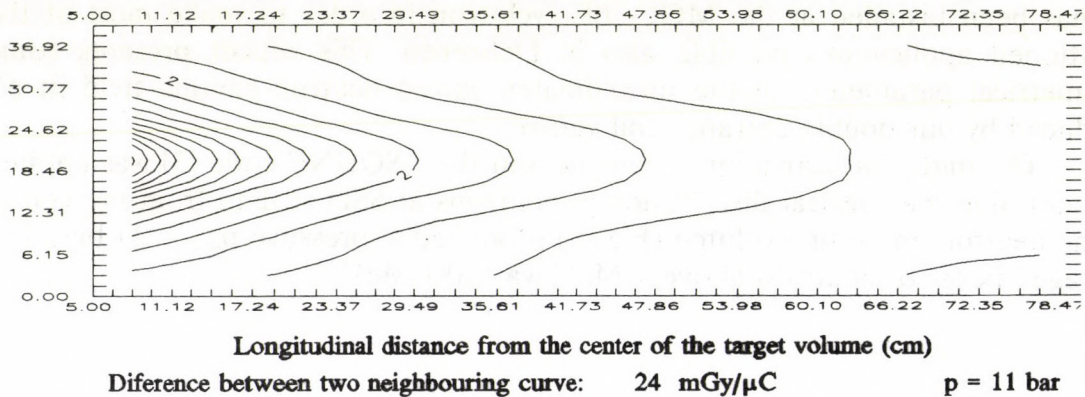


Figure 2: Isodose map of the distribution of the total dose rate of the uncollimated mixed neutron-gamma field in air in the horizontal plain containing the symmetry axis of the field.

References

+ Biomedical Cyclotron Laboratory, Medical University School, Debrecen

- 1 H. Schraube: GSF-Bericht S465
- 2 T. Molnár, A. Fenyvesi, I. Mahunka, F. Tárkányi: ATOMKI Annual Rep. 1989, p. 94
- 3 V. A. Pojarkov, T. S. Sadovnikov, J. Csikai, S. Sudár: Atomnaja Energija **67/3** 222 (1989)

Determination of RBE and OER of the p(18MeV) + Be Cyclotron Fast Neutron Source on Bacterial System

A.M. Dám⁺, L.G. Gzásó⁺, M. Rétlaki⁺
A. Fenyvesi, T. Molnár^{*}, I. Mahunka

Clinicians and researchers have a considerable interest for the radiobiological and cytogenetic effects of neutrons since their introduction as a radiotherapeutic tool more than twenty years ago. High LET (Linear Energy Transfer) radiations having lower OER (Oxygen Enhancement Ratio) than the conventional low LET radiations afford distinct advantages for radiotherapy [1]. The application of fast neutrons and other high LET radiations in radiotherapy has been stimulated by the expectation that in comparison with X-ray, the differences in radiobiological factors might result a larger RBE (relative biological effectiveness) [2]. Accepting that the biological effects of low and high LET particles are different, it is clear that the knowledge of the most important RBE and OER values are crucial in application of a fast neutron irradiation facility for radiobiological research and therapeutical purpose.

To facilitate the introduction of neutron therapy in Hungary, the basic radiobiological parameters of the p(18 MeV) + Be intense fast neutron source based on the MGC-20E cyclotron were determined. The OER and RBE were determined on bacterial model system (*Escherichia coli* B/R, ATCC No. 23277) in uncollimated mixed neutron-gamma fields ($D_{\text{gamma}}/D_{\text{neutron}} = 0.1$). The survival was investigated at end point. The absorbed dose was determined on the basis of the recommendations of the ICRU [3] and the ECNEU [4].

The RBE for *E. coli* B/R was determined in nitrogen and under oxic condition using ^{60}Co γ -ray as reference radiation. The summarized data of survival curves are shown in Fig. 1. The values are: $\text{RBE}(\text{anoxic}) = 3.92$ and $\text{RBE}(\text{oxic}) = 2.46$. The results of the calculation of OER are: $\text{OER}(^{60}\text{Co}) = 2.10$ and $\text{OER}(\text{n-}\gamma) = 1.31$.

Chemical modification of radiation response as a potential adjust to radiation in cancer treatments has received renewed interest. One potential use of chemical radiation modifiers involves the sensitization of hypoxic cells or/and the protection of normal cells. From therapeutical point of view it is essential to know the effects of these agents at high LET radiations.

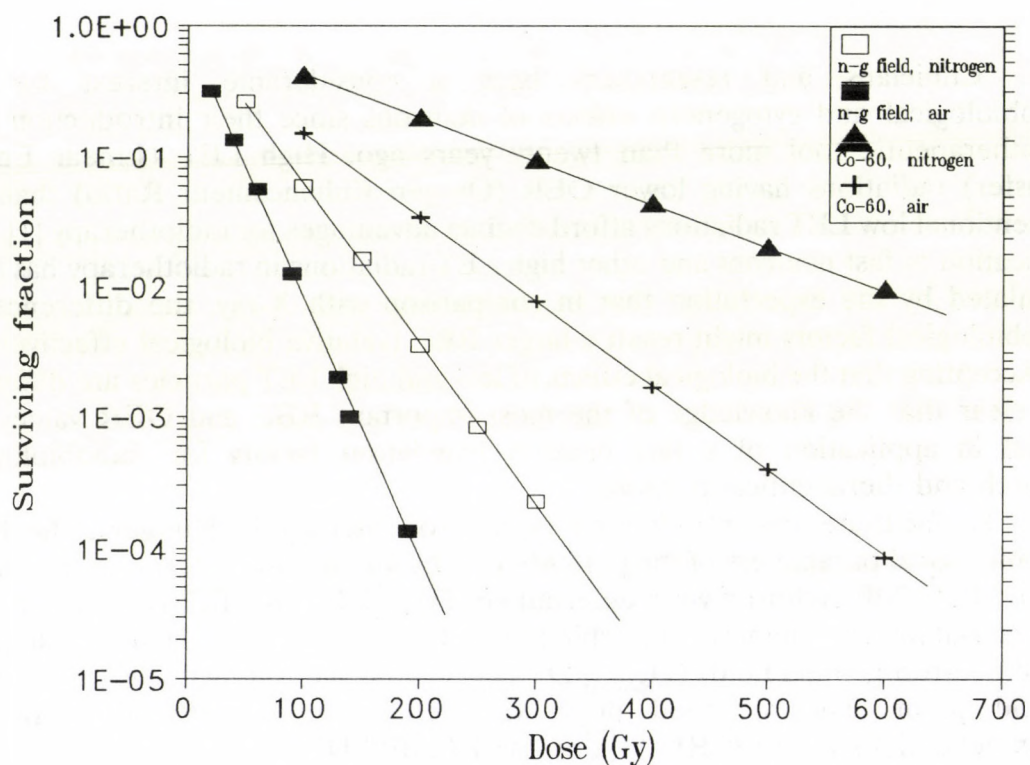
Two of the most effective compounds were tested. Misonidazole as a selective hypoxic electron affinic sensitizer was found to be lower in modulation of neutron induced cell lethality than observed for the ^{60}Co γ -rays. The sensitizer enhancement ratio (SER) for the mixed field was found to be $\text{SER}(\text{n-}\gamma) = 1.07$ and for the reference gamma radiation $\text{SER}(^{60}\text{Co}) = 1.84$.

The effect of the aminothioli type radioprotector WR 1065 was characterized by the protection factor (PF) and $\text{PF}(\text{n-}\gamma) = 1.67$ and $\text{PF}(^{60}\text{Co}) = 2.01$ were resulted for fast neutrons and gamma radiation, respectively.

Our results can promote setting up the further experimental protocol based

2. A.M. Dám⁺, ...

on mammalian cell culture systems and tumor bearing animals.



OER: 1.31 (mixed field); 2.1 (Co-60)
RBE: 3.92 (nitrogen); 2.46 (air)

Figure 1. Survival curves of *E. coli* after exposure in mixed neutron-gamma field or ⁶⁰Co gamma rays.

References

+ National Research Institute of Radiobiology and Radiohygiene, Budapest
* Biomedical Cyclotron Laboratory, Medical University School of Debrecen

1. J. F. Fowler, D. K. Bewley: Radiobiological Applications of Neutron Irradiation, IAEA, Vienna, 1972, p. 239
2. G. W. Barendsen: Int. J. Radiat. Oncol. Biol. Phys. **8** 239 (1982)
3. ICRU Report 26, ICRU Publications, 7910 Woodmont Ave., Suite 800, Bethesda, Maryland 20814-3095
4. J. J. Broerse, B. J. Mijnheer, J. R. Williams: British J. Radiol. **54** 882 (1981)

Status Report on the Nuclear Data Program for Practical Applications of Debrecen MGC-20 Cyclotron

F. Tárkányi, L. Andó, A. Fenyvesi, Z. Kovács, I. Mahunka, P. Mikecz,
T. Molnár*, F. Szelecsényi, Z. Szűcs

Nuclear data play important role in different applications of charged particle and secondary neutron beams of cyclotrons. Usually for the practical applications the decay data are measured with sufficient accuracy. The reaction data, however, are not so well known and there is an increasing demand for standardization.

The Department of Cyclotron Application have been working in this field since the commissioning of the cyclotron in Debrecen in 1985. In the last one year period in close collaboration with other institutes, this program was continued in traditional direction of charged particle induced nuclear reactions. First technical steps were done for starting measurement of some neutron induced reactions.

1. Charged Particle Induced Data

1.1. Measurements of excitation functions for isotope production

The investigated isotopes and reactions were chosen on the need of the nuclear medicine, biology and ecology.

The excitation functions for production of ^{82m}Rb , ^{38}K , ^{77}Br and ^{75}Br were studied in collaboration with the Institut für Chemie 1 (Nuklearchemie) (KfA Jülich, FRG) under a Hungarian - German bilateral scientific agreement.

The excitation function of $^{209}\text{Bi}(^3\text{He},3n)^{209}\text{At}$ was investigated for production of ^{209}At which is used for modelling and testing the chemistry of the well known ^{211}At (1). The irradiations was performed at the Accelerator Laboratory of the Abo Akademi (Turku, Finland) in a collaboration between the Hungarian Academy of Sciences and the Academy of Finland.

For optimization of production of ^{123}I on low energy cyclotrons the excitation function of the $^{123}\text{Te}(p,n)^{123}\text{I}$ nuclear reaction was remeasured in collaboration with Moscow Kurchatov Institute.

The measurement of the excitation function of the $^{40}\text{Ar}(\alpha,p)^{43}\text{K}$ reaction was completed. The produced ^{43}K was used for investigation of water transport in different plants.

Different efforts were made to measure excitation function using enriched ^{202}Hg for production of ^{201}Tl .

2. F. Tárkányi et al.

1.2. Measurements of excitation functions for monitoring charged particle beams

In the frame of a systematical study of monitor reactions for intensity and energy determinations of charged particle beams, the excitation functions of proton induced nuclear reactions on ^{nat}Ti were remeasured in collaboration with the Department of Radiopharmaceuticals of Nuclear Research Institute (Rez, Czechoslovakia)

1.3. Calculations of cross sections

It is well known that the existing nuclear models are able to predict the necessary reaction cross sections only with modest power. These models can be used as a fitting tool during data evolution. The calculated cross-sections can be useful as a guide in the case of non-measured nuclear reactions, or can help to select among data sets when large disagreements exist.

As a requirement of investigation of new reaction routes and the critical evaluation of the existing data we have started to implement and to compare the capability of different codes. First the minimal input EXIFON code of Kalka(2) and the more sophisticated STAPRE (Hauser - Feshbach plus Exiton Model) code of Uhl(3) were tested. Both of them can be useful for selecting a proper experimental conditions and to understand the measured experimental data.

1.4. Data compilation and evaluation

On the basis of experience collected on the field of nuclear data measurement in cooperation and with help of Nuclear Data Section of the International Atomic Energy Agency compilation of charged particle induced reaction data has been started. The compiled and evaluated data will be used in the international data network through the IAEA and in our local applications.

2. Neutron Induced Data

In connection with practical applications of our high intensity and broad energy spectrum cyclotron neutron beams, a quasi monoenergetic neutron source is under installation. After the investigation of the quality of the neutron source, cross section measurements for dedicated applications will be started.

References

- * Biomedical Cyclotron Laboratory, Medical University School of Debrecen
1. F. Szelecsényi, Z. Szűcs, O. Solin, J. Bergman and S-J. Heselius, ATOMKI Annual Report 1991, (1992)
2. H. Kalka, EXIFON A Statistical Multistep Reaction Code, Dresden, 1990
3. M. Uhl, B. Strohmaier, Computer Code for Particle Induced Activation Cross Sections and Related Quantities, IKR 76 01

Production of Astatine Isotopes via $^{209}\text{Bi}(^3\text{He},\text{xn})$ Processes

F. Szelecsényi, Z. Szűcs, O. Solin*, J. Bergman* and S.-J. Heselius*

* *Abo Academi, Accelerator Laboratory, SF-20500 Turku, Finland*

There is a growing interest in astatine radioisotopes from the standpoint of radiobiological and therapeutical application, particularly with respect to the use of astatine-labelled monoclonal antibodies. On the other hand, both the organic and inorganic aspects of the chemistry of astatine stimulate a continuing interest, especially in connection with the formation of complexes and stability of ionic compounds [1]. Due to the very weak gamma-rays of the medically significant ^{211}At ($T_{1/2} = 7.2$ h), developmental chemistry is best accomplished with other astatine isotopes (i.e. ^{208}At $T_{1/2} = 1.63$ h; ^{209}At $T_{1/2} = 5.41$ h; and ^{210}At $T_{1/2} = 8.1$ h) which are more suitable for gamma-ray spectroscopy.

It is known that astatine is produced directly via the irradiation of bismuth with alpha particles. However, this method of production demands a high energy accelerator with $E_{\alpha} > 30$ MeV [2]. The aim of the present study was to investigate the production possibilities of different astatine isotopes using a multiparticle compact cyclotron. Taking into account the parameters of our cyclotrons and the threshold energies of the possible charged particle induced reactions leading to At isotopes, the $^{209}\text{Bi}(^3\text{He},\text{xn})$ processes appeared most suitable.

Excitation functions were measured by the activation method using the stacked-foil technique. High purity bismuth prepared via evaporation of Bi on natural copper foils were used as target materials. The target stacks were irradiated in the external beam of the Turku cyclotron with 28 MeV incident ^3He -particle energy. The average beam current on the targets was determined using a Faraday-cup. The activity of the irradiated samples was determined by standard Ge(Li) detector gamma-ray spectroscopy. The total estimated errors in the cross sections are 12-17 %.

The measured excitation functions covering an energy range of 15 to 28 MeV are shown in Fig.1 together with the only previously reported values [3]. In the case of $^{209}\text{Bi}(^3\text{He},3\text{n})^{209}\text{At}$ reaction the present work shows good agreement with the data of Storm but for the $^{209}\text{Bi}(^3\text{He},2\text{n})^{210}\text{At}$ reaction, our values are significantly higher than the earlier published ones. Our presented excitation function shows a maximum of 21 mb at 24 MeV for ^{210}At production. The cross section data of Storm around 29 MeV (165 mb) support our values measured at lower energy regions for $^{209}\text{Bi}(^3\text{He},4\text{n})^{208}\text{At}$ reaction. Metallic bismuth targets of 0.25 g/cm² melted on Cu backings were used for thick target yield measurement. The integral thick target yields of $^{209}\text{Bi}(^3\text{He},\text{xn})^{208,209,210}\text{At}$ reactions calculated from the excitation functions are shown in Fig.2. The experimental thick target yields are in good agreement with the calculated values. For separation of astatine from the bismuth target a dry-distillation method was used with $85 \pm 5\%$ overall yield [4].

On the basis of our data the $^{209}\text{Bi}(^3\text{He},3\text{n})^{209}\text{At}$ reaction is the method of choice for the production of ^{209}At for in-house use at low energy cyclotrons.

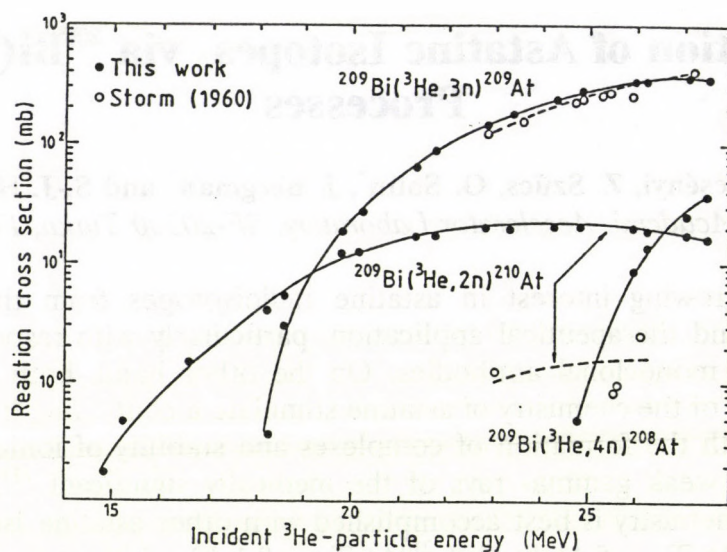


Fig. 1. Excitation functions for the formation of $^{208,209,210}\text{At}$ in ^3He -particle induced nuclear reactions on ^{209}Bi

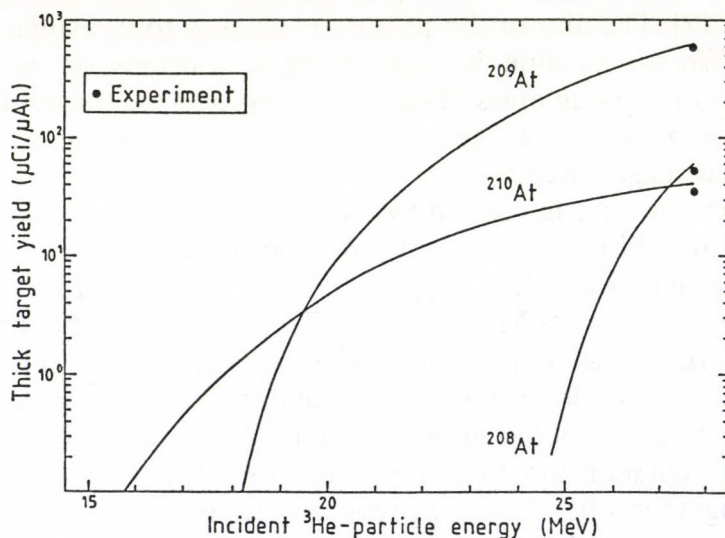


Fig. 2. Calculated thick target yields of $^{208,209,210}\text{At}$ in ^3He -particle induced reactions on natural Bi as a function of the incident ^3He -particle energy

This work was supported by the Hungarian Academy of Sciences and the Academy of Finland.

References

1. Rössler K., *Radiochimica Acta* **47**, 1 (1989)
2. Beyer G.J., Dreyer R., Oldrich H., Rösch F., *Radiochem. Radioanal. Lett.* **47**, 63 (1981)
3. Storm A., Report UCRL-9732 (1960)
4. Szűcs Z., Szelecsényi F., *Izotóptechn. Diagn.* **33**, 221 (1990)

PRODUCTION OF $^{11}\text{CH}_4$ FOR THE PREPARATION OF H^{11}CN INTERMEDIER

É. Sarkadi, Z. Kovács, P. Mikecz, F. Szelecsényi, L. Andó

^{11}C labelled radiopharmaceuticals are frequently used in the positron emission tomography. Considerable part of the syntheses of these products are carried out using H^{11}CN intermedier, like ^{11}C -labelled amino acids [1,2,3]. Two different types of methods have been described for routine H^{11}CN production via $^{11}\text{CH}_4$ precursor. In both cases the $^{14}\text{N}(p,\alpha)^{11}\text{C}$ nuclear reaction is involved. In one case the target is N_2 containing 1 % O_2 and the final product in the target gas is $^{11}\text{CO}_2$, which forms $^{11}\text{CH}_4$ after reduction steps [4]. The other procedure uses a mixture of N_2 and H_2 gases, 95% and 5% respectively, as a target gas with very low O_2 content [5,6], which directly gives $^{11}\text{CH}_4$ without further treatment. This later method was chosen to develop our H^{11}CN production procedure. We report here on the preparation of the $^{11}\text{CH}_4$ precursor and its conversion to H^{11}CN .

The target gas was prepared in an evacuated 15 l volume bottle as follows. H_2 was slowly led through a 5 Å molecular sieve trap, cooled with liquid nitrogen, filling the bottle up to 0.7 bar. Then the pressure was increased up to 14 bars during 8 hours with N_2 cleaned at 700 °C over a copper furnace regenerated with H_2 at 700 °C. The 20 cm long and 3 cm in diameter aluminum target chamber was filled up with a total pressure of 10 bars of this gas mixture through Oxisorb trap (Messer Griesheim GmbH) to reach further elimination of O_2 traces.

The water cooled target was irradiated for 40 minutes with 15 MeV protons at 10 μA beam current using our MGC 20 compact cyclotron. The yield of ^{11}C was 0.5 GBq/ μA and a small amount of ^{13}N coming from $^{14}\text{N}(p,d)^{13}\text{N}$ reaction also was detected. The composition of the irradiated target gas was determined by gas chromatography using thermal-conductivity and subsequent radioactivity detectors. The analysis were carried out on Porapak Q column (length 1.5 m, diameter 4 mm, mesh size 80-100) at a He flow rate of 10 ml/min. The temperature was programmed as follows: -30 °C for 12 min followed by a linear gradient of 10 °C/min up to 150 °C. 4 ml irradiated gas sample was injected in together with 1 ml inactive sample (25 % N_2 , 64 % CH_4 , 6 % CO and 5 % CO_2) for

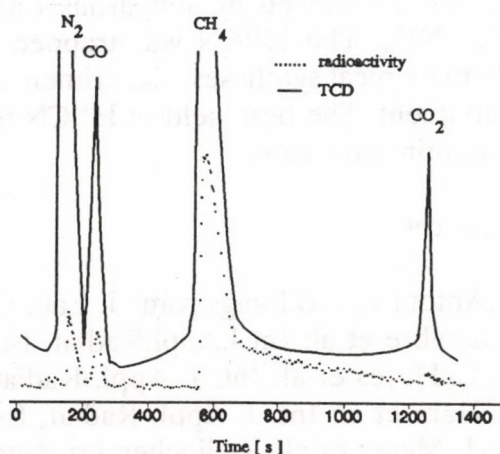


Figure 1 Radiogaschromatogram of the irradiated $\text{N}_2 : \text{H}_2$ target gas mixture

peak identification. The radiogaschromatogram is shown in Fig.1. together with the thermal-conductivity signals of identifying gases. 90 % of the total ^{11}C activity appears as $^{11}\text{CH}_4$ and only 8 % ^{11}CO and 2 % $^{11}\text{CO}_2$ was formed due to traces of O_2 in the target gas mixture.

The scheme of the $\text{NH}_3 + ^{11}\text{CH}_4 \rightarrow \text{H}^{11}\text{CN}$ conversion system is shown in Fig.2. The flow rate of the irradiated target gas was regulated by a needle valve and

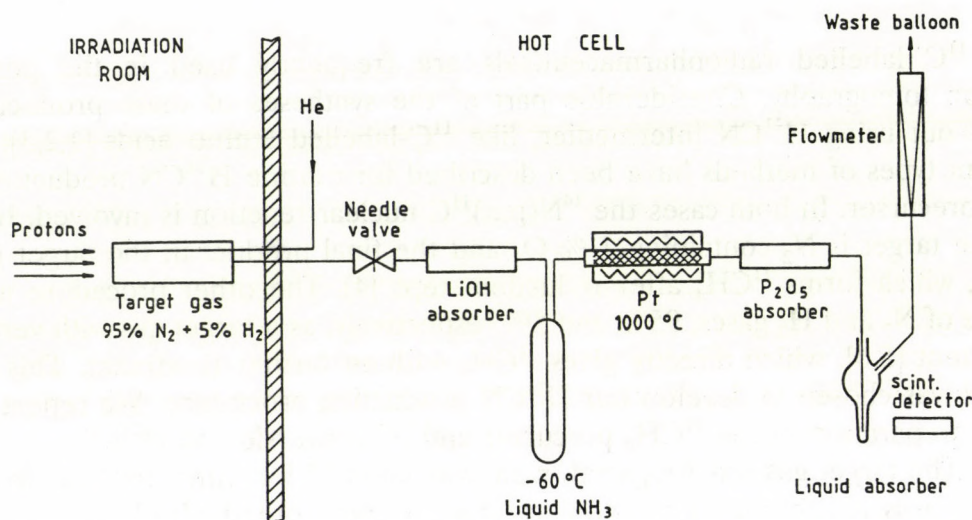


Figure 2 The scheme of the H^{11}CN production system

kept constant at 200, 400 and 600 ml/min. He gas flow was used for washing out the rest of the target gas. The NH_3 was added to the target gas by bubbling through liquid NH_3 held at $-60\text{ }^\circ\text{C}$. The Pt furnace (quartz tube with 10 mm in diameter, 16 g Pt in 8 cm length and 320 cm^2 surface) was kept at $1000\text{ }^\circ\text{C}$. The $^{11}\text{CO}_2$ and H_2O traces were removed by anhydrous LiOH absorber, while the P_2O_5 retained the surplus NH_3 . The H^{11}CN was trapped in liquid (water, THF etc.) suitable for further chemical syntheses. Experiments for conversion optimization are still under development. The best yield of H^{11}CN from $^{11}\text{CH}_4$ corrected by decay was 60 % at 400 ml/min flow rate.

References

1. G. Antoni and B. Langstrom: *J. Lab. Compd. and Radiopharm.* **27** 571 (1989)
2. J. Sambre et al: *Int. J. Appl. Radiat. Isot.* **36** 275 (1985)
3. R. L. Hayes et al: *Int. J. Appl. Radiat. Isot.* **29** 186 (1978)
4. T. Hara et al: *Int. J. Appl. Radiat. Isot.* **38** 1092 (1987)
5. G.-J. Meyer et al: *Radiochemica Acta* **50** 43 (1990)
6. D. Chrisman et al: *Int. J. Appl. Radiat. Isot.* **26** 435 (1975)

A case control study of radon and lung cancer in eastern Hungary*

Zs. Déri ^a, S. Takács ^a, I. Csige, I. Hunyadi

^aPublic Health Institute of County Borsod, Miskolc, Hungary

In joint research programs the Public Health Institute of County Borsod and the Institute of Nuclear Research of the Hungarian Academy of Sciences have made from 1989 a case control study in dwellings by track etch detectors in the eastern part of Hungary. The goal of the study was to adapt a complex survey technique and to apply it for the investigation of the possible relation between indoor radon concentration level and lung cancer. We chose the case control study as an appropriate method and constructed a well-selected questionnaire on data about the persons, the state of their health condition, smoking habits, and about their house with special attention to building materials and mode of construction. Then we designated a region for the investigation and nominated the members of the case and the control group. The selected town and its surroundings of about 52 thousand inhabitants have a closed population, and the average annual incidence of lung cancer during the last eight years was one of the highest in Borsod county but with the lowest deviation (526 ± 44 case/million people year). This average is higher than the Hungarian average of 1990 (460 case/million people year). The members of the case group were selected on the basis of data of the local oncological institute and the individuals of the control group were selected among volunteers. One radon monitor was placed in the most frequently used room of the house for one year and another one was dug in about 0.4 m depth and covered by soil nearby every measured residence for 3-4 months in the winter season. The technique for the measurement of the indoor radon activity concentration was developed by the Institute of Nuclear Research, Debrecen. The measuring device is a diffusion cup equipped by LR-115 alpha track etch detectors both inside and outside. The cup is closed by a 40 μm thick PE filter. This way the detector inside measures only the ^{222}Rn exposure, and the detector outside measures the total alpha exposure. After exposure the track detectors were developed by chemical etching in 10 wt% solution of NaOH at 60 °C during 2.5 hours and the tracks were counted manually under optical microscope. The observed track densities were in the region of 40-1200 track/cm³*30 day for dwellings and 80-3000 track/cm³*30 day for soil gas. The collected data were evaluated by LOTUS 1-2-3 software, the studies of the statistical significance were carried out by Welch test of the normalized distributions. It was presumed that the indoor radon follow log-normal distribution, as it is considered in many studies. After a careful selection we got the case group of 33 individuals and the control group of 66. The arithmetical average of the measured radon activity concentration data are 192 Bq/m³ (52-703) and a 155 Bq/m³ (22-726), respectively. Figure 1 shows the normalized distribution of the radon activity concentrations for the case and control groups. Our calculations show that the difference between the mean values of the two distributions is significant at 95 % level. The annual bronchial dose equivalent (H_b), the pulmonary dose (H_p), and

the effective dose equivalent (H_e) were estimated by the method described in the ICRP 50 Publication [1].

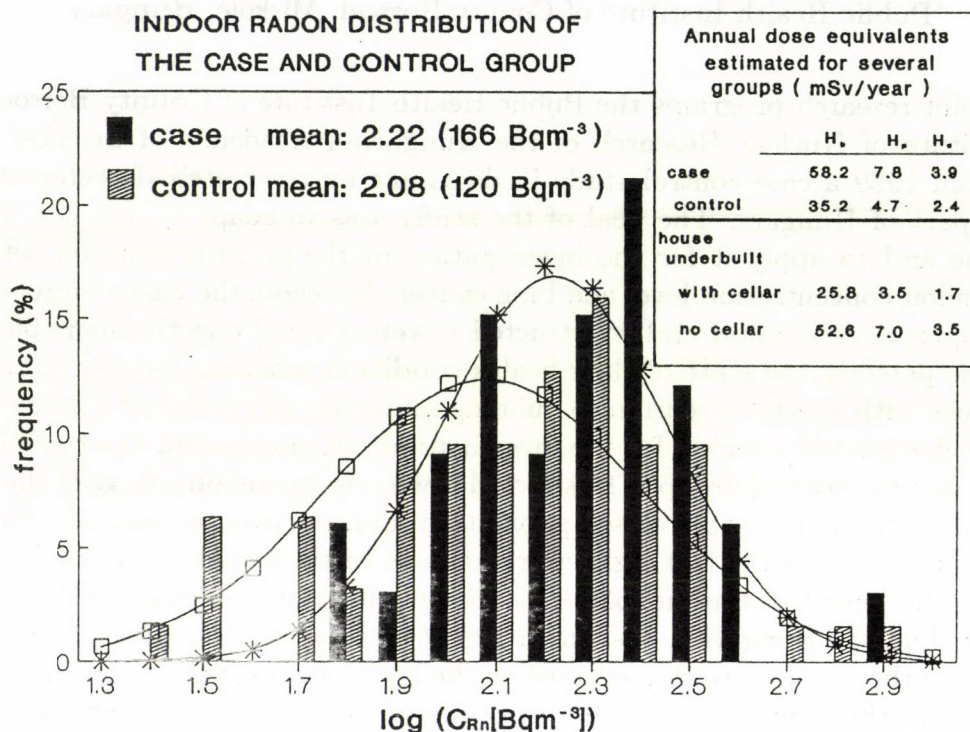


Fig. 1. Indoor radon distribution of case and control group.

The value of equilibrium factor was accepted as 0.5 from the literature, the residence probability was taken into account individually based on the questionnaires, its mean value is 0.78. The dose equivalents were derived only from the exposure of indoor radon daughter concentration in homes. We could not estimate the total exposure, thus the risk of fatal lung cancer because the radon activity concentration and the residence probabilities in other buildings (working place) and outdoor were not sufficiently known. We did not find correlation between the measured radon activity concentration in homes and in the underlying soil. The results of our investigation are not in contrast with the supposition that the most important reason of the lung cancer - after smoking - may be the elevated indoor radon activity concentration. The statistical evaluation of our data showed that the presence of an underlying cellar is more important factor than the type of building materials to decrease the indoor radon level in houses.

References

*Shortened from the paper presented at the 5th International Symposium on Natural Radiation Environment, Salzburg, Austria, Sept. 22-28, 1991.

1. ICRP Publication 50. Lung Cancer Risk from Indoor Exposures to Radon Daughters. *Annals of the ICRP*, **17** (1987) 1.

Biochemical Parameters and Ca Concentration in Hair*

J. Bacsó and I. Uzonyi

As the XRF is a powerful analytical method, by the determination of concentration of bioelements, it might promote the development of (noninvasive) diagnostic methods to gain more and more information on the health condition of the human body. With this intention we began to study the level of Ca concentration in hair (hair-Ca) in different groups of adult males in cooperation with different hospitals more than ten years ago. Namely, it was revealed from our previous measurements that the concentration of hair-Ca is decreased in ischaemic heart diseases [1,2]. The aim of the present work is to study the correlations between hair-Ca and some biochemical parameters of blood and urine measured regularly in the Aeromedical Research Institute of the Hungarian Army and to follow the mutual variation of health state and hair-Ca level.

The population consisted of males aged 19-56 years and a younger group aged ~16-18 years. In the collaborating institute the following quantities were measured: age; body weight; height; Brocka-index; blood pressure (systoles and diastoles); glycoside; uric acid; lipid; cholesterolin (total); "alfa-cholesterin" (HDL cholesterolin); "beta-cholesterin" (LDL cholesterolin); and triglicerid. The concentration of hair-Ca was measured in ATOMKI by XRFA method using Fe-55 radioisotope source for excitation. Altogether 514 and 232 data set were available in case of older and younger groups, respectively, and each of them consisted of the quantities listed above supplemented with the hair-Ca. Based on our previous results the data sets were divided into two groups according to their hair-Ca content ($\text{Ca} < 700\text{mg/kg}$ and $\text{Ca} \geq 700\text{mg/kg}$). The correlation investigations were carried out for all groups separately.

The ratio of the number of data sets (persons) falling into the $\text{Ca} \geq 700\text{mg/kg}$ and $\text{Ca} < 700\text{mg/kg}$ groups is 12:502 in the older group (which is very unfavourable) and 60:172 in the younger one (this is also unfavourable).

Tight and positive correlation has been found between cholesterolin and beta-cholesterin ($r=0.9-0.96$, see Fig. 1.) in each group, but in contrary, no correlation has been found between cholesterolin and alfa-cholesterin.

High positive correlation has been found between lipid and cholesterolin in each group, but correlation with the triglicerid has only been observed in the older group ($r \geq 0.78$) and not in the younger one ($r=0.04-0.1$). Because of the high lipid - cholesterolin and cholesterolin - beta-cholesterin correlations lipid correlates with the beta-cholesterin as well.

In case of hair-Ca the coefficients are usually low ($|r| \leq 0.56$), but in many cases they are still significant. This means, among others, that hair-Ca has a nonlinear connection with these parameters and the time dependence of the biological processes should also be taken into consideration. We observed a negative correlation with the triglicerid and lipid in all cases, and the highest being found in the older

Ca<700mg/kg group, indicating that the increasing cholesterol or triglycerid value results in decreasing hair-Ca level. The medical evaluation of the correlation data is in progress.

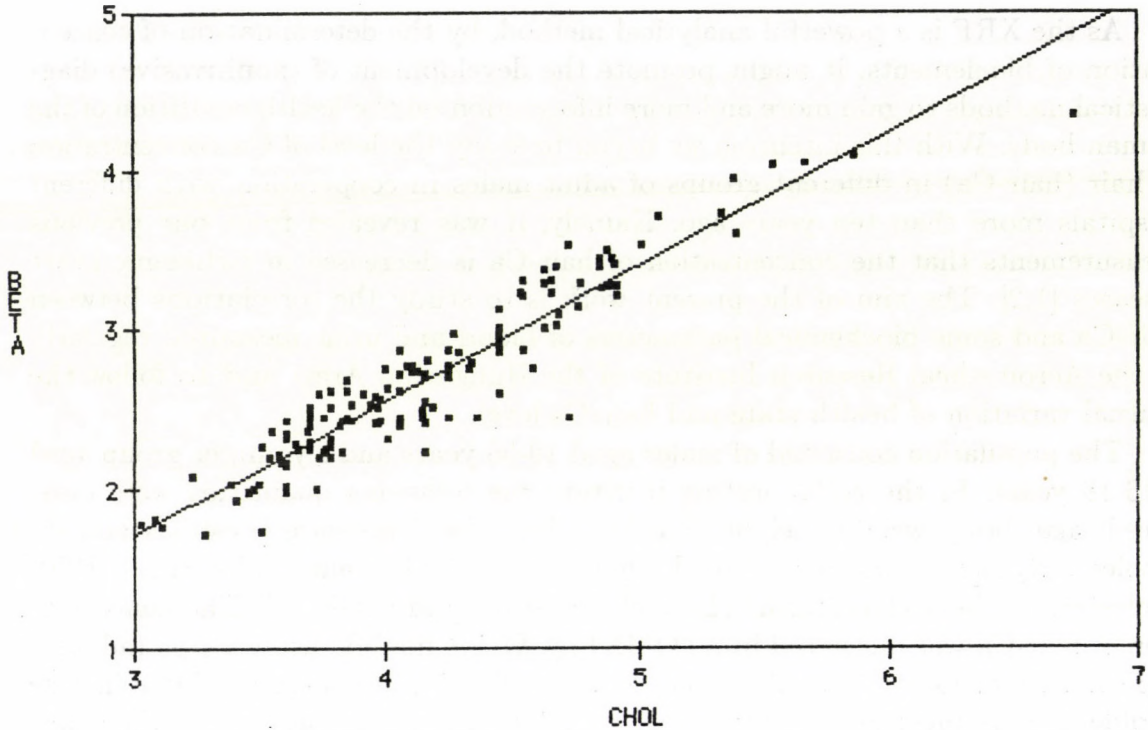


Fig.1. Beta-cholesterin as a function of cholesterol in the younger group having Ca<700mg/kg hair-Ca concentration. The linear regression equation and the correlation coefficients are: $BETA=0.84*CHOL-0.81$ and $r=0.94$ ($p\leq 0.001$), respectively.

References

* This work has been carried out in the frame of project "INTERKOZMOSZ".

1. J. Bacsó et al. : Radiochem. Radioanal. Letters **33/4** (1978) 273.
2. J. Bacsó et al. : Belorvosi Archivum **35** (1982) 245.

Investigation of Mercury and Other Toxic Heavy Metal Concentrations in Fish*

J. Bacsó

It is known that Zooplanktons and small aquatic animals concentrate the heavy metal pollutants to a marked degree over the water level. They may be of use in monitoring the level of heavy metal pollution [1]. BALOGH (1987) [2] investigated the Hg pollution in the Lake BALATON (HUNGARY). It was found that Hg content varies in zooplanktons (Cladocera, Copepoda) by time and by location in the Lake in summer period: $(0.07-0.26)\text{mgHgkg}^{-1}$.

It has been shown that Hg can be methylated in aquarial and natural sediments [3] by methanogenic bacteria [4] and by methylcobalamin [5]. These results are of great significance, as it has become apparent that Hg in all lake sediments even in inorganic form, can be mobilized and is liable for being transformed into extremely toxic methylmercury derivatives and so to enter the food chain. This way methylmercury poisoning is a widespread problem, especially in aquatic systems where various organisms can concentrate the Hg up to 1000-fold. These phenomena are strongly confirmed by the Minamata [6] and the Niigata [7] epidemic outbreaks. However, there is no evidence that methylmercury is formed in mammals.

A few years ago a relatively high concentration of Hg was observed in tinned fish by the author. Spinal column with spinal cord was selected from fish slices, dried at relatively low temperature ($\leq 70^\circ\text{C}$), pressed into pellet and measured by XRF. The concentration of Hg was equal to $(42 \pm 5)\text{ mg/kg}$. This observation inspired the author to investigate the Hg content in different parts of tinned and fresh fish products. The collection of samples is still in progress.

Sampling. Tinned fish samples of different origine and sort were collected with the permission of a number of health authorities for commerce, as well fresh fish caught in surface water (river, lake) in Hungary. All samples for measurement were selected from fish prepared for consumption. Usually a few gramms of spinal column with spinal cord, muscle from neighbor of spinal column (white muscle), and the same amount from near to skin (dark muscle) were collected.

In the first step the samples were dried with paper-napkin (to remove the oil used for production), then more dried under infrared lamp at low temperature ($\leq 70^\circ\text{C}$), ground, and finally pelletized. 100-200mg of mass was pressed into pellets with 10 mm diameter.

Measurement. The concentration of elements was determined by XRFA method.

Results. Toxic heavy metal concentrations measured in different tinned and fresh-water fishes, mg/kg (dry wt.), are shown in Table 1.

According to the recommendation of WHO (Geneva 1972) the permissible intake in mg/kg(b. wt.)/week for Cd:=0.5 for Hg:=0.005, for Pb:=0.05, which, for a person of 70 kg body weight, is equal to (mg/week): Cd=35, Hg=0.35, Pb=3.5. The table shows that the tinned and fresh-water fish species investigated, in the case of

Table 1. The code numbers mark the trade name of product or species of fish, the letters: a = bone (vertebrae) with spinal marrow or without, b = muscle (white), c = muscle (red, or near to skin) d = spinal marrow, e = bone (other than vertebrae).(*)Measured in fish from Lake BALATON [8].

Code	Ni	Cd	Hg	Pb
1a	9.1	3.2	2.3	11.5
1b	0.0	0.0	0.0	1.5
1d	6.1	0.0	2.2	0.2
2a	0.0	0.0	0.0	1.8
2b	9.1	0.0	4.2	3.6
2c	0.0	0.0	0.0	6.5
3a	3.3	1.3	0.0	9.4
3b	2.5	0.5	1.0	3.8
3c	3.1	2.0	0.0	5.4
4a	13.6	3.8	0.0	8.7
4b	0.0	0.0	0.0	4.7
4c	0.0	0.0	0.0	4.4
5a	10.9	1.0	2.1	6.5
6a	5.9	0.0	0.0	9.8
6b	0.0	0.0	0.0	4.7
7a	10.7	2.0	3.9	12.7
7b	0.7	0.8	0.8	16.9
8a	14.0	0.8	0.0	1.1
8b	0.8	0.0	0.1	9.3
8c	2.8	0.9	1.0	10.7
9a	17.4	0.2	0.0	15.3
9b	0.0	0.0(1.88)	0.0(0.089)	5.9(4.64)*
10a	0.0	2.9	4.2	10.1
11a	0.0	0.0	0.2	12.2
12a	9.8	0.0	3.9	0.0
13a	4.5	0.6	0.0	0.0

highest toxic metal concentrations [i.e.: for Cd: 1a, 4a, 10a samples ~10 kg/week; for Hg: 1a, 1d, 5a, 7a, 10a, 12a samples ~0.08-0.1kg/week; and for Pb: 1a, 3a, 6a, 7a, 7b, 8b, 8c, 9a, 10a, 11a samples ~0.35 kg/week to be consumed] are not suitable for continuous human consumption, considering the limit of heavy metals (Cd, Hg, Pb) recommended by WHO. In different tissues of fish the concentrations of Hg and Pb came the closest to the limit of tolerance. 0.1-0.2 kg (dry weight) can be consumed weekly, which, in some places, can be close or equal to the actual consumption, even in Hungary.

References

* Presented at the 1. RCM Vienna, AUSTRIA, 10-13 June 1991 for the RCP on the **ASSESSMENT OF ENVIRONMENTAL EXPOSURE TO MERCURY IN SELECTED HUMAN POPULATIONS AS STUDIED BY NUCLEAR AND OTHER TECHNIQUES.**

1. Phillips, D. J. H.: Quantitative Aquatic Biological Indicators, Applied Science Publishers LTD, London, p. 488 Pollution Monitoring Series (Adv. ed. K. Mellanby).
2. Katalin V. Balogh: Water, Air, and Soil Pollution **37** (1988) pp.:281-291.
3. Jensen S. et al. Nature, Lond. **223**, p. 753-54.
4. Wood J. M., et al. Nature, Lond. **220**, p. 173-4.
5. Imura, N., et al. Science, N.Y. **172**, p. 1248.
6. Kutsuna S. ed.: 1968. Minamata Disease. Kumamoto University, Japan: Study Group of Minamata Disease.
7. Tsubaki, T., et al. Jap. J. Med. **6**: 132 133
8. Katalin V. Balogh: The evaluation of measure of anthropogenic effect on heavy metal level of balaton fish. XXIX. GEORGIKON NAPOK KESZTHELY, 25-26. aug. 1987.

Study of Incorporation of Dimethylmercury in Small Animals*

J. Bacsó, Zs. Bacsó¹, I. Fekete², T. Ferenczy² and I. Uzonyi

¹University Medical School of Debrecen, Department of Biophysics,
Debrecen

²Kossuth University, Institute of Biology, Department of Comparative
Animal Physiology, Debrecen

Mercury is an ancient poison. Yearly 30000-150000 tons are being released into the atmosphere by degassing from the earth's crust and the oceans and additional 20000 tons of mercury are released into the environment by human activities[1]. Mercury is found in the environment in various chemical forms, and the different forms have different pharmacokinetic properties as regards absorption, bodily distribution, accumulation and excretion. Inorganic mercury can be methylated in the environment and the resultant dimethylmercury ($\text{Me}_2\text{-Hg}$) is readily taken up by some organisms, more readily than inorganic mercury.

Experiments carried out on cat with Hg compounds showed damage in brain and the highest concentration of Hg was found in liver, hair, kidney and brain, in the order of list. Hunter et al. [2] observed four cases of intoxication by $\text{Me}_2\text{-Hg}$. The symptoms were as follows: heavy general ataxia, dysarthria, and large measure of narrowing in the field of vision. In the second half of this century two serious $\text{Me}_2\text{-Hg}$ intoxication took place in Japan (Minamata; 1953-60, 111 cases of special symptoms [3], Niigata; 1964-65, 26 diagnosed cases). Other human intoxications were caused by the consumption of contaminated fish and shell-fish [4]. Animal experiments and accidental human cases show that the Hg content in hair can serve as an indicator of exposure to Hg [4, 5].

Experiments. For these very reasons we have initiated an experiment to exposure animals to $\text{Me}_2\text{-Hg}$ at different doses. The aim of this experiment is to study the accumulation of dimethylmercury in tissues and hair and to make reference material for Hg and $\text{Me}_2\text{-Hg}$ analytical quality control from the hair of animals.

The measurement was started with 33 guinea pigs and 33 rats. The animals were divided into three groups (11-11 animal in each group). Two groups were intended for experiment with different dose of $\text{Me}_2\text{-Hg}$ per day, and the third group for control. All animals were male and SPF quality. The Hg was administered partly in drinking water and partly by stomach tube. Taking into account the previous results for the lethal dose of various organic Hg compounds ($\sim 15\text{-}70$ mg/kg b. wt.) and the results of S. Ohmori and K. Hashimoto [6] we applied a lower and a higher daily dose of $\text{Me}_2\text{-Hg}$: 2.5 mg/kg (b. wt.)/day and 5mg/kg (b. wt.)/day for rats and 7.5 mg/kg(b. wt.)/day and 15.0 mg/kg (b. wt.)/day for guinea pigs. Hair cut was carried out on all animals at the set-out. On the

experimental animals the hair cut was regularly repeated every ten days in guinea pigs and every twenty days in rats. At the end of the experiment the hair cut was repeated on control animals, too. The period of experiment was two months. At the end of the experiment the animals were sacrificed and dissected. The following tissue samples were prepared: brain, liver, kidney and testis. The measurement of the concentration of Hg and other elements in the different tissues and hair was carried out by EDXRFA by using Fe-55 and I-125 sources for excitation. The tissue samples were homogenized and lyophilized and pelletized ($m=100\text{mg}$, $\emptyset=10\text{ mm}$). The hair samples were only pelletized. Approximately 400 samples were prepared and measured.

The evaluation of all the spectra has not been completed yet, only the Hg concentration in hair has been evaluated. Nevertheless, it can be seen that Hg accumulates in hair in very high concentration depending on the daily dose (Fig. 1.). Moreover, Hg appeared immediately in the hair after intake. In 40-day's time it reached a higher value than planned. These facts means that hair is a very sensitive indicator of mercury loading. We plan to carry out a correlation analysis to explore further connections between bioelemental and Hg concentrations measured in tissues and hair.

References

* This work has been carried out in the frame of a "Co-ordinated research programme (CRP) on assessment of environmental exposure to mercury in selected human populations as studied by nuclear and other techniques" which has been organized by the IAEA in collaboration with WHO (Contract No.: 6509/RB/TC).

1. M. Berlin: Handbook on the Toxicology of Metals. Vol. II, (L. Friberg, G.F. Nordberg, V.B. Vouk., Eds), Elsevier Amsterdam-New York-Oxford, 1986.
2. D. Hunter et al.: *Q.J.Med.* **9** (1940) 193.
3. T. Takeuchi: Minamata Disease, Kumamoto University, Japan, (1968) 142.
4. K. Irukayama: *Advances in Water Pollution Research* **3** (1966) 153.
5. A.C. Alfrey et al.: *Advances in X-Ray Analysis* **19** (1976) 497.
6. S. Ohmori et al.: *J. Radioanal. Nucl. Chem. Articles* **89** (1985) 277.

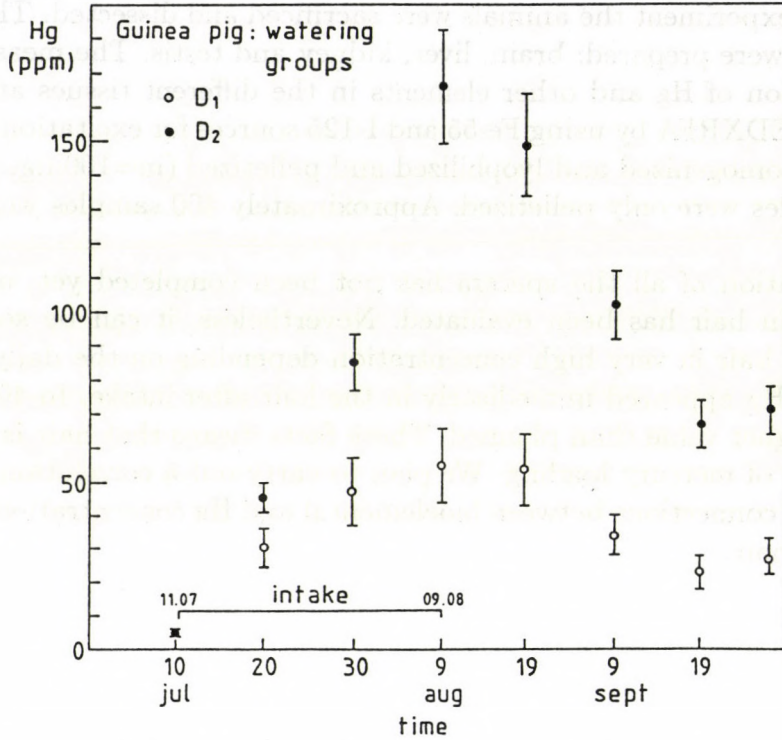


Fig. 1. Variation of Hg concentration in the hair of guinea pigs during and after the treatment with dimethyl-mercury.

The Use of XRF for the Determination of Mercurialism

J. Bacsó, L. Bognár¹ and O. Pallinger²

¹Central Hospital of Army, Department of Mental Hygiene

²Central Hospital of Army, Department of Toxicology

CASE HISTORY: A young woman got to the Department of Toxicology of Central Hospital of Army for examination and treatment due to excessive mercury. The patient had no complaint, and our examinations did not show any kind of symptoms of poisoning by mercury. There was a high level of mercury in her urine, and an extremely high level could be detected in her hair.

Since we precluded the possibility of occupational poisoning, we looked for the cause of mercurialism in the environment of the patient. In order to reduce the amount of mercury in her body, a dimercaptol (BAL) therapy was employed. After the treatment course a decreased mercury level was measured in urine.

When the patient is rubbing gold or copper things among her fingers those become white in a short while (10-20 minutes) and after a longer time (in a few hours) they break into pieces.

Sampling: On 11 of November 1990 hair sample was taken from the lady, cut near to skin. The mercury content in the sample was determined by XRF method. The measurement was carried out by steps of 17mm in length of hair. The results are shown in Fig. 1. As the lady's power for whitening the gold and copper things remained continuously in spite of the hospital treatment, the hair sampling was repeated on 7th of March 1991. At the same time, hair sample was taken from her grandmother and son living together with her. Furthermore vegetables, fruits, leaves and different parts of different plants, most of them are used as food, were collected from their garden for analysis.

Results: By the second hair sampling her hair had grown 42mm in length since the first sampling. From this figure and time interval the growing power of her hair was determined ($42\text{mm} / 116 \text{ days} = 0.3621 \text{ mm/day}$). So it is possible to fit together the results of two samplings.

It is very surprising that there was no Hg found in the second hair sample even in that part which covers a part of the first sample (overlapping part). The Hg contents in the grandmother's and son's hair were similar to that of the patient's second sample. This is a new observation in the field of hair trace element studies. The explanation of the phenomenon requires further investigations.

The authors are thankful to Dr. Uzonyi and Dr. Kovács for their technical help.

Table 1. Overlapping of the two hair sample of patient.

Hg in hair (ppm)		82.4±10.7	114±13.7	117±15.0	
		41±7.3	97.9±12.1	116.±14.	100±30
Date of sampl.	1990	23.X	06.IX	21.VII	18.IV
				04.VI	02.III
Hg in hair (ppm)		0.0	0.0	0.0	6.7±8.7
		0.0	0.0	0.0	1.7±4.4
Date	1991.16.II	14.XI	12.VIII	10.V	
	1990 31.XII	28.IX	26.VI		

Table 2. Toxic heavy metal content of vegetables and other plants.

Vegetable, plants	Ni	Cd	Hg	Pb
Strawberry, leaves	-	-	-*	1.3±2.8
			4.8**	
European hazel	3.6±8	-	-*	1.3±2.9
			4.6**	
Leaf of a nut-tree	-	0.2±2.9	-	2.5±3.1
			2.2**	
Pea leaves	4.5±7.6	-	2.2±4.7	-
			8.1**	
Bean leaves, stalk	15.5±8.3	-	-	-
			5.0**	
Nutshell	4.0±7.3	0.3±2.7	-	-
			1.3	
Brussels sprouts	11.0±7.6	4.2±2.8	4.1±4.6	-
			8.8**	
Carrot	2.7±7.4	-	-	-
			4.1**	
Parsley	-	-	-	-
			3.8**	
Kohlrabi	10.3±7.7	6.9±2.9	-	-
			3.1**	
Red cabbage	4.9±7.4	3.5±2.8	-	-
			2.4	
String beans	9.5±7.4	3.6±2.7	5.0±4.5	-
			5.4**	
Strawberry	4.1±6.9	-	3.8±4.4	-
			4.2**	
Sour-cherry	1.6±6.8	1.8±2.6	1.1±4.3	1.9±2.5
			4.3**	

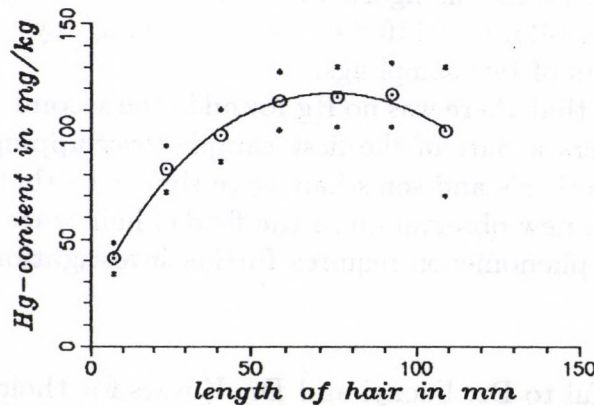


Fig. 1. The variatoin of Hg-content in length of hair sample.

DEVELOPMENT OF METHODS
AND
INSTRUMENTS

A Ge+BaF₂ Composite γ -ray Spectrometer

A. Krasznahorkay, J. Bacelar,^(a) A. Balanda,^(b) and A. Buda^(a)

^(a) Kernfysisch Versneller Instituut, 9747 AA Groningen, The Netherlands

^(b) Institute of Physics, Jagellonian University, Cracow, 30-059 Kraków, Reymonta 4, Poland

The detection of high energy γ rays following the decay of giant resonances to specific final states demands a detector system with high efficiency and good energy resolution in the 10 - 20 MeV energy region. A new Ge + BaF₂ γ -ray spectrometer fulfilling this requirements has been designed [1]. The schematic layout of the detector system is shown in Fig. 1. The energy of the γ quanta is reconstructed by summing (off-line) the energies deposited in coincidence in the Ge detector and in its BaF₂ shield.

Response function measurements have been performed at KVI Groningen at a few γ -ray energy between 4.4 and 15.1 MeV. The measured energy resolution and efficiency of the system are in agreement with the results of Monte-Carlo calculations performed with the code GEANT3. This type of spectrometer can have better than 0.5 % energy resolution and more than 10 % efficiency at 15 MeV (see in Fig. 2.).

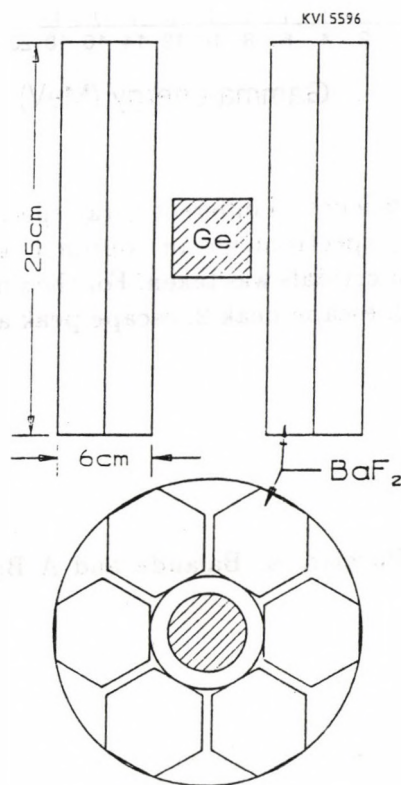


Fig. 1. Schematic layout of the Ge + BaF₂ spectrometer.

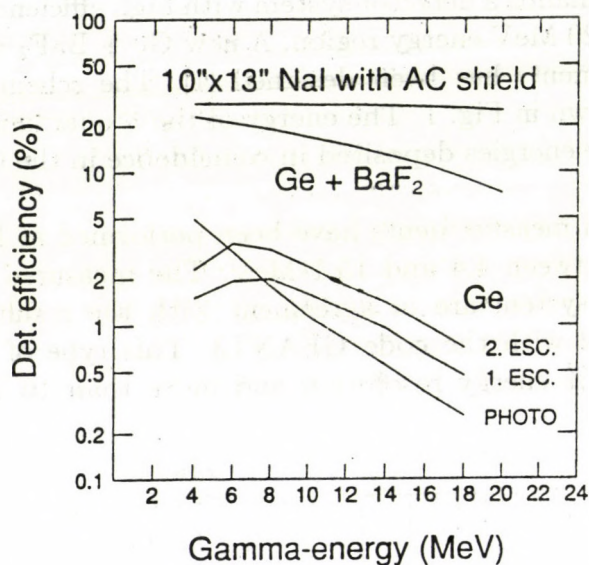


Fig. 2. Comparison of the efficiency of different γ -ray spectrometers as a function of the γ energy. For the Ge + BaF₂ spectrometer an "optimal" geometry excluding the extra spaces between the scintillator crystals was taken. For the single Ge-crystal the efficiencies are given separately for the 1. escape peak 2. escape peak as well as the photopeak.

References

- 1 A. Krasznahorkay, J. Bacelar, A. Balanda and A Buda, submitted to the Nucl. Instr. and Meth.

A UV-photoelectron spectrometer for high temperature studies

D. Varga, L. Kövér, I. Cserny, K. Tőkési

A special UV (Vacuum Ultraviolet) photoelectron spectrometer has been developed for studying free atoms and molecules, including short-lived transient species obtainable at higher temperatures.

For energy analysis of photoelectrons a hemispherical electrostatic analyzer has been built with a working radius of 150 mm and with identical entrance and exit slits of 0.5, 1.0 and 1.5 mm widths, respectively, variable without breaking the vacuum in the spectrometer. A fixed analyzer pass energy can be selected in the 2-10 eV range for electrons having kinetic energies in the 1-50 eV interval, by using a 7 elements input lens system with an object-image distance of 570 mm. This length provides a good separation between the sample chamber and analyzer (facilitating its differential pumping and preventing its contamination). Consisting of a combination of two cylindrical lenses of four elements each, the elements of the complete zoom system are operating with potentials dependent linearly on the energy of the incoming electrons. The electron optics and the analyzer is enclosed by a double layer magnetic shielding made of high permeability material.

The sample chamber of the spectrometer is pumped by a diffusion pump (600 l/s) made fully of stainless steel (making possible studies of highly reactive gases) and equipped with a special liquid nitrogen cooled cryotrap. A similar diffusion pump ensures the differential pumping of the analyzer while the sample region and the entrance slit of the lens system is separated by a watercooled blend.

Photoelectrons are excited by a capillary discharge UV lamp with a two stage differential pumping provided by a rotation pump and a diffusion pump (300 l/s), respectively. The maximum discharge current of the UV lamp is 150 mA.

Gaseous samples can be introduced into the sample chamber through special units which makes possible the use of both nozzles for narrow beam samples and gas cells for large volume homogeneous samples. Vapour samples can be obtained from a small oven by in situ evaporation of solid materials (max. temperature is 250 °C) with the possibility of fast sample changing by the help of a gate system without effecting the operation of the spectrometer. For studying transient molecules, the sample chamber is equipped by a pyrolizator unit with a quartz tube heated indirectly by thermocathodes providing controllable temperatures up to 1000°C.

The spectrometer is controlled by an IBM AT based data system. Data acquisition and recording is performed entirely on interrupt level making it possible to run any other application program without affecting the data acquisition in progress. The acquired data can be accessed for on-line evaluation by using the evaluation program EWA developed by J. Végh.

The performance of the spectrometer is illustrated by the He I α excited photoelectron spectra shown in Figs 1 and 2.

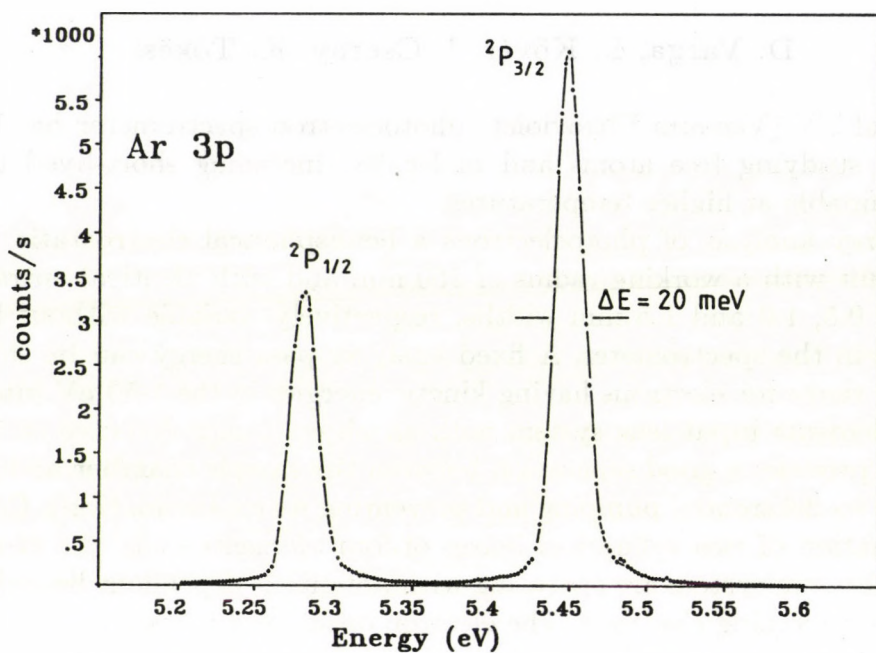


Fig. 1. The photoelectron spectrum of argon excited by He I α radiation

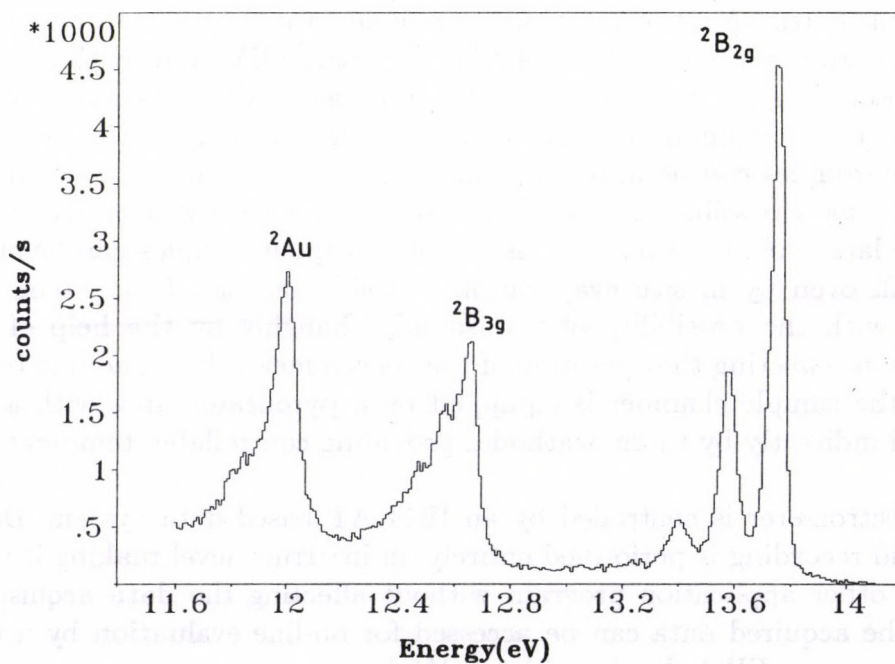


Fig. 2. A detail of the He I α excited photoelectron spectrum of anthracene

Extraction optics calculations for a hollow-cathode ion source: the first steps of the ECR program

S. Biri, J. Pálkás, A. Báder

In the last year a proposal for a heavy ion facility has been prepared in ATOMKI [1]. The key element of the planned facility is an electron cyclotron resonance (ECR) ion source, which will be installed at a 300–500 kV electrostatic accelerator and at the cyclotron of the institute. The ECR source can also be used independently (at a max. 30 kV acceleration potential) for low-energy atomic physics investigations. The ECR source will be used alternately at the two machines. During the operation of the ECR source at the cyclotron, a hollow-cathode type ion source (DANFYSIK 911A) producing single-charged heavy ions will be used at the electrostatic accelerator. This source also can be used independently, at 30 kV potential. The source was bought without any accessories (extraction lens, power supplies, etc.) Recently, the computer planning and optimization of the beam extraction optics has been carried out for this ion source.

The planning of the optics was started using the "cos-lin" method [2]. The arrangement, obtained this way, was alternated step-by-step using experiences of similar extraction optics and considering technical restrictions on the insulations and the displacement of the electrodes. Meanwhile, the axial potential distribution was continuously controlled and an effort was made not to "damage" the form came from the model. The final testing and optimization of the optics were carried out with the SIMION [3] computer code. In fig. 1 the geometry with the most suitable potentials can be seen. The potentials on the electrodes can be varied depending on the required beam energy in such a manner that the character of the axial potential distribution will not change significantly.

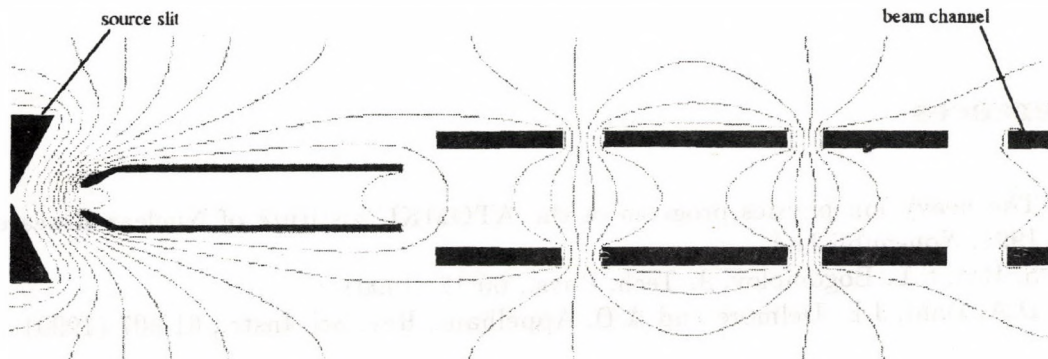


Fig. 1. Extraction ion-optics system. The electrode potentials from left to right are 20, -2, 1, 13, 1 and 0 kV, respectively

Other parameters like the distance and aperture of the electrodes and the effect of the plasma boundary, were investigated using the SIMION code. It was found that the effect of the plasma meniscus can always be compensated altering the potential of the fourth electrode (fig. 2).

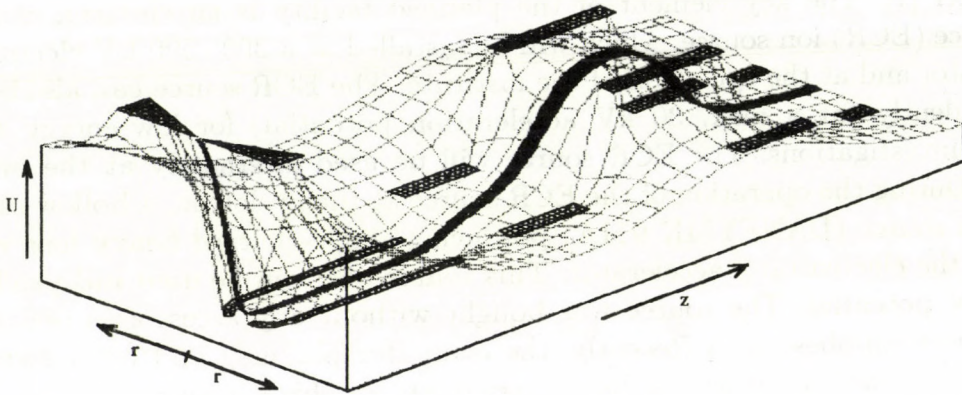


Fig. 2. Beam transport in the 3-dimensional potential field of the extraction system. The initial energy of the particle is 200 eV, plasma meniscus is 20° (convex plasma), diameter of the source slit is 1 mm. The potential of the source is 20 kV

The mechanical part of the extraction system is under construction and the electrical control system is under development. All present and future results are considered as a preparation for the installation of the ECR source and the heavy ion facility.

References

1. The heavy ion physics program of the ATOMKI. Institute of Nuclear Research, 1991. Non-published.
2. S. Biri, S.L. Bogomolov, *J. Tech. Phys.*, 60 17 (1990)
3. D.A. Dahl, J.E. Delmore and A.D. Appelhaus, *Rev. Sci. Instr.*, 61 607 (1990)

Modelling of electrostatic extraction optics of ion sources

S. Biri, S.L. Bogomolov ^a, I. Koós ^b

^aJoint Institute for Nuclear Research, Dubna, Russia

^bKossuth University, Debrecen, Hungary

Investigations on the problems of external ion source electrostatic extraction optics were carried out.

a./ Axial symmetric beam

A mathematical model was established, which is applicable for calculations in the case of ion sources producing axial symmetrical ion beams (e.g. ECR, duoplasmatron sources) [1]. It was supposed that to get a beam of suitable performance, the necessary potential distribution along the z-axis must be a special, weighted superposition of linear and cosinusoidal members. In fig. 1 simple potential distributions of this type are shown. From the potential distribution the full electrode structure can be obtained. Performances of optical systems calculated in this way and experimental results from working optics, were compared. It was found that systems by this model and the experimental optics work identically. The procedure of the model creation can be used to design electrostatic extraction optics without the usual large amount of calculations.

b./ Ribbon beam

The case, when a crossed, position depending force influences the beam extracted from the source, was studied. This is a real situation, for example, at the application of a Penning source with radial extraction. The system consists of the source, an accel-decel electrode system and an electrostatic compensator (Wien-filter) to compensate the deflecting action of the magnetic field. It is shown [2] that hyperbolic potential distribution between the filter plates provides the ion beam with minimal deflection from the axis of the ion optical system (IOS) at the exit of the IOS. The filter plates must have different absolute values of potentials and also a strong geometrical asymmetry to the IOS axis (fig. 2). The computer simulation of ion trajectories in the IOS, constructed by the proposed method, has also been carried out.

References

1. S. Biri, S.L. Bogomolov, J. Tech. Phys., **60** 17 (1990)
2. S Biri, S.L. Bogomolov, I. Koós, Nucl. Instr. Meth., **A306** 56 (1991)

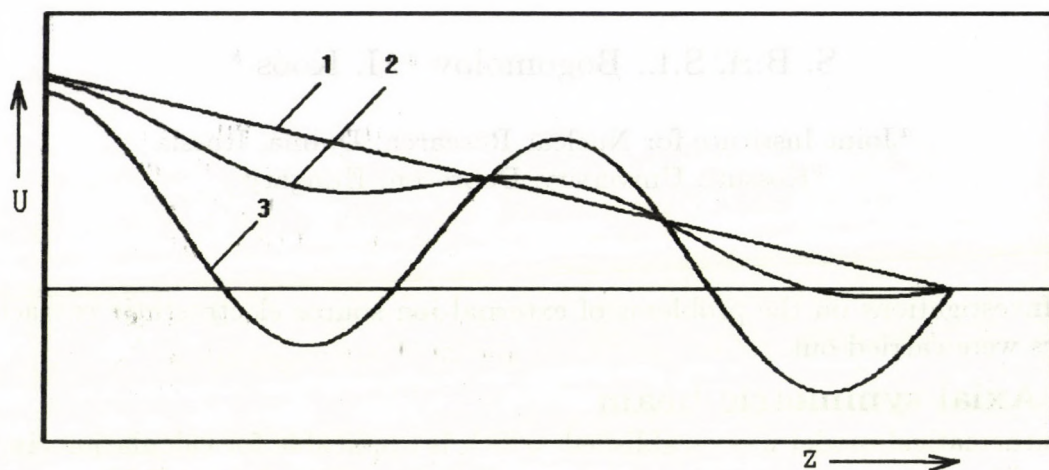


Fig. 1. Potential distribution along the axis of the IOS. 1 - $U_c=0$, 2 - $U_c/U_l=0.2$, 3 - $U_c/U_l=1.4$. U_c and U_l are the amplitudes of the cosinusoidal and linear parts of the distribution, respectively.

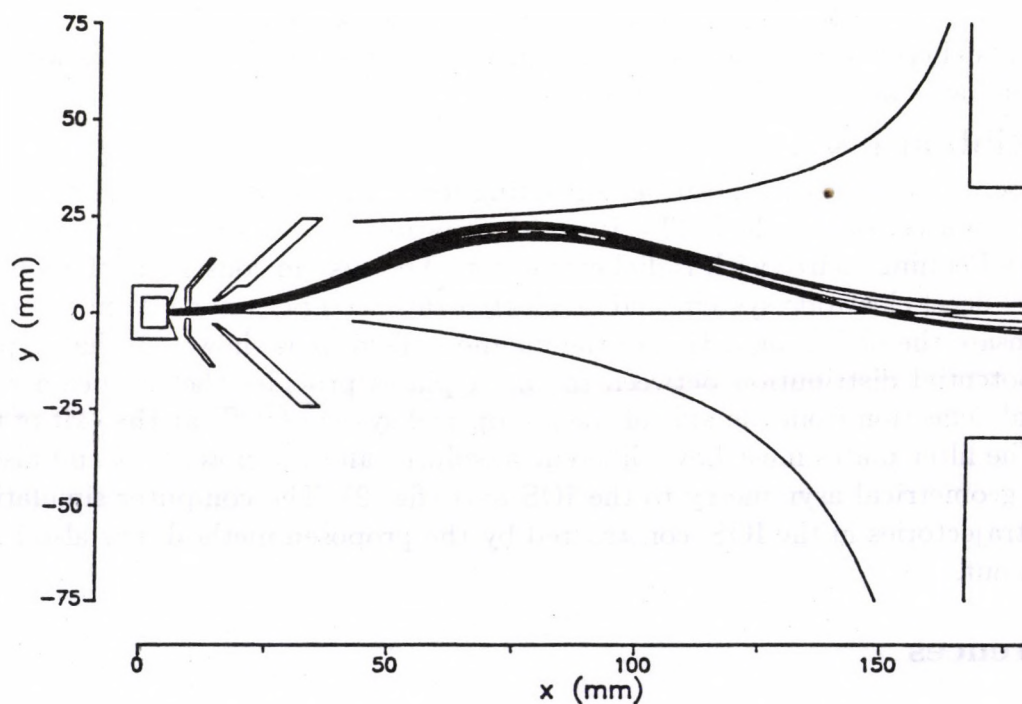


Fig. 2. IOS geometry and particle trajectories with $A/Z=3$. The injection potential is 19 kV, the potential of the extraction electrode is -5 kV, potentials of the upper and lower compensator plates are $+15.1$ and -0.5 kV, respectively.

Ion sources

S. Biri

The field of ion source research and development has grown intensively since the sixties-seventies and especially dramatically in the last decade. New kinds of ion sources have been invented and the performance of existing sources has been upgraded significantly. There are ion sources in many devices and facilities: in accelerators, in separators, in implantators, etc. The ion source is one of the most important parts of these facilities since the features of the beam on the target are basically determined by the features of the beam extracted from the source.

It is frequently necessary to identify or classify the many types and kinds of ion sources or to understand the physics of the applied source. In Hungary, in Hungarian has not been published a detailed work about ion sources yet. For this purpose a longer study was written [1], which is designed to serve as a guide and a review for the field of ion source physics and technology. The study is intended for ion source users in general, for physicists who are interested or actively engaged in ion source development or related work and for students, engineers, who have a basic knowledge of plasma physics, atomic physics and electromagnetic theory.

The contents of the study:

1. The basics of plasma physics for ion sources
 - 1.1 Basic terms
 - 1.2 Basic processes in the plasma
 2. Classification of ion sources
 3. The most wide-spread and known ion sources
 - 3.1 Penning (PIG) ion source
 - 3.2 Electron cyclotron resonance (ECR) ion source
 - 3.3 Electron beam ion source (EBIS)
 - 3.4 Laser ion source
 - 3.5 Duoplasmatron, duopigatron
 - 3.6 Cusp ion sources
 - 3.7 Negative ion sources
 - 3.8 Miscellaneous sources
 4. Comparison of ion sources
 5. Beam extraction
 6. The present and planned ion sources at the cyclotron in Debrecen
- References (94)

Reference

1. S. Biri, "Ion sources" (to be published in Hungarian)

Magnetic structure formation in ECR ion sources

S. Biri, J. Molnár

During the last few years the electron cyclotron resonance (ECR) ion sources have played an important part in heavy ion facilities. Up to the present time more than 40 ECR ion source designed for the production of high-charge-state ions have been built in different laboratories [1].

In sources of this type one of the most critical part is the magnetic system of the ionization chamber. The magnetic field in the chamber has the "minimum-B" type mirror configuration. The axial magnetic field is usually produced by solenoidal coils, the radial magnetic field is produced by SmCo or NdFeB hexapole.

In order to make the design, the measurement and the final formation of the magnetic structure of ECR sources easier and quicker, computations and instrumental developments were carried out.

1. Using a simple, but quick computer code the axial magnetic field distribution and the parameters of the coils to create this field, can be planned. In fig. 1 the result of a calculation can be seen. The calculation of the total magnetic field, which is a superposition of the magnetic field of the hexapole (radial) and the coils (axial) in the ionization chamber, is illustrated in fig. 2.

2. To measure the simple or combined magnetic field inside the coils and/or the hexapole, a semi-automatic field-meter was developed [2]. The control of the field-meter and the data acquisition was realized with a PC, via special interface developed for this purpose. In fig. 3 the main menu of the control program can be seen.

3. Another computer code transforms the results of field measurements to any required text or graphics form. Depending on the choosed parameters and on the measured data, the axial, radial or azimuthal magnetic field distributions (fig. 4, 5) and two-dimensional field maps can be obtained. The Fourier-analyzis of the $B_r(\phi)$ or $B_\phi(\phi)$ field components is also possible (fig. 6).

References

1. R. Geller, Proc. 10th Int. Conf. ECRIS, Knoxville, USA, 1990, p.381.
2. S. Biri, A.A. Efremov, V.V. Behterev, J. Molnar, in Proc. XII. All-Union Conf. Charged Part. Accel., Moscow, 1990.

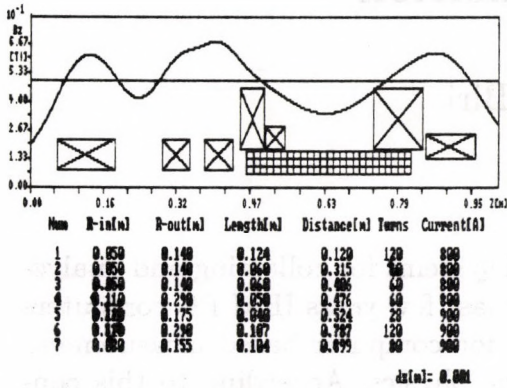


Fig. 1. Axial magnetic field distribution on the axis and coils parameters

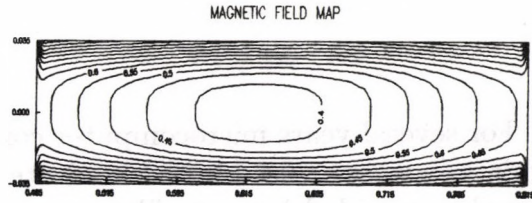


Fig. 2. The total magnetic field between the poles of the hexapole

PARAMETERS	Measurement No.: 910529/H11_A	RELAYS
Zmin = 100	Data save : c:\111r30.dat	Right : 0
Zmax = 600		Left : 0
PHImin = 0		Forward : 1
PHImax = 60		Back : 0
COORDINATES		SWITCHES
R = 30		dPhi : 0
PHI = 60	dZi : 0	
Z = 440	dZd : 1	
	Zend : 0	
	Zbeam : 0	

Fig. 3. The monitor display during the measurement

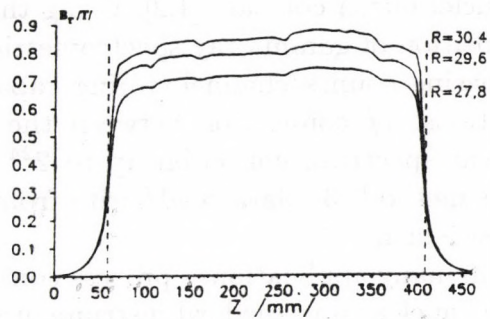


Fig. 4. The radial field component (B_r) at different radius (R)

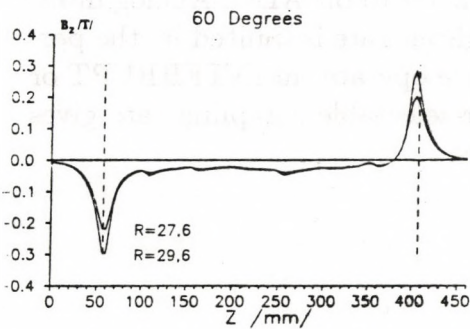


Fig. 5. The axial magnetic field component (B_z) at different radius

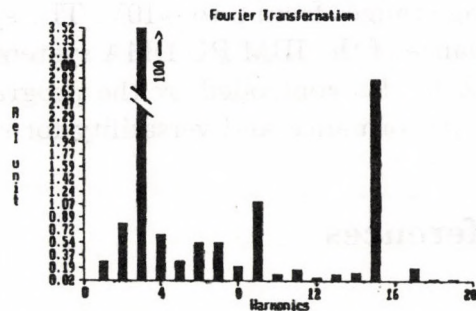


Fig. 6. The Fourier-spectra of the radial field component at a given axial position (region: 0-360°, R=33 mm)

IBM PC based interfaces for system control and data acquisition

J. Molnár, S. Biri

For several years microcomputer controlled systems for collecting and analyzing data have been used in the Institute. In the last few years IBM PC computers have also provided low cost "host computers" for computer-based measurement control and data acquisition systems in nuclear physics. According to this concept several types of interfaces were designed to solve the problem of control and recording and evaluating data measured in the experiment. Two of these interfaces are described here.

A PCA/INCREMENT MEMORY (Fig.1) interface has been developed and installed for the "GAMMA" complex for the investigation of fragmentation processes in nuclei-nuclei collision [1,2]. Using this interface reduces the measuring time for acquisition of gamma-ray spectrometric information and gives better statistics by increasing counts/channel storing capacity. The unit features the following main functions: 1/ connection between the Analog Signal Processor and the PC, 2/ nuclear spectrum collection up to 2^{24} counts/channel using increment or decrement method, 3/ data read/write from or to memory via the PC bus during the measurement.

In many applications - process control, data acquisition, automated test equipment, nuclear and medical instrumentation, robotics - the fast digitization of various analog signals, data storage and evaluation are very important requirements. An IBM PC based 16 Single-Ended Channel Interface (PC/16SECI Fig.2) was developed to meet these requirements [3]. The analog input part of the PC/16SECI unit consists of a 16 channel fully protected multiplexer, a channel address register, an operational amplifier and a complete high speed 10 bit ADC. Analog input voltage ranges from 0 to +10V. The system throughput rate is limited by the performance of the IBM PC DMA system. The interface operates in INTERRUPT or DMA modes controlled by the program. The user-selectable sampling rate gives high performance and versatility for signal analysis.

References

1. S.Biri, J.Molnar et al., JINR P1-89-298, Dubna (1989)
2. S.Biri, J.Molnar et al., JINR 13-89-297, Dubna (1989)
3. J.Molnar, S.Biri, V.N.Samoylov, Proc. Eighth Summer School on Computing Technique in Physics, Czechoslovakia Sept. 19-28. (1989)

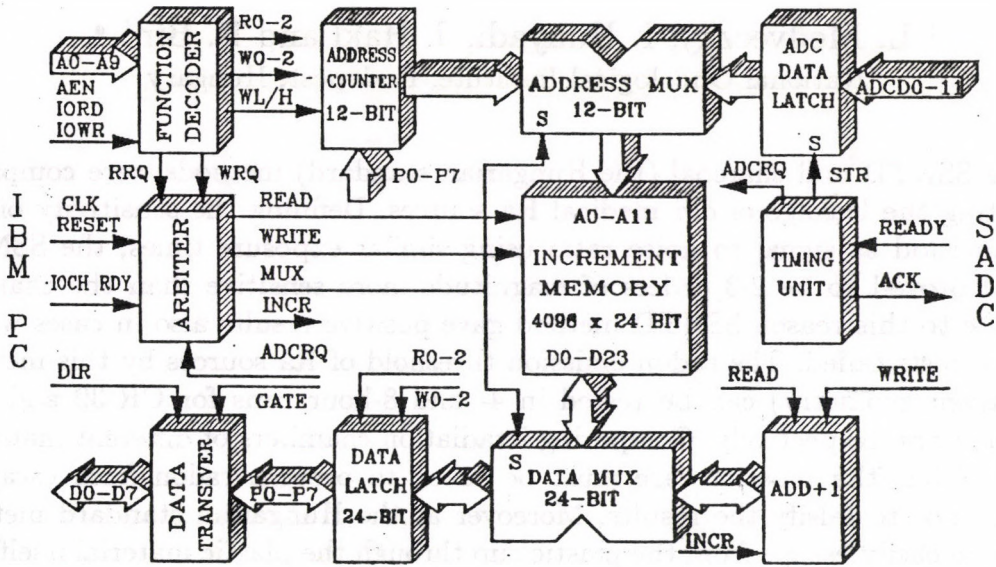


Fig. 1. Block diagram of the PCA/INCREMENT MEMORY card

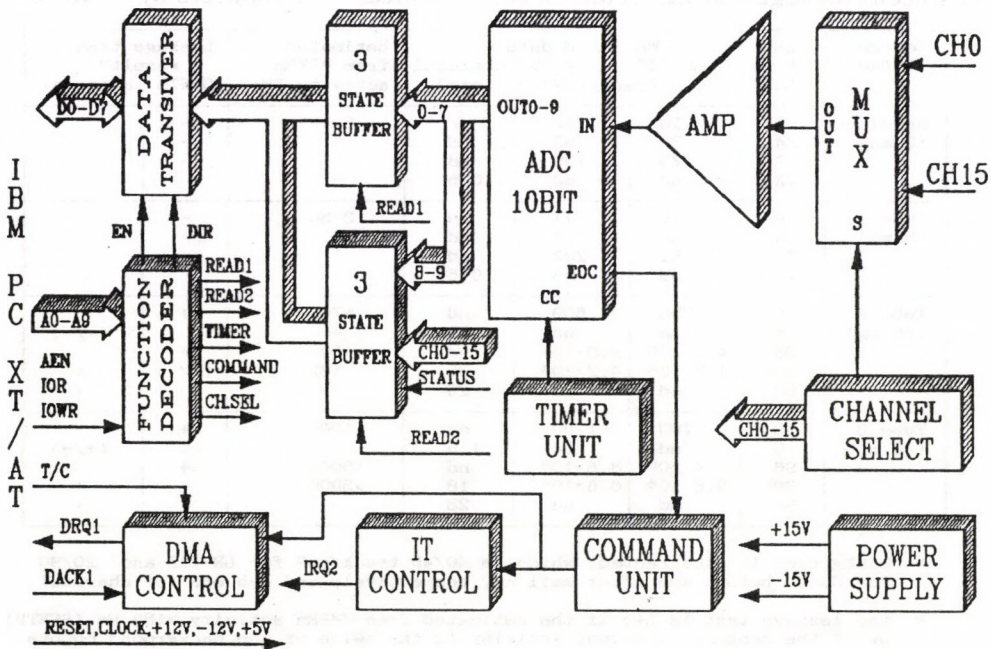


Fig. 2. Block diagram of the PC/16 SECI card

Leak testing studies of ^{226}Ra sources by radon detection with SSNTDs

¹ L. Medveczky, I. Hunyadi, J. Hakl and B. Bíró ^a

^aNational Oncological Institute, Budapest, Hungary

The SSNTD and charcoal (the Hungarian standard) methods were compared for testing the leakage of old medical Ra sources. Defining the sensitivity of the given method as signal to noise ratio using similar exposure times, the SSNTD method proved to be 2-3 orders of magnitude more sensitive than the charcoal one. Due to this reason SSNTD method gave positive results also in cases where charcoal tests failed. The radon emission threshold of Ra sources by this method (in a given geometry) can be tested in 4- and 8-hour runs for CR-39 and LR-115 detectors, respectively. Comparing irradiation chambers of different material, it turned out that special care must be taken to prevent radon from escaping in order not to falsify the results. Moreover at the Hungarian standard method radon can easily escape from the plastic cup through the plastic material itself and through smaller openings on the cup. Examining the same source in a more tight weighting bottle with a ground-in stopper also sensitivity of the charcoal tablet was increased, but never achieved the SSNTD one. As it was expected, by using simultaneously the two radon detectors in the same cup the results given by the SSNTD were also falsified due to the radon absorption in the charcoal tablet.

Table 1. Recent leakage testing results of some medical ^{226}Ra sources by ^{222}Rn detection

Source ^{226}Ra	Exp. time [h]	Measured data ^a			Estimated free ^{222}Rn activity [Bq]	Leakage test result ^b	
		LR-115 [α -track/cm ²]	CR-39	charcoal [cps]		SSNTD	charcoal
Needle (3 mg)	6	16	52	nd	5-45	-	
	24	38	92	nd	"	-	
	72	75	135	nd	"	-	
	72	nd	nd	0.5	-		-
Tube 1 (5 mg)	6	19	41	nd	3-50	-	
	24	23	111	nd	"	-	
	72	61	202	nd	"	-	
	72	nd	nd	0.5	-		-
Tube 2 (10 mg)	6	250	609	nd	>700	+	
	6	nd	nd	1	-		(+/-)
	96	$4.4 \cdot 10^5$	$9.8 \cdot 10^5$	nd	>1000	+	
	96 ^c	$1.2 \cdot 10^4$	$4.2 \cdot 10^4$	25	162	(+/-)	+
	96	nd	nd	29	-		+
Tube 3 (10 mg)	6	700	1200	nd	>1000	+	
	6	nd	nd	1.5	-		(+/-)
	96	$4 \cdot 10^5$	$8.6 \cdot 10^5$	nd	>5000	+	
	96 ^c	$2.6 \cdot 10^5$	$6.6 \cdot 10^5$	18	>3000	+	+
	96	nd	nd	23	-		+

^a background is subtracted, which is 40/45 track/cm² for LR-115 and 20/90 for CR-39 before and after mailing, respectively and 4-5 cps for charcoal

^b the leakage test is (+) if the estimated free ^{222}Rn activity >185 Bq (SSNTD) or if the measured charcoal activity is the twice of the background counts

^c simultaneous track detector and charcoal exposition

¹ Shortened from the paper presented at the Int. Workshop on Radium, Uranium Thorium and Related Nuclides in Industry and Medicine: History and Current Uses, Badgastein, Austria, Oct. 1 - 3, 1991.

Background elimination treatment for TLDs

I. Uray[†]

[†]Present address: Forschungszentrum Jülich GmbH, Jülich, Germany

A probable oxidation effect on the surface of LiF detectors may produce chemiluminescence, which appears as a high temperature background (HTBG). At lower temperatures (200-300°C) it is possibly much higher than the infrared (IR) signals. By plunging the detectors in methanol with a 0.2 % HF content before reading out, it is possible to eliminate this disturbing effect. In this way lower detection limits and better accuracy can be attained in the low dose range measurements, and there also exists the possibility of fitting and measuring the high temperature peaks more accurately than was previously possible.

Recently we investigated questions concerning the lowest possible detection limit in dose measurements, the extension of the dosimetric use of high temperature peaks and correct determination of the IR part of a glow curve.

All of these efforts, in conclusion, seem to be guiding us towards an investigation of an incalculably high temperature background (HTBG), which appears at different measurements. Its temperature region begins slightly lower than IR radiation, but it shows a form similar to a peak with a maximum in the 350-400°C region. This background in the peak 5 region of LiF detectors may measure a few 10 μ Gy. It is, of course, a strong limit to the measurement accuracy.

The dosimetric use of peak 7 is also limited. In this temperature region the HTBG may be much higher than the IR signals. It is, of course, an important disturbing effect and may be a limitation for neutron dosimetry by TLDs, as well.

To avoid destroying of the detectors, a small HF content was mixed with methanol. Experiments show that no more than 0.2 % HF in the methanol bath is necessary and no longer than 2 minutes time is required for a sufficient treatment.

To test the effectiveness of this background elimination treatment (BET) method, glow curves of TLDs were compared with and without BET before the readout. Figure 1 shows a series of measurements of detectors irradiated by a dose of 1.0 (Fig. 1a) and 0.1 (Fig. 1b) mGy dose of ¹³⁷Cs gamma rays and exposed to a room background (of about 0,08 μ Gyh⁻¹ dose rate) for 120 h (Fig. 1c), accumulating a dose of about 0.01 mGy. Curve 1 illustrates a conventional readout while curve 2 is the glow curve after a BET of the detectors.

Fig. 1a shows that the BET ensures a good measurable peak 7 also in gamma glow curves and in quite low dose ranges. This fact, above all, may be important in neutron dosimetry, and Fig. 1c suggests a very low detection limit attainable by using the BET method. The first measurements verify that applying the BET method a gamma dose of 1-2 μ Gy and a neutron dose of 10 μ Sv (in mixed γ -n-radiation field) is by LiF-s measurable.

By using this BET method both the conventional and the more complicated glow curve deconvolution methods may work more precisely.

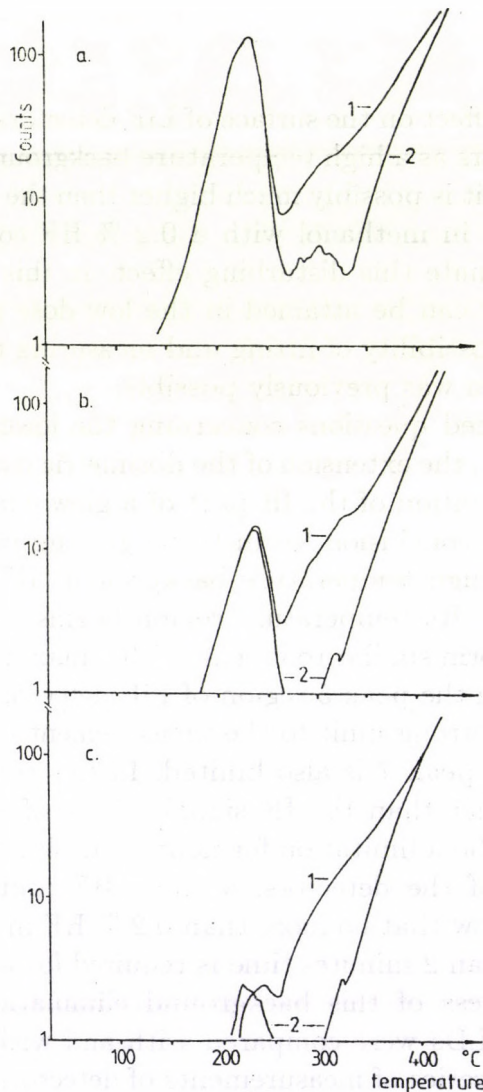


Fig. 1. Comparison of glow curves after conventional readout (curve 1) and a readout after a BET (curve 2) for detectors irradiated by doses of 1.0 mGy (Fig. 1a), 0.1 mGy (Fig. 1b) and .01 mGy (Fig. 1c), respectively.

ANAL90: a New Computer Code for Measuring and Handling X-ray Spectra

P. Kovács

The NZ-881 Digital Signal Processor and Analyser developed in our Institute by T. Lakatos [1-3] is a fully digital equipment for processing the signals of semiconductor X-ray detectors. Using a recently developed interface card [4] this equipment is connected with an IBM PC/AT. For setting the parameters of the signal processor and handling the spectra stored in the analyser memory of the interface card a computer code has been developed.

The ANAL90 is a menu controlled, easy-to-use Personal Computer Analyser Program which provides acquisition, displaying, storing and simple processing of 1K, 2K, 4K X-ray spectra. The 4096 channel acquisition memory can be divided into 4x1K or 2x2K or 1x4K sector(s) and one of them is always active i.e. in which the data acquisition can be performed.

The more than 40 functions of ANAL90 are arranged into three main menus. While the first and third groups represent functions concerning mainly the usual analyser functions the second group consists of file handling functions.

The analyser functions are as follows:

- Erase, Start/Stop measurement
- Set measuring time and NZ-881 parameters (peaking time, adaptivity, noise discrimination level, gain)
- Expand/Compress spectra in horizontal or/and vertical direction
- ROI operations (Set/Delete ROI, calculation of ROI parameters)
- Energy calibration
- Sector operations (Set active/passive sector number, set overlap mode, data transfer from active to passive sector)
- Movement of spectra and channel cursor.

Functions of file menu:

- Save/Load spectrum data in binary or/and ASCII form
- Directory of current disk
- Peak evaluation (max 100 peaks) and Save/Load results
- Smoothing of ROI data.

The desired function can be selected by pressing the appropriate function key or alphabetical key or key-combination. In some cases it is necessary to confirm the intention.

All important parameters are displayed on the screen along with the spectrum area (see Fig.1.)

A recommended minimum IBM PC/AT computer system should be equipped with 512 K of installed RAM memory, a hard disk or floppy driver, an EGA/VGA graphics card with a suitable monitor.

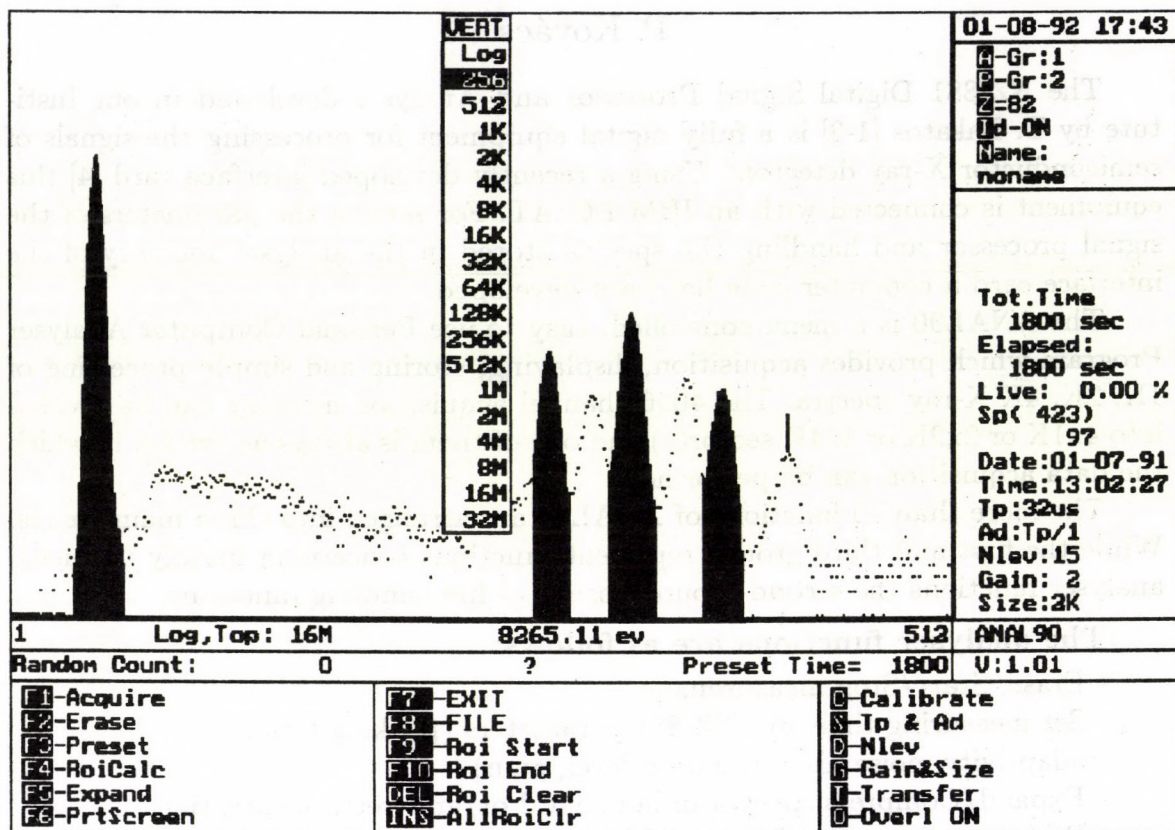


Fig. 1. The main analyser screen

References

1. T. Lakatos: Nucl. Instr. Meth. **B47** (1990) 307
2. T. Lakatos: ATOMKI Annual Report (1990) 105
3. T. Lakatos: Nucl. Instr. Meth. **B62** (1991) 289
4. T. Lakatos, P. Kovács, J. Szádai, G. Székely: ATOMKI Annual Report (1990) 125

A Computer Package for Evaluation of PIXE Spectra.

Gy. Szabó, I. Borbély-Kiss

A partly new computer package has been developed for the evaluation of PIXE spectra on the basis of experience given by the application of the previous one (PIXASE [1,2]). The changes were focussed on improvement of the stability of spectrum fitting and on an easier handling, they did not touch the principles of the concentration calculation.

The ASELES programme for spectrum evaluation except for some part of it, has been replaced with the new PFIT programme. The function modelling the X-ray spectrum, including parameters to be fitted, apart from the part modelling the background has not been changed. The background is given by the following formula [3]:

$$B(E) = f_s(E)f_a(E)f_d(E)\exp\{B_0 + \sum_{i=1}^n \exp[B_i(E - E_0)^i]\}$$

where f_s , f_a and f_d are the self absorption of the samples, the transmission of the absorbers placed between the sample and the detector and the efficiency of the detector, respectively. The last component is the background with parameters B_i . The free parameter E_0 is the energy in the middle of the fitted region of the spectrum, its introduction has only numerical reason. These functions are responsible for the sharp curvature appearing at the low energy part of the spectrum. When the experimental spectrum is divided by these functions, the logarithm of the background as a function of energy is approximately linear at low energies. By fitting a polynomial on the minima of the logarithmic spectrum we get appropriate starting values for B_i parameters to be fitted.

With the help of the present description for the background of spectrum, the proper organization of the programme and the experience collected, we ended up with a programme which requires only four starting values for parameters to be fitted. They are the two constants of energy calibration and two more for the energy dependence of the width. All the four can easily be calculated with the help of the multichannel analyser from the energy-channel relation and from the width (FWHM) of two appropriately chosen peaks.

In addition to the suitable estimation of parameters to be fitted the Newton-method used for the solution of chi-square problem in ASELES has been replaced by the Levenberg-Marquardt method [4], so the stability of fitting improved significantly.

To handle the pile-up contribution a method described in [1] was used, which is advantageous in the case of using a pile-up eliminator. It is also possible to make dead time correction applying an external pulse generator or NZ-type (NZ-870, NZ-871, NZ-881) signal processor unit [5,6].

The concentration calculation is similar to that one in PIXASE. Absolute concentrations or concentrations related to an internal standard of any element can be calculated with the help of a library file obtained by PIXEKL programme described in [2]. This programme calculates data of K and L X-ray lines and if it is necessary the contribution of secondary X-ray is also treated in a mathematically exact way.

References

1. L. Zolnai, Gy. Szabó, Nucl. Instr. Meth. in Phys. Res. B34 (1988) 118-121.
2. Gy. Szabó, L. Zolnai, Nucl. Instr. Meth. in Phys. Res. B36 (1989) 88-92.
3. E. Clayton, Nucl. Instr. Meth. 218 (1983) 221-224
4. W.H. Press, B.P. Flannery, S.A. Teukolsky, W.T. Vetterling, Numerical recipes, Cambridge University Press, 1986.
5. T. Lakatos, Proc of 10-th Int. Symp. on Nucl. Electronics, Dresden 10-16. April, (1980) p.204.
6. T. Lakatos, Nucl. Instr. Meth. in Phys. Res. B47 (1990) 307-310.

A New Data Acquisition System for Radiation Protection in ATOMKI

T.Lakatos

A new 24 channel intelligent data acquisition system was developed for collecting the activity data detected by the gamma and neutron detectors mounted in different places at the Institute.

The main function of the system is the autonomous acquisition of the hourly number of counts of each detecting channel over a period of two weeks. Using a PC with a program developed for this application (see chapter 2.2.) one can visualize or print the acquired or previously recorded data in different form and monitoring the momentary activity. Once a week it is necessary to record the data accumulated during the previous week.

1. The Data Acquisition System

The data acquisition system consists of the following main units. The data is collected in the static RAM memory of a one card microcomputer (developed at the Cyclotron Laboratory of the Institute) with a Z80 microprocessor, with EPROM program memory and with a serial input-output interface (RS-232). A direct memory access and increment (DMA) unit realises the connection between the RAM memory and the other parts of the acquisition system. The hourly changing memory group address is given by a Xtal stabilised clock with a period time of two weeks. The 24 input pulse-recognition and channel encoder unit gives the lower bites of the current address according to the serial number of the channel in which a pulse is detected. This unit also initiates the DMA memory increment action, too if an input pulse occurs.

The clock (built with CMOS IC-s) has an alternative battery power, and the static RAM memory has a battery back-up, too. Therefore, in the case of power breakdown the data acquired remains true, and the clock is working on. After the breakdown the acquisition system automatically continues working.

2. The Software

The software consists of two different programs. One for the microcomputer of the data acquisition system (written in Z80 assembly) and the other for the PC (written in Turbo Pascal).

2.1. The microcomputer program

The program for the microcomputer serves for the data transfer from the RAM memory to the PC through the serial input-output interface. Without an external command this program is in waiting station (doing nothing). If an external command arrives it recognises and acknowledges the command message, and sends the required data file to the PC. In the case of data recording if the action was successful the PC program sends a clear message. After identification this program clears the appropriate memory field which will now serve for the next week data.

2.2. The PC program

This is a menu controlled interactive program. An important function of the program is the recording of the data accumulated during the previous week. Using this program one can visualise the acquired or previously recorded data. The displayed form is a bar graph structure, which can show the hourly number of counts for one selected channel or the data of each channel collected in a selected hour. The program serves for printing the acquired or archived data in different forms, too.

In the case of monitoring the computer display shows the momentary activity of every channel in a bar graph structure. The bars serves like the hand of analog ratemeters with linear or logarithmic scale.

Activities at the Van de Graaff Accelerator Laboratory

L. Bartha, Á. Z. Kiss, E. Koltay, A. Nagy, E. Somorjai and Gy. Szabó

During 1991 the beam time of the VdG-1 machine amounted to 317 hours. The accelerator delivered proton and helium beams according to the needs of electron spectrometry group working in atomic physics, the only user this time. The outstanding feature of this machine is its high ratio of maximum and minimum energy values available; the generator covered in a series of measurements the energy interval $0.05 - 1.5\text{MeV}$. Aiming at an improvement in deflecting beams of higher magnetic rigidity the new analyzing magnet has been connected to a power supply of higher current (up to 100 A). The mass-energy product of the new analyzing system amounts to $20\text{MeV}amu/e^2$.

The 5 MeV Van de Graaff machine was operating for 2163 hours during this period (Table 1).

Field	Hours	%
Atomic physics:	915	42
Nuclear physics:	858	40
Analytical studies:	352	16
Machine tests:	43	2
Total:	2163	100

Table 1. Time distribution among different research activities at VdG-5

In the experiments protons (63 %) and helium-4 ions (37 %) were accelerated. The output current of the power supply for magnetic analyzer has been increased by 50 % with a new construction having an eye on the application of light heavy ions in experiments of ion-atom collision physics. New electrode plates have been installed in the acceleration tube, they combine straight field configuration of axial gradient modulation with an efficient screening of the insulator walls of the tube. As a result, stable beam intensity and position have been obtained up to target currents of $10 - 20\mu\text{A}$.

Status Report on the Cyclotron

A. Valek

The operation of the cyclotron and the measuring centre were very similar to those of the previous years; the later was mostly used in nuclear spectroscopy studies. The overall working time of the cyclotron was 3717 hours and the break down periods amounted only up to 83 hours. The utilization of the machine was concentrated to 9 months; January, July and August were reserved for maintenance. The cyclotron was available for users during 2779 hours, the effectively used beam time is summarized in Table 1.

Table 1. Effectively used beam time

Projects	Beam time (hours)	%
Nuclear spectroscopy	559	28
Nuclear reactions	344	17
Isotope production	859	43
Neutron source	151	8
Materials sciences	67	3
Charged particle irradiation	24	1
Total	2004	100

In the maintenance period, beside the regular repairs and tests, in January the newly installed process control system of the cyclotron was tested and the operators were practiced in its use; in the summer period the cooling system was renewed. The industrial process control system after some modifications in the software worked without any trouble and helped the operators in setting the parameters of the cyclotron and the beam transportation system. In 1991 the Cyclotron Department has not any acting project to finance upgrading the IPC system or carrying out other developments at the cyclotron.

PUBLICATIONS
AND
SEMINARS

PAPERS PUBLISHED IN 1991:

Nuclear and Particle Physics

1. Kruppa A.T., Kato, K.: **Resonances in complex-scaled orthogonality condition model of nuclear system**, Progress of Theoretical Physics **84** (1990) 1145
2. Deptula, C., Khalkin, V.A., Kim Sen Khan, Knotek, O., Konov, V.A., Mikecz P, Popinenkova, L.M., Rurarzh, E., Zaitseva, N.G.: **Excitation functions and yield for medically important generators ^{82}Sr - ^{82}Rb , ^{123}Xe - ^{123}I and ^{201}Bi - ^{201}Pb - ^{201}Tl obtained with 100 MeV protons**, Nukleonika **35** (1990) 1
3. Hildingsson, L., Klamra, W., Lindblad, Th., Lindén, C.G., Sletten, G, Székely G.: **Neutron h11/12 alignments in the triaxial nucleus ^{133}La** , Zeitschrift für Physik **A 338** (1991) 125
4. Tárkányi F., Qaim, S.M., Stöcklin, G., Sajjad, M., Lambrecht, R.M.: **Nuclear reaction cross sections relevant to the production of the ^{122}Xe - ^{122}I generator system using highly enriched ^{124}Xe and a medium-size cyclotron**, Int. Journal of Radiation Applications and Instrumentation **A42** (1991) 229
5. Tárkányi F., Qaim, S.M., Stöcklin, G., Sajjad, M., Lambrecht, R.M., Schweickert, H.: **Integral yields of ^{123}I in proton induced nuclear reactions on highly enriched ^{124}Xe** , Int. Journal of Radiation Applications and Instrumentation **A42** (1991) 221
6. Raman, S., Walkiewicz, T.A., Kahane, S., Journey, E.T., Sa, J., Gácsi Z., Weil, J.L., Allart, K., Bonsignori, G., Shriner, J.F.: **Nearly complete level scheme of ^{116}Sn below 4.3 MeV**, Physical Review **C43** (1991) 521
7. Kovács Z., Tárkányi F., Qaim, S.M., Stöcklin, G.: **Excitation functions for the formation of some radioisotopes of rubidium in proton induced nuclear reactions on nat-Kr, ^{82}Kr and ^{83}Kr with special reference to the production of ^{81}Rb (81mKr) generator radionuclide**, Int. Journal of Radiation Applications and Instrumentation **A42** (1991) 329
8. Varga K., Lovas R.G.: **Signature of cluster substructure: alpha+d spectroscopic factor of ^6Li** , Physical Review **C43** (1991) 1201
9. Krasznahorkay A., Bacelar, J., Bordewijk, J.A., Brandenburg, S., Buda, A., Van 't Hof, G., Hofstee, M.A., Kato, S., Poelhekkén, T.D., Van der Werf, S.Y., Van der Woude, A., Harakeh, M.N., Kalantar-Nayestanaki, M.: **Excitation of the isovector giant dipole resonance by inelastic alpha scattering and the neutron skin of nuclei**, Physical Review Letters **66** (1991) 1287
10. Szelecsényi F., Kovács Z., Tárkányi F., Tóth Gy.: **Production of ^{110}In for PET investigation via $\text{Cd}(^3\text{He},\text{xn})^{110}\text{Sn}$ - ^{110}In reaction with low energy cyclotron**, Journal of Labelled Compounds and Radiopharmaceuticals **30** (1991) 98
11. Bentley, M A , Alderson, A., Ball, G.C., Cranmer-Gordon, H W, Fallon, P., Fant, B., Forsyth, P.D., Herskind, B., Howe, D., Kalfas, C, Mokhtar, A R, Morrison, J D, Nelson, A.H., Nyakó B.M., Schiffer, K.J., Sharpey-Schafer, J.F., Simpson, J., Sletten, G, Twin, P.J.: **Gamma-ray spectroscopy of superdeformed states in the nucleus ^{152}Dy** , Journal of Physics **G17** (1991) 481
12. Tárkányi F., Szelecsényi F., Kopecky, P.: **Excitation functions of proton induced nuclear reactions on natural nickel for monitoring beam energy and intensity**, Int. Journal of Radiation Applications and Instrumentation **A42** (1991) 513

13. Tikkanen, P., Keinonen, J., Kangasmaki, A., Fülöp Zs., Kiss A.Z., Somorjai E.: **Short lifetimes in mirror nuclei ^{25}Mg - ^{25}Al** , Physical Review **C43** (1991) 2162
14. Zaitseva, N.G., Deptula, C., Knotek, O., Kim Sen Khan, Mikolaewski, S., Mikecz P, Rurarz, E., Khalkin, V.A., Konov, V.A., Popinenkova, L.M.: **Cross section for the 100MeV proton induced nuclear reactions and yields of some radionuclides used in nuclear medicine**, Radiochimica Acta **54** (1991) 57
15. Cseh J., Lévai G, Kato, K.: **Cluster spectroscopic factor in the vibron model**, Physical Review **C43** (1991) 165
16. Lévai G, Cseh J.: **Algebraic approach to cluster states in odd-mass nuclei. I. Energy spectrum**, Physical Review **C44** (1991) 152
17. Lévai G, Cseh J.: **Algebraic approach to cluster states in odd-mass nuclei. II. Electromagnetic and other properties**, Physical Review **C44** (1991) 166
18. Vertse T., Curutchet, P, Liotta, R. J., Bang, J., Van Giai, N.: **Continuum RPA calculation of escape widths**, Physics Letters **B264** (1991) 1
19. Tárkányi F., Kovács Z., Mahunka I., Solin, O., Bergman, J.: **Excitation function of the $^{35}\text{Cl}(\alpha, n)^{38}\text{K}$ reaction using gas targets**, Radiochimica Acta **54** (1991) 165
20. Gácsi Z., Dombrádi Zs., Fényes T., Brandt, S., Paar, V.: **Structure of ^{116}Sb nucleus**, Physical Review **C44** (1991) 642
21. Gácsi Z., Fényes T., Dombrádi Zs.: **Level scheme of ^{116}Sb from (p,n γ) reaction**, Physical Review **C44** (1991) 626
22. Cata-Danil, G., Nyakó B.M., Gizon, J., Barci, V, Bucurescu, A., Curien, D, Gizon, A, André, S., Foin, C., Genevey, J., Hildingsson, L., Klamra, W., Merdinger, J.C., Zolnai L.: **Rotational band structure in ^{128}Ce** , Zeitschrift für Physik **A339** (1991) 313
23. Szelecsényi F., Tárkányi F., Kovács Z., Bergman, J., Heselius, S.J., Solin, O.: **Production of ^{66}Ga and ^{67}Ga** , Acta Radiologica. Supplementum **376** (1991) 62
24. Tárkányi F., Szelecsényi F., Takács S.: **Determination of effective bombarding energies and fluxes using improved stacked foil technique**, Acta Radiologica. Supplementum **376** (1991) 72
25. Török I.: **Some graphic representations of solar-system abundances of nuclei**, Acta Physica Hungarica **69** (1991) 191
26. Dombrádi Zs., Brant, S., Paar, V.: **Proton-neutron multiplet structure of ^{104}In** , Physical Review **C44** (1991) 1701
27. Kruppa A.T., Nagarajan, M.A., Lilley, J.S., Thompson, I.J.: **Magnetic substate population in heavy-ion inelastic scattering at energies near the Coulomb barrier (Letter to the editor)**, Journal of Physics **G17** (1991) 209
28. Csótó A., Gyarmati B., Kruppa A.T.: **Spurious resonances in a version of the algebraic resonating-group method**, Few-Body Systems **11** (1991) 149
29. The CPLEAR Collaboration, Szilágyi S., et al.: **Determination of the relative branching ratios for pp- π^+ , π^- , and pp- K^+K^-** , Physics Letters **B267** (1991) 154
30. Lévai G.: **A class of exactly solvable potentials related to the Jacobi polynomials**, Journal of Physics "A" **24** (1991) 131

Atomic Physics

1. Sarkadi L., Vajnai T., Végh J., Kövér Á.: **A new method for measurement of post-collision interaction effects in ion-atom collision**, Journal of Physics **B24** (1991) 1655
2. Gulyás L., Szabó Gy.: **Electron capture to the continuum and simultaneous target excitation or ionization in $\text{He}^{2+} + \text{He}$ collisions**, Physical Review **A43** (1991) 5133
3. Fukuda, H., Watanabe, T., Shimamura, I., Végh L.: **Energy and angular distributions of electrons emitted and ions recoiled in proton-impact ionization of helium atoms**, Nucl. Instr. and Meth. in Phys. Res. **B53** (1991) 410
4. Kawatsura, K., Sataka, M., Naramoto, H., Imai, M., Komaki, K., Yamazaki, Y., Kuroki, K., Kanai, Y., Kambara, T., Awaya, Y., Hansen, J.E., Kádár I., Stolterfoht, N.: **High Rydberg and Auger electrons from fast projectile ions studied by zero-degree electron spectroscopy**, Nucl. Instr. and Meth. in Phys. Res. **B53** (1991) 421
5. Sulik B., Török I., Ágoston A., Kádár I.: **The intensity distribution of ion-induced K alpha L n x-ray satellites and the geometrical model of ionization**, Nucl. Instr. and Meth. in Phys. Res. **B56** (1991) 45
6. Sarkadi L., Mukoyama, T.: **Systematic study of helium-induced L shell ionization cross sections**, Nucl. Instr. and Meth. in Phys. Res. **B61** (1991) 167
7. Mukoyama, T., Ito, S., Sulik B., Hock G.: **Wave function effect on the ionization probability in the geometrical model**, Bulletin of the Institute for Chemical Research, Kyoto University **68** (1991) 281
8. Fukuda, H., Shimamura, I., Végh L., Watanabe, T.: **Proton angular distributions and highly differential cross sections for ionization of helium by proton impact**, Physical Review **A44** (1991) 1565
9. Takács E., Sarkadi L., Ricz S., Sulik B., Tóth L.: **Measurement of post-collision interaction effects for p on Ne collisions**, Journal of Physics **B24** (1991) 381
10. Kádár I., Altevogt, H., Köhrbrück, R., Montemayor, V.C., Mattis, A., Schiwietz, G., Skogvall, B., Sommer, K., Stolterfoht, N., Kawatsura, K., Sataka, M., Nakai, Y., Naramoto, H., Kanai, Y., Kambara, T., Awaya, Y., Komaki, Y., Yamazaki, Y.: **High-resolution Auger spectroscopy of Na-like argon and sulfur ions singly excited in high-energy collisions with light target atoms**, Physical Review **A44** (1991) 2900
11. Papp T., Awaya, Y., Hitachi, A., Kambara, T., Kanai, Y., Mizogawa, T., Török I.: **Angular distribution measurement of various L3 x-ray transitions**, Journal of Physics **B24** (1991) 3797
12. Berényi D.: **An analysis of the present stage and future trends in the field of atomic collisions**, Acta Physica Hungarica **69** (1991) 321
13. Ricz S., Végh J., Kádár I., Sulik B., Varga D., Berényi D.: **Fast multicharged ion-induced satellite Auger electron angular distributions** Nucl. Instr. and Meth. in Phys. Res. **B61** (1991) 411
14. Sataka, M., Kawatsura, K., Naramoto, H., Nakai, Y., Yamazaki, Y., Komaki, K., Kuroki, K., Kanai, Y., Kambara, T., Awaya, Y., Hansen, J.E., Kádár I., Stolterfoht, N.: **High-resolution L-shell Auger spectroscopy of Mg-like scandium produced in 89-MeV $\text{Sc}^{8+} + \text{He}$ collisions**, Physical Review **A44** (1991) 7290

Materials Science and Analysis

1. Török I.: **The Mg/Ca ratio determination by high resolution PIXE**, Nuclear Instruments and Methods in Physics Research **B61** (1991) 94
2. Szűcs Z., Norseev, Yu.V., K'yung, D.D., Vasáros L.: **Izomery asztatbenzójnoj kislóti**, Radiohimiya **33** (1991) 64
3. Bohátka S., Degn, H.: **Continuous measurement of water in organic solution by membrane-inlet mass spectrometry**, Rapid Communications in Mass Spectrometry **5** (1991) 433
4. Mészáros S., Vad K., Halász G., Hegman N., Katona G.: **Current conduction and macroscopic quantum interference in Bi-Sr-Ca-Cu-O screen printed films**, Superconductor Science and Technology **4** (1991) 367
5. Kovács I., Kovács Z.: **Synthesis of ethyl (14CH3)methylmalonyl thioglycolate as a possible substrate analogue of (14CH3)methylmalonyl coenzyme-A**, Journal of Labelled Compounds and Radiopharmaceuticals **29** (1991) 1181
6. Raisanen, J., Rauhala, E., Bjönberg, M., Kiss A.Z., Dominguez, J.: **Stopping powers of Al and Sn for ^4He , ^7Li , ^{11}B , ^{12}C , ^{14}N and ^{16}O ions in the energy range 0.5-2.6 MeV/amu**, Radiation Effects and Defects in Solids **118** (1991) 97

Earth and Cosmic Sciences, Environmental Research

1. Kozák M., Pécskay Z., Székyné-Fux V., Andó J.: **K/Ar radiometrikus koradatok földtani értelmezése ÉK-kubai kőzetmintákon (bevezetés, alkalmazott módszerek)**, Acta Geographica Debrecina **26** (1987) 143
2. Árva-Sós E., Balogh K., Nguyen Van Quy, Ravasz Cs., Ravasz-Baranyai L.: **Bazaltok magmatektonikai és korviszonyainak vizsgálata Bao Loc és Dilinh (dél-Vietnam) térségében**, A Magyar Állami Földtani Intézet Évi Jelentése az 1988. Évről. 1.rész (1990) 485
3. Balogh K., Lobitzer, H., Pécskay Z., Ravasz Cs., Solti G.: **Kelet-stajerországi és burgenlandi terciér vulkanitok K/Ar kora**, A Magyar Állami Földtani Intézet Évi Jelentése az 1988. Évről. 1.rész (1990) 451
4. Balogh K., Kovách Á., Pécskay Z., Svingor É., Árkai P.: **Very low- and low-grade metamorphic rocks in the pre-Tertiary basement of the Drava basin, SW-Hungary, II: K-Ar and Rb-Sr isotope geochronologic data**, Acta Geologica Hungarica **33** (1990) 69
5. Hertelendi E., Vető I.: **The marine photosynthetic carbon isotopic fractionation remained constant during the early oligocene**, Palaeogeography, Palaeoclimatology, Palaeoecology **83** (1991) 333
6. Borbély-Kiss I., Bozó L., Koltay E., Mészáros E., Molnár Á., Szabo Gy.: **Elemental composition of aerosol particles under background conditions in Hungary**, Atmospheric Environment **25** (1991) 661
7. Rozložnik, L., Jakabská, K., Dauteuil, D., Kosztolányi, Ch., Kovách Á.: **Petrogenesis and age determination of the Hodrusa granodiorite (Hodrusa Hámre, Stiavnické vrchy mts., Czecho-Slovakia)**, Geologica Carpathica **42** (1991) 77
8. Balogh K., Ravasz-Baranyai L., Dudaauri, O., Tagonidze, M.: **Dating of ore mineralization in the Kelasuri Massif, Great Caucasus, Georgia, USSR**, Chemie der Erde **51** (1991) 107
9. Hunyadi I., Hakl J., Lénárt L., Géczy G., Csige I.: **Regular subsurface radon measurements in Hungarian karstic regions**, International Journal of Radiation Applications and Instrumentation **D19** (1991) 321
10. Marenyy, A.M., Nymmik, R.A., Hunyadi I., Csige I., Spurny, F., Charvat, J., Guertzen, G.P.: **Low-energy heavy ions of cosmic rays measured on COSMOS-2044 biosatellite**, International Journal of Radiation Applications and Instrumentation **D19** (1991) 697

Biological and Medical Research

1. Deptula, C., Khalkin, V.A., Kim Sen Khan, Knotek, O., Konov, V.A., Mikecz P, Popinenkova, L.M., Rurarzh, E., Zaitseva, N.G.: **Excitation functions and yield for medically important generators ^{82}Sr - ^{82}Rb , ^{123}Xe - ^{123}I , and ^{201}Bi - ^{201}Pb - ^{201}Tl obtained with 100 MeV protons**, *Nukleonika* **35** (1990) 1
2. Szűcs Z., Szelecsényi F.: **Asztácium előállítása a debreceni mgc-20e ciklotronnal**, *Izotoptechnika, Diagnosztika* **33** (1990) 221
3. Smakova, N.L., Norseev, Yu.V., Vajnsón, A.A., Szűcs Z., Fadeeva, T.A., Fomenkova, T.E., Halkin V.A., Cherevatenko, A.P.: **Dejstvie alfa-izlucheniya ^{211}At na kletki astsitnogo raka Erliha**, *Eksperimental'naya Onkologiya* **12** (1990) 58
4. Lauritsen, F.R., Nielsen, L.T., Degn, H., Lloyd, D., Bohátka S.: **Identification of dissolved volatile metabolites in microbial cultures by membrane inlet tandem mass spectrometry**, *Biological Mass Spectrometry* **20** (1991) 253
5. Fenyvesi A., Mahunka I., Molnár T.: **Status report on the fast neutron irradiation facility for radiobiological purposes at the Debrecen cyclotron**, *Zeitschrift Für Medizinische Physik* **1** (1991) 30
6. Kovács Z., Tárkányi F., Qaim, S.M., Stöcklin, G.: **Production of 6.5h ^{82}mRb via the $^{82}\text{Kr}(p,n)$ -process at a low-energy cyclotron - A potential substitute for ^{82}Rb** , *International Journal of Radiation Applications and Instrumentation* **A42** (1991) 831
7. Bacsó J., Uzonyi I., Földes I., Bakulin, A.V., Rachmanov, A.S., Oganov, V.S.: **Investigations of mineral concentrations, mechanical and biochemical parameters in rat's hair and bone, and correlations between them**, *Acta Physica Hungarica* **69** (1991) 365

Development of Instruments and Methods

1. Berez I., Balogh K., Bohátka S., Hertelendi E., Kövér L., Langer G.: **Developments in mass and electron spectrometry**, Acta Chimica Hungarica **127** (1990) 525
2. Berényi D., Bibók Gy., Berez I.: **Spektroskopicheskie izmeritel'nye pribory, razrabotannye v Institute Yadernyh Issledovanij Vengerskoj Akademii Nauk**, Scientific Instrumentation **5** (1990) 203
3. Kövér Á.: **Design parameters of an electrostatic analyser for recording the energy and angular distribution of positrons and electrons simultaneously**, Measurement Science and Technology **2** (1991) 448
4. Dajkó G.: **Etching characteristic of a CR-39 track detector at room temperature in different etching solutions**, International Journal of Radiation Applications and Instrumentation **D18** (1991) 297
5. Freyer, K., Treutler, H.C., Dietze, K., Hunyadi I., Csige I., Somogyi Gy.: **Vacuum treatment of CR-39 for the reduction of background in neutron induced autoradiography of boron**, International Journal of Radiation Applications and Instrumentation **D18** (1991) 309
6. Biri S., Bogomolov, S.L., Koós I.: **A method for radial extraction of ions from a PIG source using an asymmetrical Wien filter**, Nucl. Instr. and Meth. in Phys. Res. **A306** (1991) 56
7. Bhattacharyya, D., Basu, B., Pal, P., Rakshit, R., Chakrabarty, S., Hunyadi I.: **Interactions of 0.45 GeV/n ^{84}Kr ions on CR-39(MA-ND)**, Nucl. Instr. and Meth. in Phys. Res. **B61** (1991) 197
8. Trajber Cs, Simon M., Csatlós M.: **On the Use of pre-filters in quadrupole mass spectrometers**, Measurement Science and Technology **2** (1991) 785
9. Székely G., Klamra, W., Lindblad, Th., Lund-Jensen, B.: **A small multiparameter data acquisition system-based on a VME-PC/AT**, Nucl. Instr. and Meth. in Phys. Res. **A306** (1991) 540
10. Gál I., Takács S., Tárkányi F., Andó L.: **Beam splitting for parallel isotope production**, Acta Radiologica. Supplementum **376** (1991) 73
11. Ujhelyi Cs.: **New determination of the true net count rates by measuring the decay of two sources of a radioisotope at the same distance**, International Journal of Radiation Applications and Instrumentation **A42** (1991) 475
12. Bacsó J., Uzonyi I., Földes I., Bakulin, A.V., Rachmanov, A.S., Oganov, V.S.: **Investigations of mineral concentrations, mechanical and biochemical parameters in rat's hair and bone, and correlations between them**, Acta Physica Hungarica **69** (1991) 365
13. Hafez, A.F., Kotb, M.A., Tóth-Szilágyi M.: **Contribution of radon daughters plated-out in a cylindrical device by track-technique**, Isotopenpraxis **27** (1991) 211
14. Hafez, A.F., Hunyadi I., Kotb, M.A.: **The etch-induction time T_i and etch-critical time T_c in CR-39 plastic nuclear track detector**, Isotopenpraxis **27** (1991) 214

15. Bohátka S., Degn, H.: **Continuous measurement of water in organic solution by membrane-inlet mass spectrometry**, Rapid Communications in Mass Spectrometry **5** (1991) 433
16. Csige I., Hunyadi I., Charvat, J.: **Environmental effects on induction time and sensitivity of different types of CR-39**, International Journal of Radiation Applications and Instrumentation **D19** (1991) 151
17. Medveczky L., Hakl J., Fenyvesi A., Molnár T.: **Fast neutron radiation field measurement in a water phantom**, International Journal of Radiation Applications and Instrumentation **D19** (1991) 507
18. Hakl J., Hunyadi I., Tóth-Szilágyi M.: **Radon permeability of foils measured by SSNTD technique (Non-equilibrium approach)**, International Journal of Radiation Applications and Instrumentation **D19** (1991) 319
19. Turek, K., Bednar, J., Dajkó G., Spurny, F.: **Study of parameters influencing the internal heating effect during electrochemical etching at room temperature**, International Journal of Radiation Applications and Instrumentation **D19** (1991) 227
20. Biri S., Butcev, V.S., Molnár J., Samojlov, V.N.: **Interfejs PCA/increment memory dlya analogovykh protsessorov na linij s IBM PC-XT/AT**, Pri-bory i Tekhnika Eksperimenta (1991) 88
21. Baksay, L., Lökös S., Magahiz, R., Bencze Gy.L., Fodor Z., Bujak, A., Banicz, K.: **Apparatus for precise drift time change measurements by means of photoelectrons emitted from the cathode**, Nucl. Instr. and Meth. in Phys. Res. **A310** (1991) 607
22. Lakatos T.: **Noise and resolution with digital filtering for nuclear spectrometry**, Nucl. Instr. and Meth. in Phys. Res. **B62** (1991) 289
23. Turek, K., Bednar, J., Dajkó G.: **Variation of temperature with time during electrochemical etching. (Short communication)**, International Journal of Radiation Applications and Instrumentation **D18** (1991) 415

CONFERENCE CONTRIBUTIONS AND TALKS:

Nuclear and Particle Physics

1. Szelecsényi F., Tárkányi F., Kopecky, P., Rydl A., Mikecz P, Tóth Gy., Andó L.: **Excitation functions of proton induced nuclear reactions on ^{111}Cd and ^{112}Cd . Production of ^{111}In** , (abstr.: p.67), International Conference on Nuclear Data for Science and Technology. Jülich, Germany, 13-17 May,1991 (1991)
2. Lovas R.G.: **Összetett rendszerek relatív mozgása**, Budapesti Műszaki Egyetem Fizikai Intézete, Bp., 1991.jan.11. (1991)
3. Lovas R.G.: **Paradoxical phenomena in nuclear clustering**, Manne Siegbahn Institute För Fysik. Stockholm, Sweden, 1991.Jan.30. (1991)
4. Lévai G.: **Algebraic description of cluster structure of light nuclei**, Institut für Theoretische Physik, Justus-Liebig Universität, Giessen, Germany, 1991.Jan.8. (1991)
5. Cseh J., Lévai G.: **The vibron model and the nuclear clusterisation**, (abstr.:Verhandlungen der Deutschen Physikalischen Gesellschaft. Darmstadt, Physik-Verlag,1991,no.6, fachsitzung a7-f7,p7) Frühjarstagung, Darmstadt, 1991, Physik der Hadronen und Kerne. Darmstadt, Germany. 15 March,1991. (1991)
6. Kovács Z., Tárkányi F., Qaim, S.M., Stöcklin, G.: **Cross section of proton induced nuclear reactions on Kr gas relevant to the production of medically important radioisotopes ^{81}Rb and ^{82}mRb** (abstr.:66), International Conference on Nuclear Data for Science and Technology. Jülich, Germany, 13-17 May,1991 (1991)
7. Tárkányi F., Szelecsényi F., Kopecky, P.: **New data for p, alpha, and ^3He induced reactions on nat-Ni, nat-Cu and nat-Ti for monitoring the beam performance**, (abstr.: p.230), International Conference on Nuclear Data for Science and Technology. Jülich, Germany, 13-17 May,1991 (1991)
8. Somorjai E.: **Kísérleti magreakció kutatás és a nukleáris asztrofizika**, A fizika fejlődési irányjai. Az MTA Matematikai és Fizikai Tudományok osztálya tudományos ülése. BP., 1991.május 7. (1991)
9. Zaitseva, N.G., Deptula, C., Knotek, O., Kim Sen Khan, Mikolaewski, S., Mikecz P, Rurarzh, E., Khalkin, V.A., Konov, V.A., Popinenkova, L.M.: **Cross section for the 100 MeV proton induced nuclear reactions and yields of some radionuclides used in nuclear medicine**, (abstract book 044), Nuclear Data for Science and Technology. Jülich, Germany, 13-17 May,1991. (1991)
10. Nyakó B.M., Cata-Danil, G., Gizon, J., Barci, V, Bucurescu, A., Curien, D, Gizon, A, André, S., Foin, C., Genevey, J., Hildingsson, L., Klamra, W., Merdinger, J.C., Zolnai L.: **Spectroscopy of high spin states in ^{128}Ce** , European Research Conference on Nuclear Shapes, Balatonfüred, 2-6 Sept.,1991 (1991)
11. Ditrói F., Takács S., Mahunka I., Mikecz P, Tóth Gy.: **Investigation of oxigen in high purity gallium samples by using charged particle activation analysis**, 2nd ECAART, European Conference on Accelerators in Applied Research and Technology. Frankfurt am Main, Germany, 3-7 Sept.,1991. (1991)
12. Keinonen, J., Tikkanen, P., Kuronen, A, Kiss A.Z., Somorjai E., Wildenthal, B.H.: **Short lifetimes for tests of sd-shell states**, Contemporary Topics in Nuclear Structure Physics, Mexico, 9-14 June, 1988 (1991)
13. Tikkanen, P., Keinonen, J., Kangasmaki, A., Kiss A.Z., Somorjai E., Wildenthal, B.H.: **Transition strenghts in the mirror nuclei ^{25}Mg , ^{25}Al** , (abst.: Tampere Univ. of Technology Department of Electrical Engineering, physics report 7-90 p.13:8) XIV. Annual Meeting of the Finnish Physical Society, Tampere, Finland, 29-31 March, 1990 (1991)

14. Lovas R.G.: **Signature of cluster substructure in microscopic cluster models**, Clusters in Hadrons and Nuclei. Tübingen, Germany. 15-17 July, 1991. (1991)
15. Fényes T.: **Structure of odd-odd In and Sb nuclei:shape co-existence**, European Research Conference on Nuclear Shapes. Balatonfüred, 1991.szeptember 2-6. (1991)
16. Gyarmati B.: **Complex scaling: a method for determining resonant states in nuclear systems**, Clusters in Hadrons and Nuclei. Tübingen, Germany. 15-17 July, 1991. (1991)
17. Zolnai L.: **Low energy proton OMP for tin isotopes**, Abo Academy, Department of Physics, Turku, Finland, 1991.nov.27. (1991)
18. Zolnai L.: **Debrecen-EUROGAM future prospects**, Department of Physics, University of Jyväskylä, Finland, 1991.nov.22. (1991)
19. Vertse T.: **Oriásrezonanciák parciális szélességének számítása**, BME Fizikai Intézet, Budapest, 1991.május 31. (1991)
20. Lovas R.G., Varga K., Kruppa A.T.: **Microscopic versus macroscopic treatment of clusters in nuclei**, International Conference on Clustering in Nuclei and Atoms. Turku, Finland, 3-7 June, 1991. (1991)
21. Lévai G.: **Application of the Vibron-Fermion model to cluster states of light nuclei**, Institut für Theoretische Physik, Justus-Liebig-Universität, Giessen, Germany, 1991.nov.1. (1991)
22. Szilágyi S.: **Search for non-leptonic transitions in CPLEAR**, CERN, Geneva, Switzerland, 1991. May 17. (1991)
23. Cseh J., Gupta, R.K., Scheid, W.: **Cluster radioactivity within an algebraic approach**, (Contributed papers. Eds.: R.Caplar et al. p.7) 7th Adriatic International Conference on Nuclear Physics, Heavy-Ion Physics Today and Tomorrow. Brioni, Yugoslavia, 27 May - 1 June, 1991. (1991)
24. Cseh J.: **Non-closed-shell nuclear clusters and the algebraic approach**, (Invited papers, Springer Verlag) International Conference on Clustering in Nuclei and Atoms. Turku, Finland, 3-7 June, 1991. (1991)
25. Cseh J., Scheid, W.: **On the relation between cluster and superdeformed states of light nuclei**, European Research Conference on Nuclear Shapes, Balatonfüred, 2-6 Sept.,1991 (1991)
26. Cseh J.: **Algebraic treatment of internal cluster degrees of freedom**, (Contributed papers. Eds.:R.Caplar et al. p.3) 7th Adriatic International Conference on Nuclear Physics, Heavy-Ion Physics Today and Tomorrow. Brioni, Yugoslavia, 27 May - 1 June, 1991. (1991)
27. Galés, S., Krasznahorkay A., et al. **Neutron decay of giant states excited in transfer reactions**, Workshop on Giant Resonances and Related Phenomena. Notre Dame University Indiana, USA, 21-23 Oct., 1991. (1991)
28. Krasznahorkay A., Bacelar, J., Bordewijk, J.A., Brandenburg, S., Van der Werf, S.Y., Van der Woude, A., Harakeh, M.N., Kalantar-Nayestanaki, M.: **Excitation of the isovector GDR by inelastic alpha scattering and the neutron skin of nuclei**, (Abstr.: Bulletin of the American Physical Society. Sept.1991, Vol.36, No.8. p.2154) 1991 Annual Fall Meeting of the Division of Nuclear Physics (DNP). East Lansing, Michigan, USA, 23-27 Oct., 1991. (1991)
29. Krasznahorkay A., Bacelar, J., Balanda, A., Bordewijk, J.A., Brandenburg, S., Van der Werf, S.Y., Van der Woude, A., Harakeh, M.N., Kalantar-Nayestanaki, M.: **Excitation of the isovector GDR by inelastic alpha scattering and**

- the neutron skin of nuclei**, 6th International Conference on Nuclear Reaction Mechanisms. Varenna, Italy, 10-15 June, 1991. (1991)
30. Krasznahorkay A., Bacelar, J., Balanda, A., Bordewijk, J.A., Brandenburg, S., Van der Werf, S.Y., Van der Woude, A., Harakeh, M.N., Kalantar-Nayestanaki, M.: **Excitation cross section of the isovector GDR in (α , α') reactions as a measure of the neutron skin of nuclei**, Nederlandse Natuurkundige Verebiging. Petten, The Netherlands, 1 Nov., 1991. (1991)
 31. Krasznahorkay A.: **Excitation cross section of the isovector GDR in (α , α') reactions as a measure of the neutron skin of nuclei**, Universite Catholique de Louvain, Département de Physique, Institut de Physique Nucleaire. Louvain-la-Neuve, Belgium, 1991. Dec.3. (1991)
 32. Krasznahorkay A.: **A novel method for determination of the neutron skin thickness of nuclei**, Institut de Physique Nucléaire. Orsay, France, 1991. Feb.13. (1991)
 33. Cseh J., Gupta, R.K., Scheid, W.: **An algebraic approach to cluster radioactivity**, (Contributed papers. Eds.: T. Lönnroth. Turku, 1991, p.9) International Conference on Clustering in Nuclei and Atoms. Turku, Finland, 3-7 June, 1991. (1991)
 34. Lévai G.: **Dinamikai szimmetria atommagokban**, KLTE-Atomki közös szeminariumsorozat, Debrecen, 1991. febr. 28. (1991)
 35. Fényes T.: **Magspektroszkopiai eredmények a debreceni ciklotronnál**, Szalay Sándor Fizikai Centrum, Debrecen, 1991. április 4. (1991)
 36. Fényes T.: **A magyarországi magfizikai kutatás külkapcsolatai: Közép- és Kelet-Európa**, MTA Magfizikai Albizottság, Debrecen, 1991.junius 26. (1991)
 37. Fényes T.: **A magyarországi magfizikai kutatás külkapcsolatai: Egyesített Atomkutató Intézet (Dubna)**, MTA Magfizikai Albizottság, Debrecen, 1991.junius 26. (1991)
 38. Koltay E.: **Az atomenergia és magkutatás újabb eredményei**, (szerk.) BP., Akadémiai K. **7** (1990) 267
 38. Carlson, P., Kerek, A., Szilágyi S.: **First biennial conference on low energy antiproton physics**, LEAP'90. Stockholm, Sweden, 2-6 July 1990. (eds.) World Scientific, Singapore, New Jersey, London, etc. (1991) 545
 39. Fényes T.: **G.N.Fljorov (1913-1990)**, Fizikai Szemle **41** (1991) 196
 40. Kovách Á.: **Teller Ede Debrecenben**, Fizikai Szemle **41** (1991) 148

Atomic Physics

1. Pálinkás J., Papp T., Sarkadi L.: **M2-E1 mixing in ion induced L x-ray transitions**, X-ray and inner-shell processing, Knoxville, TN., 1990. ed.:T.A.Carlson, M.O.Krause, S.T.Manson. New York, AIP. AIP conference proceedings 215 (1990) 441
2. Gulyás L., Kövér Á., Szabó Gy., Vajnai T., Berényi D.: **Testing the series expansion method used for studying the 'cusp' spectra**, High-energy ion-atom collisions. Proceedings, Debrecen, Hungary 1990. eds.:D. Berényi, G. Hock, Berlin, Heidelberg, New York, etc., Springer-Verl. (Lecture Notes in Physics) 376 (1991) 56
3. Kádár I., Ricz S., Végh J., Sulik B., Varga D., Berényi D.: **Winkelverteilung von Schwerionen Induzierten Auger Satelliten**, Energiereicheatomare Stösse, Riezlern, Austria, 1991.Jan.27-Feb.2. (1991)
4. Sarkadi L.: **Study of cusp, alignment and post-collision interaction effects applying coincidence technique**, Institut für Kernphysik, J.W.Goethe Universität, Frankfurt Am Main, Germany, 1991. Apr.29. (1991)
5. Török I., Petukhov, V., Blokhin, S., Závodszky, P., Pálinkás J., Sarkadi L.: **The polarization of Ti KL x-ray satellites**, 2nd Debrecen-Uzhgorod-Miskolc Triangle Seminar on Atomic Collision Processes. Miskolc, 1991.máj.30. (1991)
6. Petukhov, V., Blokhin, S., Török I., Závodszky, P., Pálinkás J., Sarkadi L., Papp T., Sulik B., Takács E.: **Polarization measurements of light element K alpha Ln x-ray satellites**, International Symposium on Ion-Atom Collision - ISAC XII. ANA Hotel, Gold Coast, Australia, 18-19 July, 1991. (1991)
7. Takács E., Sarkadi L., Ricz S., Sulik B., Tóth L. **Measurement of post-collision interaction effects for p on Ne collisions**, Seventeenth International Conference on the Physics of Electronic and Atomic Collisions (XVII.ICPEAC), Brisbane. Brisbane, Australia, 10-16 July, 1991 (1991)
8. Takács E., Sarkadi L., Ricz S., Sulik B., Tóth L.: **Measurement of post-collision interaction effects for p on Ne collisions**, 2nd Debrecen-Uzhgorod-Miskolc Triangle Seminar on Atomic Collision Processes. Miskolc, 1991.máj.30. (1991)
9. Berényi D.: **Recent results on the cusp phenomena in the electron spectrum from ion-atom collisions in Atomki, Debrecen**, Institute for Physics, Bergen University, Bergen, Germany, April 22,1991. (1991)
10. Gulyás L., Berényi D., Sarkadi L., Pálinkás J., Kövér Á., Vajnai T.: **Study of the electron distribution measured at He⁺(200,600 KeV)-He, Ar collision systems**, 2nd Debrecen-Uzhgorod-Miskolc Triangle Seminar on Atomic Collision Processes. Miskolc, 1991.máj.30. (1991)
11. Török I.: **The Mg/Ca ratio determination by high resolution**, 2nd ECAART, European Conference on Accelerators in Applied Research and Technology. Frankfurt am Main, Germany, 3-7 Sept.,1991. (1991)
12. Végh L., Nagy L.: **Stopping of slow antiprotons in hydrogen**, Mini-workshop on Slowing Down and Stopping of Slow, Heavy, Charged Particles in Matter. Budapest, 1991.sept.9-10. (1991)

13. Sarkadi L.: **Theoretical study of L-shell ionization induced by energetic ions**, 2nd Debrecen-Uzhgorod-Miskolc Triangle Seminar on Atomic Collision Processes. Miskolc, 1991.máj.30. (1991)
14. Nagy L., Végh L.: **Theoretical ionization cross sections for p-H₂ collisions**, 2nd Debrecen-Uzhgorod-Miskolc Triangle Seminar on Atomic Collision Processes. Miskolc, 1991.máj.30. (1991)
15. Kádár I.: **Structure effects in the excitation of sodium-like ions**, 2nd Debrecen-Uzhgorod-Miskolc Triangle Seminar on Atomic Collision Processes. Miskolc, 1991.máj.30. (1991)
16. Berényi D.: **Recent results on the cusp in the electron spectrum**, Nuclear Physics Department, ANU, Canberra, Australia. July 22,1991. (1991)
17. Berényi D.: **Some new results and ideas on the cusp shape**, (Invited talk) ISIIAC XII., Gold Coast, July 19, 1991. (1991)
18. Cserny I., Kövér L., Brabec, V., Fiser, M., Dragoun, O., Novák J.: **Chemical effects on the 3p and 3d core-level widths in technetium; a study by internal conversion electron spectroscopy**, (Abstr.: ECASIA 91 Abstracts, p.150) ECASIA 91. 4th European Conference on Applications of Surface and Interface Analysis. Budapest, Hungary, 14-18 Oct.,1991. (1991)
19. Sarkadi L.: **Investigations of atomic collisions by detection of electrons**, Sophia University, Tokyo, Japan, Oct.17,1991. (1991)
20. Sarkadi L.: **Investigations of atomic collisions by detection of electrons**, Metropolitan University, Tokyo, Japan, Oct.17,1991. (1991)
21. Berényi D.: **Why the "cusp" issue in the electron spectrum ejected in ion-atom collisions is still actual?**, Seminar talk Hahn-Meitner-Institut. Berlin, Germany, Nov.29,1991. (1991)
22. Berényi D.: **Investigation on the cusp-stage in the electron spectrum emitted in ion-atom collision**, Seminar talk IKF, Frankfurt, Germany. Nov.27,1991. (1991)
23. Tóth J.: **Instrumentation in the NAO and ESAO in Atomki for atomic physics and surface- and interface research**, University of Reims, Laboratory of Analysis of Solid Surfaces and Interfaces in the Group of the Research of Surfaces and Thin Films. L.A.S.S.I.(G.R.S.M.). Reims, France, March 26, 1991. (1991)
24. Ricz S., Kádár I., Végh J., Fülöp Zs., Takács E., Wakiya K., Szabó Gy., Tóth L.: **A possible post collision interaction in the electron capture to continuum process**, Hahn-Meitner Institut GmbH, Berlin, Germany, 1991.Nov.28. (1991)
25. Gulyás L., Sarkadi L., Pálincás J., Kövér Á., Vajnai T, Szabó Gy., Berényi D.: **ELC cusp-shape in the electron spectrum from the collisions He⁺ (0.20,0.57 MeV)-He**, (Abstr.:Book of Abstracts. Ed.:I.E.McCarbly. p.481) Seventeenth International Conference on the Physics of Electronic and Atomic Collisions (XVII.ICPEAC), Brisbane. Brisbane, Australia, 10-16 July, 1991 (1991)
26. Pálincás J.: **Observation of electron capture induced by electron-electron interaction in p-He collisions at 1 MeV**, Physics Department, Sophia University, Tokyo, Japan, 1991.Oct.19. (1991)
27. Pálincás J.: **Az elektron-elektron kölcsönhatás megfigyelése elektronbefogási folyamatban**, József Attila Tudományegyetem Fizikai Tanszékcsoport Szeminárium, Szeged, 1991. m rc.8. (1991)
28. Pálincás J.: **Egzotikus elektronbefogási folyamatok**, Központi Fizikai Kutatóintézet Szemináriuma, Budapest, 1991. ápr.22. (1991)

29. Pálinkás J.: **Observation of electron-electron interaction in electron capture by 1 MeV protons from He**, Joint Institute for Nuclear Research, Dubna, USSR, 1991. ápr.19. (1991)
30. Pálinkás J.: **Electron-electron interaction in transferionization** Laboratory for Atomic Physics, The Institute of Physical and Chemical Research (RIKEN), Tokyo, Japan, 1991.okt.25. (1991)
31. Pálinkás J.: **Inner-shell alignment in ion-atom collisions**, (Invited talk) Seventeenth International Conference on the Physics of Electronic and Atomic Collisions (XVII.ICPEAC), Brisbane. Brisbane, Australia, 10-16 July, 1991 (1991)
32. Berényi D., Hock G.: **High-energy ion-atom collisions**, Proceedings, Debrecen, Hungary 1990. (eds.) Lecture Notes in Physics. Berlin, Heidelberg, New York, etc., Springer-Verlag 376 (1991) 364
33. Berényi D.: **Világunk jelene és jövője**, Mozgalom egy globális parlamentért. Szarvas,1991.márc.13. (1991)
34. Berényi D.: **A tudományos ismeretterjesztés ma**, Emlékkülés a természettudományi társulat alapításának 150. évfordulója tiszteletére. Nyíregyháza, 1991. márc.25. (1991)
35. Berényi D.: **"Exodus" vagy bekapcsolódás a világ normális tudományos vérkeringésébe?**, Természet Világa **122** (1991) 246
36. Berényi D.: **Gondolatok a Magyar Tudományos Akadémia kiadói koncepciójáról (A tudományos műhely problémái)**, Magyar Tudom ny **97** (1991) 717
37. Berényi D.: **A mai fizika fejlődési iránya**, Bessenyei Tanárképző Főiskola. Nyíregyháza, 1991.május 8. (1991)
38. Berényi D.: **The content of the message of the scientists to the public**, Talk at the Working Group C-10 at the Berlin congress. "Challenges" international congress of scientists and engineers. Berlin, Germany, 29 Nov. - 1 Dec.,1991. (1991)
39. Berényi D.: **Foundation of the network "INES"**, Plenary talk at the Berlin congress. "Challenges" international congress of scientists and engineers. Berlin, Germany, 29 Nov. - 1 Dec.,1991. (1991)
40. Berényi D.: **Quo vadis physica?** VEAB Klub. Veszprém, 1991.okt.16. (1991)
41. Berényi D.: **Az atomfizika helye és szerepe a mai fizikában**, ELFT Veszprémi Csoportja. 1991.okt.16. (1991)

Materials Science and Analysis

1. Biswas, S.K., Borbély-Kiss I., El-Ghawi, U.M., Koltay E., Szabó Gy.: **On the applicability of PIXE microanalysis at 100 keV bombarding energies**, International Conference Proceedings. Applications of Nuclear Techniques, Heraklio, Crete, Greece, June 1990. Ed.: G.Vourvopoulos, Th.Paradellis. Singapore Etc., World Scientific (1991) 179
2. Vad K., Mészáros S., Hegman N., Katona G., Besenyei E.: **Current conduction properties of BiPbSrCaCuO thick films**, Proceedings of the Sixth International Symposium on Weak Superconductivity. Smolenice, Czechoslovakia, 20-24 May 1991. Eds.: S.Benacka, M.Darula, M.Kedro. Singapore, New Jersey, London, etc., World Scientific (1991) 64
3. Vad K., Kirsch, É.: **Analogue simulation of RF SQUID**, Proceedings of the Sixth International Symposium on Weak Superconductivity. Smolenice, Czechoslovakia, 20-24 May 1991. Eds.: S.Benacka, M.Darula, M.Kedro. Singapore, New Jersey, London, etc., World Scientific (1991) 215
4. Vad K., Mészáros S., Halász G., Hegman N., Katona G., Besenyei E.: **Hysteretic magnetoresistance of high-TC superconductors**, Proceedings of the Sixth International Symposium on Weak Superconductivity. Smolenice, Czechoslovakia, 20-24 May 1991. Eds.: S.Benacka, M.Darula, M.Kedro. Singapore, New Jersey, London, etc., World Scientific (1991) 35
5. Mészáros S., Halász G., Vad K., Hegman N.: **Measuring system for studying superconductive properties of high TC superconductors**, Proceedings of the Sixth International Symposium on Weak Superconductivity. Smolenice, Czechoslovakia, 20-24 May 1991. Eds.: S.Benacka, M.Darula, M.Kedro. Singapore, New Jersey, London, etc., World Scientific (1991) 56
6. Kiss A.Z., Fülöp Zs., Borbély-Kiss I., Gesztelyi T., Koltay E., Szabó Gy.: **Analysis of ancient glass sealing by the PIXE-PIGE method**, University of Helsinki, Accelerator Laboratory, Helsinki, Finland, 1991.Jun.5. (1991)
7. Szabó Gy.: **Auswertung von PIXE-Spectren mit einem neuen Programm**, Institut für Kernphysik, Frankfurt/Main, Germany, 1991.aug.6. (1991)
8. Kövér L., Varga D., Cserny I., Tóth J., Tőkési K.: **High energy, high resolution Auger-electron spectroscopy using bremsstrahlung radiation**, (Abstr.:ECASIA 91 Abstracts, p.30) ECASIA 91. 4th European Conference on Applications of Surface and Interface Analysis. Budapest, Hungary, 14-18 Oct.,1991. (1991)
9. Tőkési K, Kövér L., Varga D.: **A new type of electrostatic electron analyzers**, (Abstr.: ECASIA 91 Abstracts, p.141) ECASIA 91. 4th European Conference on Applications of Surface and Interface Analysis. Budapest, Hungary, 14-18 Oct.,1991. (1991)
10. Varga D., Kövér L., Cserny I., Tóth J., Tőkési K.: **A photoelectron spectrometer for high energy XAES**, (Abstr.: ECASIA 91 Abstracts, p.142) ECASIA 91. 4th European Conference on Applications of Surface and Interface Analysis. Budapest, Hungary, 14-18 Oct.,1991. (1991)

- Materials Science and Analysis
11. Cazaux, J., Bardoux, T., Mouze, D., Patat, J.M., Salace, G., Thomas, X., Tóth J.: **Why (and how) to obtain simultaneously two Auger spectra at the same point?**, (Abstr.: ECASIA 91 Abstracts, p.148) ECASIA 91. 4th European Conference on Applications of Surface and Interface Analysis. Budapest, Hungary, 14-18 Oct., 1991. (1991)
 12. Gémesi Z., Ditrói F., Takács S., Mahunka I., Bódizs D.: **Microelemental investigation of different types of glasses by using cyclotron beams and nuclear reactor** 2nd International Conference Advances in the Fusion and Processing of Glass. Düsseldorf, Germany. 22-25 Oct., 1990. (1991)
 13. Ditrói F.: **Materialanalyse mit Zyklotron in Debrecen**, Institut für Kernphysik J.W.Goethe Universität, Frankfurt, FRG, 1991.Apr.18. (1991)
 14. Mahunka I.: **Cyclotron based thin layer activation for wear measurement**, Sumitomo Heavy Industries, Ltd., Toyo, Japan. 1991.okt.25. (1991)
 15. Mahunka I.: **Cyclotron in the practice**, Department of Nuclear Engineering, Nagoya University, Nagoya, Japan. 1991.nov.1. (1991)
 16. Tóth J. **Instrumentation in the NAO and ESAO in Atomki for atomic physics and surface- and interface research**, University of Reims, Laboratory of Analysis of Solid Surfaces and Interfaces in the Group of the Research of Surfaces and Thin Films. L.A.S.S.I.(G.R.S.M.). Reims, France, March 26, 1991. (1991)
 17. Kis-Varga M., Költő L., Kovács P., Fekete S.: **XRF analyser for archaeological use**, MTA Veszprémi Akadémiai Bizottságának Archaeometriai és Iparrégészeti Munkabizottsága felolvasóülés. Veszprém, 1991.nov.28. (1991)
 18. Futó I., Simon M., Bohátka S.: **Nagy tömegszámú oldott komponensek mérése tömegspektrométerrel**, Kutatási jelentés, Atomki, Debrecen (1991) 9

Earth and Cosmic Sciences, Environmental Research

1. Sokhi, R.S., Randle, K., Takács S., Gardiner, K.: **Characterisation of atmospheric particulates with PIXE and NAA**, Aerosols, Their Generation, Behaviour and Applications. Loughborough Univ. of Technology. Loughborough, England. 26-27 March, 1991. (1991)
2. Marton L., Mikó L., Ránk, D., Hertelendi E.: **Isotopenpydrogeologische Untersuchungen in der Grossen Ungarischen Tiefebene**, A 20 éves magyarosztrák földtani együttműködés jubileumi kötete. Szerk: Harald Lobitzer, Géza Császár **1** (1991) 369
3. Hertelendi E., Marton L., Mikó L.: **Isotope hydrological evidence of topographical changes in North-Eastern Hungary**, International symposium on the use of isotope techniques in water resources development. Wien, Austria, 11-15 March, 1991. (1991)
4. Bacsó J., Hakl J., Hunyadi I., Mikó L., Toth-Szilágyi M., Uzonyi I., Varga K.: **Hévízek össz-alfa-radioaktivitásának és kémiai elem tartalmának összehasonlító vizsgálata**, (Előadás és poszter kivonatok, p.17) XVI. Sugárvédelmi Továbbképző Tanfolyam, Balatonkenese, 1991.május 8-10. (1991)
5. Pécskay Z., Edelstein, O., Bernad, A., Kovács, M.: **Constraints on the neogene time-scale by K-Ar dating of Gutii Mts. volcanic rocks (Romania)**, Interpretarea de prospectiuni si explorari geologice Maramures, Baia Mare. Baia Mare, /Nagybánya/, Romania, 1991. June 27. (1991)
6. Amemiya, S., Katoh, T., Borbély-Kiss I., Koltay E., Szabó Gy., Biswas, S.K.: **Short-range transport of aerosols emitted by a point source of mixed character in complex terrain**, (abstract booklet, p.133. 1991) 2nd European Conference on Accelerators in Applied Research and Technology. Frankfurt/Main, Germany. 3-7 Sept.,1991. (1991)
7. Amemiya, S., Katoh, T., Borbély-Kiss I., Koltay E., Szabó Gy., Mészáros E., Molnár Á., Varga M.: **Vertical concentration profiles of fine and coarse aerosol particles collected over a suburban sampling site in the out skirts of Budapest, Hungary**, (abstract booklet p.132,1991) 2nd European Conference on Accelerators in Applied Research and Technology. Frankfurt/Main, Germany. 3-7 Sept.,1991. (1991)
8. Karamata, S., Knezevic, V., Bilik I., Árva-Sós E.: **Petrography and geochronology of some triassic volcanic rocks in Budva area, Yugoslavia**, Symposium on Central European Alkaline Volcanic Rocks (SCEAVR), Praga, Czechoslovakia, 24-29 June, 1991. (1991)
9. Bilik I., Harangi Sz., Árva-Sós E.: **Geochemistry, geochronology and tectonic setting of the basalt-tephrite-phonolite series in South Hungary**, Symposium on Central European Alkaline Volcanic Rocks (SCEAVR), Praga, Czechoslovakia, 24-29 June, 1991. (1991)
10. Balogh K.: **K-Ar mérések szerepe a pannoniai kronosztratigráfiában**, Magyarhoni Földtani Társulat, Budapest, 1991.okt.14. (1991)

11. Balogh K., Colantoni, P., Guerrero, F., Majer, V., Ravasz-Baranyai L., Vener, F.: **Radiometric age of Eholeiitic rocks from Jabuka Island (Adriatic sea, Yugoslavia)**, (Abstr.:eds.:I.Velic, I.Vlacovic. Institute of Geology, Zagreb, 1991. p.27) The Second International Symposium on the Adriatic Carbonate Platform. Zadar, Yugoslavia, 12-18 May, 1991. (1991)
12. Béres Cs., Fenyvesi A., Molnár T.: **Ciklotron által termelt rövid felezési idejű izotópok alkalmazása a fák vízzállítási vizsgálatára**, II. Ökológus Kongresszus, Keszthely, 1991.július 4-7. (1991)
13. Hámor T., Hertelendi E., Kovács L.: **Sulphur isotopic composition of sedimentary sulphides and sulphates of the Pannonian basin Hungary**, 29.International Geological Congress. Kyoto, Japan. 11-18 Sept.,1991. (1991)
14. Szöör Gy., Scheuer Gy., Schweitzer F., Hertelendi E., Balázs E., Sümegi P.: **Isotopegeochemical investigation of Quaternary and Neogene fresh-water limestone with faciological and stratigraphical evaluation**, XIIIrd INQUA Congress. Peking, China. 2-9 Aug., 1991. (1991)
15. Szöör Gy., Sümegi P., Hertelendi E.: **New potential in tracing climatic changes in the Quaternary period by malacofaunal and isotope geochemical methods**, XIIIrd INQUA Congress. Peking, China. 2-9 Aug., 1991. (1991)
16. Hertelendi E., Sümegi P., Szöör Gy.: **Geochronologic and paleoclimatic characterization of Quaternary sediments in the Great Hungarian Plain**, 14th International Radiocarbon Conference. Tucson, Arizona, USA. 20-24 May, 1991. (1991)
17. Benton, E.V., Frank, A.L., Benton, E.R., Csige I., Parnell, T.A., Watts, J.W.: **Radiation exposure of LDEF: initial results**, 1st Post-Retrieval LDEF Symposium. Kissinnee, Florida, USA. 2-8 June, 1991. (1991)
18. Csige I., Benton, E.V., Frank, A.L., Frigo, L.A., Benton, E.R., Parnell, T.A., Watts, J.W.: **Charged particle LET-spectra measurements aboard LDEF**, 1st Post-Retrieval LDEF Symposium. Kissinnee, Florida, USA. 2-8 June, 1991. (1991)
19. Hakl J., Hunyadi I., Csige I., Géczy G., Zámbo L., Lénárt L., Töröcsik I.: **Outline of natural radon occurrences on karstic terrains of Hungary**, Fifth International Symposium on the Natural Radiation Environment. Salzburg, Austria. 22-28 Sept.,1991. (1991)
20. Déri Zs., Takács S., Csige I., Hunyadi I.: **A case-control study of radon and lung cancer in eastern Hungary**, Fifth International Symposium on the Natural Radiation Environment. Salzburg, Austria. 22-28 Sept.,1991. (1991)
21. Géczy G., Hakl J., Hunyadi I., Zámbo L.: **Karsztlégzési modell a felszín alatti radon mérések alapján**, Oktatási és Kutatási Intézmények Karszt- és Barlangkutató Tevékenységének III. Országos Tudományos Konferenciája. Jósvalfő, 1991. május 17-19. (1991)
22. Hakl J., Töröcsik I., Hunyadi I.: **Radonaktivitás koncentráció mérések a Baradla barlangban (1984-1991)**, Oktatási és Kutatási Intézmények Karszt- és Barlangkutató Tevékenységének III. Országos Tudományos Konferenciája. Jósvalfő, 1991. május 17-19. (1991)
23. Lénárt L., Hakl J., Hunyadi I.: **A földtani környezet hatása a barlangi radonszint alakulására**, Oktatási és Kutatási Intézmények Karszt- és Barlangkutató Tevékenységének III. Országos Tudományos Konferenciája. Jósvalfő, 1991. május 17-19. (1991)

24. Várhegyi A, Hakl J., Futó K.: **DLC radon monitoring rendszer**, MFT és MGE 1991. évi Közös Vándorgyűlése. Szeged, 1991. május 16-18. (1991)
25. Lénárt L., Hakl J., Hunyadi I., Orbán J.: **A miskolc-tapolcai termál-forrás vízszintjének, víz hőmérsékletének és radonkoncentrációjának változása**, SITH XXVIIe Congress. Hajdúszoboszló, 1991. szept. 15-19. (1991)
26. Varga K., Hunyadi I., Tóth-Szilágyi M., Uzonyi I., Hakl J., Bacsó J., Mikó L.: **Hévizetek össz-alfa-radioaktivitásának és kémiai nyomelem tartalmának vizsgálata**, SITH XXVIIe Congress. Hajdúszoboszló, 1991. szept. 15-19. (1991)
27. Mikó L., Varga K., Hunyadi I., Tóth-Szilágyi M., Uzonyi I., Hakl J., Bacsó J.: **Kelet magyarországi hévizetek komplex nukleár analitikai vizsgálatából levonható földtani összefüggések**, Földtani Előadónap a DAB-ban. Debrecen, 1991. okt. 1. (1991)
28. Amemiya, S., Katoh, T., Borbély-Kiss I., Koltay E., Szabó Gy., Mészáros E., Molnár Á., Varga M.: **PIXE studies on horizontal and vertical distributions of atmospheric aerosols**, Department of Nuclear Engineering, Faculty of Engineering, Nagoya University. Nagoya, Japan. 1991.nov.1. (1991)
29. Hunyadi I., Hakl J., Várhegyi A.: **Real-time monitoring by Silicon photodiodes**, Second Workshop on Radon Monitoring in Radioprotection, Environmental and/or Earth Sciences. Trieste, Italy, 25 Nov.-6 Dec., 1991. (1991)
30. Géczy G., Hakl J., Hunyadi I.: **Long-term radon studies at the thermalkarst region of Budapest**, Second Workshop on Radon Monitoring in Radioprotection, Environmental and/or Earth Sciences. Trieste, Italy, 25 Nov. - 6 Dec., 1991. (1991)
31. Kovách Á.: **A Föld klímája és az emberi tevékenység**, MTESz, 1991 évi fizikusnapok, Nyíregyháza, 1991.okt.7. (1991)
32. Hertelendi E., Horváth F.: **Radiocarbon chronology of Late-Neolithic settlements in the Tisza-Maros region, Hungary**, 14th International Radiocarbon Conference. Tucson, Arizona, USA. 20-24 May, 1991. (1991)
33. Árva-Sós E., Balogh K., Pécskay Z.: **Balatonfelvidéki és villányi vulkanitokon végzett K-Ar módszeres kormeghatározások**, (Jelentés a MÁFI és Atomki között létrejött 5232/91. nyilvántartási sz. kut. szerződés keretében végzett K-Ar módszeres geokronológiai vizsgálatokról), Atomki, Debrecen (1991) 7
34. Pécskay Z., Balogh K., Árva-Sós E.: **Vulkanit kőzetminták abszolút korának meghatározása dunántúli és alföldi szénhidrogén-kutató fúrásokból**, A GKV és az Atomki 425/1991sz.szerződés keretében végzett K/Ar módszeres kormeghatározásokról. Témafelelős: Pécskay Z., Atomki, Debrecen (1991) 27
35. Balogh K., Árva-Sós E., Pécskay Z.: **A Bükkium kronológiai vizsgálata K/Ar módszeres kormeghatározásokkal**, Jelentés a Központi Földtani Hivatal és az Atomki 24/91sz. kutatási szerződés keretében végzett vizsgálatokról. Témafelelős: Balogh K., Atomki, Debrecen (1991) 9
36. Balogh K., Árva-Sós E., Pécskay Z.: **Mediterrán, miocén alapszelvényekből és alapfúrásokból származó kőzetminták K/Ar kormeghatározása**—, Jelentés a MÁFI és az Atomki 5231/91sz. szerződés keretében végzett kutatásokról. Témafelelős: Balogh K., Atomki, Debrecen (1991) 10
37. Balogh K., Árva-Sós E., Pécskay Z.: **K/Ar kormeghatározások az Alföld mezozoikum előtti képződményein**, Jelentés a Központi Földtani Hivatal és az Atomki között létrejött 256/kg-57/1991.sz. szerződés keretében végzett kormeghatározásokról, Atomki, Debrecen (1991) 7
38. Bohátka S., Futó I., Simon M.: **Fermentációs gázok mérése nagyüzemi fermentoron**, Kutatási jelentés, Atomki, Debrecen (1991) 7

Biological and Medical Research

1. Kispéter J., Horváth L., Kiss L., Bara-Herczeg O., Bacsó J., Uzonyi I., Eszes F.: **The effect of additional Se and ionizing radiation on the physical properties of milk protein powder**, 4th European Seminar of the EOQ Food Section. Berlin (West), Germany, Oct.24-27,1990. (1990)
2. Béres Cs., Fenyvesi A., Molnár T., Mahunka I., Tárkányi F.: **Field experiments on water transport of oak traced by cyclotron produced isotopes**, Az Élő Rendszerek Biomatematikai Modellezőse, Siófok, 1991. szept.6-7. (1991)
3. Déri Zs., Takács S., Csige I., Hunyadi I.: **Tüdőrák kockázat és radon**, (előadás és poszter kivonatok, p.46), XVI. Sugárvédelmi Továbbképző Tanfolyam, Balatonkenese, 1991.május 8-10. (1991)
4. Kovács Z., Tárkányi F., Qaim, S.M., Stöcklin, G.: **Cross section of proton induced nuclear reactions on Kr gas relevant to the production of medically important radioisotopes ^{81}Rb and ^{82}mRb** , (abstr.:66); International Conference on Nuclear Data for Science and Technology. Jülich, Germany, 13-17 May,1991 (1991)
5. Bohátka S.: **Biotechnological measurements with quadrupole mass spectrometers**, Budapest 91: Informal Meeting on Mass Spectrometry, Budapest, 1991.Jun.3-5. (1991)
6. Béres Cs., Fenyvesi A., Molnár T.: **Water transport in oak trees**, (book of poster abstracts, D4) First European Symposium on Terrestrial Ecology: Forests and Woodlands. Florance, Italy, 20-24 May,1991. (1991)
7. Fenyvesi A., Mahunka I., Tárkányi F., Molnár T., Béres Cs., Kovács Z., Mikecz P., Szücs Z.: **Production of ^{24}Na and ^{43}K radioisotopes in carrier-free form for use in radioecological studies at the forest area of the Síkfőkút project**, (Book of abstracts C10), First European Symposium on Terrestrial Ecology: Forests and Woodlands. Florance, Italy, 20-24 May,1991. (1991)
8. Béres Cs., Mahunka I., Molnár T., Fenyvesi A., Tárkányi F.: **Water transport of oak trees traced by cyclotron produced ^{24}Na and ^{43}K** , (abstr.: KLTE, Debrecen - GSF, Neuherberg, 1991), International Symposium on Ecological Approches of Environmental Chemicals. Debrecen, Hungary, 15-17 April,1991. (1991)
9. Fenyvesi A., Tárkányi F., Mahunka I., Molnár T., Szelecsényi F., Szücs Z., Béres Cs.: **Production of ^{43}K and $^{81,82m,83,84}\text{Rb}$ isotopes at the Debrecen cyclotron for ecological purposes**, (abstr.:KLTE, Debrecen - GSF, Neuherberg, 1991), International Symposium on Ecological Approches of Environmental Chemicals. Debrecen, Hungary, 15-17 April,1991. (1991)
10. Szücs Z., Dombi I., Kovács Z.: **^{67}Ga -citrát hazai gyártása az Atommag Kutató Intézetben**, Magyar Orvostudományi Nukleáris Társaság VII.Kongresszusa. Kecskemét, 1991.aug.15-17. (1991)
11. Bacsó J., Bacsó Zs., Fekete I., Ferenczy T., Uzonyi I.: **The effect of methylmercury on small animals and the use of hair as a reference material for Hg and methylmercury analytical quality control**, Research Co-operation Meeting on "The Assesment of Environmental Exposure to Mercury in Selected Human Population as Studied by Nuclear and Other Techniques". Wien, Austria, 10-13 June, 1991. (1991)

12. Bacsó J.: **Investigation of mercury concentration in fish**, Research Co-operation Meeting on "The Assessment of Environmental Exposure to Mercury in Selected Human Population as Studied by Nuclear and Other Techniques". Wien, Austria, 10-13 June, 1991. (1991)
13. Bacsó J., Bognár L., Pattinger, O.: **An unusual form of mercurialism**, Research Co-operation Meeting on "The Assessment of Environmental Exposure to Mercury in Selected Human Population as Studied by Nuclear and Other Techniques". Wien, Austria, 10-13 June, 1991. (1991)
14. Tóth Gy., Mikecz P., Molnár T., Trón L.: **(¹⁸F)2-fluoro-2-dezoxi-d-glükóz in vivo radiofarmakon előállítása**, (előadások és poszterek kivonata p.101), Magyar Biofizikai Társaság XVI.Vándorgyűlése, Budapest, 1991.július 2-4. (1991)
15. Mikecz P.: **Izotópok és radiofarmakonok előállítása a debreceni ciklotronon**, (Izotóptechnika, Diagnosztika 34,1991,1sz. p.24), Magyar Orvostudományi Nukleáris Társaság VII.Kongresszusa. Kecskemét, 1991.aug.15-17. (1991)
16. Dám A.M., Rétlaki M., Gázsó L., Fenyvesi A., Molnár T., Mahunka I.: **Basic radiobiological parameter of p(18 MeV)+Be fast neutron source in Hungary**, (book of abstracts), 9th International Congress of Radiation Research, Toronto, Canada, 7-12 July, 1991 (1991)
17. Csejtei A., Fenyvesi A., Molnár T., Márián T., Pásti G., Trón L., Miltényi L., Mahunka I., Kovács P.: **Physical and biological dosimetry with regard to further neutron therapy applications at the cyclotron in Debrecen**, (Book of abstracts), First Biannual Meeting on Physics in Clinical Radiotherapy, Budapest, 14-17 Oct., 1991. (1991)
18. Béres Cs., Fenyvesi A., Molnár T.: **Vízszállítás sebességének vizsgálata tölgyfákban gyors felezési idejű izotópokkal**, IV.magyar Növényélettani Kongresszus. Szeged, 1991.július 10-12. (1991)
19. Csejtei A., Molnár T., Fenyvesi A., Márián T., Kovács P., Pásti G.: **Preliminary report on the preclinical experiments required for neutron therapy at the cyclotron in Debrecen**, Az Élő Rendszerek Biomatematikai Modellezése, Siófok, 1991. szept.6-7. (1991)
20. Dám A.M., Rétlaki M., Gázsó L.G., Fenyvesi A., Molnár T., Mahunka I.: **A hazai ciklotron neutronforrás sugárbiológiai paramétereinek bemérése**, A Magyar Biofizikai Társaság XVI. Vándorgyűlése, Budapest, 1991. július 2-4. (1991)
21. Körösi F., Jezierska E.Szabó, Szőke P., Hunyadi I.; **Az ionizáló sugárzás hatása a növények életfolyamataira**, Magyar Biofizikai Társaság XVI. Vándorgyűlése. Budapest, 1991.július 2-4. (1991)
22. Körösi F., Hunyadi I.: **A nitrogén és a bór növényélettani jelentősége; szilárdtestnyomdetektoros meghatározásuk ¹⁴N(n,p)¹⁴C és ¹⁰B(n,α)⁷Li magreakciókkal**, 4. Növényélettani Konferencia, Szeged, 1991. július 10-12. (1991)
23. Mikecz P.: **Isotope production at the Atomki (Debrecen) cyclotron**, 1st Meeting of Producers and Traders of Radioisotopes. Veszprém, Hungary, 14-18 Oct.,1991. (1991)
24. Mahunka I.: **Classification of cyclotrons for medical use**, Japan Steel Works, Ltd, Baby Cyclotron. Muroran, Japan. 1991.okt.19. (1991)
25. Mahunka I.: **Target systems for the production of cyclotron isotopes**, CYRIC Cyclotron and Radioisotope Center, Tohoku University, Sendai, Japan. 1991.okt.21. (1991)

26. Béres Cs., Fenyvesi A., Molnár T.: **Ciklotron által termelt rövid felezési idejű izotópok alkalmazása fák vízszállításának vizsgálatára**, II. Ökológus Kongresszus, Keszthely, 1991.július 4-7. (1991)
27. Végh L.: **A fizika alaptörvényei és az élet**, Fizikusnapok. Debrecen, 1991.március 1. (1991)
28. Végh L.: **A fizika alaptörvényei és az élet**, Fizikatanári továbbképzés. Nyíregyháza, 1991. aug. 28. (1991)

Development of Instruments and Methods

1. Efremov, A.A., Kutner, V.B., Biri S., Chugreev, V.A.: **Problemy formirovaniya magnitnogo polya ECR-istochnika**, Soobshchenie OIYAI, P9-91-263 (1991) 12
2. Kormány Z., Lakatos T., Valek A.: **A microcomputer-based versatile profile monitoring system**, Twelfth international conference on cyclotrons and their applications. Berlin, Germany May 8-12, 1989. Ed.: B.Martin, K.Ziegler. World Scientific, Singapore (1991) 309
3. Paál A., Szádai J., Székely G.: **A Q300PC típusú kvadrupol tömegspektrométer IBM PC alapú mérési adatgyűjtő és vezérlő rendszere, XXXIV. Magyar Szinképelemző Vándorgyűlés. VII. Magyar Molekulaspektroszkópai Konferencia, Nyíregyháza, 1991.aug. 27-30. Nyíregyháza, Gépipari Tudományos Egyesület (1991) 155**
4. Kalinka G.: **X-ray spectroscopy using semiconductor detectors**, 159TH x-ray workshop, Kansai University, Osaka, Japan, 18 January, 1991. (1991)
5. Váhegyi A, Hakl J., Futó K.: **DLC radon monitoring rendszer**, (előadás és poszter kivonatok, p.51), XVI. Sugárvédelmi Továbbképző Tanfolyam, Balatonkenese, 1991.május 8-10. (1991)
6. Medveczky L., Biró B., Hunyadi I., Hakl J.: **Orvosi rádium készítmények zártóságának vizsgálata**, (előadás és poszter kivonatok, p.50), Sugárvédelmi Továbbképző Tanfolyam, Balatonkenese, 1991.május 8-10. (1991)
7. Bohátka S.: **Biotechnological measurements with quadrupole mass spectrometers**, Budapest 91: Informal Meeting on Mass Spectrometry, Budapest, 1991.Jun.3-5. (1991)
8. Langer G.: **Quadrupole mass spectrometry and its application**, Bernath Atomic GmbH, Wennigsen, Germany, 1991.jun.6-7 (1991)
9. Molnár T., Tóth Gy., Trón L., Gál I., Kiss J.: **^{18}F termelő céltárgykamra a debreceni MGC-20 ciklotronhoz**, (Előadások és poszterek kivonata p.87), Magyar Biofizikai Társaság XVI.Vándorgyűlése, Budapest, 1991.julius 2-4. (1991)
10. Medveczky L., Hunyadi I., Hakl J., Biró B.: **Leakage testing of ^{226}Ra sources by radon detection**, International Workshop on Radium, Uranium, Thorium and Related Nuclides in Industry and Medicine: History and Current Uses. Badgastein, Austria. 1-3 Oct., 1991. (1991)
11. Biri S., Bogomolov, S.L., Kutner, V.B., Tretyakov, Yu.P.: **Investigation of injector with an arc multicharged ion source**, 4.International Conference on Ion Sources. Bensheim, Germany, Sept.30-Oct.4,1991. (1991)
12. Dajkó G.: **Application of track detectors in neutron dosimetry**, University College of Science. Calcutta, India. 1991.okt.4. (1991)
13. Dajkó G.: **Neutron spectrometry using SSNTD**, Seventh National Conference on Particle Tracks in Solid: Application in Environmental Monitoring. Jodhpur, India. 9-11 Oct., 1991. (1991)
14. Dajkó G.: **Track detectors and their applications**, Saha Institute of Nuclear Physics. Calcutta, India. 1991.okt.7. (1991)
15. Dajkó G.: **Production and application of particle track membranes in Hungary**, 2nd Meeting on Particle-Track Membranes and Their Applications. Bielsko Biala, Poland. 2-6 Dec.,1991. (1991)

16. Mahunka I.: **Ciklotronok és alkalmazásaik**, KLTE Kísérleti Fizikai Tanszék, Debrecen, 1991.nov.26. (1991)
17. Paál A., Szádai J., Székely G.: **Data acquisition and control system for quadrupole mass spectrometer using an add-on card to IBM PC**, Budapest'91 : Informal Meeting on Mass Spectrometry. Budapest, 1991.junius 3-5 (1991)
18. Szilágyi J., Pólya K., Bohátka S., Langer G.: **Development of an industrial quadrupole mass spectrometer system for monitoring fermentations**, Bioreactor Engineering Course of European Federation of Biotechnology. Supetar, Yugoslavia, 26-30 Sept.,1991 (1991)

Theses completed

CANDIDATE OF THE PHYSICAL SCIENCES:

Nyakó, B.M. Superdeformation and shape coexistence in ^{152}Dy , (in Hungarian)

Végh, J. Results and applications of the electron and Röntgen-spectroscopic research, (in Hungarian)

Pál, K.F. The effect of rotation on the structure of nuclear states, (in Hungarian)

Langer, G. Home-market introduction and applications of the continuous, mass-spectrometric measurement of gases dissolved in liquid (in Hungarian)

Hertelendi, E. Developments of methods and instruments for the purpose of isotope analysis and their applications (in Hungarian)

Mészáros, S. Experimental study of current-conducting properties of weakly coupled superconducting transitions (in Hungarian)

Ricz, S. Röntgen- and Auger-electron-spectroscopic results in studies of high energy, charged-particle-atom collisions (in Hungarian)

Hunyadi, I. Study of low energy nuclear reactions by track detectors (in Hungarian)

DOCTORAL DEGREES:

Szabó I. Computer control of quadrupole mass spectrometric measuring system (in Hungarian)

Biri, S. Investigation of heavy-ion sources' operation and the possibilities of heavy-ion acceleration on the Debrecen cyclotron (in Hungarian)

Csige, I. Development and application of solid-state track-detector technique in space and radon dosimetry (in Hungarian)

Tókési, K. **Investigation of electrooptic characteristics of electronspectrometer units** (in Hungarian)

DIPLOMA WORKS:

Vámosi, Gy. **Design of position-sensitive detector for electrostatic electronspectrometer** (in Hungarian), supervisor: Cserny, I.

Medve, I. **Investigation of the current-conducting properties of high-transition-temperature BI-SR-CA-CU-O superconducting film** (in Hungarian), supervisor: Vad, K.

Tóth, L. **Study of angular distribution of Auger electrons in p-Ne collisions** (in Hungarian), supervisor: Ricz, S.

HEBDOMADAL SEMINARS

January 17

Ab initio stopping power calculations

G. Schiwietz (Hahn-Meitner Institute, Berlin)

January 24

Description of molecular-like states of nuclei by group-theoretical methods

G. Lévai

February 21

Experiments with ultracold antiprotons

D. Horváth (Central Research Institute of Physics, Budapest)

March 7

Photoeffect induced by intensive laser impulses

Gy. Farkas (Central Research Institute of Physics, Budapest)

March 14

Mass spectrometer system for monitoring of fermentation processes

S. Bohátka

March 21

Excitation of Na -like ions in high-energy ion-atom collisions

I. Kádár

March 28

Final state interaction in Auger processes induced by $p - Ne$ reaction

E. Takács

April 4

Experimental nuclear spectroscopy at the Debrecen cyclotron

T. Fényes

April 11

Computer modelling for data processing of spectrometer signals

T. Lakatos

April 25

Environmental analytical activities at GKSS in Geesthacht

W. Michaelis (Forschungszentrum Geesthacht)

April 30

Ion optics of energy-dispersive and transport elements of electronspectrometers

K. Tökési

May 2

Investigation of neutron radiation of palladium plates saturated electrically by deuterium

S. Daróczy (Kossuth University, Debrecen)

May 9

Past, present and future at the Institute of Isotopic and Molecular Technology, Cluj

C. Cuna (Institute of Isotopic and Molecular Technology, Cluj)

Research activities at the Mass Spectroscopy Department

A. Pamula (Institute of Isotopic and Molecular Technology, Cluj)

May 23

Mechanism of $(n, 2n)$ reactions at 14 MeV neutron energies

G. Pető (Kossuth University, Debrecen)

May 30

Calculation of partial widths for giant resonances

T. Vertse

June 6

Intermediate energy heavy-ion collisions in the framework of quantum molecular dynamics

A. Rosenhauer (University of Bergen)

June 13

Classical Monte Carlo methods for atomic collisions

G. Hock

June 20

Controlling and data acquisition systems of magnetic and quadrupole spectrometers

A. Paál, J. Szádai, and G. Székely

July 9

Cold fusion studies at OCTAVIAN

A. Takahashi (Osaka University)

September 5

Proton - hydrogen molecule ionization cross sections

L. Nagy

September 11

Elementary nuclear states in new approximation

T. Kibédi

September 12

High-energy atomic collision processes

L. Sarkadi

September 26

CRYRING - an accelerator and storage ring in Stockholm

U. Rosengard (Manne Siegbahn Institute of Physics)

October 10

The baryon-baryon forces in skyrmion approximation

J. Eisenberg (University of Tel Aviv)

October 17

Investigation of magnetic properties of high-temperature superconductors

N. Hegmann

October 24

Analogue simulation of nonlinear systems

É Kirsch

October 31

Research and development of $Si(Li)$ detectors

G. Kalinka

November 7

Creating and applications of ultrahigh-power laser impulses

G. Szabó (József Attila University, Szeged)

November 14

High resolution PIXE method and its applications

I. Török

November 21

Production of labelled compounds for diagnostics

Z. Kovács

November 28

PIXE analysis of atmospheric aerosols

S. Takács

December 5

What is patch clamp?

S. Damjanovich (Medical University, Debrecen)

December 12

Measurement of CP -violation at CERN

S. Szilágyi

Author Index

- Algora A. 14, 16
 Amemiya *S. 112, 114
 Andó L. 121, 125
 Angulo *C. 1
 -
 Árva-Sós E. 108
 -
 Bacelar *J. 139
 Bacsó J. 129, 131, 134, 137
 Bacsó *Zs. 134
 Balanda *A. 139
 Balogh K. 108
 Bang *J. 58
 Bardoux*T. 96
 Bartha L. 161
 Báder A. 143
 Berényi D. 65, 79
 Bergman*J. 123
 Biri S. 143, 145, 147, 148, 150
 Biswas*S.K. 112
 Bíró *B. 152
 Bognár *L. 137
 Bogomolov *S. L. 145
 Borbély-Kis I. 103, 112, 114, 157
 Brabec *V. 81
 Brant*S. 27, 29, 31
 Buda*A. 139
 -
 Cazaux *J. 96
 Curutchet*P. 58
 -
 Cseh J. 41, 43, 45, 47, 48, 50
 Cserny I. 81, 141
 Csige I. 106, 127
 Csótó A. 33, 35, 37, 39
 -
 Dám *A. M. 119
 Déri *Zs. 127
 Ditrói F. 85
 Dombrádi Zs. 10, 12, 22, 24, 27, 29, 31
 Dragoun*O. 81
 Engstler *S. 1
 Elston *S. B. 79
 -
 Fekete *I. 134
 Fekete *S. 97
 Fenyvesi A. 117, 119, 121
 Ferenczy *T. 134
 Fényes T. 10, 12, 22, 24
 -
 Gázsó *L. G. 119
 Gácsi Z. 14, 16, 19, 21
 Géczy *G. 106
 Giai *N. Van 58
 Greife*U. 1
 Greiner *W. 50
 Gulyás J. 18, 22, 24
 Gulyás L. 65, 79
 Gupta *R. K. 48, 50
 -
 Hakl J. 106, 152
 Hassan *M. F. F. M. 22, 24
 Hegman N. 104, 105
 Hertelendi E. 110
 Hock G. 67, 69
 Hunyadi I. 6, 106, 127, 152
 -
 Józsa M. 26
 Julin *R. 8, 10, 18, 24
 -
 Kalinka G. 87, 89, 91, 97, 99
 Katoh*T. 112, 114
 Kádár I. 63
 Keinonen*J. 4
 Kirch*B. 1
 Kiss Á. Z. 3, 4, 6, 161
 Kis-Varga M. 97, 99, 101
 Koltay E. 4, 112, 114, 161
 Koós *I. 145
 Kovács P. 97, 99, 155
 Kovács Z. 121, 125
 Költő *L. 97

- Kövér Á. 79
 Kövér L. 81, 94, 141
 Krasznahorkay A. 8, 10, 12, 139
 Kruppa A. T. 33, 39
 Kumpulainen *J. 8, 10, 18, 24
 Kopeczky *P. 7, 14
 Kovács P. 127
 Kovács Z. 5, 102
 Kövér Á. 49, 57
 Kövér L. 71, 119
 Krasznahorkay A. 10, 12
 Kruppa A. T. 33
 Kumpulainen *J. 12, 21
 -
 Lakatos T. 159
 Langanke *K. 1
 Lénárt *L. 106
 Lévai G. 43, 45, 52
 Liotta *R. J. 52, 58
 Lovas R. G. 33, 35, 37, 39, 54
 Ludu *A. 50
 -
 Mahunka I. 85, 117, 119, 121
 Máté Z. 26
 Medveczky L. 152
 Mészáros *E. 114
 Mészáros S. 104, 105
 Mikecz P. 121, 125
 Molnár *Á. 114
 Molnár J. 148, 150
 Molnár *T. 117, 119, 121
 Monze *D. 96
 Mukoyama *T. 69, 83
 -
 Nagy A. 161
 Nagy L. 77, 78
 Nakamatsu *H. 69
 Novák *J. 81
 -
 Paar *V. 12, 27, 29, 31
 Pallinger *O. 137
 Patat *J. M. 96
 Pál K. F. 39
 Pálkás J. 65, 71, 79, 143
 Pécskay Z. 108
 -
 Quang T. X. 8, 10, 12, 14, 16
 -
 Rahula *E. 6
 Raimann *G. 1
 Räisänen *J. 6
 Rétlaki *M. 119
 Ricz S. 63
 -
 Salace *G. 96
 Sarkadi É. 125
 Sarkadi L. 65, 71, 79, 83
 Scheid *W. 43, 45, 47, 48, 50
 Schröder *U. 1
 Sohler D. 14, 16
 Solin *O. 123
 Somorjai E. 1, 3, 4, 161
 Sümegi *P. 110
 -
 Szabó Gy. 63, 79, 112, 114, 157, 161
 Szádai J. 97
 Szelecsényi F. 121, 123, 125
 Szilágyi S. 60
 Szöőr *Gy. 110
 Szűcs Z. 121, 123
 -
 Takács E. 63
 Takács S. 85
 Takács *S. 127
 Tárkányi F. 121
 Thomas *X. 96
 Tikkanen *P. 4
 Tímár J. 8, 10, 12
 Tóth J. 96
 Tóth L. 63
 Török I. 71, 73, 75
 Törőcsik *I. 106
 Tökési K. 67, 69, 141
 -
 Uray I. 153
 Uzonyi I. 129, 134
 -
 Vad K. 104, 105
 Vajnai *T. 65, 79
 Valek A. 162
 Varga D. 141

Varga K. 39, 54, 56
 Varga *M. 114
 Vasváry L. 85
 Vertse T. 58
 Végh J. 63, 79, 101
 Végh L. 77, 78
 -
 Wakiya *K. 63
 -
 Závodszy P. 65, 73
 Zolnai L. 26

(* denotes author from other establishment)

Kiadja a
Magyar Tudományos Akadémia Atommag Kutató Intézete
A kiadásért és szerkesztésért felelős
Dr. Pálinkás József, az Intézet igazgatója
Készült a Bogáti vállalkozás nyomdájában
Törzsszám: 65783
Debrecen, 1992. március.

1871
1872
1873
1874
1875
1876
1877
1878
1879
1880
1881
1882
1883
1884
1885
1886
1887
1888
1889
1890
1891
1892
1893
1894
1895
1896
1897
1898
1899
1900

